FAST ATOM BOMBARDMENT MASS SPECTROMETRY OF THE COORDINATION COMPLEXES OF THE LIGAND 5,5,7,12,12,14-HEXAMETHYL-1,4,8,11-TETRAAZACYCLOTETRADECANE

Cindy Lee MacLaurin, B. Sc.

A thesis submitted to the
Department of Chemistry
in partial fulfilment of the requirements
for the degree of
Master of Science

Brock University,
St. Catharines, Ontario
Sept., 1985

© Cindy Lee MacLaurin

To my mother

for her love and encouragement

ABSTRACT

A number of metal complexes containing the ligand 5,5,7,12,12,14-hexamethyl-1,4,8,11-tetra-azatetradecane were synthesized and analyzed using electron impact (EI) and fast atom bombardment (FAB). The FAB mass spectra were obtained in positive and negative ion mode. FAB in the positive ion mode proved to be the most successful technique for the identification of these compounds. In the majority of cases the spectra obtained using positive ion FAB were structurally informative, although not all showed molecular (M^+) or quasimolecular ($[M+H]^+$) ions. The fragmentations observed were characteristic of the ligands, and were interpreted based on the chemistry of these compounds.

ACKNOWLEDGEMENTS

The author would like to express her sincere appreciation to Professeur Jack Miller and Professeur Mary Richardson, the supervisors of this work, for their guidance and patience.

Special thanks to Tim Jones for his aid in familiarizing me with the mass spectrometer and for his invaluable advise.

I would like to express my deep gratitude to Dr. Rothstein for his unfaltering assistance with the computing required for the use of the Bayesian Statistical Method.

Thanks are due the people in the inorganic lab and the chemistry staff for their support and encouragement. Special thanks to Greg Waters and Mel Farquharson for their inspiration and assistance.

TABLE OF CONTENTS

Table of Contents cont'd

LIST OF TABLES

LIST OF FIGURES

I. INTRODUCTION

A. Mass Spectroscopy

1. Desorption Ionization Techniques in Mass Spectrometry

The mass spectrometer is essentially a sophisticated weighing machine. Its purpose is to convert the sample into measurable products which are indicative of the original molecule. To accomplish this, the instrument requires that the sample molecules to be weighed be in the gas phase and that they be ionized (1). It is the ion source which produces this ionization. The mass spectrometer consists basically of an inlet, ion source, mass analyzer, detector and a recorder.

Since its first use in organic analysis, mass spectrometry has relied largely on electron impact (EI) to create ions from the vaporized neutral molecules. In this method an electron beam, usually with an energy of 70 electron volts, interacts with a neutral molecule in the gas phase and strips an electron to leave a positive radical ion, $M^{+\cdot}$. This interaction is illustrated in equation 1.

[1] $$M + e^- \text{----->} M^{+\cdot} + 2e^-$$

This radical molecular ion reflects the molecular weight of the analyte, and it is this ion and the fragment ions which result

from its dissociation which make up the mass spectrum. It is the interpretation of these fragments which may reveal the structure of the molecule. Sample vaporization is a prerequisite with EI, and therefore the sample must be heated. For nonvolatile or thermally fragile samples, heating the sample to vaporize it often leads to thermal degradation.

Various alternative strategies have been developed to make possible the analysis of these thermally labile compounds. The basic concept of these alternative methods is the desorption of ions directly from a condensed phase. Desorption ionization (DI) or particle-induced desorption are general terms often applied to these techniques (2,3), and includes such ionization techniques as secondary ion mass spectrometry (SIMS), fast atom bombardment (FAB), plasma desorption (PD), field desorption (FD), electrohydrodynamic ionization (EHMS), and laser induced desorption (2).

FD is the precursor of this family of ionization methods. It was first used for a compound of low volatility in 1969 by Beckey (4), who published the mass spectrum of glucose using this technique. In this method the sample is placed on microdendrites, usually carbon grown on a fine metal wire, and introduced into a special ion source. A high field causes both ionization and desorption to occur. This technique is difficult in practice and the ions providing molecular weight information, if produced at all, are frequently only transient (5).

Plasma desorption was developed as an outgrowth of work in

which the decay of californium was studied by the time-of-flight measurement of its fission fragments (2). This method uses the interactions of high energy (hundreds of Mev) heavy ions in a solid matrix to induce desorption and ionization (3). The essential feature of ^{252}Cf PDMS was that the beam of energy was highly concentrated and the excitation lasted for only short periods of time. Under these conditions, large thermally labile molecules were able to survive intact and to desorb from the surface as ionized species.

Other means of obtaining the same results were sought and found. SIMS was one such method. Samples, usually in solid form, are energized by ions with energy in the Kev range. Up until 1976 this method had been used routinely for surface analysis of inorganic species. It was Benninghoven who showed that these energetic ions impinging on the surface of a thin film of biomolecules induced the same desorption-ionization process observed in PDMS (6). In 1978, Meuzelaar introduced laser desorption (LD) (7). Samples are prepared in a variety of manners as both reflection and transmission experiments are performed. Excitation of the sample is initiated by laser pulses of short duration and produces patterns of desorbed molecular ions similar to ^{252}Cf PDMS and SIMS. The most recent particle-induced desorption technique to be studied is fast atom bombardment FAB.

2. FAB and its Advantages

This technique was first introduced by Barber in 1981, and since then it has become a widely used soft ionization technique (8). In this method, samples, usually in solution, are energized by neutral atoms of kev energy. The neutral beam of atoms bombards the sample and sample ions are produced as a result of the interaction of the beam with the sample, see Figure 1. In the initial interaction of the incident particles, a large amount of energy is deposited into a highly localized region of the sample. Some of this energy is transformed into internal vibrational modes and into molecular translation/rotation of the surface molecules. This initiates fragmentation and desorption into the gas phase. Both positive and negative ions can be formed in the bombardment process. Molecular weight information is often obtained from quasimolecular ions especially for molecules of biological interest; $(M+H)^+$ in positive ion spectra and typically from $(M-H)^-$ ions in negative ion spectra rather than simple molecular ions. The earliest experiments using the FAB technique required that the sample be deposited directly on the probe tip from solution and evaporated to dryness before analysis. This method of preparation resulted in mass spectra of a transient nature. It was found by Barber et al (9), that the use of low vapor pressure liquids and oils gave spectra that lasted for hours. These liquids are commonly referred to as the matrix. Matrix liquids commonly encountered are; glycerol,

Figure 1: Simplified Diagram of a FAB Source (15).

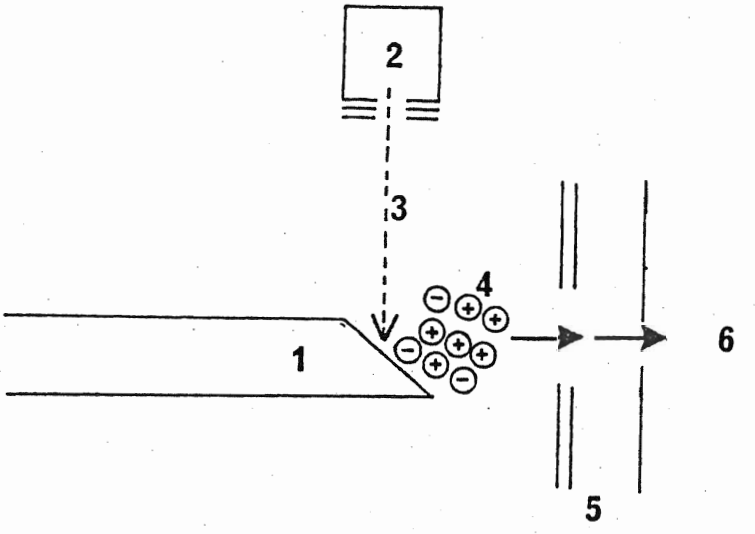

(1) Probe tip

(2) Atom gun

(3) Fast atom beam

(4) Sputtered ions

(5) Source ion optics

(6) To mass analyzer

sulfolane, thioglycerol, nitrophenyl-octylether,and nujol. Glycerol is by far the most popular. The sample preparation consists of dissolving the sample of interest in a suitable matrix and placing it on the probe tip.

Among the recently developed mass spectroscopy techniques FAB has been considered one of the more successful. This success is due in part to the advantages that are inherent to FAB.

1. The ionization and evaporation process occurs from either the solid or the dissolved solid and thus, no separate sample volatilization is required.
2. The sample preparation is fairly simple as compared to the derivatization techniques required for EI or the involved sample preparations required for field desorption. In fact, when both FAB and FD give useful results FAB is preferred due to the minimized sample preparation and the generally more informative fragmentation which results (1,10).
3. FAB in many cases has a high pseudomolecular or molecular ion sensitivity, and provides structurally significant fragmentation. Fragmentation is quite often absent in some of the other softer ionization techniques. For example, FD and EHMS produce spectra which have reduced fragmentation (2).
4. Mass spectra may be obtained from molecules of relatively high molecular weight. In fact it is still not known how large a molecule can be lifted from the matrix surface by FAB, although results have been obtained above 23,000 for

biologically interesting molecules using PD-MS (11), and above 30,000 for inorganic ion clusters with SIMS (12).

5. The final advantage has to do with the spectra that may be obtained. Both positive and negative ion spectra may be obtained with equal facility and without any need to make major changes in the ion source conditions, although changes in the power supply polarities are necessary.

It can be noted that in the literature the main focus for FAB has been towards molecules of biomedical interest. Applications to inorganic compounds have not been as extensive, but the advantages that FAB presents make it a potentially useful technique for these compounds.

3. Applications

Mass spectroscopic analysis of non-volatile, thermally labile inorganic complexes has generally proved so difficult that in the past mass spectroscopy has not been a common tool of the inorganic chemist. FAB makes it possible to obtain mass spectra of organometallic and coordination compounds that could not be analyzed previously. A mass spectroscopic technique should provide (a) information concerning the parent ion's molecular weight, (b) give an indication of structural complexity through fragmentation and (c) perhaps predict the chemical reactivity of the compound of interest. Such information is particularly important for complexes containing for example, paramagnetic

sites where NMR spectral studies are of limited value. The following examples from the literature are provided to emphasize not only the obvious advantages of FAB, but to illustrate that FAB does satisfy the above criteria.

(a) Organometallic Compounds

The most extensively studied organometallic compound using FAB is Vitamin B_{12} and its coenzymes. Vitamin B_{12} was featured in the first paper published by Barber *et al.* on FAB (8). The basic structure of the coenzyme is illustrated in Figure 2. The bond to the carbon atom of the deoxyribose moiety is labile, and as a result the ligand attached to the cobalt at that coordination site is variable. This fact made it possible for Barber to not only study Vitamin B_{12}, but also the cyano-, methyl- and hydroxy-derivatives (13). In all cases a reasonably intense quasi-molecular ion (M+1), was obtained. The next peak of importance appears at m/z 1329, corresponding to loss of the axial ligand. Barber reported the relative abundances of the quasimolecular ions are m/z 1355>1344>1579>1346, which corresponds to cyano, methyl, adenosine, and hydroxy compounds respectively. This series mimics the π-acceptor ability of ligands noted in other transition metal complexes.

FAB is known to produce the best results for polar or ionic species. FAB, however has been found to be applicable to non-polar species as well. This is exemplified by the silyl

Figure 2: Basic Structure of Cobalamine (15).

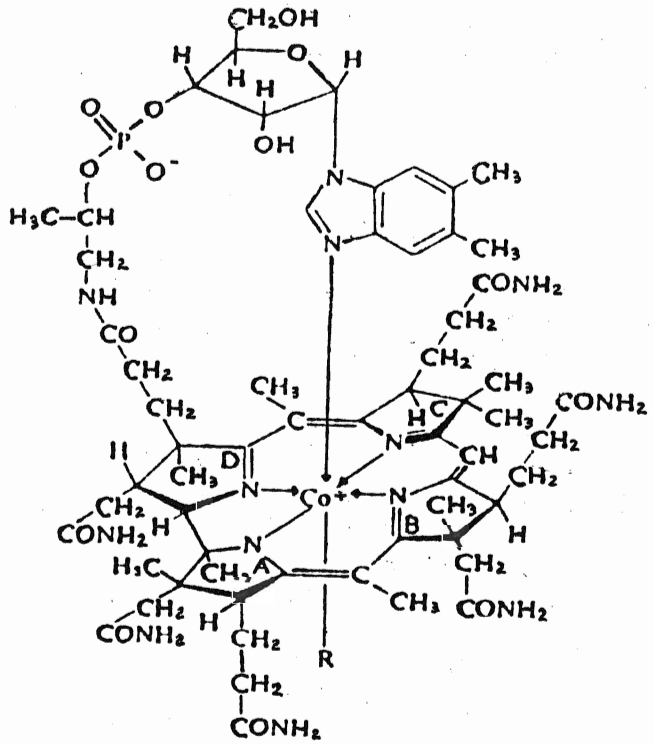

	R
Cyanocobalamin	CN
Methylcobalamin	CH_3
Hydroxocobalamin	OH

Coenzyme B_{12}

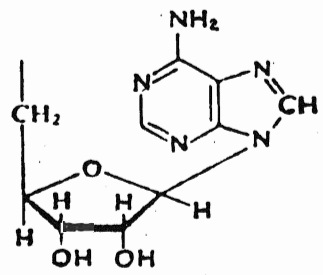

cyclopentadiene/cyclooctadienerhodium(I) compound. This compound emphasizes the obvious advantages of FAB. No worthwhile structural information could be obtained by conventional techniques as it is water sensitive as well as thermally labile. Also, it was applied as a liquid to the probe tip which eliminated any type of sample preparation. A strong parent ion was observed at m/z 438, with losses due to C_8H_4, $(CH_3O)_3SiH$ and $(CH_3O)_3SiCH{=}CH$ creating the most important high mass ions (9). This compound is typical of many organometallics for which molecular ions rather than quasi-molecular ions are observed.

FAB has also been used in an analytical context in that it has been used to identify organoarsenic compounds in seafoods (14). This particular study involved the use of both FAB and FD. The authors concluded that FAB was more practical, producing more fragment ions than FD. The arsenic compound of interest was the arsenobetaine $(CH_3)_3As^+CH_2CO_2^-$ isolated from plaice. Using high resolution FAB and an ion counting multichannel analyzer system it was possible to detect the protonated parent ion at m/z 179.0053.

The number of studies involving transition metal organometallics are far more extensive than those of the main group metals (15-19). In a recent paper by Cerny et al. , FAB proved to be quite successful in giving interpretable fragment ions for a series of organometallic derivatives of Os(II) and Ru(II) (16). The purpose of this study was to determine the applicability of both FAB and FD techniques in studying π

-bonding ligand groups. In most cases the FD spectrum yielded only information on the intact cation, whereas FAB revealed structural aspects of the cation through its fragment ions. In most instances, the most intense peaks were due to loss of the π-bonding ligand and the π-bonding ligand+HCl. FAB proved to be a better characterization technique as it produced fragment ions which aid in compound identification.

In a similar study by Sharp and co-workers, a series of rhodium, iridium and platinium organometallic complexes in which a cumulene ligand is attached to the metal in either σ or π bonding fashion, were examined (17). The cumulene ligand was lost intact in all the complexes studied. The observed fragmentation occurred at the metal-ligand bonds, and not within a ligand, which is consistent with the known strength of the metal-ligand bonds and the bonds between atoms within the ligands. In general, they found the most easily lost ligands are the anionic ones. In the iridium complex series, the triflate ligand (OSO_2CF_3) was lost and in the rhodium series, the chloride was lost. The unsaturated organic ligands are less easily lost, and the acids carbon monoxide and triphenylphosphine are relatively difficult to lose. The relative ordering of the bond strengths mimics the solution chemistry of this series of complexes. Sharp concluded that the FAB mass spectroscopy of these compounds is the most useful method for structure determination short of x-ray crystallography. The FAB-MS of the rhodium complexes were more readily analyzed and potentially less ambigious than various

optical and magnetic spectra available (17).

Davis and coworkers applied FAB-MS to a range of mono- and poly nuclear transition metal complexes which did not yield EI spectra (18). Organometallic complexes of rhodium, ruthenium, rhenium, palladium, platinum, as well as the metal clusters of iron and osmium, were studied. Good FAB spectra were obtained for the triphenylphosphine complexes for which EI gives only ions arising from Ph_3P, which is produced as a result of thermal decomposition of the complexes. The compounds $[RhX(PPh_3)_3]$ where X=Cl or Br gave peaks corresponding to the cations of $(M+H)^+$, M^+, $(M+H-X)^+$, $(M-X)^+$, $(M+H-PPh_3)^+$, and $(M-PPh_3)^+$. The $[RuCl_2(PPh_3)_3]$ complex gave $[(M+H)-PPh_3]^+$ as its highest mass ion, which is consistent with known solution behaviour. The complexes $[ReCl(CO)_3(P(C_3H_4F\text{-}p)_3)\ ]$ and $[Re(NO_3)(CO)_3(P(C_6H_4Me\text{-}p)_3)_2]$ have $[(M+H)-X]^+$ where X=Cl or NO_3 as the highest mass ion. However there are no published results to the effect that these molecules behave like this in solution. The platinum and palladium phosphines undergo extensive dissociation in accord with their solution behaviour. The cluster compounds of Fe and Os were also identified using FAB. Davis demonstrated the potential of FAB for transition metal complexes, in particular organometallics and stated that FAB will become an important weapon in the organometallic chemist's arsenal.

Minard and Geoffroy also studied a number of organometallic cluster compounds (19). It is known that as carbonyl groups of carbonyl clusters are replaced by triphenylphosphine,

diphenylphosphito and chloro groups, the volatility of the organometallic compounds decreases, and thus, EI spectra cannot be obtained. The matrix used for the FAB spectra was 18-crown-6 with 10% tetraglyme to depress the melting point. The spectra obtained contained structurally significant fragmentations; such as, stepwise loss of all carbonyls,chloro, phenyl, triphenylphosphine and other coordination groups and in almost all cases molecular ions were observed.

(b) Coordination Compounds

Cerny, Sullivan, Bursey and Meyer found that FAB fragments could be useful in predicting the solution chemistry of some neutral, 1+ and 2+ cationic transition metal coordination complexes (20). They obtained both parent ion information and fragments for the 1+ complexes. For example, the compound $[Re^{I}(bpy)(PMe_2Ph)_2(CO)_2]PF_6$ had a peak at m/z 675 which represents the quasi-molecular ion. The next peak of interest was the loss of PMe_2Ph at m/z 537. No peaks were obtained for sequential loss of CO, see Figure 3. The weaker of the two possible monodentate π-acceptor ligands, the tertiary phosphine is lost in preference to the carbonyl. It was possible for a number of generalizations to be drawn from this study. First, monodenate ligands are lost in preference to bidentate ligands. Second, if redox processes occur then the spectrum is complicated with many fragment peaks, most of these fragments being formed by

Figure 3: FAB Mass Spectrum of $[Re^{I}(bpy)(PMe_2Ph)_2(CO)_2](PF_6)$ (20).

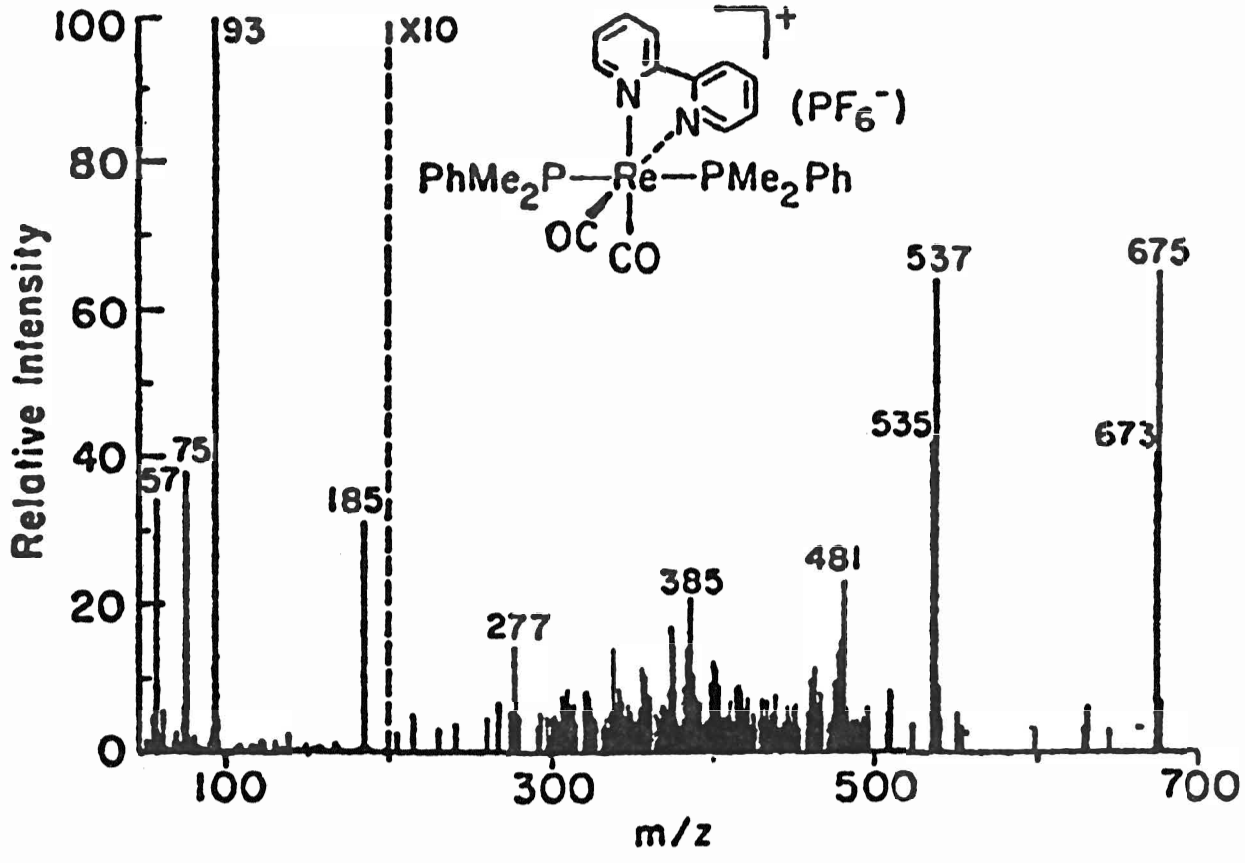

the reduction of a higher oxidation state to a lower one. In those compounds in which metal reduction was disfavored, simple ligand loss occurred. The final generalization made was that in every case where the solution chemistry of the complex was known it was paralleled by FAB fragmentation. The same group studied copper complexes which were of biological interest, and found it to be a useful characterization technique (21).

Applications of FAB-MS to biomedical compounds has received a great deal of attention. Barber's group applied both the FD and the FAB procedures to the analysis of hydroxamate containing siderophores as iron(III) complexes (22). Siderophores are low molecular weight chelating agents possessing a high affinity for iron(III) and are secreted by a wide range of micro-organisms. The FAB spectra obtained exhibited good molecular ion sensitivity, and FAB was recommended as the preliminary screening technique, as FD spectra were difficult to obtain. It was suggested that because of the high sensitivity of FAB, (good spectra were obtained of μg quantities), it offers a means for identification of siderophore metabolites.

Dell and Morris studied bleomycins which are a family of glycopeptide-derived antibiotics (23). These compounds had proved to be difficult to characterize due to their complexity, high molecular weight and thermal instability. The metal complexes of these compounds yielded pseudomolecular $(M+H)^+$ ions in the FAB spectra. The FAB-MS gave m.w. information on all bleomycins studied as both native material and as metal

complexes. It was concluded that FAB-MS could be used to characterize a wide variety of bleomycins and may be used as a method of structure elucidation for other members within the family.

Other interests have included the study of metal complexes involved in medical research. Puzo *et al.* studied the bis-guanosine adduct of the cisplatin anticancer drug (24). The results were encouraging for the use of FAB spectrometry in the charcterization of DNA adducts of platinum containing drugs. Cohen *et al.* (25) and Costello *et al.* (26,27) studied technetium compounds in a variety of oxidation states. These compounds are of interest as technetium-based radiopharmaceutical agents have become important clinical diagnostic agents. Cohen found that the best results were obtained using monothioglycerol as the matrix. FAB was discovered to be a useful technique in identification of these compounds.

Johnstone *et al.* studied crown ether complexes of metallic cations using FAB (28,29). In the past the methods for investigating these complexes were cumbersome and time-consuming usually requiring calorimetry, potentiometry and spectroscopy to determine stability constants. Johnstone obtained molecular ions of the type, $[crown+M^{n+}+A^{(n-1)-}]^{+}$ where A is the anion. The range of metallic salts included the chlorides, acetates, and nitrates of Li, Na, K, Rb, Cs, Mg, Ca, Ba, Cu, Hg, etc. All yielded molecular ions but not with equal facility. The competitive reactions showed that the order of preference for

complex formation in Group 1 is K >Cs >Na, which reflects the trends found in solution. This trend is different for each crown ether investigated. It was suggested that this method could be used to rapidly analyze trace metals as low as 10^{-10}M. Johnstone also proposed a method by which stability constants could be measured (28). The predicted stability constants closely paralleled published results.

The 18-crown-6 ligand was the topic of another FAB-MS study (30), the complex of interest being [$HgCl_2$(18-crown-6)]. The FAB-MS showed a cluster of peaks centered at m/z 501 which corresponds to the $[HgCl(18\text{-crown-6})]^+$ ion. The appearance of this ion as the highest mass peak is normal for chlorinated compounds, which normally exhibit much stronger $[M-Cl]^+$ peaks than $[M]^+$ peaks. The importance of this study stems from the fact that the mercury ion remained associated with the 18-crown-6 ligand despite the weak mercury-to-oxygen bonds. This hints that FAB-MS could have useful applications in the identification of other macrocyclic compounds not amendable to EI. It was this study which sparked the interest in the examination of the macrocyclic compounds discussed herein.

B. Area of Interest

The compounds chosen for this study were the metal complexes of the macrocyclic ligand 5,5,7,12,12,14-hexamethyl-1,4,8,11-tetraazacyclotetradecane, (see Figure 4(a)), often abbreviated

Figure 4(a): Basic Structure of $Me_6[14]aneN_4$ (31).

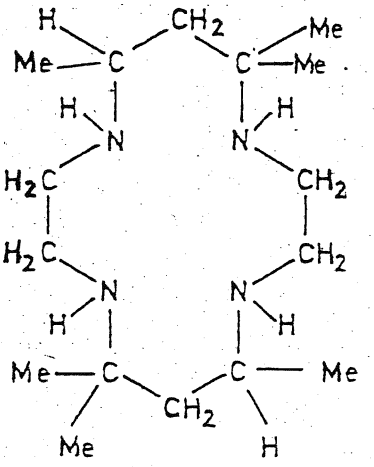

Figure 4(b): The Isomers of $Me_6[14]aneN_4$

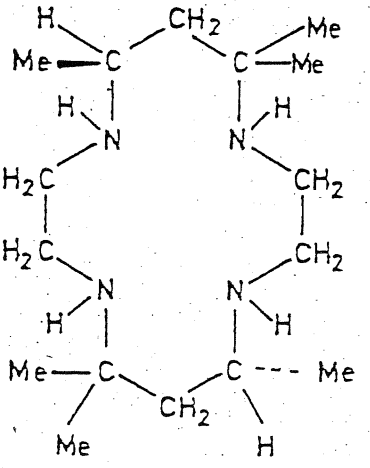

teta

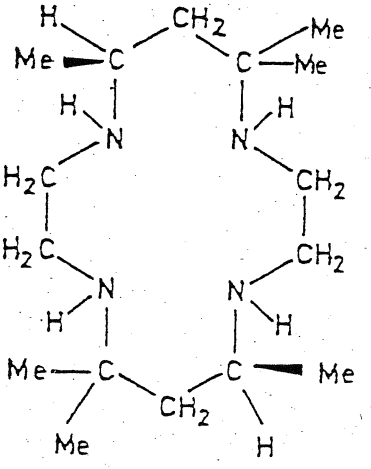

tetb

$Me_6[14]aneN_4$. The abbreviation used indicates the number of methyl substituents, the size of the ring in brackets, followed by the type and number of hetero atoms in the ring. There are two isomers of this ligand and these are illustrated in Figure 4(b). The coordination compounds of the $Me_6[14]aneN_4$ were thought to be a good choice for FAB, as FAB had previously proven itself successful with oxygen containing macrocyclic compounds (28-30).

Another reason for this choice was the fact that these complexes contained nitrogen and in general coordination complexes of nitrogen have low sample volatility (32). The use of EI to study these complexes, would therefore, require high source temperatures. Such temperatures would mean that sample decomposition was likely to be a problem. Due to this, mass spectrometry has not been used to any appreciable extent as a characterization technique for the complexes of $Me_6[14]aneN_4$. In the past, much of the work involving these compounds has involved crystalline complexes, and as a result the two main characterization techniques have been crystallography and infared spectrometry.

The main reason for the choice of these complexes was the fact that these complexes are remarkably stable, and are relatively inert to dissociation. This was an important factor as earlier work envolving the metal complexes of Vitamin-B_6 produced spectra of the metal complexed to the matrix instead of Vitamin-B_6.

The principal emphasis of this study was to determine whether FAB was a suitable technique for the identification of these compounds based on the three requirements of a good mass spectrometry technique (see section C).

II. EXPERIMENTAL

A. Instumentation

Mass spectra of all compounds were obtained using a Kratos MS-30 double beam, double focusing mass spectrometer, retrofitted with a Kratos FAB source in beam 1. A resolution of 1000 and an accelerating voltage of 4kv were used. Scan rates of 10 sec/decade and 30 sec/decade were used.

The samples were introduced by a heated solid probe for EI with an ionization voltage of 70ev. The source temperature was varied between 180-220^{0}C depending upon the decomposition point of the coordination compound.

The samples for FAB were introduced on a stainless steel probe at room temperature. The FAB ion gun (Ion Tech) was operated at a voltage of 6-8 kev and at a source pressure of 10^{-5}torr and a current of 1-2 mA. All data collection and computation were carried out on a Kratos DS-55 data system modified with Brock software. Both positive and negative FAB ion spectra were obtained, using Xe as the primary beam.

The FORTRAN program BMASROS was used to calculate isotopic patterns of specific ions. The DS-55 programs PKAVG, PLOT and QUAN were used to obtain qualitative and quantitive mass spectral data. The relative abundances of overlapping isotopic multiplets were computed by a least squares fit of the output BMASROS to the observed spectrum using the FORTRAN program BMASABD. The Bayesian Statistical method (33) was also used to provide a more

statistically valid method of deconvoluting overlapping species in the spectra.

B. General Techniques

Decomposition points were taken using an Electrothermal melting point apparatus. Infared spectra in the 4000 cm^{-1} to 400 cm^{-1} range were recorded on an Analect FX-6260 FTIR spectrometer to confirm the presence of the ligand in the complexes synthesized. The shift in the ν(N-H) peaks were used to determine if complexation had occurred, see Table 1. A decrease in the N-H absorption frequency implies a weakening of the N-H bond due to withdrawl of electron density by the metal. All samples were prepared as KBr pellets.

Elemental analysis were preformed by Galbraith Laboratories Inc., and Guelph Chemical Laboratories Ltd.

C. Chemicals

The $Me_6[14]aneN_4$ ligand was obtained from the Parish Chemical Co., and Strem Chemicals Inc. The forms in which this ligand were obtained are given in Table 2. The Parish chemical is a mixture of teta and tetb isomers and will be referred to as $Me_6[14]aneN_4$. The chemical obtained from Strem has only the teta isomer present, and will be referred to as teta. (See Figure 4.) Two different batches of the ligand were obtained from Strem, as

Table 1: ν(N-H) Infared Absorption Frequencies

Compound	ν(N-H)
teta	3274, 3240
$CdCl_2$(teta)	3270, 3233
$PtCl_4$(teta)	3212
$CuCl_2$(teta)	3223, 3143
$NiCl_2$(teta)	3235, 3185
$ZnCl(NO_2)$(teta)	3266, 3200
$ZnCl_2$(teta)	3243, 3212

Table 2: Reagents

Chemical	Formula	Supplier
$Me_6[14]aneN_4$	$C_{16}H_{36}N_4.H_2O$	Parish Chemical Co. Orem, Utah
teta	$C_{16}H_{36}N_4$	Strem Chemicals, Inc. Newbury, Massachusetts
Manganous Chloride	$MnCl_2.4H_2O$	BDH Chemicals Ltd. Poole, England
Cobaltous Chloride	$CoCl_2.6H_2O$	BDH Chemicals Ltd. Poole, England
Cadium Chloride	$CdCl_2.2\ H_2O$	J. T. Baker Chemical Co. Phillipsburg, New Jersey
Cupric Acetate	$(CH_3CO_2)_2Cu.H_2O$	BDH Chemicals Ltd. Poole, England
Sodium Nitrite	$NaNO_2$	McArthur Chemical Co. Ltd. Montreal, Canada
Sodium Cyanide	NaCN	Matheson Coleman & Bell Manufactoring Chemists Norwood, Ohio
Silver Nitrate	$AgNO_3$	McArthur Chemical Co. Ltd. Montreal, Canada
Zinc Chloride	$ZnCl_2$	Fisher Scientific Co. FairLawn, New Jersey
Nickel Chloride	$NiCl_2.6H_2O$	BDH Chemicals Ltd. Poole, England
Sodium Azide	NaN_3	Fisher Scientific Co. FairLawn, New Jersey
Sodium Thiocyanate	NaSCN	Fisher Scientific Co. FairLawn, New Jersey
Cupric Chloride	$CuCl_3.2H_2O$	BDH Chemicals Ltd. Poole, England
Zinc Nitrate	$Zn(NO_3)_2$	Fisher Scientific Co. FairLawn, New Jersey
Potassium Tetra-chloroplatinate (II)	K_2PtCl_4	Alfa Products Danvers, Massachusetts

the first batch, lot# 158K, was found to be contaminated with chloride. The Parish reagent had been used in previous synthesis work done by M. R. Burke (34). The remaining reagents used in the synthesis are also listed in Table 2.

D. Synthesis

The list of compounds synthesized and their molecular weights and decomposition points are provided in Table 3. The starred complexes were synthesized using the Parish ligand lot# 1065, and therefore are a mixture of teta and tetb isomers. See figure 4 for an explanation of the abbreviations used for the ligand. The $(HgCl_2)_2$(tetb) was previously prepared by M. R. Burke and provided in crystal form (35). An elemental analysis was obtained to ensure that the mercury complex was the desired compound. Data from the elemental analysis is provided in Table 4.

1) Cobalt Complexes

The cobalt complex Co_2Cl_4(teta) was prepared according to the basic procedure of Endicott *et al.* (36). The remaining cobalt complexes were synthesized in accordance with the preparations of Whimp and Curtis (37) found in the literature.

Table 3: $Me_6[14]aneN_4$ Complexes

Complex	m.w.	d.p. (^0C)
$[Co(C_{16}H_{36}N_4)(NO_3)(OH)]ClO_4,H_2O$	524	160
$Co_2Cl_4(C_{16}H_{36}N_4)$	544	280
$[Co(C_{16}H_{36}N_4)(NO_2)_2]ClO_4,1/2H_2O$	544	190
$[Co(C_{16}H_{36}N_4)ClN_3]ClO_4,H_2O$	538	130
$[Co(C_{16}H_{36}N_4)Cl_2]Cl,4H_2O$	522	215
$[Co(C_{16}H_{36}N_4)(CN)_2]ClO_4,H_2O$	513	250
$[Co(C_{16}H_{36}N_4)(SCN)_2]SCN,H_2O$	535	140
*$[Co(C_{16}H_{36}N_4)Cl_2]ClO_4$	514	210
$[Mn(C_{16}H_{36}N_4)Cl_2]Cl,3H_2O$	500	115
$[Ni(C_{16}H_{36}N_4)]Cl_2,2H_2O$	450	>300
*$[Cu(C_{16}H_{36}N_4)](ClO_4)$	547	>300
$[Ag(C_{16}H_{36}N_4)](NO_3)_2$	516	220
*$Cd(C_{16}H_{36}N_4)Cl_2$	467	280
$(HgCl_2)_2(C_{16}H_{36}N_4)$	828	249
$Cu(C_{16}H_{36}N_4)Cl_2,H_2O$	436	220
$Zn(C_{16}H_{36}N_4)Cl_2,H_2O$	437	290
$(PtCl_4)[H_2C_{16}H_{36}N_4]$	621	>300
$Zn(C_{16}H_{36}N_4)ClNO_2,H_2O$	449	260

* Complexes synthesized with $Me_6[14]aneN_4$

2) Cadmium Complex

The complex of $CdCl_2 2.5H_2O$ and $Me_6[14]aneN_4$ was prepared by dissolving 0.40g of $CdCl_2 2.5H_2O$ in 10 ml of warm distilled water and allowing it to cool. The $Me_6[14]aneN_4$ was dissolved in 10 ml of 1-butanol and cooled. The ligand solution was then layered on top of the cadium solution in a separatory funnel and was allowed to stand for 48 hrs. A large quantity of precipitate formed at the interface. A small amount of precipitate had formed in the aqueous layer and this was drawn off. The precipitate from the interface was filtered and washed with 10 ml of cold 1-butanol and allowed to air dry. The results of the elemental analysis of this compound are provided in Table 4. Both the infared spectrum and the mass spectrum showed the compound to be unique, and not merely a mixture of starting materials.

3) $ZnCl_2$(teta)

The zinc complex was prepared by dissolving 0.14g of $ZnCl_2$ in 5 ml of ethanol, and 0.23g of the teta ligand in another 5 ml of ethanol. Both solutions were filtered and then combined. The resulting solution clouded and a white precipitate formed. The product was recrystallized using ethanol as the solvent. The results of the elemental analysis for this compound are provided in Table 4. The mass spectrum confirmed that the compound was that which was proposed. The infared spectrum showed the

Table 4: Analytical Data for Complexes of $Me_6[14]aneN_4$

Formula		Metal	C	H	N
$Hg_2Cl_4(C_{16}H_{36}N_4)$	%Found	48.07	23.43	4.50	----
	%Calculated	48.48	23.22	4.38	----
$CdCl_2(C_{16}H_{36}N_4)$	%Found	25.21	38.04	7.09	----
	%Calculated	24.03	41.09	7.76	----
$PtCl_4(C_{16}H_{38}N_4)$	%Found	----	30.70	6.07	8.93
	%Calculated	----	30.85	6.10	8.99
$ZnCl(NO_2)(C_{16}H_{36}N_4),H_2O$	%Found	----	40.61	7.78	16.23
	%Calculated	----	42.76	8.46	15.59
$ZnCl_2(C_{16}H_{36}N_4),H_2O$	%Found	----	43.16	8.41	12.45
	%Calculated	----	43.79	8.65	12.76
$NiCl_2(C_{16}H_{36}N_4),2H_2O$	%Found	----	40.99	8.51	11.91
	%Calculated	----	42.67	8.88	12.44
$CuCl_2(C_{16}H_{36}N_4),H_2O$	%Found	----	44.13	8.68	13.18
	%Calculated	----	43.93	8.23	12.82

compound to be unique.

4) $NiCl_2$(teta)

The $NiCl_2$(teta) complex has been previously prepared by Tasuko Ito and Koshiro Toriumi (38). The method used in this work was not that published. The synthesis used was similar to that used for the zinc complex, in that both the teta and $NiCl_2.6H_2O$ were dissolved in hot 1:1 ethanol/water and combined. The characteristic orange crystals of the low-spin [Ni(teta)]Cl_2 complex were obtained. The product was observed to turn mauve at approximately 160-165^{0}C which represents a conversion of this product to the high-spin Ni-complex as stated by Ito (38). The composition of this complex, as illustrated through elemental analysis, is provided in Table 4. The infared spectrum had the expected sharp band near 3200 cm^{-1} due to the N-H vibration (39).

5) $CuCl_2$(teta)

The copper(II) chloride teta complex was prepared by dissolving 0.43g of teta in 10 ml of absolute ethanol. The $CuCl_2.2H_2O$ was dissolved in 5 ml of abs. ethanol and added to the teta solution. The combined solution was heated for 15min, and filtered. After 24 hrs a blue ppt formed and was filtered and recrystallized from hot ethanol. The results from the elemental

analysis are presented in Table 4. Both the mass spectrum and the infared spectrum showed this compound to be unique.

6) $(PtCl_4)[H_2(teta)]$

The complex was prepared by dissolving 0.23g of the teta in 10ml of DMF. The solution was then heated slightly and filtered. Approximately 0.28g of K_2PtCl_4 was dissolved in 15ml of DMF, this solution was heated and then filtered. The warm solutions were combined and allowed to cool to room temperature. The pink precipitate which formed was washed with cold DMF and dried under vacuum. The results from the elemental analysis agree well with the prosed formula, however, no satisfactory mass spectral data has been obtained for this complex. The infared spectrum confirmed that this was a new compound, and not merely a mixture of starting materials. The spectra for the uncomplexed ligand, teta and the platinum complex are given in Figure 5.

7) $ZnCl(NO_2)(teta)$

This complex was prepared by dissolving 0.14g of $Zn(NO_3)_2 6H_2O$ in 2ml of methanol and adding this solution drop by drop, to a solution of 0.14g of teta, Strem lot# 158K, dissolved in 5ml of methanol. Upon addition the solution remained clear but a white precipitate formed overnight. The precipitate was collected and washed with a small amount of 1-butanol.

Figure 5: Infared Spectra of $(PtCl_4)[H_2(teta)]$ and Teta

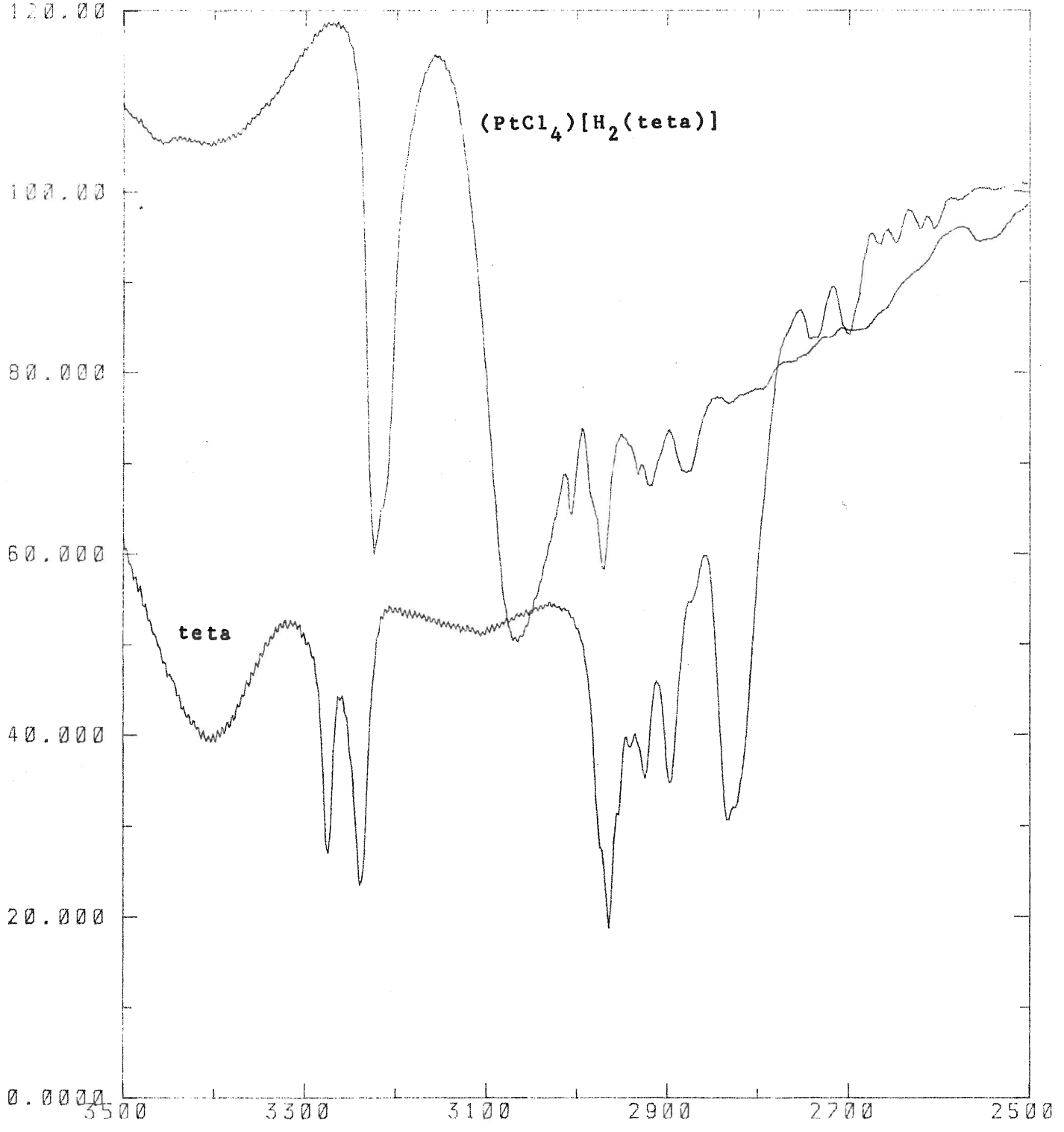

Note: The $(PtCl_4)[H_2(teta)]$ spectrum is displaced 4 cm vertically

It was originally believed that the compound was $Zn(NO_3)_2$(teta). However, elemental analysis of this compound disproved this formulation. The mass spectral analysis clearly showed the presence of chloride. The infared spectrum showed this compound to be unique.

The remaining metal complexes, (Ag,Mn and Cu) were prepared from standard preparations (40-42).

E. FAB-MS Sample Preparation

The FAB samples were prepared by adding approximately 0.1g of the complex to 0.05 ml of the matrix liquid. A variety of matrices were used in an attempt to produce suitable spectra. A listing of the matrices utilized can be found in Table 5.

The complexes proved to be relatively insoluble in most of the matrix liquids. To increase the amount dissolved and thus, improve the quality of spectra, samples were left in the matrix for 12-24 hrs, which greatly improved the quality of the spectra obtained. Heating the sample slightly also improved the results obtained.

Obtaining mass spectra for a number of the cobalt complexes proved to be rather difficult and to improve the spectra a doping technique was employed. This method consisted of dissolving approximatedly 0.1g of the sample in a glycerol matrix and then further adding 0.05 ml of a 0.1M anion solution. NH_4Cl was used to provide the doping anions in the majority of the cobalt

Table 5: Matrices

2-nitro-phehyloctylether (NPOE)
di-tert-amylphenol (DAP)
nujol
glycerol
thioglycerol
30% glycerol in sulfolane
sulfolane
Dithiothreitol/dithioerythritol 5:1
polyethylene glycol (PEG)
glycerol/DMF 1:1
glycerol/H_2O 1:1
Diethylforamide
18-crown-6 with 10% tetraglyme

compounds with some success. However, the chloride anion did not produce useful results for cobalt compounds that contained nitrite. 0.1M $NaNO_2$ was used as the doping agent for the NO_2^- anion containing compounds.

The method of sample preparation proposed by Zhang and Liang (43), was used on a number of the more intractible complexes. This method consists of dissolving the sample in a suitable solvent and transferring 2µl of this solution to the surface of the liquid matrix on the probe tip using a microsyringe. The probe is then inserted into the vacuum lock, where the solvent is evaporated, then after 1-2 minutes the probe is inserted into the ioniztion chamber.

F. Spectra Reproducibility and Stability

The reproducibility of spectra was checked using the $[Co(teta)Cl_2]ClO_4$ complex. Two samples were prepared with approximately the same w/w sample to glycerol ratio. Sample A was prepared with a sample:glycerol ratio of 1:123. Sample B had a 1:143 ratio. Both samples were heated at a low temperature until all the complex had dissolved. The samples were then cooled to room temperature and left in solution for a few days. Twenty scans were collected for sample A and twenty-five scans were collected for sample B. The data collection was done on the same day for both samples with sample B being run directly after sample A.

A linear regression was performed on each peak of interest

using a TI programmable 58C calculator. The mean and standard deviation of the TIC and the absolute intensity of each peak were calculated over the 20 scans of each sample. The correlation coefficient of the absolute peak intensity versus the TIC were also calculated. The results are presented in Table 6 and will be discussed in Chapter III.

Table 6: Statistical Data for Reproducibility Runs

Sample	Peak	Absolute Intensity	r_{pc} (relation of absolute peak intensity to TIC)	%TIC
85RP1	285	$1.56(11)\times10^{4}$	0.30	0.35(03)
	341	$1.61(12)\times10^{5}$	0.89	3.59(30)
	378	$4.56(11)\times10^{5}$	-0.21	10.16(48)
	413	$4.17(27)\times10^{4}$	0.69	0.93(07)
TIC		$4.49(18)\times10^{6}$		
85RP2	285	$2.52(41)\times10^{4}$	0.96	0.35(07)
	341	$2.50(30)\times10^{5}$	0.98	3.51(58)
	378	$6.09(46)\times10^{5}$	0.92	8.5(1.2)
	413	$9.56(46)\times10^{4}$	-0.59	1.34(17)
TIC		$7.13(82)\times10^{6}$		

III. Results and Discussion

A. Electron Impact Ionization

In the past, mass spectral studies of the Me_6[14]aneN_4 ligand and its complexes have been concerned with m.w. determination only (44,45). The mass spectrum of the teta or tetb show the parent ion peak at m/z 284, with a peak at m/z 269 corresponding to the loss of one methyl group (44), none of the other fragments in the spectrum being identified.

The EI and FAB mass spectra of the Me_6[14]aneN_4 are given in Figure 6. The two spectra of the ligand are very similar; however, the electron-impact spectrum is not as clean as the FAB spectrum, nor is the intensity of the parent ion as high. The parent ion intensity is 1.9% of the total ion current in the electron impact spectrum. The pseudomolecular ion $(M+H)^+$ at m/z 285 is 21.0% of the TIC in the FAB spectrum and represents the highest peak in the spectrum. The TIC is 355,136 counts for the electron impact spectrum compared to 3,345,408 counts for FAB. Although, the ligand is well behaved in EI, precautions in interpretation of the spectra of the metal complexes are necessary as thermal decomposition of the sample is a possiblity (32).

Application of electron impact mass spectroscopy to these complexes proved to be difficult. Spectra could not be obtained for the following complexes: Co_2Cl_4(teta), [Co(teta)$(CN)_2$]ClO_4,

Figure 6: FAB and EI Spectra of $Me_6[14]aneN_4$

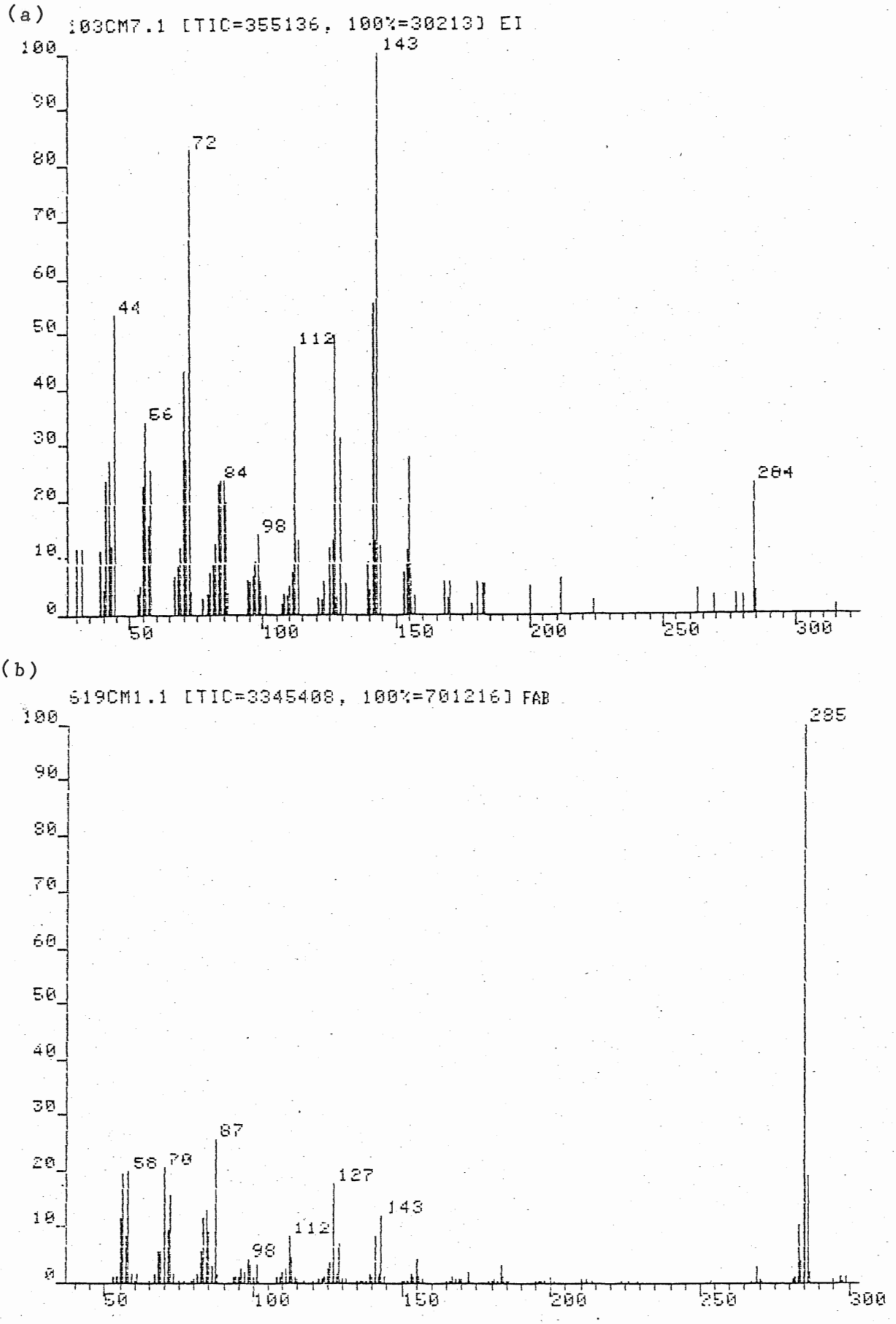

$[Co(teta)Cl_2]Cl$, $[Co(teta)(SCN)_2]SCN$, $Cu(teta)Cl_2$, $Zn(teta)Cl_2$, $(PtCl_4)[H_2(teta)]$ and $[Zn(teta)ClNO_2]$ as these complexes decomposed rapidly under EI conditions. The first and second scans collected contained approximately fifteen hundred peaks, after which the ion current decayed to the point where sample peaks were not observed. The total ion current (TIC) for EI spectra was a factor ten times less than the spectra obtained by FAB (after background subtraction). The inability to obtain spectra using electron impact is believed to result from the involatility and thermal lability of these compounds. This belief is reinforced by Busch's work on iron complexes of the $Me_6[14]aneN_4$ ligand. The mass spectra obtained had only low m/z values due to the decomposition of the complex (45).

Although spectra were obtained for a number of the complexes studied, molecular ions were not observed. The spectra contained peaks due only to the decomposition of the complex. The EI spectra of the dinitro and dichloro cobalt complexes had in common peaks at m/z 333, 315, 301 and 287; as well as peaks due to the decomposition of the $Me_6[14]aneN_4$ ligand. The loss of 14 mass units 315-301 and 301-287 appears to be the predominant decomposition pathway. Figure 7 is representative of the spectra obtained for the cobalt compounds. It should be noted that the cobalt complexes of $[Co(teta)ClN_3]ClO_4$ and $[Co(teta)(OH)(NO_2)]ClO_4$ also gave similar spectra, however, the peaks obtained were below 2000 counts and were not considered statistically valid. The Ag, Mn and Cd compounds had peaks due only to the decomposition of

Figure 7: The EI Spectrum of $[Co(Me_6[14]aneN_4)Cl_2]ClO_4$

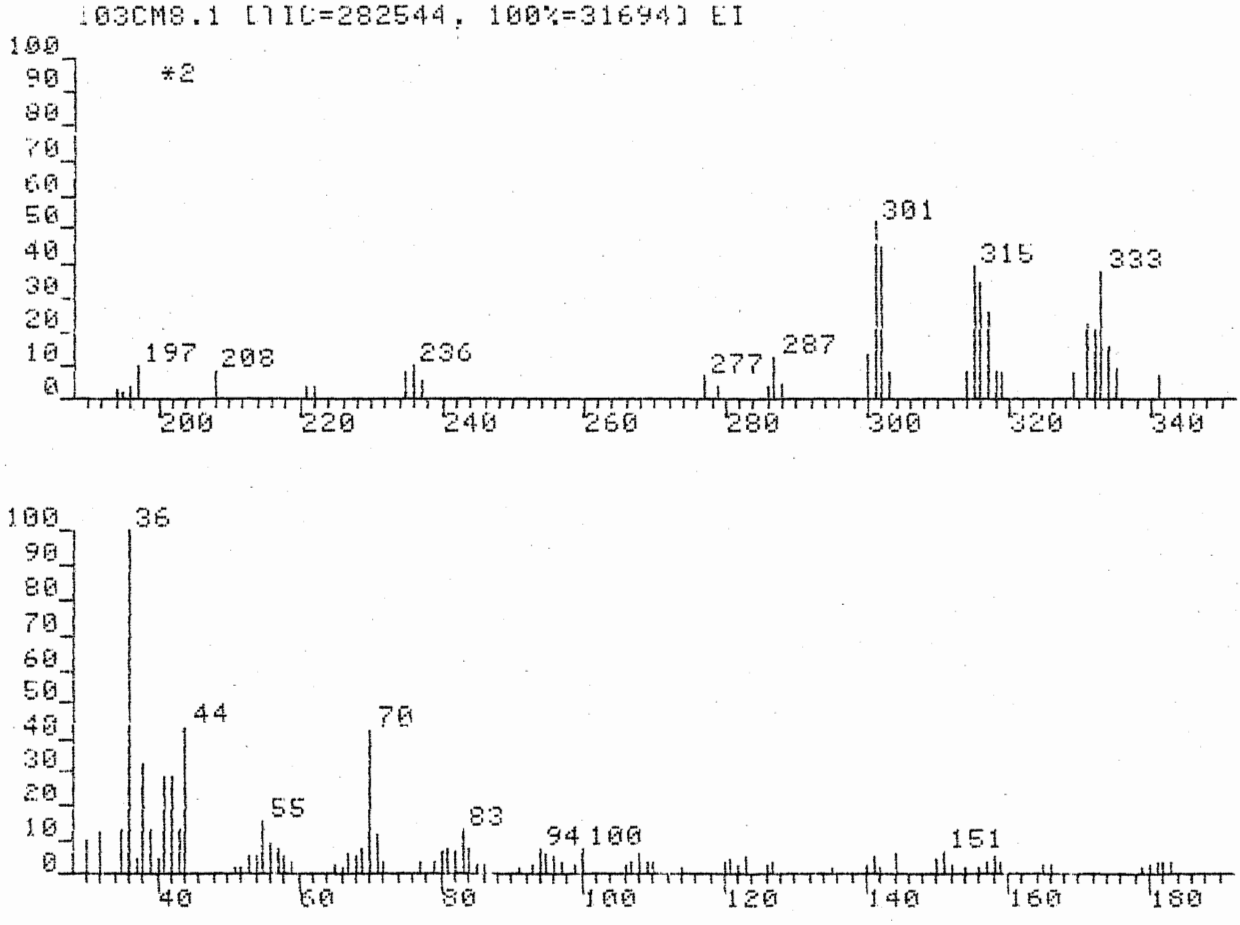

the ligand, teta. The mercury complex had peaks corresponding to Hg^+ and $HgCl_2^+$, as well as ligand decomposition peaks. The $Cu(teta)(ClO_4)_2$ spectrum had peaks due to the presence of $[Cu(teta)]^+$ and $[Cu(teta)ClO_4]^+$, however, these peaks were of extremly low intensity. The $Ni(teta)Cl_2$ complex showed a peak due to $[Ni(teta)]^+$. The isotope pattern for the nickel species was not correct, as the smaller peaks in the isotope pattern were below the detection limits of the instrument. The major peaks in the spectra of the Ni, and Hg complexes are given in Table 7. The fragmentation pattern of the nickel complex is similar to the cobalt complexes, as it has the same peaks present in the 300-350 range as the cobalt complexes, refer to Figure 7. Note also that the fragmentation products from the ligand are easily observed in all the EI spectra of the complexes as well as the ligand itself.

B. Negative Ion FAB

Negative ion FAB was attempted for about one third of the complexes. The results were rather unproductive in terms of providing molecular ions or fragment ions containing the ligand. The complexes for which negative ion FAB results were obtained were $Co(teta)(CoCl_4)$, $[CoCl_2(teta)]ClO_4$, $[Cu(teta)](ClO_4)_2$ and $[CdCl_2(teta)]$. The major fragments obtained for these complexes are presented in Table 8. Results could not be obtained either for the $(HgCl_2)_2(tetb)$ or the $[Ni(teta)Cl_2]$ complexes.

In the $[CoCl_2(teta)]ClO_4$ spectrum, the base peak was the

Table 7: Major Peaks in the EI Spectra of the Ni and Hg Complexes of $Me_6[14]aneN_4$

(a) $(HgCl_2)_2(tetb)$			(b) $NiCl_2(teta)$		
Fragment	m/z	(%TIC)	Fragment	m/z	(%TIC)
$^*HgCl_2^+$	272	(1.0)	$Ni(teta)^+$	342	(0.6)
$^*Hg^+$	202	(8.7)		332	(1.4)
				315	(1.3)
				300	(1.0)
	155	(0.9)			
fragmentation	143	(3.3)	fragmentation	143	(3.0)
due to the	127	(2.5)	due to the	127	(1.5)
ligand	112	(2.7)	ligand	112	(2.1)
	84	(1.6)		82	(2.0)
	72	(7.2)		72	(5.8)
	56	(3.5)		56	(2.6)
	44	(5.6)		44	(3.7)

* Sum of all isotopic contributions

Table 8: Major Peaks in the FAB Negative Ion Spectra of the $Me_6[14]aneN_4$ Complexes

Compound											
$(Co(teta)(CoCl_4)$			$[Co(teta)Cl_2]ClO_4$			$[Cu(teta)](ClO_4)_2$			$CdCl_2(teta)$		
Fragment	m/z	%(TIC)	Fragment	m/z	%(TIC)	Fragment	m/z	%(TIC)	Fragment	m/z	%(TIC)
Cl^-	35	(68.5)	Cl^-	35	(30.5)	Cl^-	35	(24.1)	$CdCl_2^-$	184	(18.8)
$CoCl_2^-$	129	(4.6)	ClO_4^-	99	(50.1)	ClO_4^-	99	(44.5)	$CdCl_3^-$	219	(45.2)
$CoCl_3^-$	164	(5.2)				$Cu(ClO_4)Cl^-$	199	(2.1)			
						$Cu(ClO_4)(ClO_3)^-$	247	(0.9)			
						$Cu(ClO_4)_2^-$	263	(4.9)			

perchlorate ion, followed in intensity by the peak due to the chloride ion with the remaining peaks of low intensity. The most intense peak in the [Co(teta)($CoCl_4$)] complex corresponded to the chloride ion, with other peaks due to $CoCl_2^-$ and $CoCl_3^-$ ions.

The [Cu(teta)](ClO_4)$_2$ spectrum was remarkably similar to the [Co(teta)Cl_2]ClO_4 in that the anion with the greatest intensity was the perchlorate. The second most intense peak was due to the chloride ion, most likely resulting from the perchlorate species. A reasonably intense cluster of peaks was obtained around mass m/z 263, which corresponded in isotope pattern to $Cu(ClO_4)_2^-$. A peak was observed 16 mass units below the $Cu(ClO_4)_2^-$ which corresponded to $Cu(ClO_4)(ClO_3)^-$. A peak was also observed at m/z 199 which was identified as $CuCl(ClO_4)^-$. The fact that peaks were observed at m/z 247 and m/z 199, loss of 16 from the peak at 263 and 199 loss of 64, indicates that the perchlorate ion does decompose under FAB conditions to produce chloride ion. This is consistent with the reducing nature of the matrix under FAB conditions.

The $CdCl_2$(teta) spectrum had peaks corresponding to Cl^-, $CdCl_2^-$ and $CdCl_3^-$. The isotope patterns matched well for the cadium containg fragments. Figure 8 compares the observed isotope pattern to the BMASROS calculated cluster for $CdCl_2^-$ and $CdCl_3^-$.

The loss of the counter ion, ClO_4^- in the [Co(teta)Cl_2]ClO_4 spectrum was expected in terms of what has been found by other workers (14,16,25). This work was concerned mainly with the

Figure 8: A Comparison of the Observed and Calculated Isotope Patterns for the $CdCl_2^-$ and $CdCl_3^-$ Species.

(a) Observed Isotope Patterns

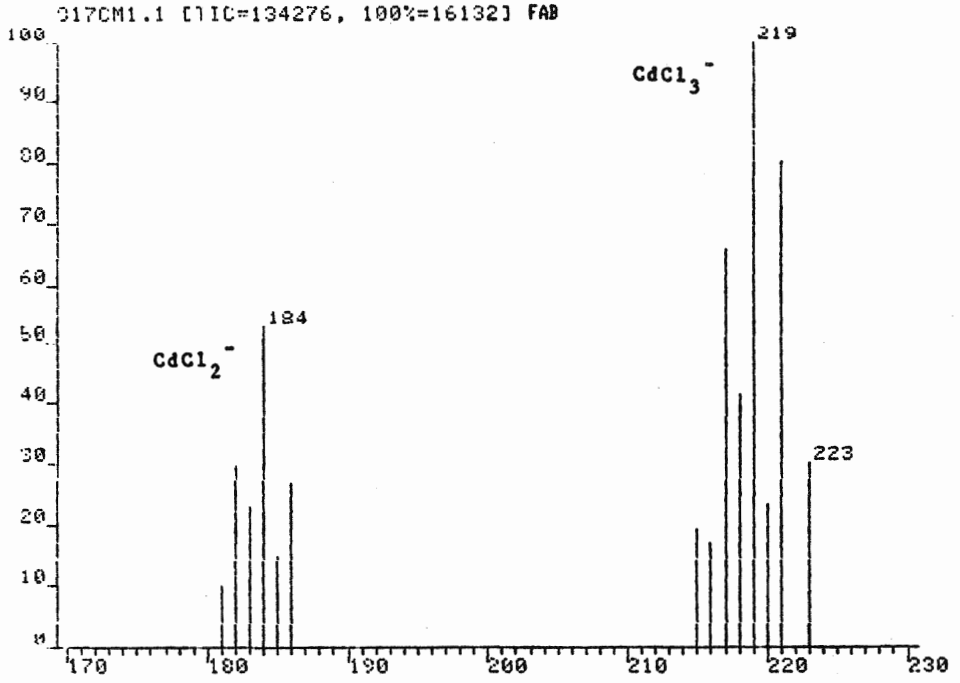

(b) Calculated Isotope Patterns

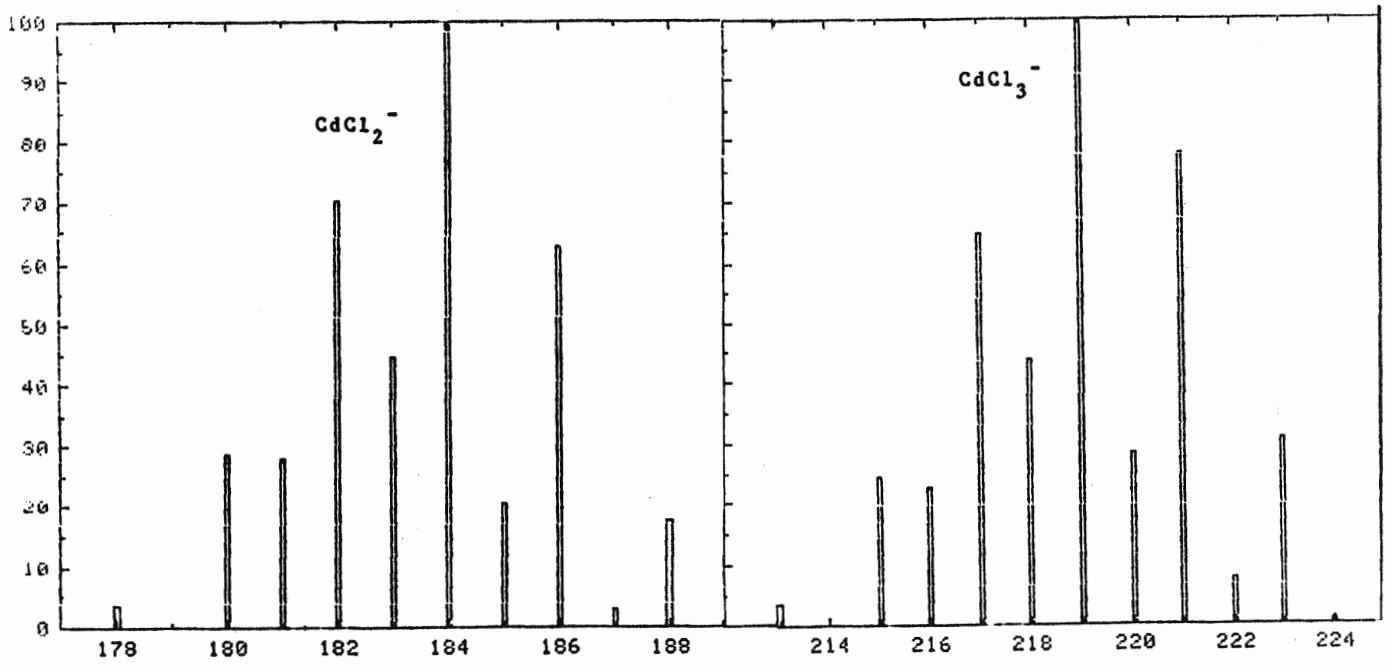

hexafluorophosphate anion, although the chloride and the perchlorate anions had been used in a study by Cohen (25). As with our present work, Cohen found that negative ions of any significance were not observed.

C. Positive Ion FAB Mass Spectra

1) Reproducibility of Spectra

The check on reproducibility of spectra was preformed to ensure that the data obtained were as precise as possible. Figure 9 presents the spectra from the two successive sample trials of the complex $[Co(teta)Cl_2]ClO_4$. The spectrum 85RP1 represents the 1:123 sample:glycerol ratio and 85RP2 represents the 1:143 ratio. (Refer to section F in chapter II.) The spectra obtained for these trials are very similar with the expected peaks at m/z 285, 343, 378 and 413. These peaks correspond to the $(teta+H)^+$, $Co(teta)^+$, $Co(teta)Cl^+$ and $Co(teta)Cl_2^+$ species respectively. In both spectra, over 50% of the ion current is carried by the teta containing species. Particular attention should be paid to the Co(teta) region of the spectra in Figure 9. Note that the cluster of peaks associated with successive loss of hydrogen are identical for both spectra; this implies that the losses are inherent in the matrix-compound solution and the FAB requirement and are not an artifact of the instrument.

Table 6 lists the percent TIC for the peaks of interest in

Figure 9: The Spectra of the Reproducibility Trials.

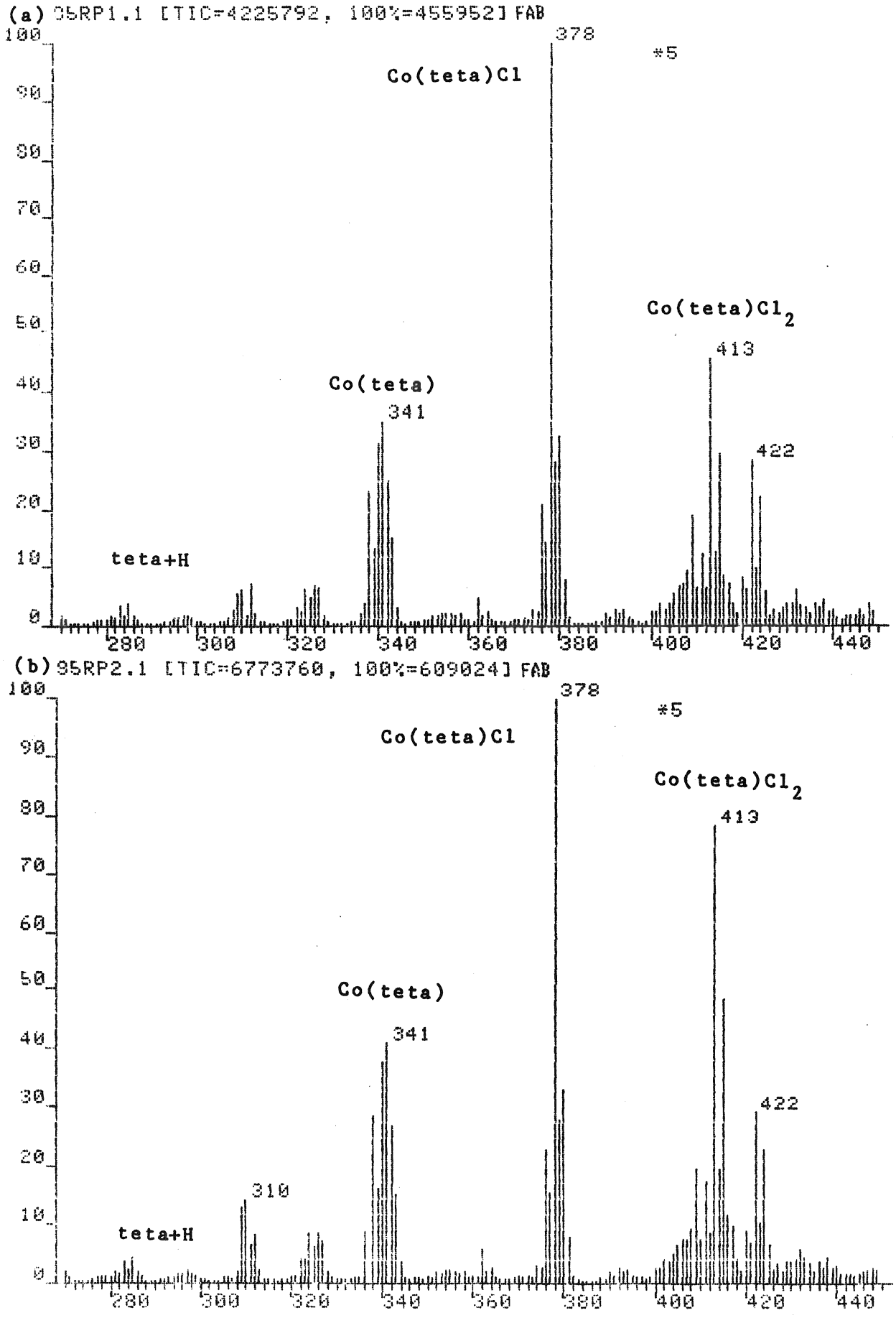

the spectra 85RP1 and 85RP2. The peaks m/z 285, 341, 378, and 413 were chosen as they represent the largest peaks of importance to the complex being studied. (The peak at m/z 341 has been identified as the species Co(teta)-2H) Observation of the %TIC for both spectra illustrates clearly the excellent reproducibility of the spectra. (The %TIC is calculated by dividing the absolute intensity of each peak by the total ion current.) The intensity of the peaks at m/z 285, 341, and 378 in the 85RP1 spectrum are well within the standard deviations calculated for their analogues in the 85RP2 spectrum. The peak at m/z 413 in the 85RP1 spectrum, however is not within the standard deviations associated with this peak in 85RP2.

The peak at m/z 413 must be interacting with the matrix as the statistical results obtained for this peak do not agree in the two spectra. It has been previously observed that the glycerol spectrum changes drastically as the length of irradation with the fast atom beam is prolonged (46). It was discovered that new ions formed in the course of the fast atom bombardment which were not present in the first scans. The intensity of these ions grow as the bombardment is prolonged and the intensity of the $(glycerol+H)^+$ at m/z 93 falls in intensity (46). A check on the intensity of the peak at m/z 93 in the spectra of 85RP1 and 85RP2 showed the peak to drop as predicted, this is illustrated in Figure 10. Thus it is probable that the peak at m/z 413 contains a component that is increasing with the increasing radiation damage of the matrix. To obtain better

Figure 10: Cross Scan Reports for the Sample Trials 85RP1 and 85RP2, Showing the Decrease of the $(glycerol+H)^+$ Species with Increasing Scan Number.

(a) DS-55 CROSS SCAN REPORT, RUN: 850371

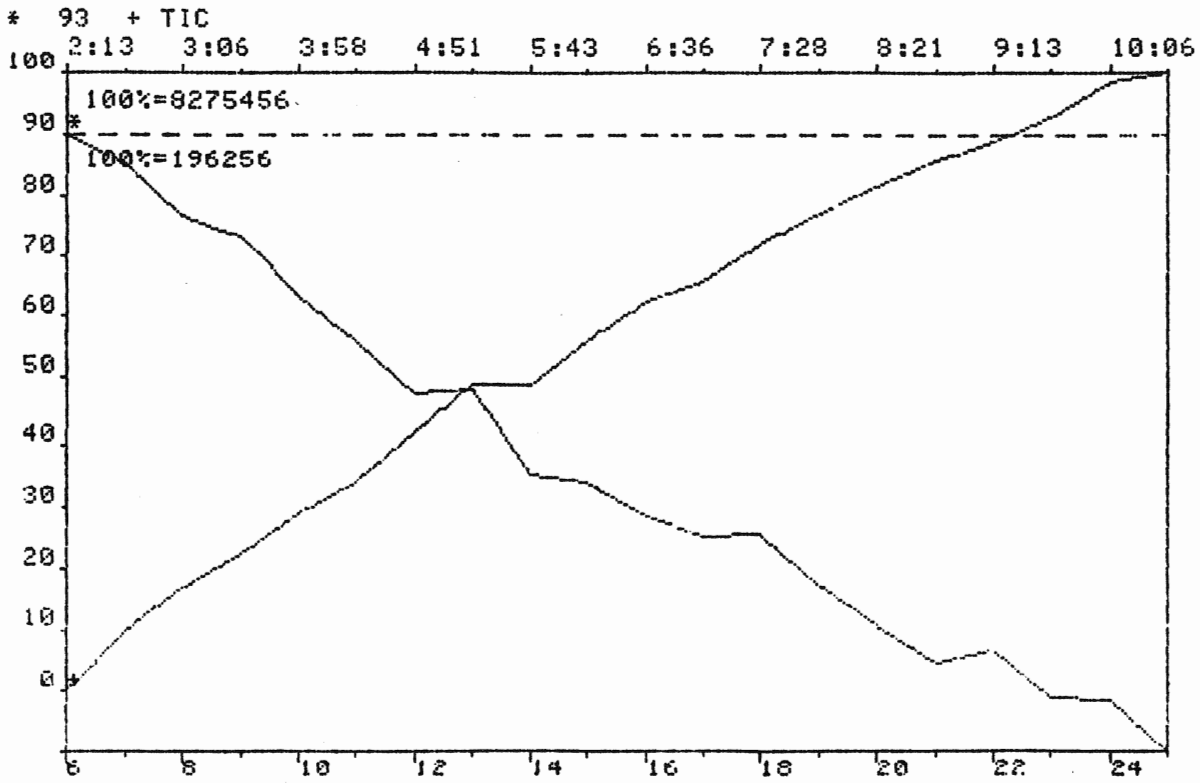

(b) DS-55 CROSS SCAN REPORT, RUN: 850370

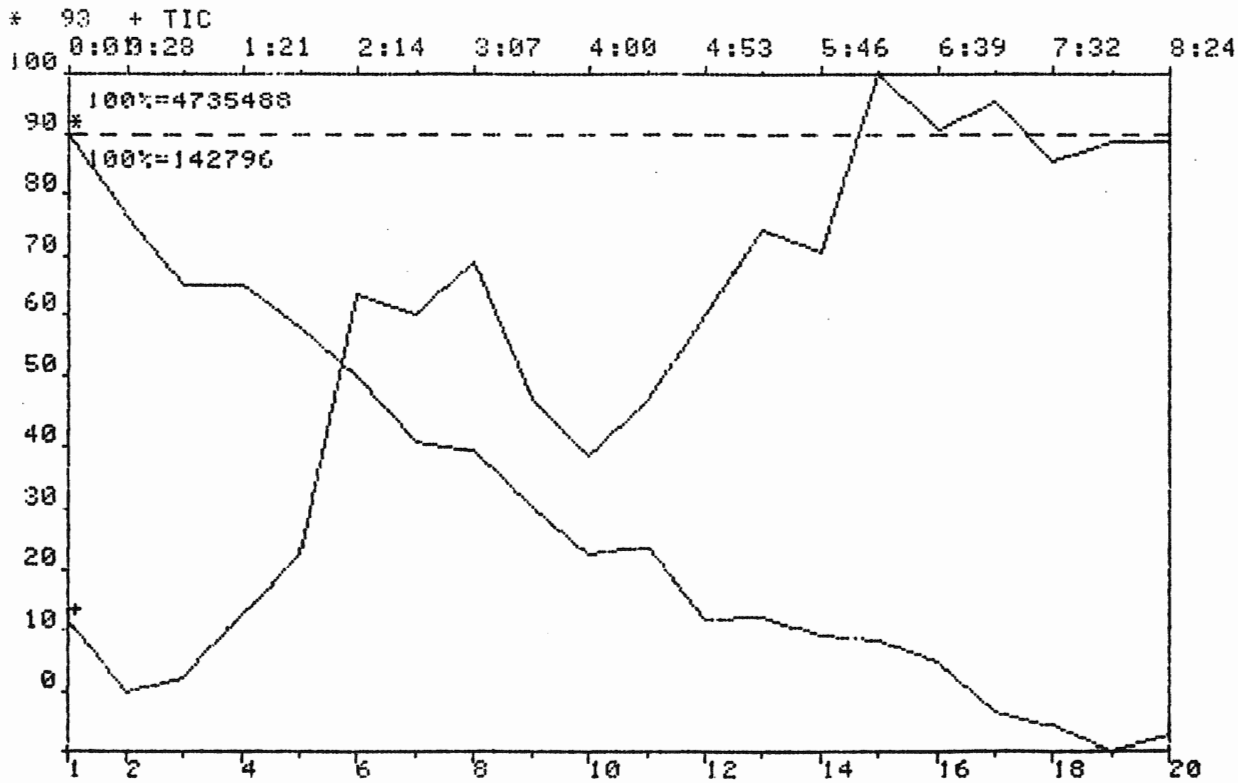

850370 = 85RP1

850371 = 85RP2

statistics for the peak at m/z 413 it would be necessary to decrease the length of time of bombardment so that the species which forms as a result of sputtering damage does not have time to build in intensity.

2) Stability of Spectra

Stability by definition is a continuance without change, a reliable steadiness (47). To determine the stability of the Me_6[14]aneN_4 complexes under FAB conditions, correlation coefficients were calculated for the absolute peak intensities as a function of the total ion current (TIC) for two sample runs of the complex [Co(teta)Cl_2]ClO_4. Table 6 lists the peaks and their corresponding correlation coeffients.

The data from the 85RP1 sample suggests that the complex is unstable. The correlation coefficients are poor for both the m/z 285 and 378 peaks. The m/z 341 peak has a good value associated with its correlation coeffient of 0.89. The peak at m/z 413 has a correlation coefficient of 0.69, but this by no means represents linearity.

The 85RP2 sample has much improved correlation coefficients associated with its data. The peaks m/z 285, 341, and 378 all represent good linear fits. Again m/z 413 does not represent a reasonable fit, this is to be expected if the peak has an interference due to the decomposition of the matrix, glycerol. The improved linearity of spectrum 85RP2 results from the fact

that 85RP2 was run after spectrum 85RP1 and as a result, the instrument had more time to stabilize. In fact spectrum 85RP1 was the first sample run on that particular day, and therefore, it is not representative of the stability of the spectra. It is thus concluded that the complex $[Co(Me_6aneN_4]ClO_4$ is stable under FAB conditions, providing the instrument itself has had time to stabilize. Spectrum 85RP2 is representative of the stability possible in the dichloro complex and the $Me_6[14]aneN_4$ complexes in general.

3) Studies on the Cobalt(III) Complexes of $Me_6[14]aneN_4$

The reaction scheme for the synthesis of the cobalt complexes is given in Figure 11. Figures 12-19 illustrate the positive ion FAB spectra of the cobalt compounds of interest. The matrix used for all the spectra illustrated was monothioglycerol. The TIC as mentioned earlier is much better in FAB than in electrom impact even after subtraction of the matrix. Initially glycerol was the matrix employed, but the spectra obtained using this matrix were not very intense. (The spectra obtained using glycerol as the matrix may be found in the appendix I.) The use of monothioglycerol as the matrix improved the intensity of the spectra. The principle positive ions result from the liberation of the cation $[C^+]$, the subsequent loss of the anion ligands followed by Co(III) loss, and the formation of ions originating from the teta ligand.

Figure 11: The Reaction Scheme for the Preparation of the Cobalt Compounds

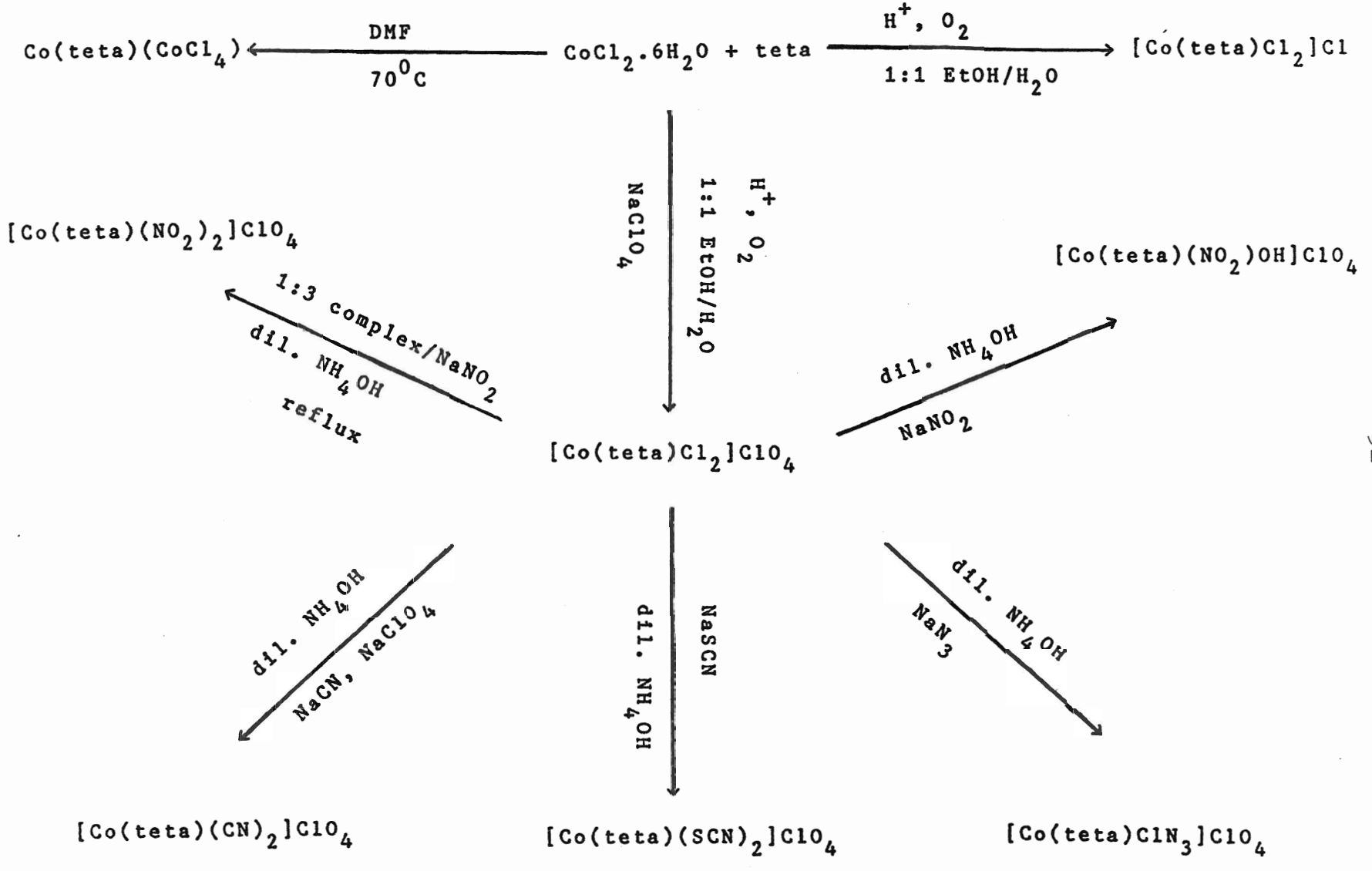

Figure 12: The Positive Ion FAB Mass Spectrum of $[Co(Me_6[14]aneN_4)Cl_2]ClO_4$ in Thioglycerol

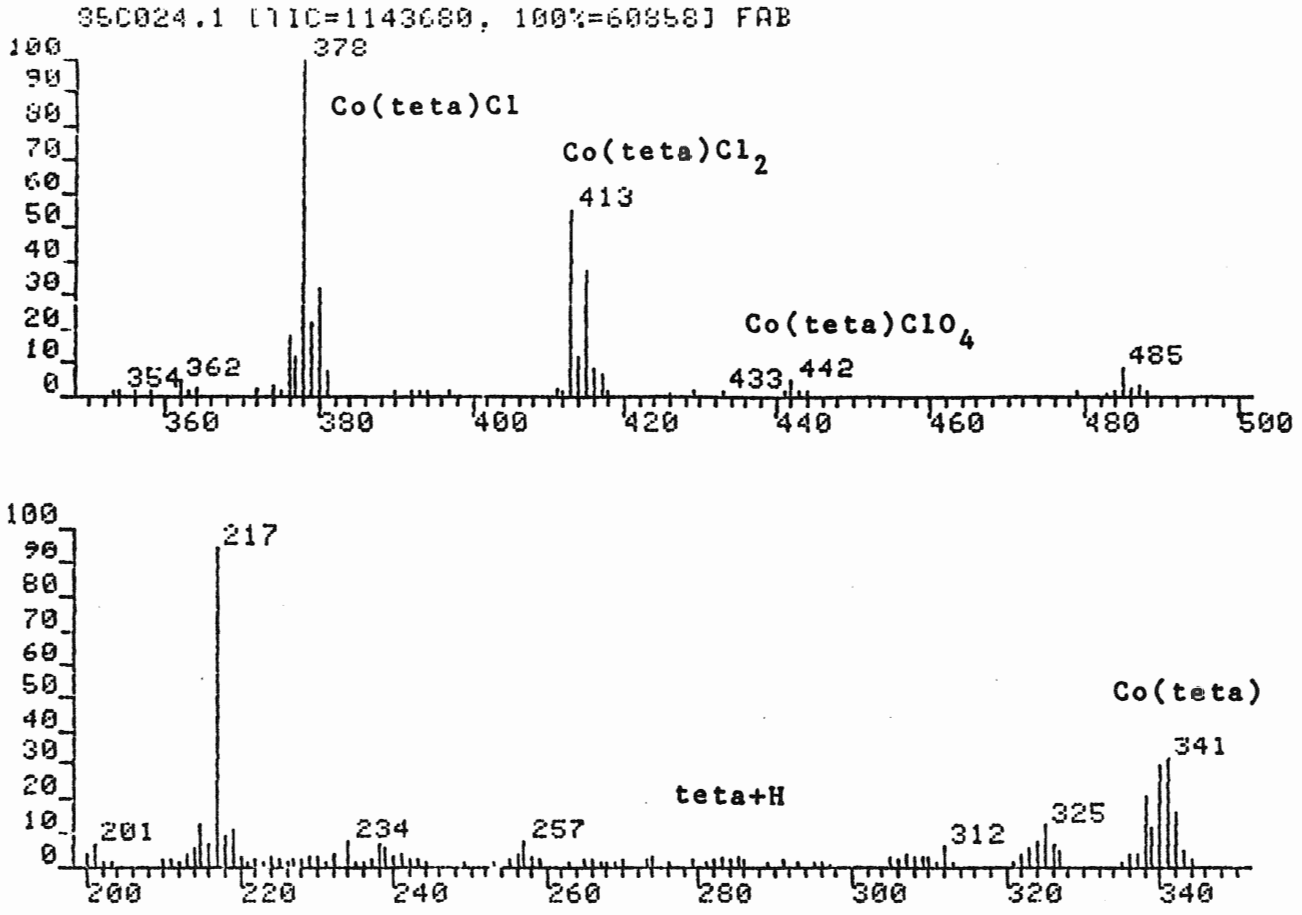

Figure 13: The Positive Ion FAB Mass Spectrum of $[Co(teta)Cl_2]Cl$ in Thioglycerol

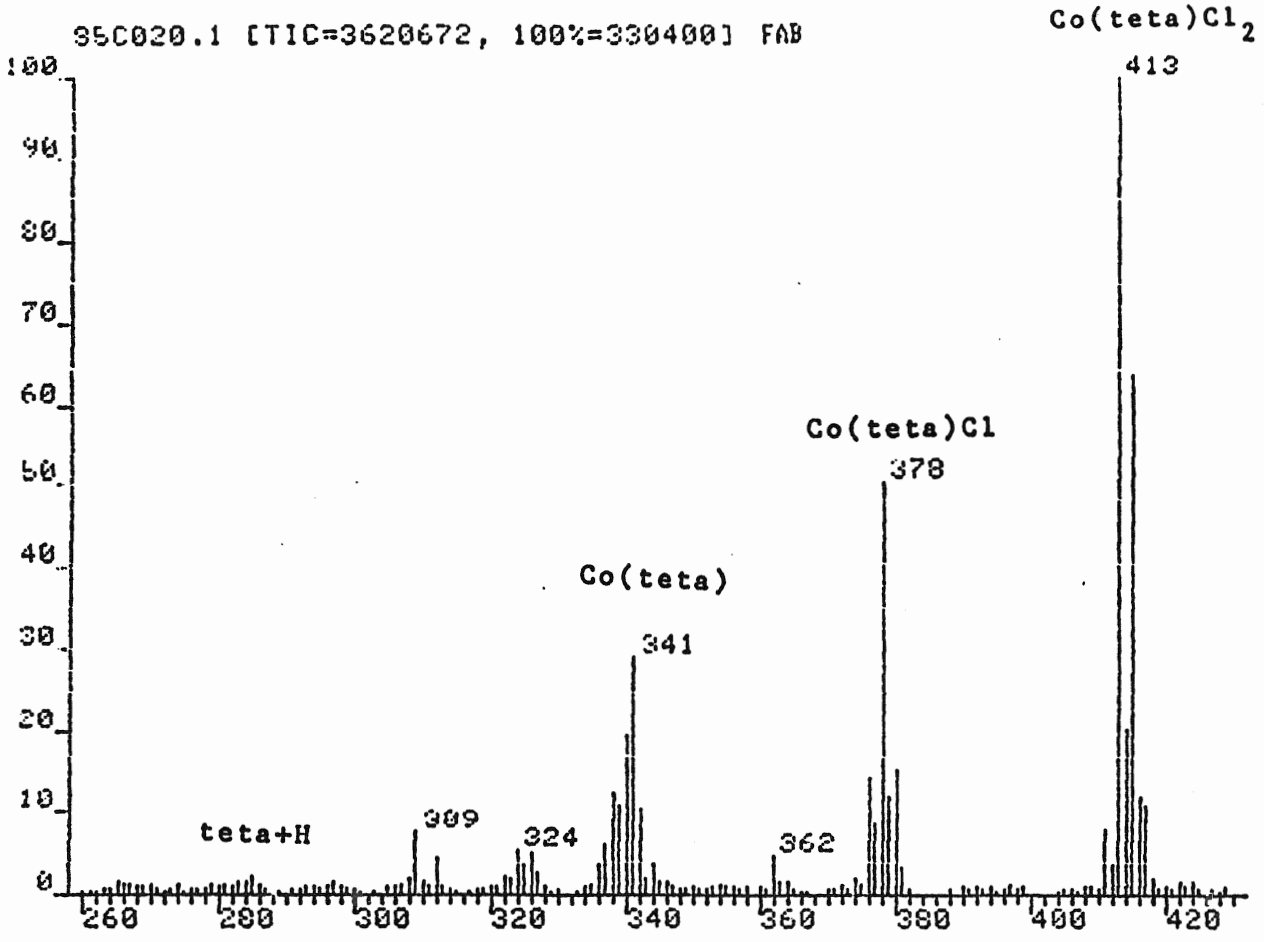

Figure 14: The Positive Ion FAB Mass Spectrum of $(Co(teta))(CoCl_4)$ in Thioglycerol

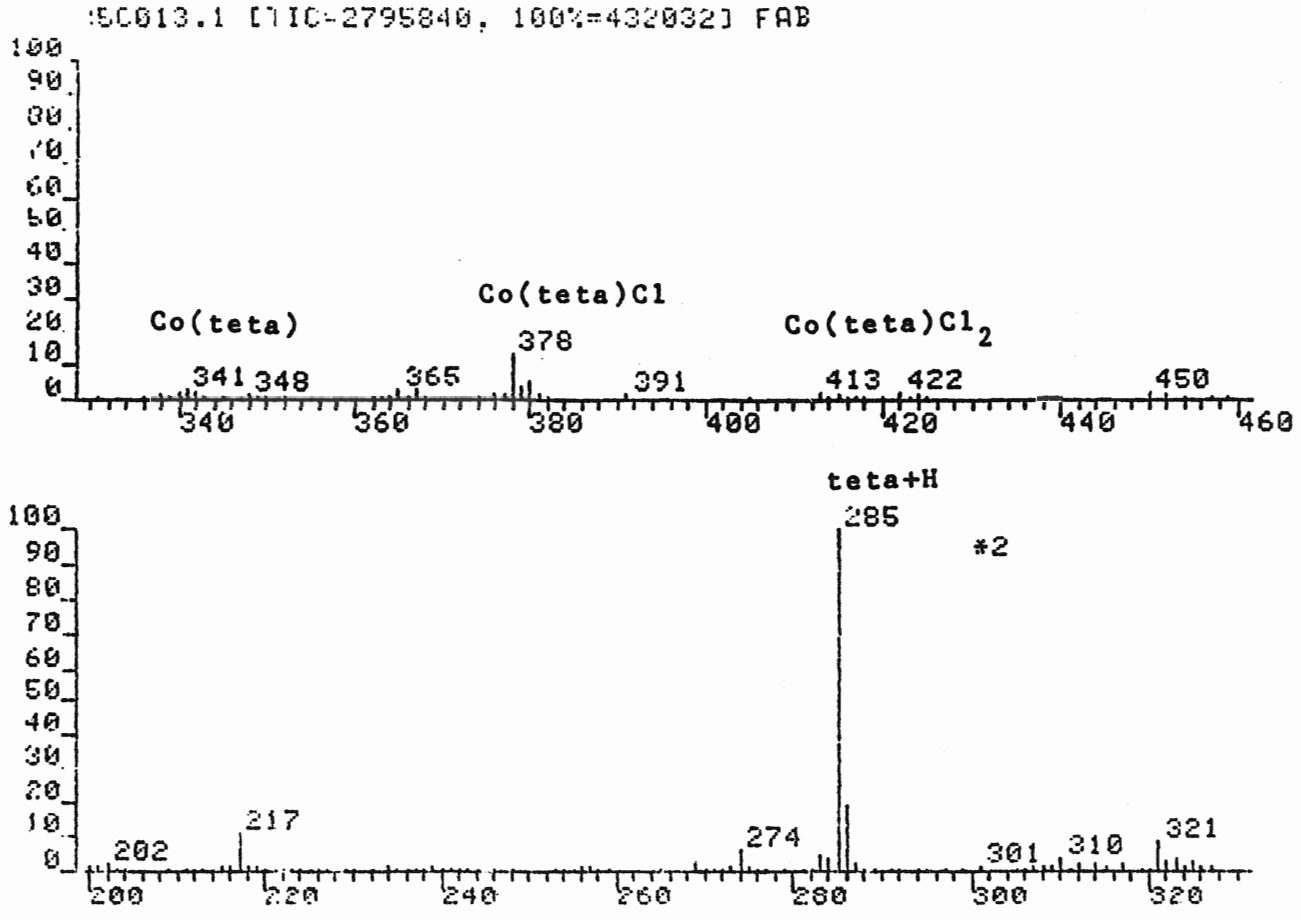

Figure 15: The Positive Ion FAB Mass Spectrum of $[Co(teta)ClN_3]ClO_4$ in Thioglycerol

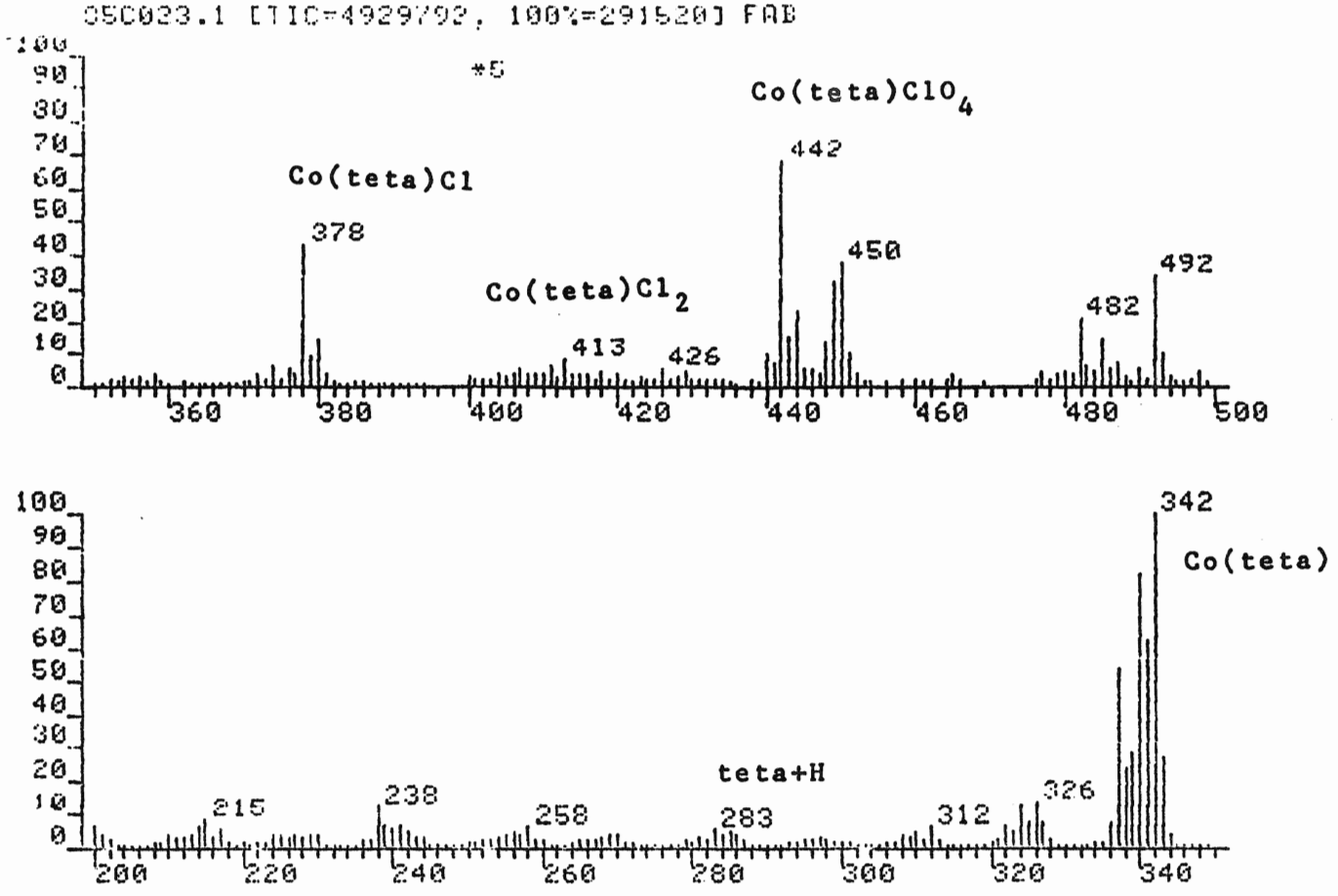

Figure 16: The Positive Ion FAB Mass Spectrum of $[Co(teta)(NO_2)_2]ClO_4$ in Thioglycerol

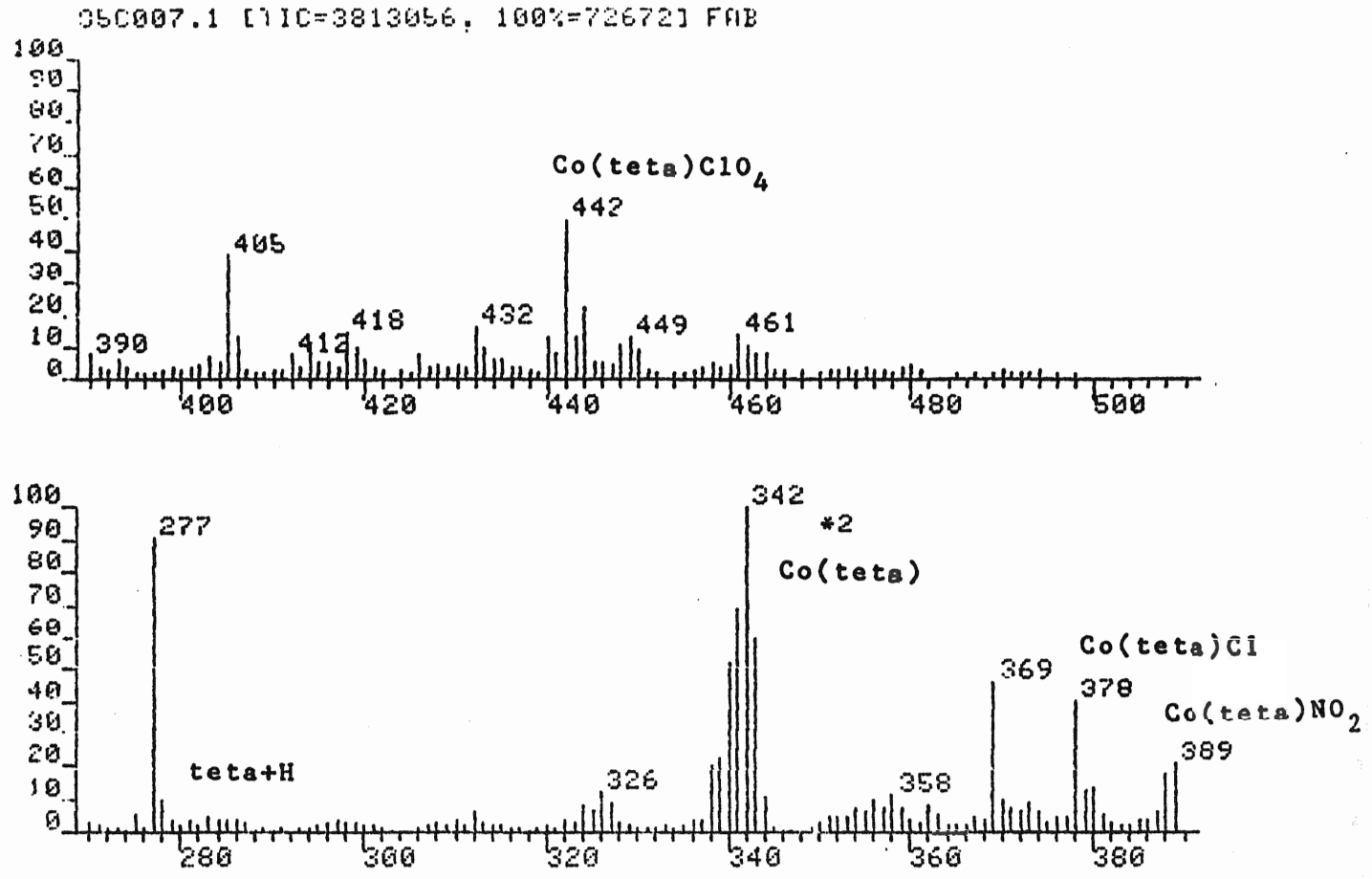

Figure 17: The Positive Ion FAB Mass Spectrum of $[Co(teta)NO_2OH]ClO_4$ in Thioglycerol

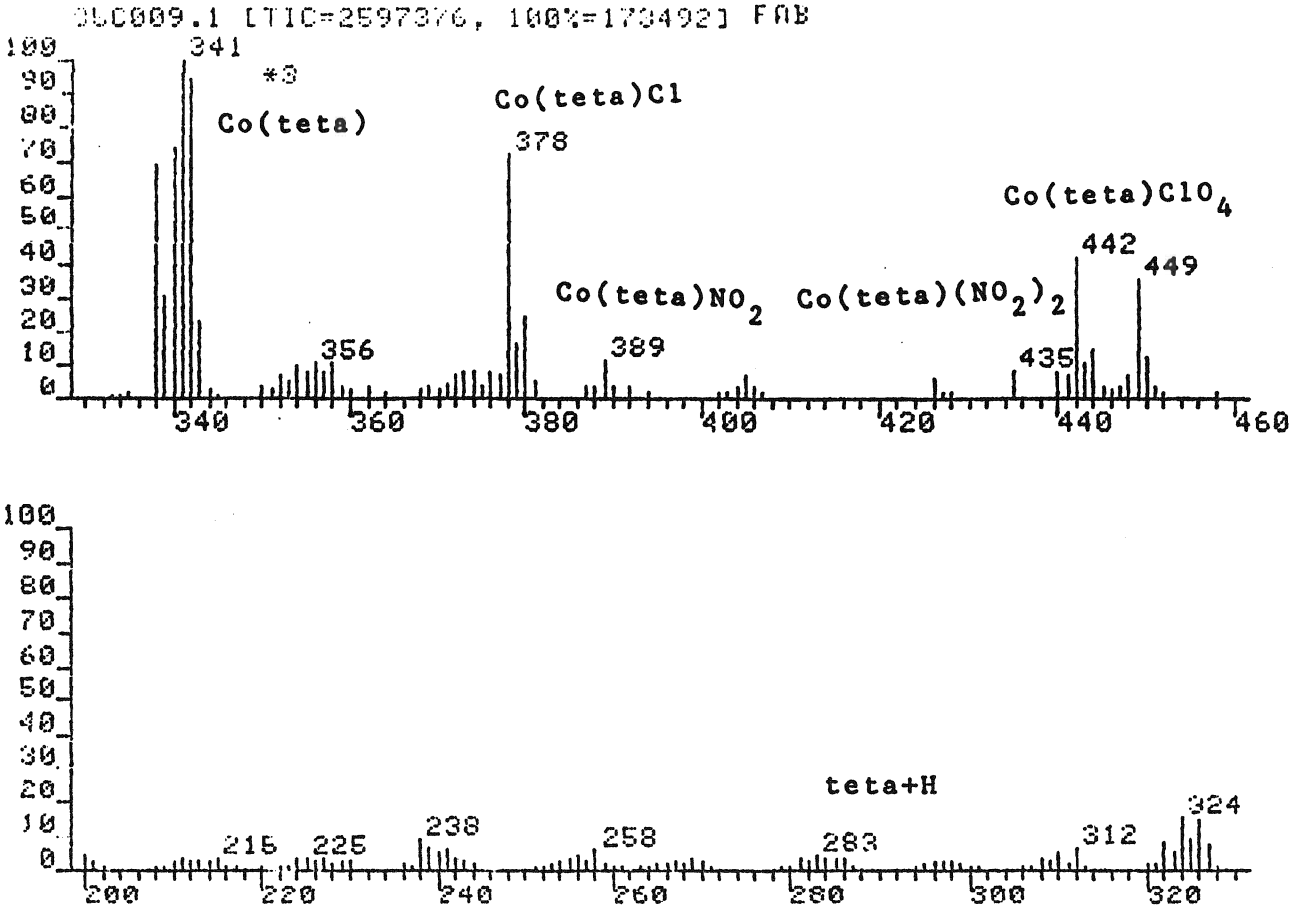

Figure 18: The Positive Ion FAB Mass Spectrum of $[Co(teta)(CN)_2]ClO_4$ in Thioglycerol

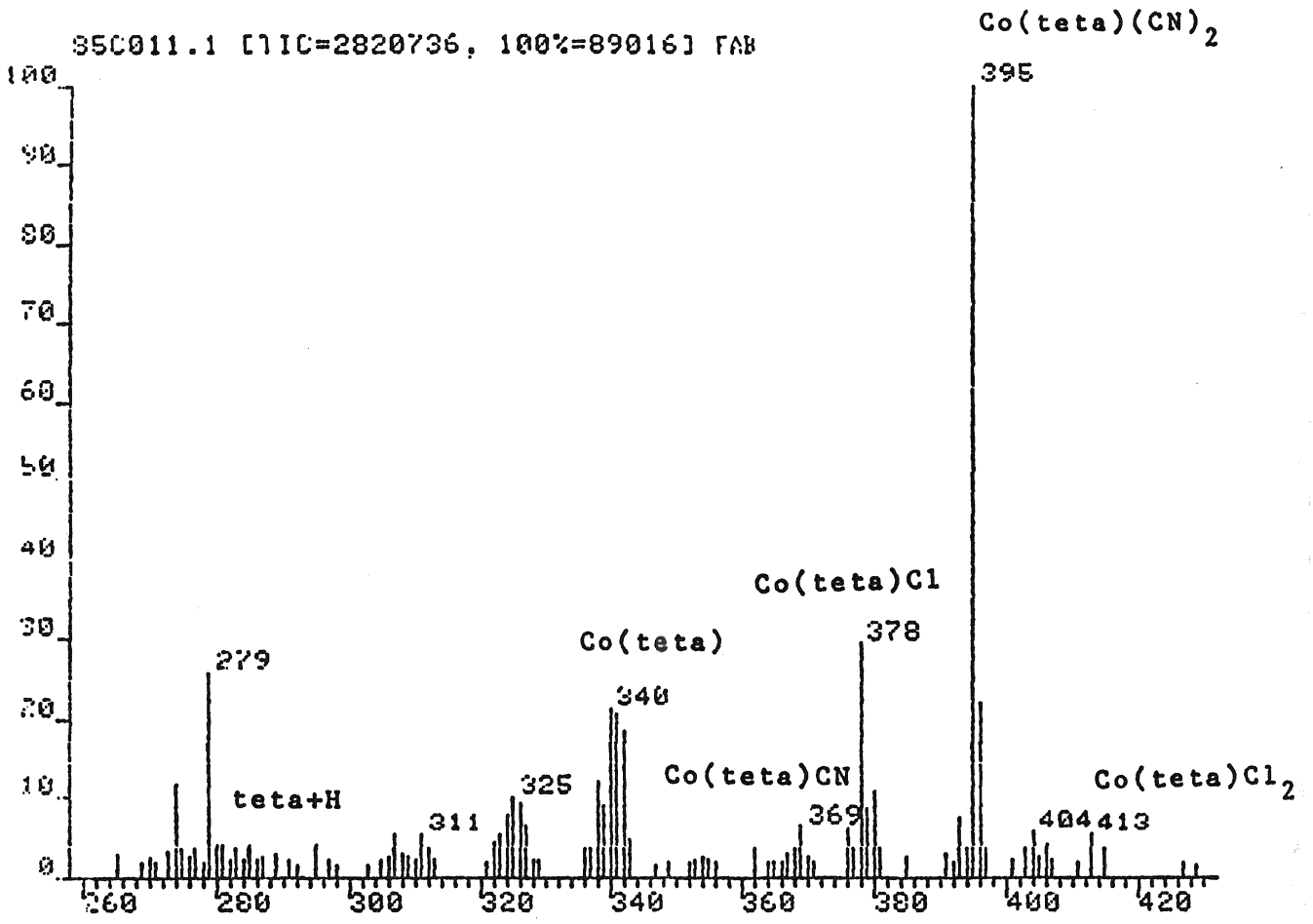

Figure 19: The Positive Ion FAB Mass Spectrum of $[Co(teta)(SCN)_2]SCN$ in Thioglycerol

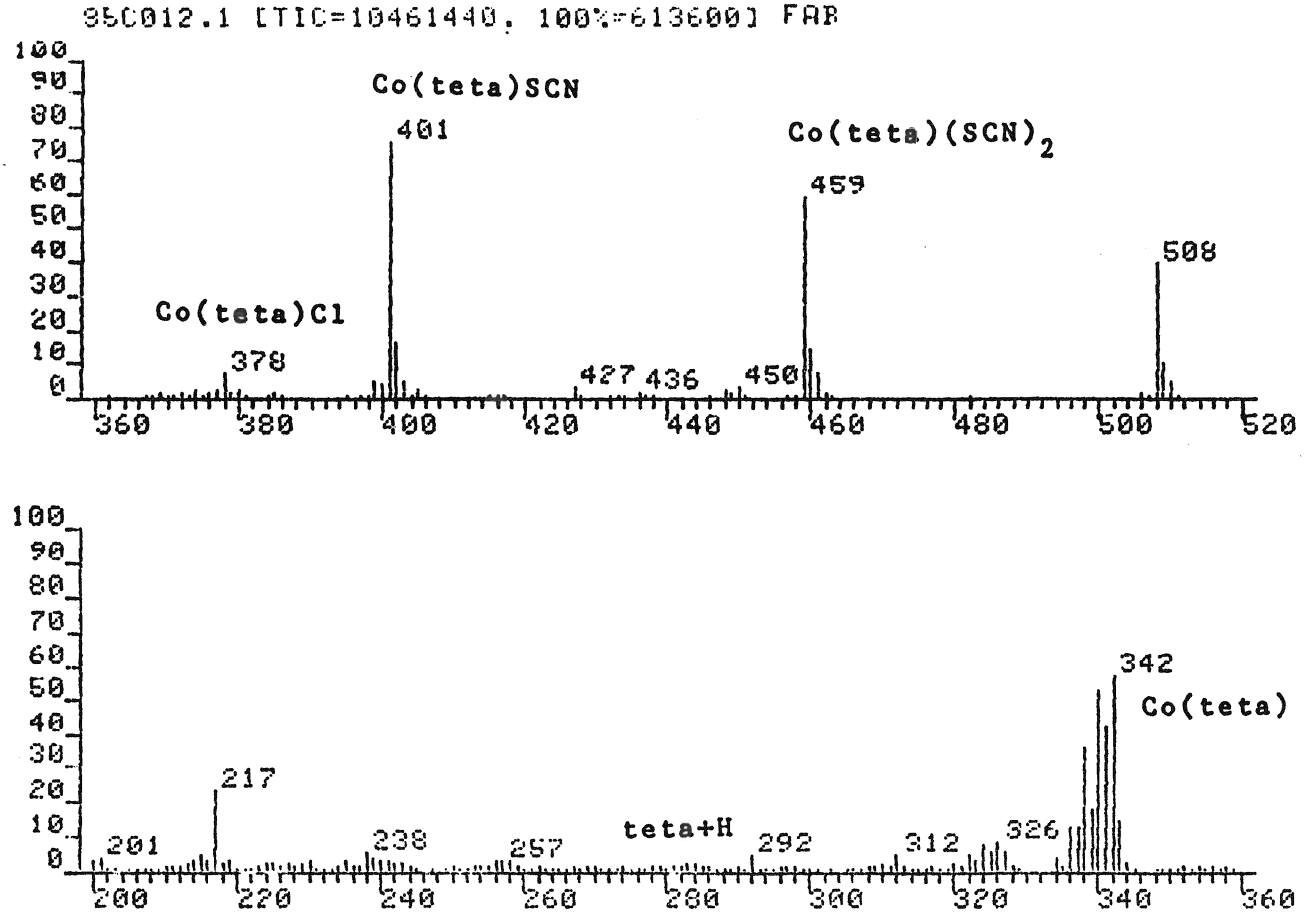

The $[teta]^+$ and the $[Co(teta)]^+$ species are common to all the positive ion spectra of the cobalt compounds. These species, however, did not appear in the expected isotope pattern. A conglomeration of peaks was observed for these species due to successive loss and gain of hydrogen via ion/molecule or matrix/molecule reactions. This result was observed regardless of the matrix utilized.

The spectrum of the uncomplexed ligand also had peaks due to addition and subtraction of hydrogens. The quasimolecular ion at m/z 285 was very intense, and the peaks due to hydrogen loss were of minor intensity. In the cobalt spectra the quasimolecular ion associated with the teta species is weak and the surronding peaks are more intense. Compare the quasimolecular ion for the teta species in the spectrum of the ligand, (Figure 6(b)), and in the spectrum of the complex $[Co(teta)Cl_2]ClO_4$, (Figure 12). The reason for the strange dehydrogenation of these species will be discussed at a later point in this report. Data will also be presented in a later section to corroborate that it is loss and addition of hydrogens that is being observed.

In the cobalt cations which have perchlorate as the counter ion (See Table 3), a peak is observed corresponding to $[Co(II)(teta)ClO_4]^+$. This is unusual in the sense that the perchlorate ion has relatively little tendency to serve as a ligand and is often used where an anion unlikely to coordinate is required (48). It is known that when no other donor is present

to compete with the perchlorate, it is possible for the perchlorate ion to exercise a donor capacity and can be monodentate, bridging bidentate, or chelating bidentate (49). The perchlorate is probably not a contaminant as it is soluble in alcohol and cold water, therefore the peak identified as the $[Co(II)(teta)ClO_4]$ species most probably results from some type of matrix/molecule or ion/molecule reaction. The intensity of this species is weak in all the cobalt perchlorate complexes. The observation of coordination due to the counter ion is unusual in that previous workers have found that the counter ion does not have any effect on the observed spectrum (25).

The results obtained for the cobalt complexes, however, indicate that the counter ion does have an effect on the spectra. The complexes $[Co(teta)Cl_2]ClO_4$ and $[Co(teta)Cl_2]Cl$ basically differ only in the outersphere anion, however, there is a great difference in the intensity of the peaks that are obtained in the spectra of these compounds, (See Figures 12 and 13). The peak corresponding to the species $Co(teta)Cl_2$ has a much greater intensity in the spectrum of the $[Co(teta)Cl_2]Cl$ complex. The cluster of peaks due to the dehydrogenation of the Co(teta) species has a very different pattern in the two spectra. Table 9 presents the normalized intensity for the peaks with mass greater than and including the $[teta]^+$ species. As no other chloride complex was studied with a counter ion other than ClO_4^- and Cl^-, it is not known as to whether this behaviour represents an anomaly or is in fact consistent with these compounds. If the

Table 9: Comparison of the Ion Intensities in the FAB Mass Spectra of the $[Co(teta)Cl_2]Cl$ and $[Co(teta)Cl_2]ClO_4$ Complexes.

	$[Co(teta)Cl_2]Cl$		$[Co(teta)Cl_2]ClO_4$	
	Ion Intensities [a]			
Ions Observed	glycerol	thioglycerol	glycerol [b]	thioglycerol
C^{+} [c]	22.3	50.8	2.2	27.1
C^{+}-Cl	30.0	24.1	45.2	44.5
C^{+}-2Cl	45.2	23.1	45.2	28.4
C^{+}-2Cl-Co	2.6	0.2	7.5	0.0

(a) Ion intensities are a percentage of the teta containing species Isotope cluster peak intensities of the same elemental composition are summed and included with the parent species. Peaks due to deprotonation of an elemental cluster are also summed and included with the parent peak.

(b) $C^{+} = Co(teta)Cl_2$

(c) Data from spectrum 622CM1

counter ion does cause differences in the observed spectrum, comparisions between complexes would have to be done only among complexes with the same counter ion.

Molecular cations or molecular ions could not be obtained for a number of the cobalt complexes. The $(Co(teta))(CoCl_4)$ complex proved to be very difficult to analyze, and a molecular ion could not be obtained. The ions that were observed were similar to $[Co(teta)Cl_2]ClO_4$ or $[Co(teta)Cl_2]Cl$ complexes. Peaks were observed at masses which corresponded to $(Co(teta)Cl_2)^+$, $(Co(teta)Cl)^+$, $(Co(teta))^+$ and the $teta^+$. Of the matrices used for this compound, thioglycerol produced the best results. The blue $(Co(teta))(CoCl_4)$ turned pink upon dissolving in most of the matrices used. These included the coprecipitation method using DMF on glycerol, DMF on thioglycerol, and DMF on DAP. Other matrices used included glycerol, DAP, NPOE, 30% glycerol in sulfolane, DMF/glycerol and sulfolane. Doping with NH_4Cl was also used with DMF/glycerol as the matrix. The complex only had limited solubility in the majority of the matrices used. The pink colour which occurred upon dissolving is characteristic of Co(II) and usually indicates formation of an octahedral cobalt(II) complex and destruction of the deep blue $CoCl_4^{2-}$ ion.

It was hard to obtain spectra of the nitro- containing complexes, and the ions that were observed were of low intensity. The problem is believed to be due mainly to the poor solubility in glycerol matrices. Even the doping method using NH_4Cl and $NaNO_2$ did not produce worthwhile results. The problem with

solubility is not surprising as it is well known that the teta complexes have lower solubilities than the complexes of tetb (50). (Increased solubility implies greater difficulty in isolating the metal complexes, and therefore many of the complexes that can be isolated for teta can not be isolated for tetb.) FAB is greatly hindered when solubility is low, and as these complexes dissolve to a greater extent in sulfur-containing matrices such as sulfolane and thioglycerol, these matrices produce better quality spectra. The C^+ molecular ion was not obtained for $[Co(teta)(NO_2)(OH)]ClO_4$ complex, nor was a peak observed for the $[Co(teta)(OH)]^+$ species even in the sulfur matrices.

The cation molecular ion peak was obtained for the di-nitrite containing complex, as well as the peak created by the loss of one nitrite in both glycerol and thioglycerol. The intensities of these species were low particularly in glycerol. In fact, the parent ion intensity in glycerol was only 2000 counts in terms of absolute intensity, which is borderline in terms of whether it exists or is merely noise.

The $[Co(teta)ClN_3]ClO_4$ did not produce a C^+ parent ion. The azide was not observed in any of the peaks present in the spectrum. This is not an uncommon observation, as previous work done on the electron impact spectra of inorganic azides had shown that these compounds show a distinct preference for N_3 loss (51). The major peaks were $[Co(teta)^+$ and the $[Co(teta)Cl]^+$. Other peaks included the $Co(teta)Cl_2$ and the $Co(teta)ClO_4$ species. The

$Co(teta)Cl_2$ might be a result of contamination from the $[Co(teta)Cl_2]ClO_4$ species used as starting material to form this compound. However, it might also be due to perchlorate decomposition which will be discussed in the next section.

Good quality spectra were obtained for the $[Co(teta)(CN)_2]ClO_4$ and the $[Co(teta)(SCN)_2]SCN$ complexes in both glycerol and thioglycerol. Solubility was good in both glycerol and thioglycerol, and therefore the spectra were equally good in both matrices. (Compare the spectra obtained for these complexes in glycerol and in thioglycerol given in the appendix I, pages A7-A10.)

4) Studies on the Metal Complexes Other Than Cobalt

Figures 20-23, 25 and 26 show the positive FAB ion spectra of the metal complexes in thioglycerol. In these metal complexes, the matrix did not have a great effect on the spectrum observed, as the spectra appeared the same in both glycerol and thioglycerol. (See appendix II for the spectra of the complexes in glycerol.)

Spectra of the complexes $Ag(teta)(NO_3)_2$ and $(HgCl_2)_2(tetb)$ proved to be extremely difficult to obtain. Both the silver and the mercury complex showed the quasimolecular ion of the ligand as the most intense peak. The di-mercury complex behaved similarly to the complex $(Co(teta))(CoCl_4)$ in that spectra of this compound were not easily obtained. The matrices used

included: NPOE, 18-crown-6 with 10% tetraglyme, glycerol, PEG, thioglycerol, nujol, DMF in 30% glycerol in sulfolane and 30% glycerol in sulfolane. A mixture of methanol and glycerol doped with NH_4Cl was also tried without any success. Unlike $(Co(teta))(CoCl_4)$, results were obtained when the coprecipitation technique was employed. Methanol was the solvent used to dissolve the complex and glycerol was the matrix layered on the probe tip. The spectrum of the mercury complex is given in Figure 20. It should be noted that the intensities of the peaks obtained were extremely low. (See the quantitative report for the spectrum of this complex in appendix II, page A19.) The peaks at m/z 485, m/z 521 and m/z 593 were identified as the $Hg(tetb)^+$, $Hg(tetb)Cl^+$ and $Hg(tetb)Cl_3$ species respectively, although the isotope patterns for these clusters were not as expected.

Both glycerol and thioglycerol were used as matricies in an attempt to obtain spectra of the silver complex. The glycerol matrix produced only the $(teta)^+$ peak at m/z 285. In thioglycerol, a doublet was observed for the species $[Ag(teta)]^+$ in the second scan taken, however the averaged scan did not have this pattern of peaks. Both coprecipitation and the doping techniques were attempted, but without any success.

The dichloro complexes containing Cd, Mn and Zn all had the $(\underline{M}(teta)Cl)^+$ as the most intense peak in the spectrum. The spectra of these complexes are illustrated in Figures 21-23, and in each case the BMASROS plot for the $(\underline{M}(teta)Cl)^+$ is also

Figure 20: The Positive Ion FAB Mass Spectrum of $(HgCl_2)_2$(tetb) using Coprecipitation

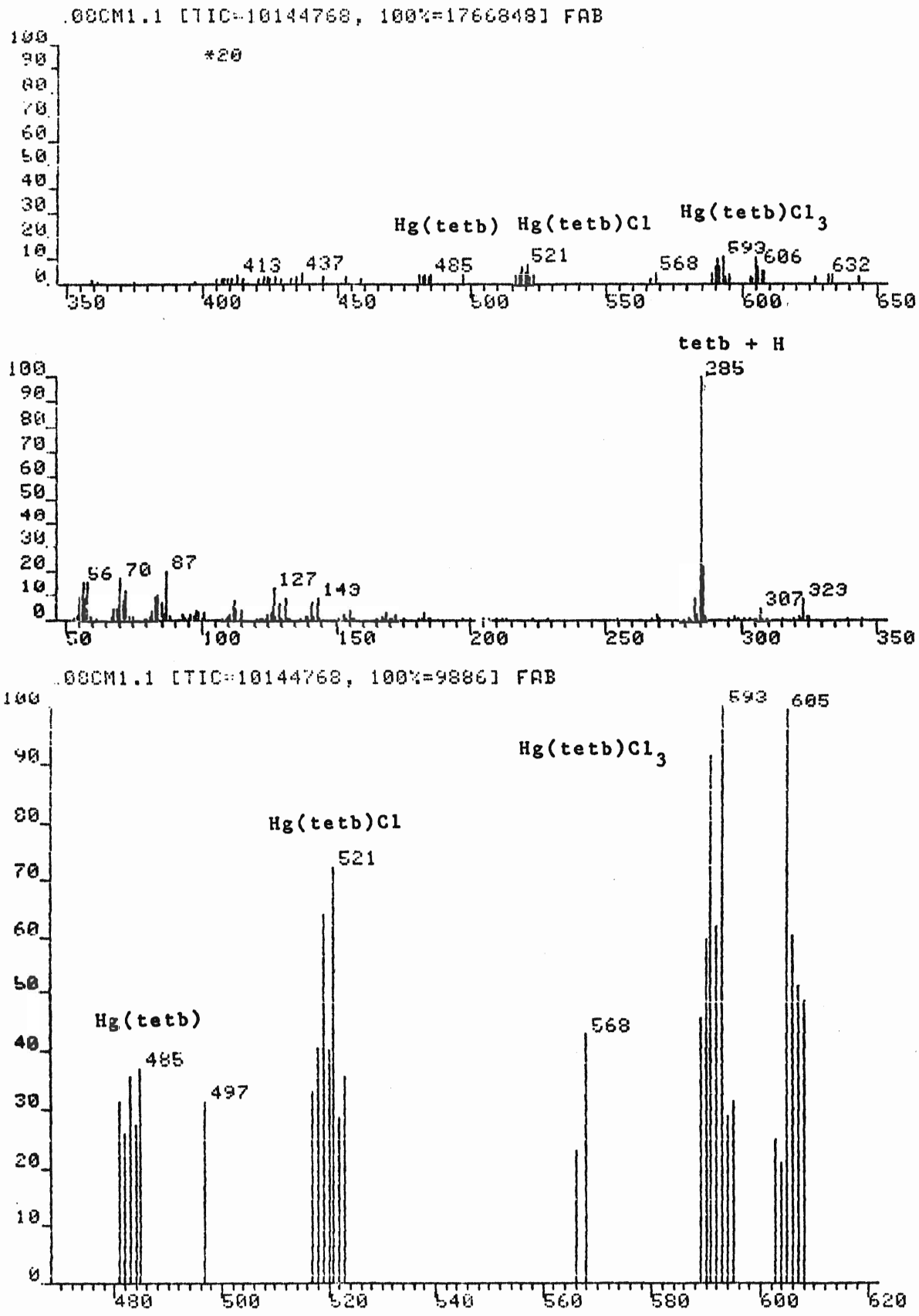

Figure 21(a): The Positive Ion FAB Mass Spectrum of $Cd(teta)Cl_2$ in Thioglycerol

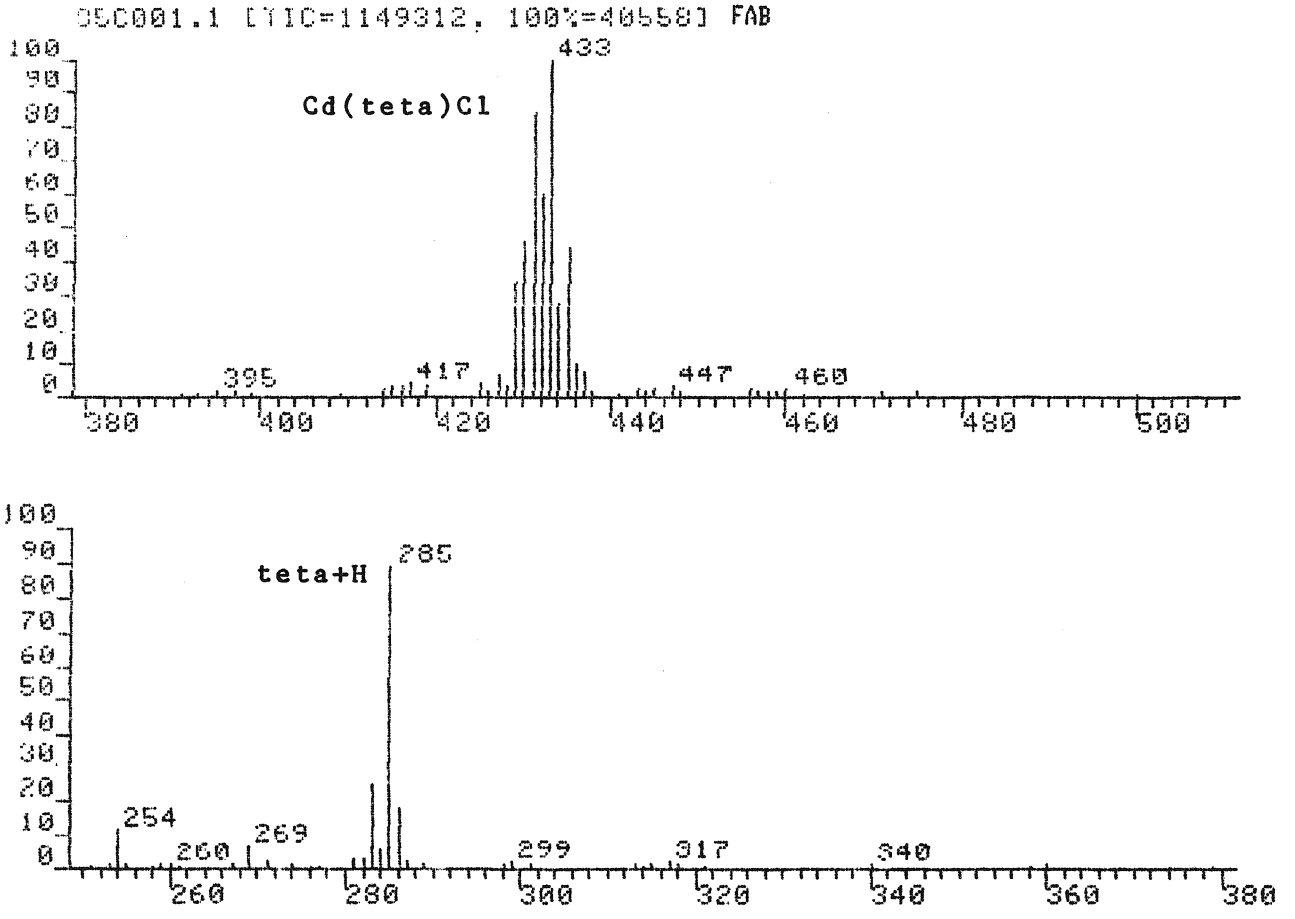

(b) The Calculated Isotope Pattern of Cd(teta)Cl

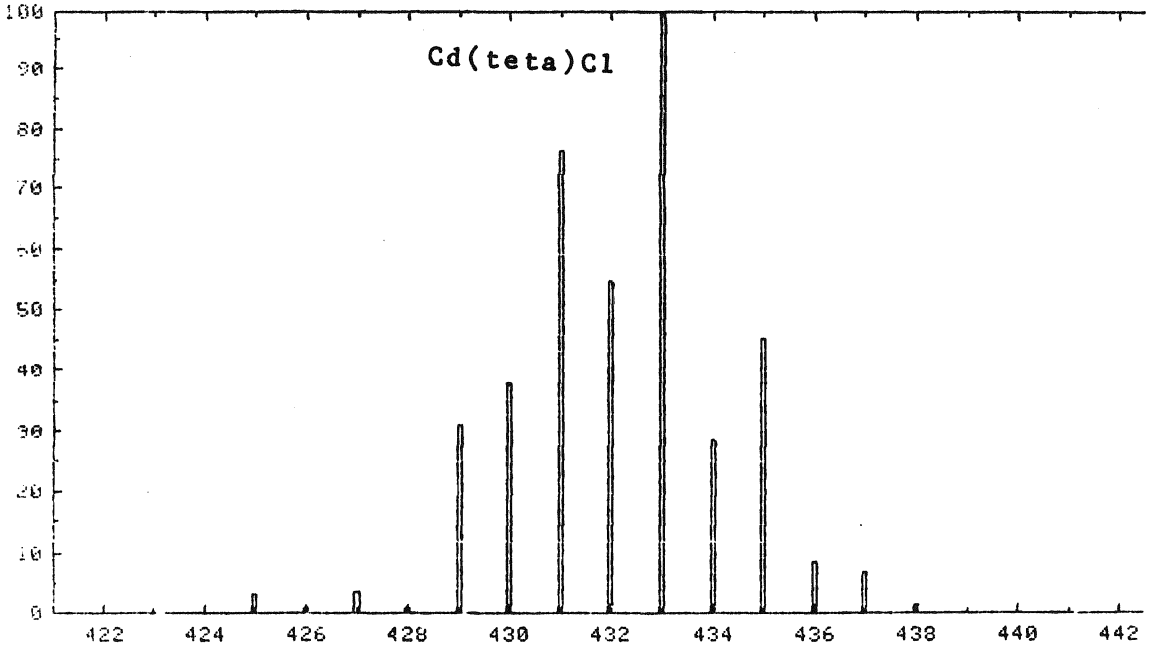

Figure 22(a): The Positive Ion FAB Mass Spectrum of $[Mn(teta)Cl_2]Cl$ in Thioglycerol

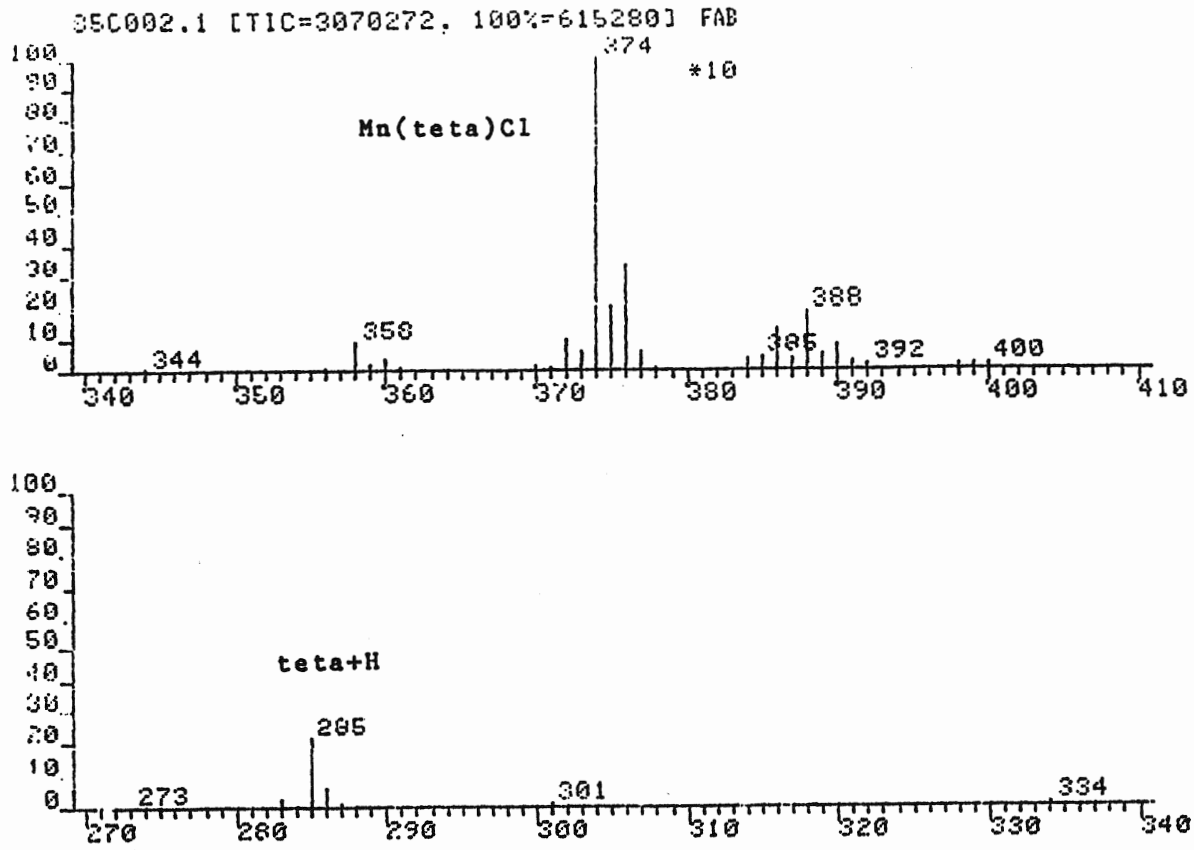

(b) The Calculated Isotope Pattern of Mn(teta)Cl

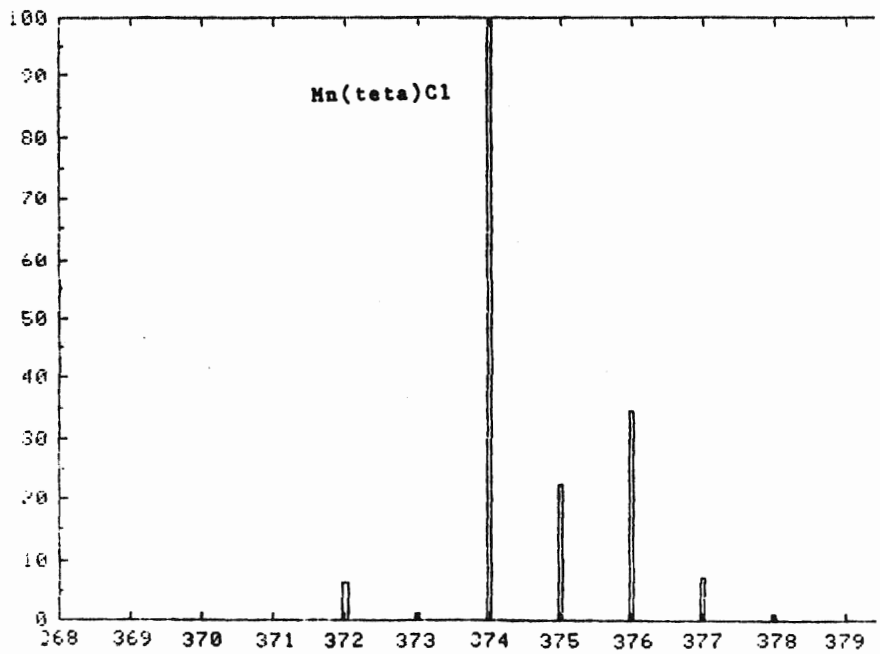

Figure 23(a): The Positive Ion FAB Mass Spectrum of $Zn(teta)Cl_2$ in Thioglycerol

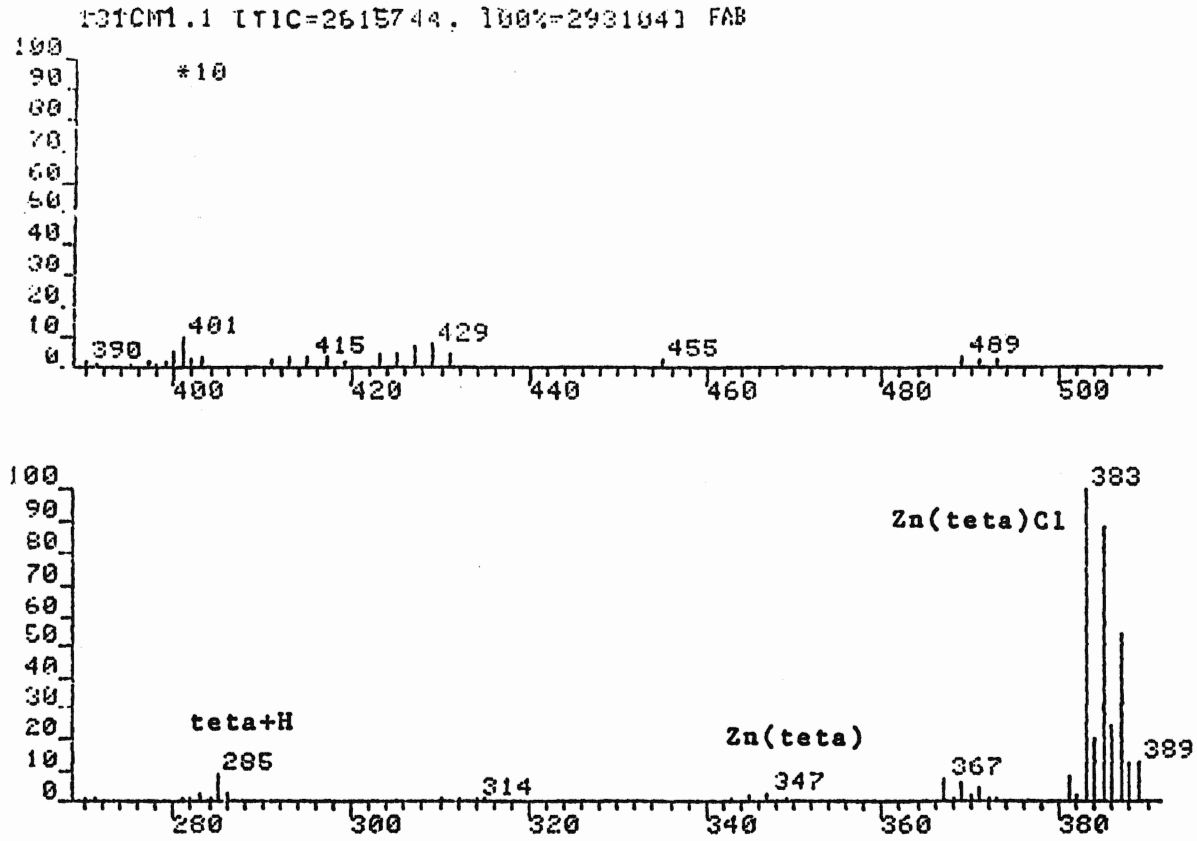

(b) The Calculated Isotope Pattern of Zn(teta)Cl

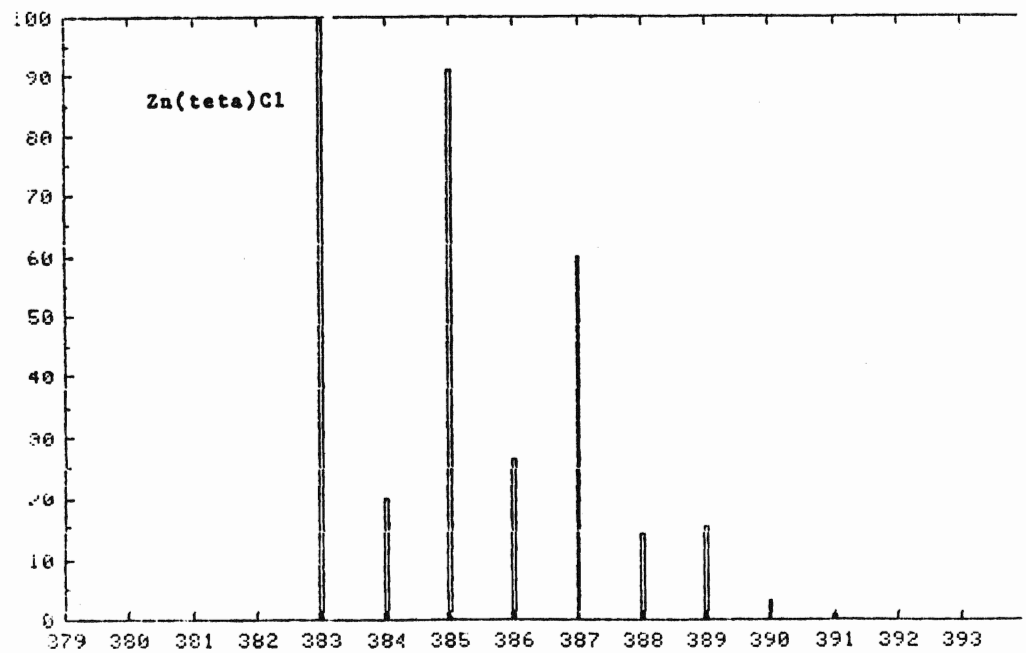

provided. The cluster due to the (M (teta)Cl)$^+$ represented more than 35% of the TIC for the Cd, Mn, and Zn complexes in glycerol. This was also true of the Mn and Zn complexes in a thioglycerol matrix; however, the cluster was reduced to 15% for the Cd complex using thioglycerol. The only other peak of significant intensity in the spectra of the Cd and Mn complexes was the teta peak. The zinc complex had a peak corresponding to the (Zn(teta)-H)$^+$ species as well as the teta+H$^+$ species. The spectrum of the Zn(teta)Cl_2 in glycerol also has a peak which corresponded in isotope pattern to the species $(Zn(teta))_2Cl_3$. (The observed peak at m/z 805 and the calculated isotope pattern are given in figure 24 for this dimerized species.) It should be noted that these peaks are of minor intensity in comparison to the (M (teta)Cl)$^+$ peak which overwhelms the spectra. Table 10 gives the intensities of the peaks obtained in the spectra of the Zn, Cd, and Mn complexes.. The appearance of the M (teta)Cl$^+$ ion as the highest-mass peak is normal for chlorinated compounds, which usually exhibit much stronger [M-Cl]$^+$ peaks than [M]$^+$ peaks (29,30). (The notation M represents the metal, and the notation M is used to represent the molecular ion.) This is contrasted against the Cu and Ni complexes which do not give significant [M(teta)Cl]$^+$ species.

The spectra of Cu(teta)$(ClO_4)_2$ and the Cu(teta)Cl_2 are similar as they are both four coordinate copper complexes. The species common to these compounds included (teta)$^+$, [Cu(teta)]$^+$ and [Cu(teta)X]$^+$, where X is the anion either ClO_4^- or Cl^-. The

Figure 24: The Observed and Calculated Isotope Patterns for $(Zn(teta))_2Cl_3$

(a) Observed Isotope Pattern

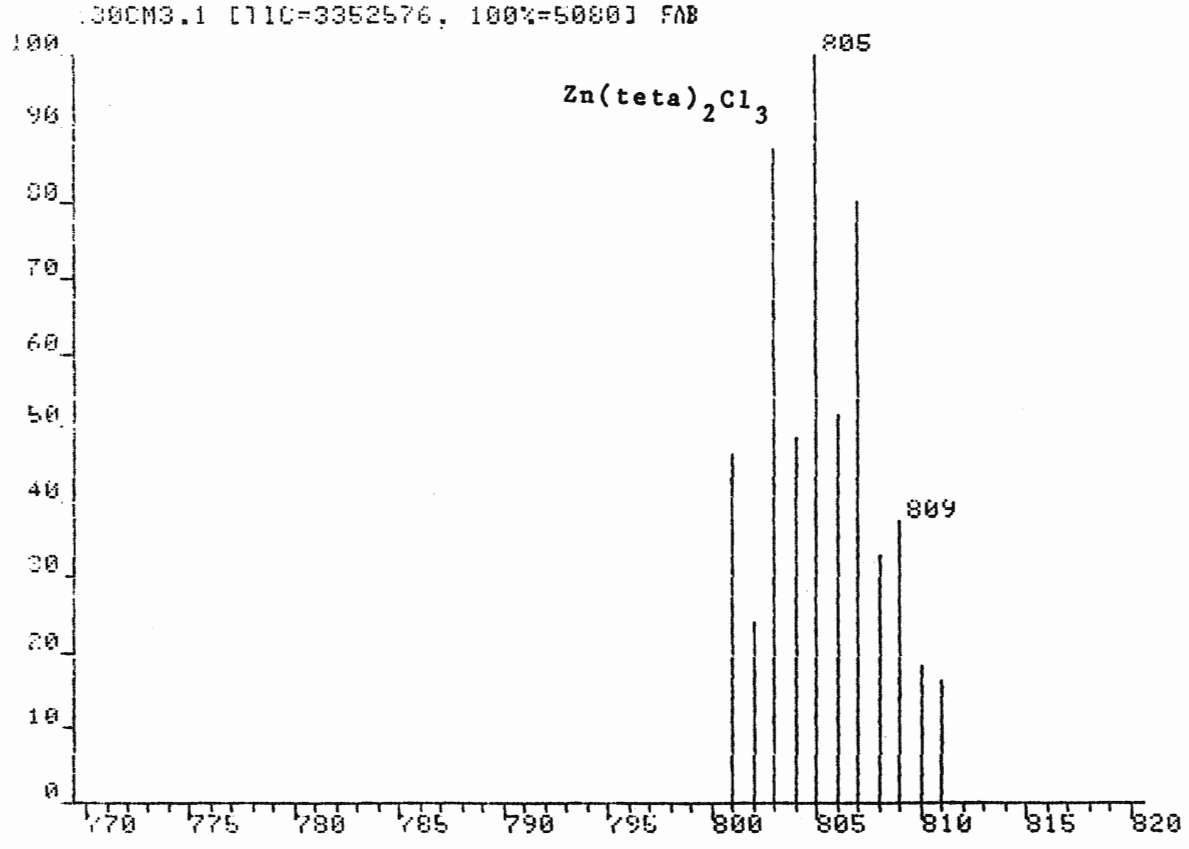

(b) The Calculated Isotope Pattern

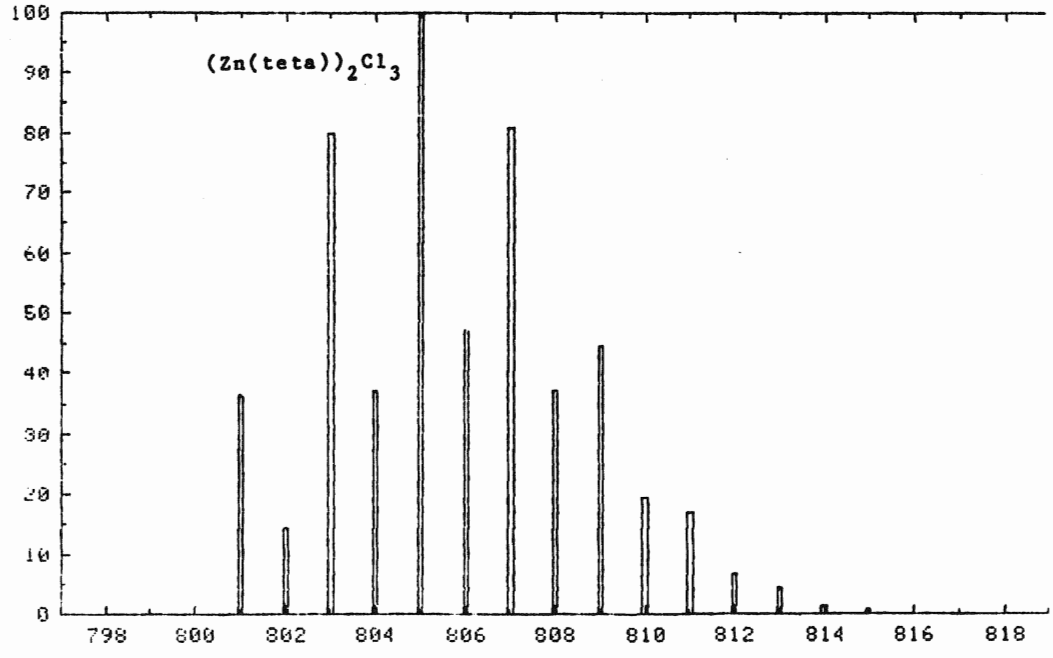

Table 10: The Observed Ion Intensities in the Positive Ion FAB Mass Spectra of the $Me_6[14]aneN_4$ Metal Complexes of Cd, Zn and Mn in Glycerol and Thioglycerol

Compound								
$CdCl_2$(teta)			$Zn(teta)Cl_2$			$[Mn(teta)Cl_2]Cl$		
Fragment	m/z	%(TIC)	Fragment	m/z	%(TIC)	Fragment	m/z	%(TIC)
Thioglycerol								
teta+H	285	(4.9)	teta+H	285	(2.3)	tet+H	285	(4.3)
Cd(teta)Cl	433	(14.9)	Zn(teta)-H	347	(0.9)	Mn(teta)Cl	375	(35.3)
			Zn(teta)Cl	383	(35.5)			
Glycerol								
teta+H	285	(3.3)	teta+H	285	(1.3)	teta+H	285	(1.4)
Cd(teta)Cl	433	(35.7)	Zn(teta)-H	347	(1.1)	Mn(teta)Cl	375	(32.8)
			Zn(teta)Cl	383	(35.0)			
			$(Zn(teta))_2Cl_3$	805	(0.4)			

spectrum of $Cu(teta)Cl_2$ in thioglycerol has a peak at m/z 800 which corresponds to $(Cu(teta))_2Cl_3$-H, as well as the other common peaks (see appendix 2).

Figure 25 gives the spectrum of the copper perchlorate complex in thioglycerol. The $Cu(teta)(ClO_4)_2$ spectra includes a cluster of peaks due to the $Cu(teta)Cl^+$ species. This cluster is believed to be a result of ClO_4^- decomposition and is more predominant in thio- matrices. This is consistent with the results obtained in the negative ion FAB mass spectrum of this complex, as ions were observed which were formed as a result of the decomposition of perchlorate. The chlorinated $\underline{M}(teta)^+$ has been observed before in cobalt complexes containing no coordinated chloride, however, perchlorate was the outersphere anion present. It is thus probable that the peaks observed in the cobalt complexes due to $[Co(teta)Cl]^+$ results from ClO_4 decomposition as well as from incomplete conversion of the dichloro-perchlorate into the desired complex.

There is a strong correspondence between the copper complexes and the nickel complex in terms of the species obtained in the FAB spectra, (compare Figures 25 and 26). The nickel complex has peaks due to $(teta)^+$, $[Ni(teta)]^+$ and $[Ni(teta)Cl]^+$. A peak also appears at m/z 423 whose identity is unknown; it may result from some type of matrix interaction. As in the mercury and silver complexes the quasimolecular ligand peak at m/z 285 is the most intense peak in this spectrum.

Figure 25: The Positive Ion FAB Mass Spectrum of $[Cu(teta)](ClO_4)_2$ in Thioglycerol

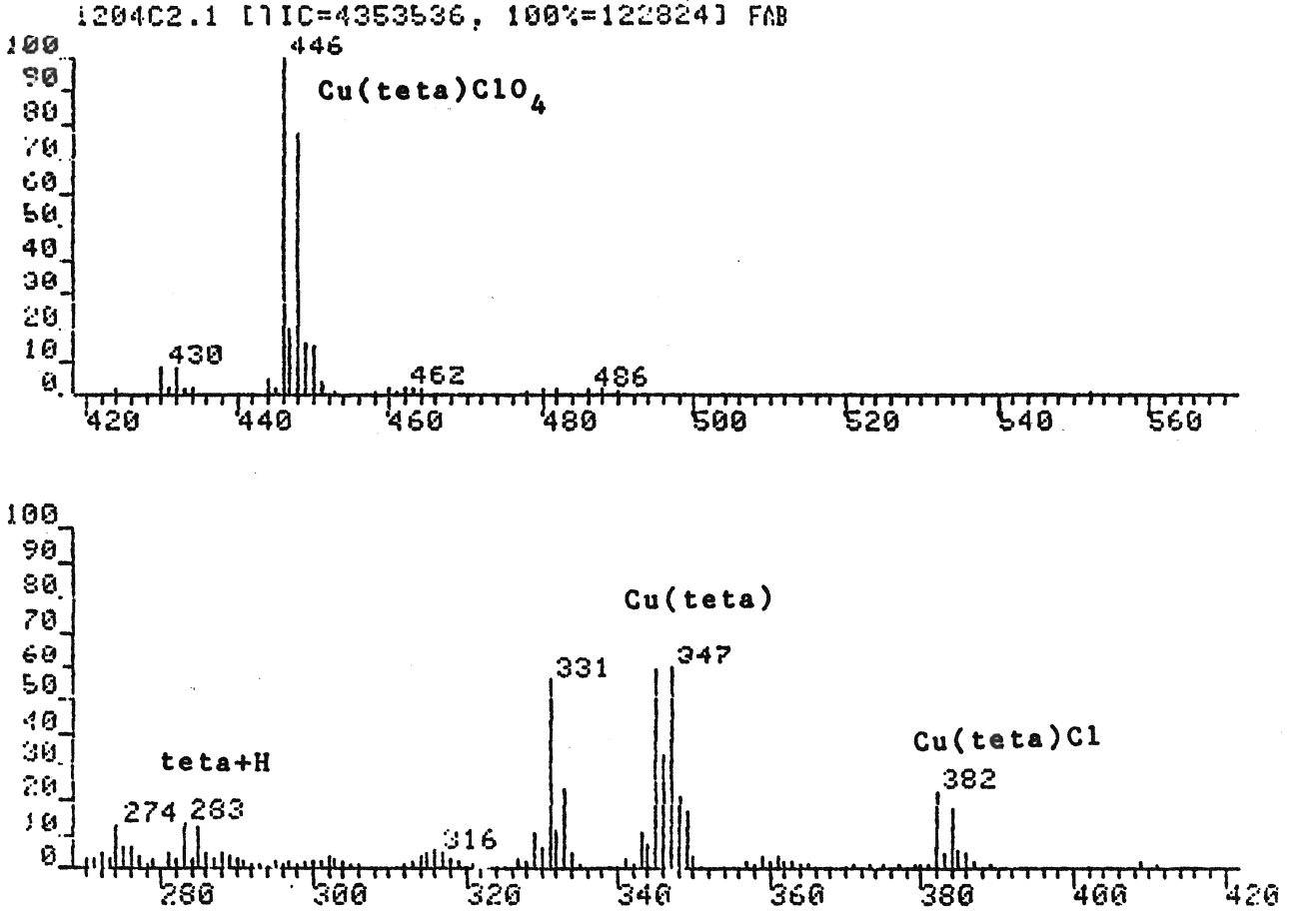

Figure 26: The Positive Ion FAB Mass Spectrum of $[Ni(teta)]Cl_2$ in Thioglycerol

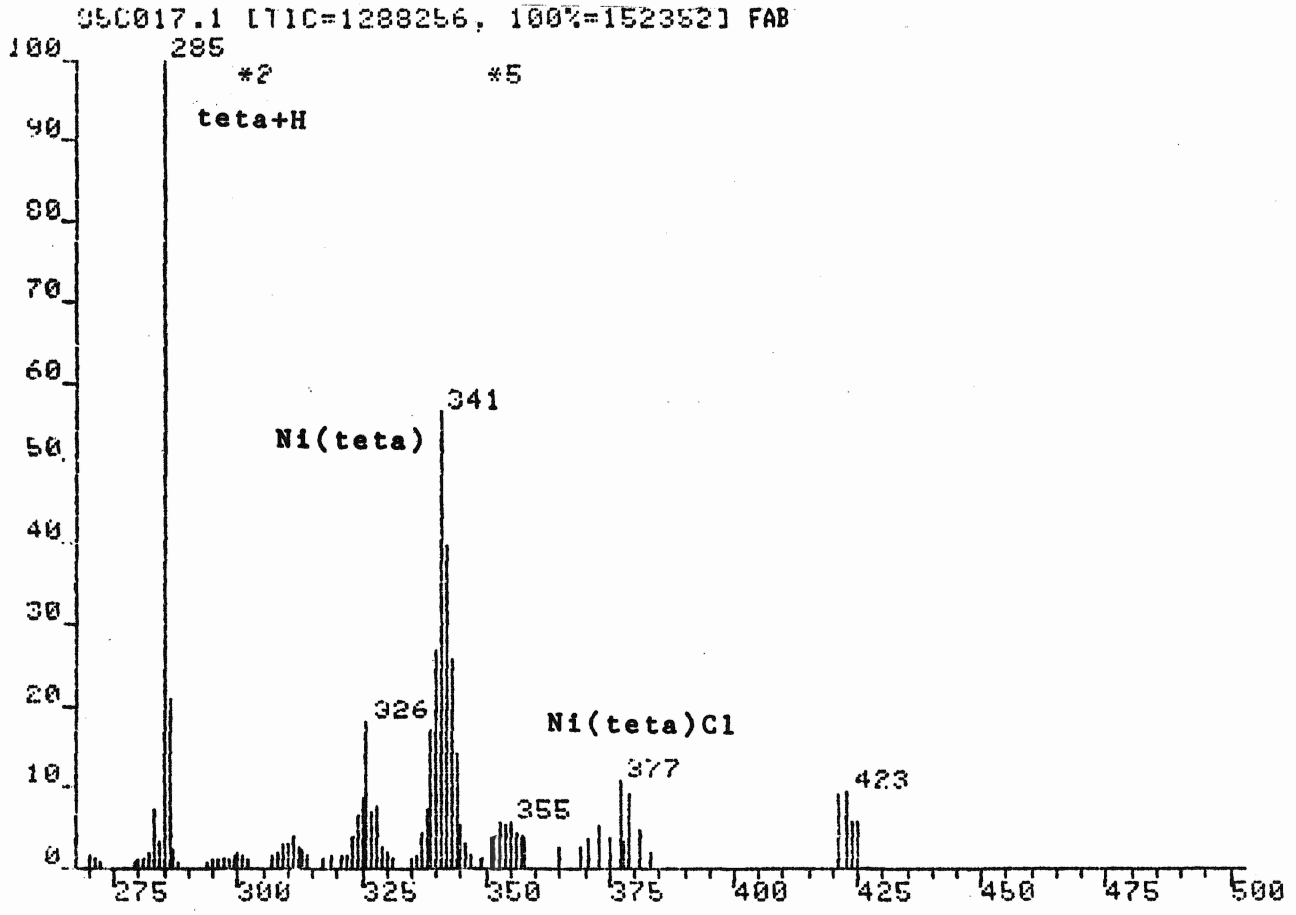

5) Dehydrogenation

As previously mentioned, it is common in the $Me_6[14]aneN_4$ complexes for dehydrogenation of the main fragments in the FAB spectrum to occur. The cobalt complexes commonly gave a cluster of peaks associated with the $[Co(teta)]^+$ species. These peaks were identified as being due to the dehydrogenation of the macrocyclic ring.

The Fortran program BMASABD was used to show that the peaks could be associated with successive loss of hydrogen. The program BMASABD performs a least squares fit of the observed intensities of the peaks to the calculated intensities (assuming dehydrogenation). The results obtained from the BMASABD calculation on the experimental data for $[Co(teta)(SCN)_2]SCN$ are provided in Table 11. From this data, it is evident that there is a good correlation between observed and calculated peak intensities. BMASABD calculations were also performed on $[Co(teta)(CN)_2]ClO_4$, $[Co(teta)Cl_2]ClO_4$ and $[Co(teta)Cl_2]Cl$ in glycerol, as well as $[Co(teta)(SCN)_2]SCN$ in a thioglycerol matrix. All three spectra 622CM1, 85RP1 and 85RP2 of the $[Co(teta)Cl_2]ClO_4$ had BMASABD calculations done on the Co(teta) cluster. In each instance, the percent composition obtained for each fragment was comparable (see appendix III, pages A37-A39), which reinforces the earlier statement that spectra of these complexes are reproducible. The BMASABD results for the $[Co(teta)(SCN)_2]SCN$ complex in glycerol and thioglycerol are also

Table 11: The Data from the BMASABD Calculation of the Complex $[Co(teta)(SCN)_2]SCN$

(a) The % Composition of the Dehydrogenated Fragments

Fragment	% Composition
Co(teta)	4.97756
Co(teta)-H	26.58000
Co(teta)-2H	12.02710
Co(teta)-3H	22.77330
Co(teta)-4H	5.41171
Co(teta)-5H	15.21020
Co(teta)-6H	11.13720
Co(teta)-7H	1.42633
Co(teta)-8H	0.45658

(b) Observed and Calculated Averaged Intensities

m/z	Observed	Calculated	Difference
347	0.00000	0.00005	-0.00005
346	0.00000	0.00142	-0.00142
345	0.00000	0.02543	-0.02543
344	0.32800	0.30795	0.02005
343	2.14300	2.14653	-0.00353
342	5.99200	5.99164	0.00036
341	3.39900	3.39902	-0.00002
340	4.91900	4.91900	0.00000
339	1.76200	1.76200	0.00000
338	3.55500	3.55500	0.00000
337	2.32800	2.32800	0.00000
336	0.30900	0.30900	0.00000
335	0.09300	0.09300	0.00000

Average Deviation = 0.004

*Note: Species with % composition's less than 1, are not statistically valid but are known to exist on a chemical basis

very similar. The results for the thiocyanide complex are given in appendix III, page A41. In all the calculations done on the cobalt complexes, the average deviation obtained between the observed and calculated intensities was less than 0.04. Dehydrogenation of the teta species and the Co(teta)X species has been observed in the spectra, but the intensity of these peaks are minor in comparision to the Co(teta) cluster.

The teta complexes of Cu and Ni also display dehydrogenation of the M (teta) species. The nickel complex and the copper complexes are analogous to the cobalt complexes with the dehydrogenation occurring with losses of one hydrogen at a time. The BMASBD data for the copper complexes of $[Cu(teta)](ClO_4)_2$ and $[Cu(teta)]Cl_2$ are given in appendix III, pages A42-A43. The results for the nickel complex may also be found in appendix III, page A44.

The least squares method of obtaining mole fractions for successive loss and gain of hydrogens does not represent the best statistical approach (33). It was suggested that the Bayesian Statistical Method would prove to be a more appropriate method to analyze this data. The Bayesian method had been used successfully in the analysis of data obtained from the EI spectra of such compounds as $H_3B_3N_3Cl_3$ and $GeC_{12}H_{10}$ which produced overlapping spectra as a result of successive loss and gain of hydrogens (33). The Bayesian program was written in Fortran by S. M. Rothstein and L. M. Karrer as part of the latter's 4th year thesis (52).

The compound chosen for analysis was the $[Co(teta)Cl_2]ClO_4$ complex. The reproducibility run 85RP2, which had 25 scans collected, was the data set selected. Twenty scans of the 85RP2 sample run were selected as it had been previously shown that this represented a good data set. (See sections C1 and C2 of this chapter.) The program was debugged and results were obtained for the $[Co(teta)Cl_2]ClO_4$ complex. The mole fractions obtained from the Bayesian analysis gave a poor fit for observed versus calculated peak intensities. The program reduced the input six species to five. The species which were input were Co(teta), Co(teta)-H, Co(teta)-2H, Co(teta)-3H, Co(teta)-4H and Co(teta)-5H. The Co(teta) and Co(teta)-4H were found to have approximately the same mole fraction using the Bayesian method . The Bayesian method reduced these parameters to 5, eliminating the Co(teta)-4H species. This elimination resulted in a final least squares fit and a Bayesian result which exhibited an extremely poor correlation for observed versus calculated values, (see appendix III, page A45).

This poor correlation of data was thought to be a result of two possible problems. The first concerned the possibility that the data from the 85RP2 sample was not within the necessary experimental requirements. It had been found previously that variations in the number of peaks as high as 20% had no adverse affects on the quality of the data (33). A check on the 20 scans showed that the number of peaks varied by approximately 21%, which was slightly higher than allowed. The last 5 scans were

eliminated, reducing the number of scans used to 15 and reducing the variation in the number of peaks detected to 19%. The data improved slightly, but there was still a large discrepancy between observed and calculated intensities.

As the experimental data appeared to be within the designated requirements, the only other possibility was that the poor correlation in observed and calculated intensities was due to poor precision in the data returned from the Burroughs computer. One of the subroutines designed to find a minimum of a function required that the calculated data be returned with four digit accuracy. It was thought that the possibility existed that only one digit accuracy was being returned. To eliminate this possibility the subroutine was rewritten in double precision. With a number of other minor revisions, the program was again run on the 15 scans from the 85RP2 sample.

The revisions to the program using double precision produced very similar data to the single precision program, (see Appendix III, page A46). It is now believed that the problem is not with the program itself. The inability to obtain data that produces a reasonable agreement between observed and calculated intensities, is most probably a result of statistically poor experimental data. To obtain statistically reproducible data of reasonable quality for the Bayesian Method, it may be necessary to collect data in which the experimental parameters vary by only a small margin; this is difficult with samples that produce low sensitivity data. BMASABD does not impose the same rigorous

statistical requirements on the data as does the Bayesian Method. The data in Table 11, while not having the statistical rigour of the Bayesian approach, are still valid on chemical and mass spectrometric grounds.

6) Explanation for Dehydrogenation

It is not uncommon for complexes of the $Me_6[14]aneN_4$ ligand to undergo dehydrogenation reactions. In fact, oxidative dehydrogenations have been very useful in the synthesis of new macrocyclic complexes (53). The reaction involves the oxidation of the macrocyclic amine complex to form an imine complex. It was observed by workers in this field that the macrocyclic amine complexes of Ni^{2+}, Cu^{2+} and Fe^{2+} undergo oxidative dehydrogenations, whereas, the complexes of Co^{3+} are resistant to oxidation (54). This indicated that the net reaction involved prior oxidation of the metal ion, followed by oxidation of the ligand and subsequent reduction of the metal ion. Figure 27 illustrates the typical reactions for two of the better characterized systems (55). The reactions illustrated may be carried out in steps and the trivalent metal intermediate isolated for the Cu, Ni and Fe complexes. Note that the maximum possible hydrogen loss is eight (see Figure 27). A stepwise reaction scheme involving a +3 intermediate has been proposed for these ligand reactions and is illustrated in Figure 28. The reaction is believed to operate through a coordinated ligand radical intermediate (56).

It has been observed in this study that the spectra of the

Figure 27: The Products of the Oxidation of the $Me_6[14]aneN_4$ Complexes of Fe and Ni

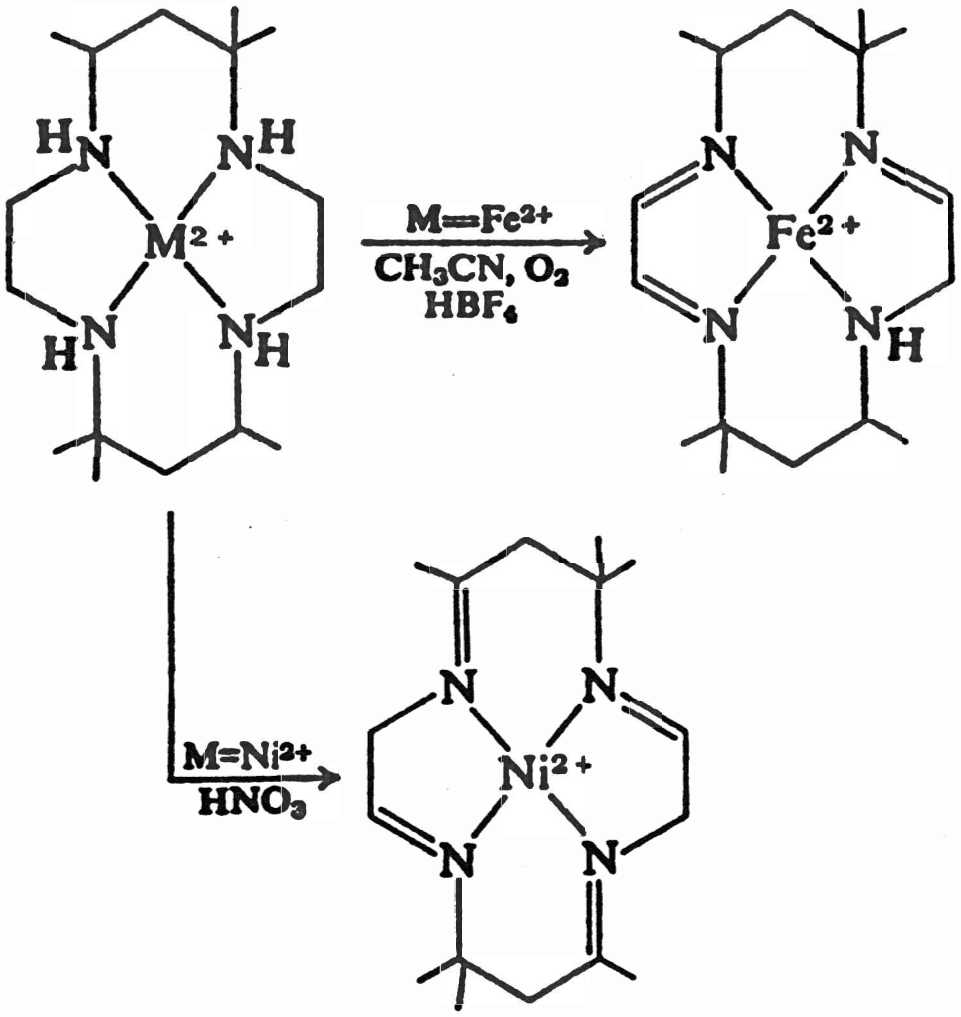

Figure 28: The Reaction Scheme Proposed for the Dehydrogenation of the Metal Complexes of $Me_6[14]aneN_4$

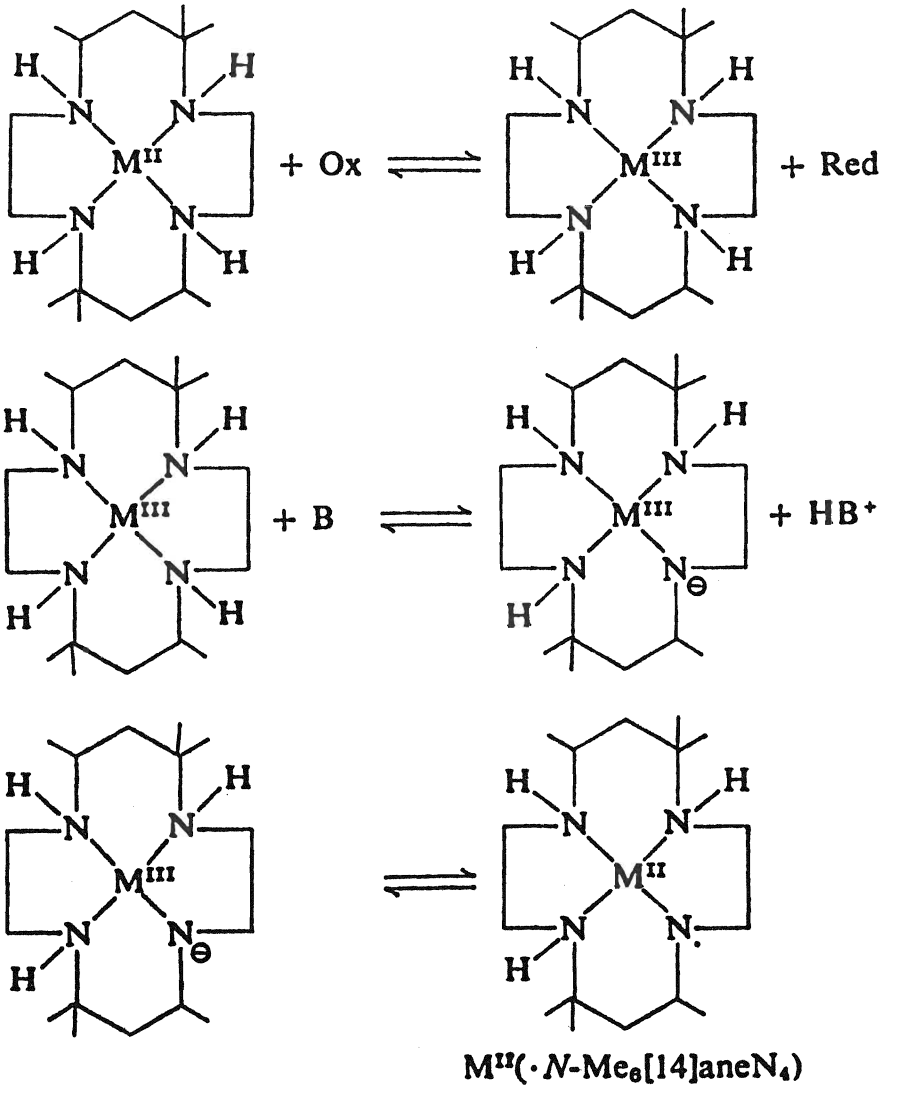

$M^{II}(\cdot N\text{-}Me_6[14]aneN_4)$

$M^{II}(\cdot N\text{-}Me_6[14]aneN_4) + Ox \rightleftharpoons M^{III}(\cdot N\text{-}Me_6[14]aneN_4) + Red$

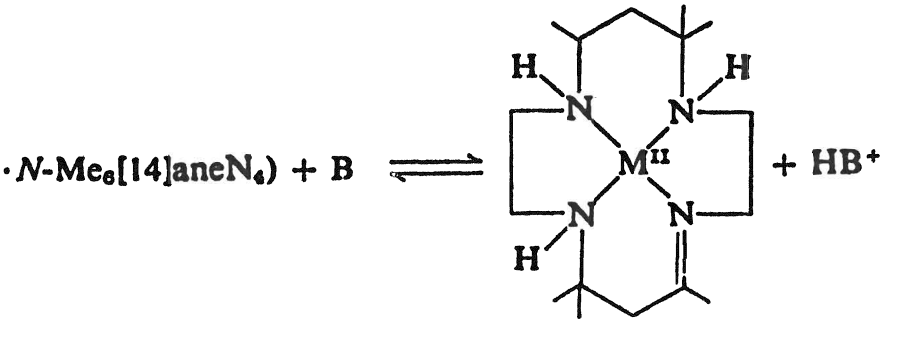

cobalt complexes may contain peaks due to loss of up to 8 hydrogens, for the Co(teta) species, provided there is a strong enough signal. This loss is consistent with what has been observed previously in reactions of the Cu and Fe complexes (53,54). When absolute intensities are poor, loss of up to 5 hydrogens for the cobalt species is still easily observed. A five proton loss has also been observed in the spectra of the nickel complex for the Ni(teta) species. Loss of hydrogens for the coordinated ligand copper species has also been observed in the FAB spectra of $[Cu(teta)]Cl_2$ and $[Cu(teta)](ClO_4)_2$, (refer to the BMASABD calculations in appendix III). This loss of hydrogens occurs in glycerol, thioglycerol and 30% glycerol in sulfolane. The reaction occurs independently of the matrix which indicates that it is not due to a specific matrix/ion reaction.

As all the complexes behave similarly, it is unlikely that the oxidative dehydrogenation mechanism (Figure 28) is operative, as cobalt is not known to undergo this type of reaction. For Co^{3+} to undergo this particular mechanism, cobalt would have to exist as a +4 intermediate. The +4 oxidation state exists only for a few compounds of cobalt and therefore it is unlikely that the +4 intermediate is formed. (Reduction is more commonly observed in the FAB spectra of coordinated compounds (16,20,57)). The mechanism given for dehydrogentation illustrated in Figure 28 requires that the metal in the +2 oxidation state dehydrogenate in the Cu and Ni complexes and the metal in the +3 oxidation state dehydrogenate for the Co complexes. Dehydrogenation of the metal complex in the +2 state is observed to a small extent in the Cu and Ni complexes, but

it is minor in comparision to what is observed in the spectra for the complexes in the +1 oxidation state. In the cobalt complexes no dehydrogenation is observed in the +3 oxidation state, but dehydrogenation does occur in the +1 oxidation state. The oxidative dehydrogenation mechanism illustrated in figure 28 does not fit what has been observed using FAB mass spectrometry, for the obove mentioned reasons.

The solution chemistry of these complexes in the +1 oxidation state have no parallel to the reaction observed in FAB-MS. Dehydrogenation of the +1 oxidation state has not been observed in the electrochemistry of these complexes (58-60). It has been noted by Busch and coworkers, however that the overall oxidation-reduction behavior of the macrocyclic metal complexes is a function of the degree and type of ligand unsaturation (60). In general, it has been found that cyclic tetramine complexes are slightly more difficult to reduce than the diene complexes of Co, Fe, Ni and Cu (41). This is a result of the increased stability of the +1 oxidation state due to unsaturation of the ligand. It is therefore possible that the dehydrogenation observed for the +1 oxidation state is a result of stabilization of the +1 oxidation state.

In the Cu(I) complexes it is necessary to have some degree of unsaturation in the ligand in order for Cu(I) macrocyclic complexes to exist in solution. It has been postulated that this behaviour was related to σ and π-bonding features of the Cu(I) macrocycle (61). It is possible if unsaturation exists for Cu(I) to transfer electron density to low energy antibonding orbitals of the ligand through a π mechanism (62), and as a result stabilize the Cu(I)

complex. The stabilization possible when unsaturation exists is evident if one considers the following example; $Ni^{II}(Me_4[14]1,3,8,10\text{-tetraeneN}_4)^{2+}$ undergoes two electrochemically reversible one-electron reductions at -0.82v and -1.15v producing Ni(I) and Ni(0), contrasted with $Ni^{II}([14]1,4,8,11\text{-tetraeneN}_4)^{2+}$ whose reduction occur at -1.35v and -2.0v. The first complex, which undergoes reduction much more readily, contains an α-diimine ligand while the second complex contains an isolated imine. The conjugated diimine delocalizes the added electron density to a large degree, and the added electron has predominantly ligand character, which stabilizes the lower valence states (60).

It should be noted from the above discussion that the complexes of Cu(I), Ni(I) and Co(I) are more stable if some degree of unsaturation is present to allow delocalization of the electron density into the macrocyclic ring. In the FAB spectra of these complexes, dehydrogenation is observed for the +1 oxidation state. This dehydrogenation results to produce a more stable form for the complexes in the +1 oxidation state, which accounts for the large peaks observed around the $\underline{M}^{I}$(teta) species in FAB-MS.

The dehydrogenation occurs to stabilize the +1 oxidation state, however the mechanism of this reaction is not known. Although the oxidative dehydrogenation mechanism given in the literature has been eliminated as a possibility, it is possible that a mechanism similar to this is operative, involving a lower oxidaton state intermediate than +3 or +4. In the Ni and Cu complexes, the $\underline{M}^{I}$(teta) ion may be oxidized to $\underline{M}^{II}$(teta) and then dehydrogenate. This explanation would account for the abundance of dehydrogenated species observed

for the $\underline{M}^{I}$(teta) ion in the spectra of the copper and nickel complexes. The cobalt complex could also undergo a similar reaction, oxidation of the $Co(teta)X^{+}$ ion from +2 to +3 which would explain the presence of the dehydrogenated $Co(II)(teta)X^{+}$ ions. The unsaturated +2 ions thus generated could then be readily reduced to the +1 state, as unsaturation stablizes the +1 oxidation state. Further experimentation is required in order to determine whether the oxidative dehydrogenation mechanism proposed is operative. The use of partially oxidizing matrices containing nitro groups such as nitrobenzyl alcohol and nitrophenyl octyl ether could be tried to see their effect on the dehydrogenation reactions. The results obtained using nitrobenzyl alcohol as the matrix for $[Co(teta)(CN)_2]ClO_4$ and $[Cu(teta)](ClO_4)_2$ are given in Appendix V as this work was done after the thesis was submitted.

7) Ring Size

In Section C of chapter I, three criteria were introduced that a mass spectroscopic technique should provide. One of these provisions was that the technique predict the chemical reactivity of the compounds of interest. Perhaps one of the most important aspects of these compounds chemically is their pronounced ability to bind metal ions. Therefore, it would be useful if in FAB a trend could be observed, parallelling the strength of the metal to ligand bond.

When a metal ion is coordinated within the $Me_6[14]aneN_4$ ligand, the donor atoms are constrained to occupy the coordination sites

about the metal ion, with the lone pairs of electrons oriented toward the metal ion. In most instances, the four nitrogen atoms lie in the plane, thus allowing the ligand to adopt a relatively strain-free conformation. Strain is introduced if the donor atoms are required to move inwards or outwards from these preferred sites to accomodate a metal ion. The distance from the center to a nitrogen is approximately 2.07 A^0 for the least strained conformation for $Me_6[14]aneN_4$ (63). Therefore, for greatest stability of the complex, the metal-ion must be within this best-fit distance to provide the best metal-nitrogen interaction.

A number of studies have involved the determination of which metal ion best fits the macrocycle and as a result determine which metal ion will bind the strongest to the ligand. Busch and coworkers studied the relationship between metal-donor distance and ring size in macrocyclic complexes (64). Table 12 gives the ideal bond lengths for a variety of ring sizes. Busch demonstrated that there is an ideal ring size for any given metal ion having a given metal-donor atom distance and that ring sizes slightly smaller (0.1-0.2 A^0 in terms of M-N distance) than the best fit ring show abnormally strong metal-donor bonds, while rings that are slightly oversized show substantially decreased metal-donor interactions. Most transition metal-nitrogen linkages fall within the 1.8-2.4 A^0 range spanned by the values given in Table 12.

If the metal-nitrogen distances for the macrocyclic complex are known, it is possible to predict a trend in terms of the relative strength of the bond to the macrocycle. Table 13 gives the metal-nitrogen distances for a number of tetradentate nitrogen

Table 12: Ideal Metal-Nitrogen Bond Lengths and Planarity of Macrocyclic Ligands (64).

Ring Size	Average Ideal Bond Length (A^0)	Average Deviation from the ideal N_4 plane A^0
[12]	1.83	0.41
[13]	1.92	0.12
[14]	2.07	0.00
[15]	2.22	0.14
[16]	2.38	0.00

Table 13: Metal-Nitrogen Distances in some Tetradentate Complexes.

Complex	M -N(a)	[M -N]	Atomic Radii (70)
$[CoLa(N_3)_2]N_3$ (65)	1.94	-0.13	0.69
$[Ni(teta)]Cl_2$ (38)	1.96	-0.11	0.63
$[Ni(teta)Cl_2]$ (38)	2.08	0.01	0.83
$[Ni(cyclam)Cl_2]$ (66)	2.06	-0.01	0.83
$[Cu(teta)](ClO_4)_2$ (67)	2.04	-0.03	0.71
$[Cu(cyclam)](ClO_4)_2$ (68)	2.02	-0.05	0.71
$[ZnL_bCl]ClO_4$ (69)	2.20	0.13	0.82

(a) All the distances and atomic radii are given in A^0

L_a = C-meso-5,12-dimethyl-1,4,8,11-tetra-azacyclotetradecane

cyclam = 1,4,8,11-tetra-azacyclotetradecane

L_b = 1,4,8,11-tetramethyl-1,4,8,11-tetra-azacyclotetradecane

containing complexes whose structures are known. The metal-nitrogen distances for the Co and Ni teta complexes have not been published. There is, however, a reasonable correlation between the structures of other tetra-aza ligands and teta in terms of their binding to nitrogen and so these have been cited. Note that the cyclam M-N distances are given for those teta analogues whose structures have been published and that these distances are in good agreement with those of teta.

The atomic radii can also be used as an indication of the strength of the metal to ligand bond. As the atomic radius increases in size, the fit between the ring and the metal ion becomes poorer. The increased size means that the metal ion will no longer fit in the hole of the macrocyclic ring and as a result, alteration will occur in the metal-donor linkage which reduces the strength of the M-N bond (71). The atomic radii are also given in Table 13.

From the consideration of a substantial array of data derived from x-ray structure determinations, Co(III) complexes have been found to coordinate in a trans-octahedral geometry and to have in general a range of 1.94-2.03 A^0 for their Co(III)-N distance (64), which is consistent with the structure given in Table 13. Busch found that the octahedrally coordinated Ni(II) ion has a Ni(II)-N distance approxiamtely 0.1-0.15 A^0 greater than the Co(III)-N distance. He also found on examination of x-ray data that the square planar Ni(II) complexes had approximately the same M-N distance as the low-spin octahedral Co(III). Therefore, the

14-membered macrocyclic ring fits low spin Co(III) and Ni(II) best (72), and the [15]aneN$_4$ fits the high spin Ni(II). This is in agreement with the data presented in Table 12 and Table 13. The bond distances and atomic radii provided in Table 13 indicates that the trend in terms of decreasing bond strength should be Co(III) >Ni(II)(square planar) >Cu(II) >Ni(II)(octaheral) >Zn(II).

Table 14 provides the mass spectral data for the metal complexes. The trend observed in terms of the intensity of the $[\underline{M}(teta)]^+$ peak in the glycerol matrix is as follows: Co(III)>Ni(II)>Cu(II)>Zn(II). The intensity of the metal-ligand peak thus seems to provide a good estimate of the ability of the metals to bind to the macrocycle. The trend observed in the glycerol matrix is not observed in the thioglycerol matrix. The copper complex is out of sequence, which is not surprising as copper has a tendency to bind strongly to sulfur. It is probable that in this instance the complex is reacting with the sulfur containing matrix which causes the copper complex to appear out of sequence. The remainder of the series does not appear to be effected by the thioglycerol matrix.

8) π-Acidity

Another aspect of the chemical reactivity of these compounds that was hoped would be mimicked using FAB was their solution

Table 14: Metal Complexes of Teta.

Matrix	Compound	Ion Intensities[a] $[N]^{+}$.[b]	$[N-Cl]^{+}$	$[N-2Cl]^{+}$	$[N-M-2Cl]^{+}$
Glycerol					
	[c] $[Co(teta)Cl_2]^{+}$	5	100	100	17
	$[Ni(teta)]Cl_2$	---	7	75	100
	$[Cu(teta)]Cl_2$	---	19	31	100
	$Zn(teta)Cl_2$	---	100	3	4
Thioglycerol					
	$[Co(teta)Cl_2]^{+}$	61	100	64	---
	$[Ni(teta)]Cl_2$	---	3	71	100
	$[Cu(teta)]Cl_2$	---	70	100	49
	$Zn(teta)Cl_2$	---	100	3	6

a Relative intensities are normalized to the most intense ion above or equal to the mass of the $[teta]^{+}$ ion. Isotope cluster peak intensities of the same elemental composition are also summed and included with the parent species.
b N= M (teta)Cl_2 where M is the metal ion of interest.
c Cobalt compound is $[Co(teta)Cl_2]ClO_4$

chemistry. The complexes of the type $[Co(teta)X_2]Y$ were studied with the desire to see if a π-acidity trend might be discovered by FAB. The complexes studied were Y=SCN or ClO_4 and X=NO_2, SCN, CN and Cl. Two different matrices were used for the study, glycerol and thioglycerol. In the glycerol matrix, it was discovered that the C^+-X species was more intense than the C^+ species. In thioglycerol, the opposite trend was observed. This type of effect is not uncommon and may be explained in terms of the reducing potential of the matrix. Pelzer et al investigated the oxidation-reduction chemistry of glycerol solutions submitted to ion (SIMS) or atom (FAB) bombardment. It was discovered that a reduction process occurred in glycerol for both inorganics and organics (73). It was concluded that the reduction process occurring in the FAB of glycerol solutions could be governed by a simple redox equilibrium between hydrogen atoms produced in glycerol by bombardment and the oxidized species present in solution. In other common solvents, such as diethanolamine and tetraglyme, the reduction process was less severe. Meili and Seibl also investigated matrix effects in the FAB analysis of cobalamines (74). They concluded that if any metal containing system appears to give as the highest ion in FAB a species corresponding to the reduction of the metal, then a slightly oxidizing matrix is advisable.

In glycerol, C^+-X is more intense than C^+, which coincides with glycerol's reducing behaviour (11). This corresponds to the following equation:

[2] $[Co^{III}(teta)X_2]^{+*} \rightarrow [Co^{II}(teta)X]^{+} + X^{\cdot}$

The asterisk on the precursor complex indicates a thermally excited vibrational state. The process in equation 1 involves reduction of the Co(III) center to Co(II) accompanied by the formation of a X radical; this process is favored over X dissociation (shown in equation 2) since no peak is seen where the dicationic species would appear.

[3] $[Co^{III}(teta)X_2]^{+*} \rightarrow [Co^{III}(teta)X]^{2+} + Cl^{-}$

Since glycerol is enhancing reduction, according to Meili a slightly oxidizing matrix should produce the opposite affect, increase the C^{+} cation. This is in fact what is observed, the C^{+} peak is more intense than the $C\text{-}X^{+}$ peak. Thus, the thioglycerol is sufficiently oxidizing to produce the desired molecular ion. It may then be concluded that the matrix must be kept constant in comparing trends among complexes. Table 15 lists the intensity of the C^{+} and the C^{+}-X species for the complexes of interest in both glycerol and thioglycerol. Previous workers have used a ratio of C^{+}/C^{+}-X when making comparisons in spectra of similar complexes (75), where C+ is the cation and C^{+}-X represents the cation minus an axial ligand.

In both matrices, the trend observed is that of $CN^{-} > NO_2^{-} > SCN^{-} > Cl^{-}$ in terms of the relative intensity of the parent ion versus loss of the axial ligand. This is a familar trend in terms of the ability of the ligand to split the d-orbitals.

The ordering of ligands in terms of decreasing Dq is termed the spectrochemical series. This may be written as: $I^{-} < Br^{-} < Cl^{-}$

Table 15: Comparison of C^+ and C^+-X for the Series of Cobalt Complexes $[Co(teta)X_2]Y$ in Glycerol and Thioglycerol.

Complex	C^+	C^+-X	C^+/C^+-X
Matrix: Glycerol			
$[Co(teta)Cl_2]ClO_4$	2.2	45.2	1/21
$[Co(teta)(SCN)_2]SCN$	1.2	17.6	1/15
$[Co(teta)(NO_2)_2]ClO_4$	1.9	5.6	1/3
$[Co(teta)(CN)_2]ClO_4$	3.1	6.3	1/2
Matrix: Thioglycerol			
$[Co(teta)Cl_2]ClO_4$	27.1	44.5	0.6/1
$[Co(teta)(SCN)_2]SCN$	18.0	22.7	0.8/1
$[Co(teta)(NO_2)_2]ClO_4$	9.5	3.2	3/1
$[Co(teta)(CN)_2]ClO_4$	53.3	2.7	20/1

$<dsep^{-}=S^{2-}=dtp^{-}<N_3^{-}<F^{-}<dtc^{-}<urea=OH^{-}=IO_3^{-}<oxalate^{2-}=malonate^{2-}=O^{2-}<H_2O<SCN^{-}<NO_2^{-}$=bipy=o-phen $<CH_3^{-}$=ph$^{-}<CN^{-}$ <constrained phosphite=CO (76). Those ligands which are pi-acceptors lie at the high end, while ligands such as halides with moderately large pi-donor character fall at the low end of the series. The series obtained by mass spectrometry for the teta cobalt complexes parallels the spectrochemical series (see Table 15). This is in accord with known solution behavior of these type of complexes. In a study by Martin and Busch on complexes of the type $Ni([14]aneN_4)X_2$, it was found that the Dq^z decreased according to the normal spectrochemical series $Br^{-}<Cl^{-}<N_3^{-}<NCS^{-}$ (77).

The ultraviolet data for a number of the cobalt complexes synthesized was provided in a study by Whimp and Curtis (37) and is given below.

Table 16: Reflectance Spectra for the Complexes $[Co(teta)X_2]Y$ in 10^{-3} cm^{-1}.

Complex	$^1A_{1g}$--->$^1T_{1g}$	$^1A_{1g}$--->$^1T_{2g}$
$[Co(teta)Cl_2]ClO_4$	20.9,15.3	25.2,28.1
$[Co(teta)(CN)_2]ClO_4,H_2O$	20.4,16.0	28.7
$[Co(teta)(NCS)_2]SCN,H_2O$	20.0,18.7	24.0,26.7
$[Co(teta)(NO_2)_2]ClO_4,1/2H_2O$	20.0	25.2,26.3

Using this data and the method developed by Wentworth and Piper

(78), the crystal field splitting parameters Dq^{xy} and Dq^{z} may be calculated, where Dq^{xy} is the in plane ligand field splitting parameter and Dq^{z} is the axial ligand field splitting parameter. As observed, the $^1T_{1g} <--- {}^1A_{1g}$ band is split into two components the $^1E_g{}^a <--- {}^1A_{1g}$ and $^1A_{2g} <--- {}^1A_{1g}$, and a complete ligand field analysis may be done based on a D_{4h} model. When both low symmetry components derived from the first octahedral band are observed, a complete calculation of Dq^{xy} and Dq^{z} is possible according to:

[4] $Dq_{xy} = (1/10)(\ ^1A_{2g} <--- {}^1A_{1g} + C)$

[5] $Dt = (-4/35)(^1E_g{}^a <--- {}^1A_{1g} - \ ^1A_{2g} <--- {}^1A_{1g})$

[6] $Dq^{z} = Dq^{xy} - (7/4)Dt$

where C is commonly taken as 3800 cm^{-1} (71). Table 17 below provides the values of Dq^{xy} and Dq^{z} obtained.

Table 17: Ligand Field Spectral Parameters for the Complexes of the type $[Co(teta)X_2]Y$.

Compound	Dq^{xy}	Dq^{z}
$[Co(teta)Cl_2]ClO_4$	2470	1350
$[Co(teta)(NCS)_2]SCN$	2380	2120
$[Co(teta)(CN)_2]ClO_4$	1980	2860

Note that for the nitro complex the first octahedral band is not split and therefore cannot be interpreted in any detail. Three

bands are observed for the dicyano complex; however, the ^1A2g level has dropped below the ^1Eg level because cyanide is a stronger ligand than the macrocycle (71), see Table 16. From Table 17 the following trend is observed in terms of the ability to split the d orbitals $CN^- > SCN^- > Cl^-$. The FAB results parallel this trend. The variation in the Dq^{xy} parameter is a result of the variation of the axial ligand. It has been previously found that the value of Dq^{xy} decreases as the value of Dq^z increases which is also the trend observed in Table 17 (72).

9) FAB as an Identification Method for Coordination Compounds

In an attempt to prepare $Zn(NO_3)_2$(teta), a compound was obtained whose elemental analysis was inconsistent with the dinitrate formulation (see chapter II Table 4).

A positive ion FAB-MS was done on the unknown compound in both glycerol and thioglycerol. (The spectra obtained for the zinc complex in glycerol and thioglycerol are given in appendix II, pages A33 and A34.) In glycerol a large conglomeration of peaks was obtained centered around m/z 429. The isotope pattern did not match any of the expected fragments, but it did appear to contain zinc. The thioglycerol spectrum had a large peak at m/z 383, as well as the peak at m/z 429. Figure 29 gives the BMASROS calculation of the $(Zn(teta)Cl)^+$ species and the peak obtained at m/z 383. Note that the pattern obtained from the BMASROS matches well the pattern obtained in the thioglycerol spectrum. The

spectrum clearly indicated the presence of chloride in the complex. The presence of chloride was not possible unless there was contamination in either $Zn(NO_3)_2.6H_2O$ or the teta ligand. (The teta turned out to contain chloride; see appendix IV.)

The peak at m/z 429 corresponded to $Zn(teta)Cl(NO_2)$. The BMASROS calculated intensities of this species along with the observed pattern is also given in Figure 29. The discrepancy observed between the calculated pattern and the observed cluster is a result of dehydrogenation of the $Zn(teta)Cl(NO_2)$ species. The BMASABD results given in Table 18, provides evidence that this is what had occurred. The elmental analysis of this complex matched $Zn(teta)Cl(NO_2)$ with one water of hydration.

It appears that FAB is a useful technique in the identification of this compound. The FAB-MS of the $Zn(teta)(NO_2)Cl$ provided not only the molecular weight for this complex but also gave an indication of the complexity of the compound through identifiction of the fragments present. This satisfies the other two criteria of a good mass spectroscopic technique listed in the introduction.

Figure 29: A Comparison of the Observed and Calculated Isotope Patterns for the Zn(teta)Cl(NO_2) and Zn(teta)Cl(NO_2)-2H Species.

(a) Observed Isotope Patterns

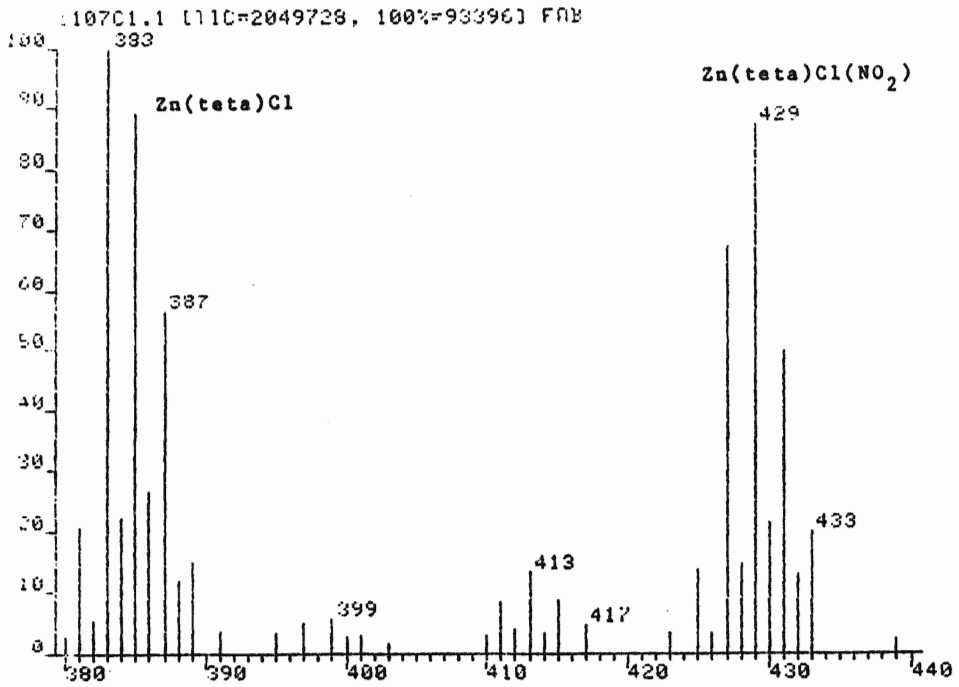

(b) Calculated Isotope Patterns

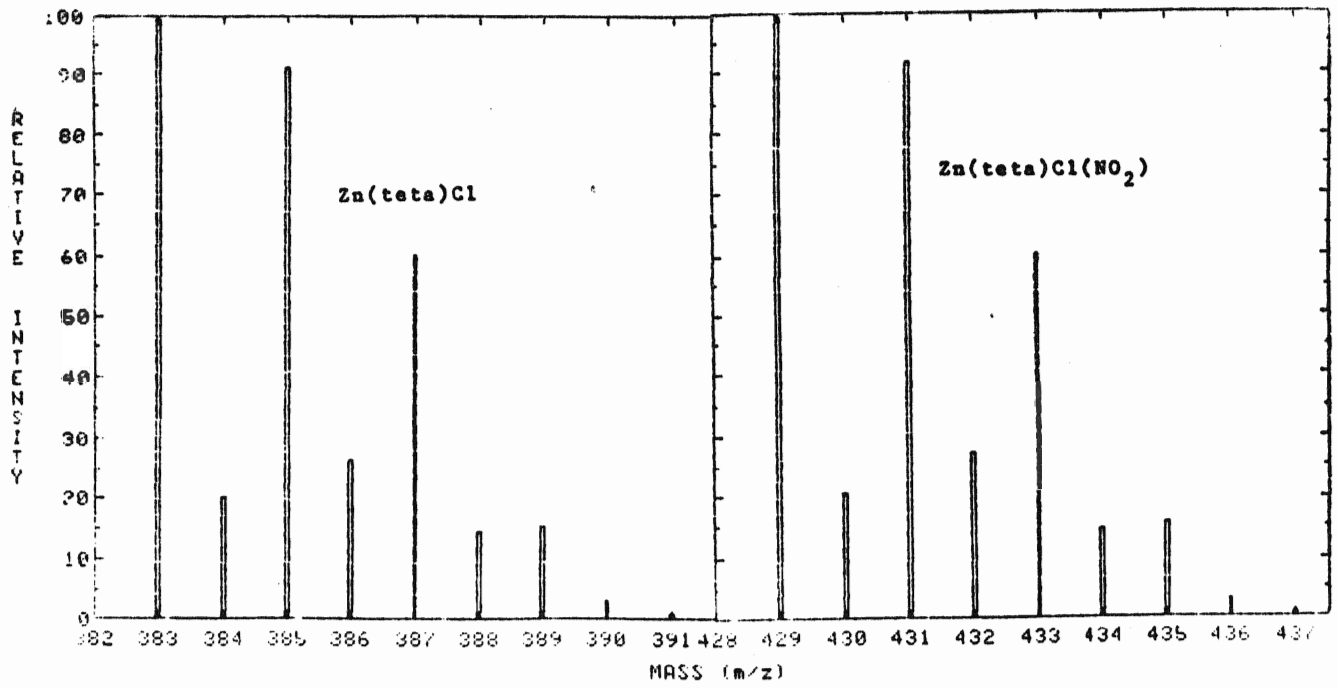

Table 18: The Data from the BMASABD Calculation of the Complex $Zn(teta)Cl(NO_2)$

(a) The % Composition of the Fragments

Fragment	% Composition
$Zn(teta)Cl(NO_2)$	17.77760
$Zn(teta)Cl(NO_2)$-2H	82.22240

(b) Observed and Calculated Averaged Intensities

m/z	Observed	Calculated	Difference
435	0.00000	0.19757	-0.19757
434	0.00000	0.13245	-0.13245
433	0.90000	0.92140	-0.02140
432	0.60000	0.65989	-0.05989
431	2.30000	2.58594	-0.28594
430	1.00000	1.00951	-0.00951
429	4.00000	3.65751	0.34249
428	0.70000	0.65951	0.04049
427	3.10000	3.22840	-0.12840

Average Deviation = 0.135

IV CONCLUSION

The major emphasis in this study was to determine whether FAB was a suitable technique for the identification of the 5,5,7,12,12,14-hexamethly-1,4,8,11-tetra-azacyclotetradecane metal complexes. To be considered a suitable technique, the spectra obtained should provide; (a) molecular weight information (b) information concerning the structural complexity through fragmentation and (c) predict the chemical reactivity of the complexes of interest.

Molecular weights were obtained in the majority of the spectra. There were exceptions such as the nitrite-containing cobalt complexes and the complexes containing two metal ions. The problem in producing quality spectra for these complexes was their insolubility, a prerequisite for obtaining a good spectrum being sufficient solubility in the matrix.

In those complexes which yielded good spectra, the ion with the greatest intensity at high m/z could be attributed to the complex. Peaks did occur at high m/z values which could not be attributed to the complex (see Figure 12 the peak at 485), but these were usually of minor intensity. The cobalt complexes gave spectra containing the intact cation $[Co(teta)X_2]$, and the fragments from this cation. These complexes did not have ions corresponding to the (cation+anion) in positive ion FAB. Information concerning the anion could be easily obtained using negative FAB-MS.

There was some confusion caused by the perchlorate counterion in the cobalt and copper complexes. A peak was observed in the cobalt complexes which was identified as the $[Co(teta)ClO_4]^+$ ion. This would cause some confusion in the spectra where the cation intensity is weak, as the intensity of the $[Co(teta)ClO_4]^+$ peak would dominate the spectra. Such confusion would occur in the nitrite and azide complexes where only peaks of low intensity were observed. The perchlorate ion also decomposed to produce Cl^- ions, which complexed with the M (teta) species in the spectra of the $[Cu(teta)](ClO_4)_2$ complex and the perchlorate-containing cobalt complexes. Due to this complexation, peaks were observed which would indicate the presence of a chloride ion where it should not have been observed. This would result in the incorrect formulation of the compound.

The metal complexes in the +2 oxidation state had the M (teta) peak as the highest peak in the spectrum. No other peaks could be identified at higher m/z values. Although this provides information concerning the metal and the anion present, it would not allow for the complete identification of the complex. The oxidation state of the metal would still be lacking for a total determination. In the zinc complex $ZnClNO_2$(teta) it was possible to identify both the anions through the fragments obtained in the FAB spectrum of this compound. However, the coordination sphere of the complex cannot be identified. The complex could be either four, five or six coordinate, although a five coordinate complex

is more probable (69).

The information obtained through a comparison of peak heights allowed for the determination of the chemical reactivity of the complexes. A π-acidity trend was determined through a comparison of the C^+ and C^+-X peaks which parallelled known solution behavior. The strength of the metal-to-teta bond was determined by a comparison of the height of the M $(teta)^+$ ion, which was comparable to known bond strengths. The utility of FAB mass spectral data to predict the chemistry of these complexes should not be overlooked.

The FAB-MS fulfilled the requirements to be considered a good mass spectral method for the characterization of the complexes of teta. FAB should provide a reliable and quick method for the identification of these macrocyclic complexes as well as others. Care is required where the solubility of the compound is poor or where the counterion could cause interferences. The use of FAB-MS for macrocyclic compounds has shown itself to be a dependable technique and should greatly facilitate the progress in the area of macrocyclic coordination compounds.

REFERENCES

1. L. C. E. Taylor, Industrial Research and Development, Sept. (1981).

2. K. L. Busch and G. Cooks, Science, 218 , 247 (1982).

3. Ronald D. MacFarlane, Acc. Chem. Res., 15 , 268-275 (1982).

4. H. D. Beckey, Int. J. Mass Spectrom. Ion Phys., 2 , 500 (1969).

5. D. H. Williams, C. Bradley, G. Bojesen, S. Santikarn and L. C. E. Taylor, J. Am. Chem. Soc., 103 , 5700 (1981).

6. A. Benninghoven, D. Jaspers, W. Sichtermann, Appl. Phys., 11 , 35 (1976).

7. M. A. Posthumus, P. G. Kistemaker, H. L. C. Meuzelaar, M. C. ten Noever de Brauw, Anal. Chem., 50 , 985 (1978).

8. M. Barber, R. S. Bordoli, R. D. Sedgwick, A. N. Tyler, J. Chem. Soc., Chem. Commun., 325 (1981).

9. M. Barber, R. S. Bordoli, E. J. Elliott, R. P. Sedgwick and A. N. Tyler, Anal. Chem., 54 , 645A (1982).

10. M. Barber, R. S. Bordoli, R. D. Sedgwick and A. N. Tyler, Nature, 293 , 270 (1981).

11. B. Sundqvist, P. Roepstorff, J. Fohlman, A. Hedin, P. Hakansson, I. Kamensky, M. Lindberg, M. Salehpour and G. Sawe, Science, 226 ,696 (1984).

12. I. Katakuse, H. Nakabushi, T. Ichihara, Int. J. Mass Spec. Ion Processes, 57 , 239-242 (1984).

13. M. Barber, R. S. Bordoli, R. D. Sedgwick and A. N. Tyler; Biomed. Mass Spec., 8 , 492, (1981).

14. J. Van der Greef and M. C. ten Noever de Brauw, Int. J. Mass Spec. Ion Phys., 46 , 379-382 (1983).

15. J. M. Miller: "Fast Atom Bombardment Mass Spectrometry and Related Techniques," in Adv. Inorg. Chem. and Radiochem., H. J. Emeleus and A. G. Sharp, eds., Academic Press, New York, 28 , (1984).

16. R. L. Cerny, B. P. Sullivan, M. M. Bursey and T. J. Meyer, Inorg. Chem., 24 , 397 (1985).

17. T. R. Sharp, M. R. White, J. F. Davis and P. J. Stang, Org. Mass Spectrom., 19 , 107-117 (1984).

18. R. Davis, I. F. Groves, J. L. A. Durrant, J. Organomet. Chem., 241 , C27-C30 (1983).

19. R. D. Minard, and G. L. Geoffroy, 30th Anual Conference on Mass Spectrometry, 321 (1982).

20. R. L. Cerny, B. P. Sullivan, M. M. Bursey, T. J. Meyer, Anal. Chem., 55 , 1954-1958 (1983).

21. R. L. Cerny, M. M. Bursey and J. R. Hass: Abstr. 31st Conference ASMS, Boston, 369, May (1983).

22. A. Dell, R. C. Hider, M. Barber, R. S. Bordoli, R. D. Sedgwick and A. N. Tyler, J. B. Neilands, Biomed. Mass Spectrom., 9 , 158 (1982).

23. A. Dell, H. R. Morris, M. D. Levin and S. M. Hecht, Biochem. and Biophys. Res. Commun., 102 , 730 (1981).

24. G. Puzo, J. C. Prome, J. P. Macquet and I. A. S. Lewis, Biomed. Mass Spec., 9 , 552 (1982).

25. A. I. Cohen, K. A. Glaven and J. F. Kronauge, Biomed. Mass Spectrom., 10 , 287-9 (1983).

26. C. E. Costello, J. W. Brodack, A. G. Jones, A. Davison, D. L. Johnson, S. Kasina and A. R. Fritzberg, J. Nucl. Med., 24 , 353-355 (1983).

27. C. E. Costello, H. Pang, A. Davison and A. G. Jones; Abstr. 31st. Conf. ASMS, Boston, 377, May (1983).

28. R. A. W. Johnstone and M. E. Rose, J. Chem. Soc. Chem. Commun., 1268, (1983).

29. R. A. W. Johnstone and I. A. S. Lewis, Int. J. Mass Spectrom. and Ion Phys., 46 , 451-454 (1983).

30. C. R. Paige and M. F. Richardson, Can. J. Chem., 62 , 332-335 (1985).

31. G. A. Melson, "Coordination Chemistry of Macrocyclic Compounds", Plenum Press, New York, 10 (1979).

32. M. R. Litzow and T. R. Spalding, "Mass Spectrometry of Inorganic and Organometallic Compounds", Elsevier Scientific Publishing Co., New York, N. Y. 559 (1973).

33. L. M. Karrer, H. L. Gordon, S. M. Rothstein, J. M. Miller, and T. B. Jones, Anal. Chem., 55 , 1724 (1983).

34. M. R. Burke, H. B. Sc. Thesis, Brock University, 1981

35. M. R. Burke and M. F. Richardson, Inorg. Chim. Acta., 69 , 29-35 (1983).

36. D. P. Rillema, J. F. Encicott, and E. Papaconstaninou, Inorg. Chem., 10 , 1739 (1971).

37. P. O. Whimp and N. F. Curtis, J. Chem. Soc. (A), 867-871 (1966).

38. Tasuku Ito and Koshiro Toriumi, Acta. Cryst., B37 , 88-92 (1981).

39. M. Tait and D. H. Busch, Inorganic Synthesis, 18 , 13 (1978).

40. K. B. Mertes, Inorg. Chem., 17 , 49-52 (1978).

41. P. S. Bryan and J. C. Dabrowiak, Inorg. Chem., 14 , 296-299 (1975).

42. N. F. Curtis, J. Chem. Soc., 2644-2650 (1964).

43. Mei-Yi Zhang and Xi-Yun Liang, Anal. Chem., 56 , 2288 (1984).

44. B. E. Douglas ed., Inorg. Syn., 18 , 12 (1978).

45. J. C. Dabrowiak, P. H. Merrell and D. H. Busch, Inorg. Chem., 11 , 1979 (1972).

46. F. H. Field, J. Phys. Chem., 86 , 5115 (1982).

47. "The Random House College Dictionary", edited by J. Stein, Random House,Inc., New York, N. Y. (1984).

48. F. A. Cotten and G. Wilkinson, "Advanced Inorganic Chemistry", 4th ed., John Wiley and Sons, Inc., New York, 174 (1980).

49. Ref. 48, p. 560

50. P. O. Whimp, and N. F. Curtis, J. Chem. Soc. (A), 188 (1968).

51. J. M. Miller and T. R. B. Jones, "The Chemistry of Functional Groups" Part 1, John Wiley and Sons, edited by Saul Pati and Zvi Rappoport, Great Britain, 96 (1983).

52. L. M. Karrer, H. B. Sc. Thesis, Brock University, 1982

53. C. J. Hipp, L. F. Lindoy and D. H. Busch, Inorg. Chem., 11 , 1988 (1972).

54. G. M. Brown, T. R. Weaver, F. R. Keene and T. J. Meyer, Inorg. Chem., 15 , 190 (1976).

55. Ref. 31, p.431

56. E. K. Barefield and M. T. Mocella, J. Am. Chem. Soc., 4238 97 , (1975).

57. Gustav Bojesen, Organic Mass Spectrometry, 20 , 413 (1985).

58. J. Vasilevskis and D. C. Olson, Inorg. Chem., 10 1228 (1971).

59. D. C. Olson and J. Vasilevski, Inorg. Chem., 10 , 463 (1971).

60. F. V. Lovecchio, E. Gore, and D. H. Busch, J. Am. Chem. Soc., 96 , 3109 (1974).

61. L. Fabbrizzi, A. Lari and A. Poggi, Inorg. Chem. 21 , 2083 (1982).

62. L. Fabbrizzi and A. Poggi, J. Chem. Soc. Dalton Trans., 2191 (1983).

63. Ref. 31, p. 228

64. L. Y. Martin, L. J. DeHayes, K. H. Zompa and D. H. Busch, J. Am. Chem. Soc., 96 , 4046 (1974).

65. R. J. Restivo, G. Ferguson, R. W. Hay & D. P. Piplani, J. C. S. Dalton, 1131 (1978).

66. B. Bosnich, R. Mason, P. J. Pauling, G. B. Robertson, & M. L. Tobe, Chemical Commun., 97 (1965).

67. R. Clay, J. Murray-Rust & P. Murray-Rust. J. C. S. Dalton, 1135 (1979).

68. P. A. Tasker & L. Skalar, J. Cryst. Mol. Structrue, 5 , 329-344 (1975).

69. N. W. Alcock, N. Herron & P. Moore, J. C. S. Dalton, 1282 (1978).

70. J. E. Huheey, "Inorganic Chemistry" 2nd ed., Harper & Row Publishers, New York, N. Y., 71-74 (1978).

71. Y. Hung, L. Y. Martin, S. C. Jackels, A. M. Tait and D. H. Busch, J. Am. Chem. Soc., 99 , 4029 (1977).

72. D. H. Busch, Acc. Chem. Res., 11 , 392 (1978).

73. G. Pelzer, E. DePauw, Dao Viet Dung, and J. Marien, J. Phys. Chem., 88 , 5065 (1984).

74. J. Meili & J. Seibl, 31st Annual Conf. on Mass Spec. (ASMS) Boston, May (1983).

75. J. Miller, J. Organomet. Chem., 249 , 299-302 (1983).

76. A. B. P. Lever, "Inorganic Electronic Spectroscopy 2nd.", Elsevier Science Publishers B. V. New York, N. Y. (1984) p.751

77. L. Y. Martin, C. R. Sperati and D. H. Busch, J. Am. Chem. Soc., 99 , 2968 (1977).

78. R. A. D. Wentworth and T. S. Piper, Inorg. Chem., 4 , 709 (1965).

APPENDIX I

The Positive Ion FAB Mass Spectra of the Cobalt Complexes of Teta

FAB of $[Co(teta)Cl_2]ClO_4$ in Thioglycerol

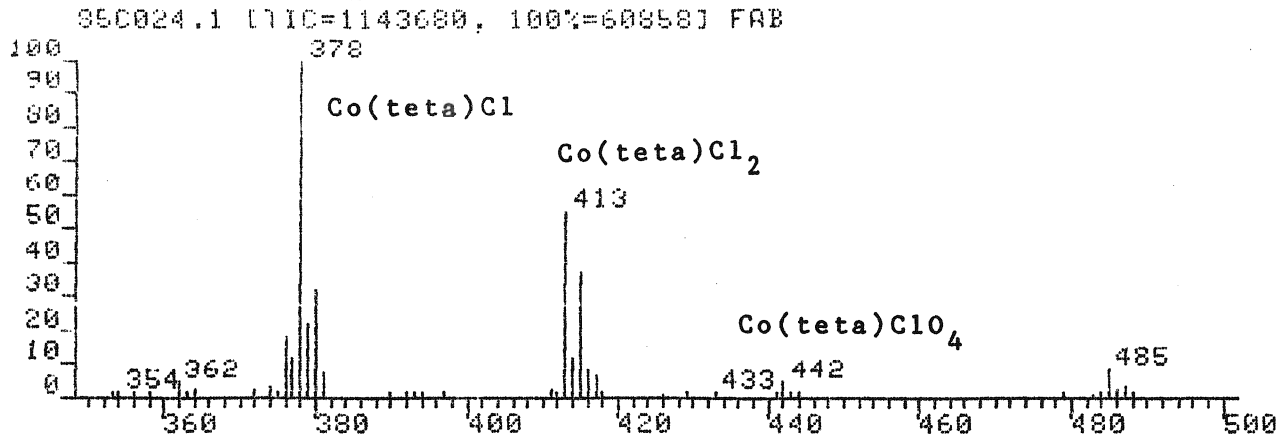

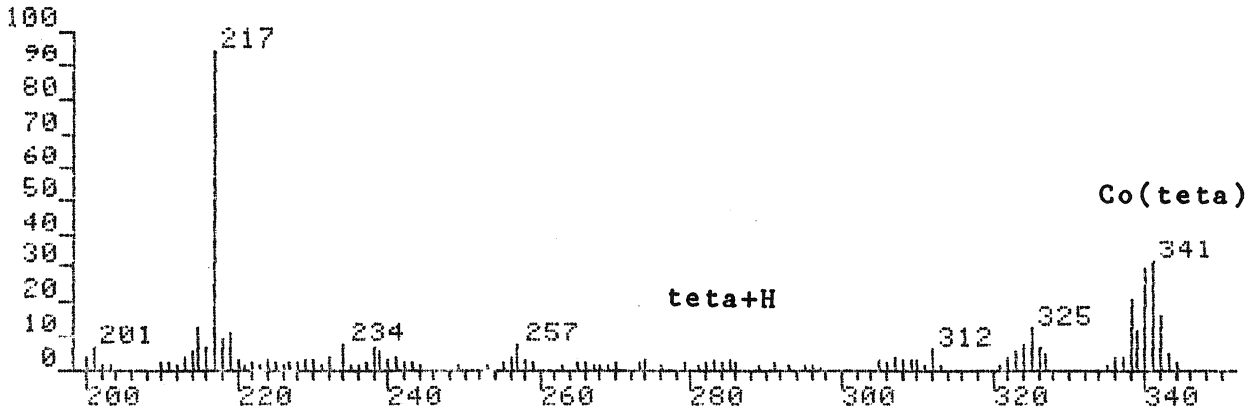

DP4:85C024.MS
SCAN: 1. 6/26/85 13: 8

IONISATION: FAB
NO. PEAKS: 247
BASE/NREF INT: 140292./ 140292.
TIC: 1143680.
MASS RANGE: 69 - 488

PEAK NO.	MEASURED MASS	NO. POINTS	ABSOLUTE INTENSITY	% INT. BASE	% INT. NREF	% TOT. ION
2	487	25	1895.	1.4	1.4	0.2
3	486	25	1493.	1.1	1.1	0.1
4	485	35	5194.	3.7	3.7	0.5
10	442	29	2846.	2.0	2.0	0.2
16	417	29	3967.	2.8	2.8	0.3
17	416	35	4828.	3.4	3.4	0.4
18	415	43	22578.	16.1	16.1	2.0
19	414	35	7177.	5.1	5.1	0.6
20	413	43	33568.	23.9	23.9	2.9
22	411	25	1540.	1.1	1.1	0.1
28	381	35	4218.	3.0	3.0	0.4
29	380	43	18961.	13.5	13.5	1.7
30	379	35	13460.	9.6	9.6	1.2
31	378	51	60858.	43.4	43.4	5.3
32	377	35	7068.	5.0	5.0	0.6*
33	376	43	11247.	8.0	8.0	1.0
35	374	29	1849.	1.3	1.3	0.2*
36	372	29	1495.	1.1	1.1	0.1
39	362	29	3124.	2.2	2.2	0.3
45	343	35	2977.	2.1	2.1	0.3
46	342	43	9927.	7.1	7.1	0.9
47	341	43	19568.	13.9	13.9	1.7
48	340	59	18132.	12.9	12.9	1.6*
49	339	43	7216.	5.1	5.1	0.6*
50	338	59	12565.	9.0	9.0	1.1*
51	337	43	2292.	1.6	1.6	0.2*
52	336	29	2014.	1.4	1.4	0.2
54	327	35	3011.	2.1	2.1	0.3
55	326	43	4308.	3.1	3.1	0.4
56	325	43	7383.	5.3	5.3	0.6
57	324	35	4805.	3.4	3.4	0.4
58	323	35	3403.	2.4	2.4	0.3
59	322	29	2186.	1.6	1.6	0.2
62	312	35	3800.	2.7	2.7	0.3
64	310	29	1872.	1.3	1.3	0.2
65	309	29	1637.	1.2	1.2	0.1
66	308	29	1559.	1.1	1.1	0.1*
67	307	25	1997.	1.4	1.4	0.2
69	305	25	1516.	1.1	1.1	0.1
77	285	29	1801.	1.3	1.3	0.2
79	283	25	1569.	1.1	1.1	0.1
84	274	29	1809.	1.3	1.3	0.2
94	258	29	1719.	1.2	1.2	0.2
95	257	35	4396.	3.1	3.1	0.4
96	256	29	2019.	1.4	1.4	0.2
102	242	21	1413.	1.0	1.0	0.1
103	241	35	2209.	1.6	1.6	0.2
104	240	29	1757.	1.3	1.3	0.2
105	239	35	3224.	2.3	2.3	0.3
106	238	35	3936.	2.8	2.8	0.3
110	234	35	4800.	3.4	3.4	0.4
111	232	29	2446.	1.7	1.7	0.2
113	230	25	1752.	1.2	1.2	0.2
114	229	25	1648.	1.2	1.2	0.1
119	224	25	1608.	1.1	1.1	0.1
123	220	25	1676.	1.2	1.2	0.1
124	219	35	6711.	4.8	4.8	0.6
125	218	35	5723.	4.1	4.1	0.5
126	217	51	57498.	41.0	41.0	5.0
127	216	35	4301.	3.1	3.1	0.4
128	215	43	7576.	5.4	5.4	0.7
129	214	35	3363.	2.4	2.4	0.3
130	213	29	2004.	1.4	1.4	0.2
136	201	35	4322.	3.1	3.1	0.4
137	200	29	2224.	1.6	1.6	0.2

FAB of $[Co(teta)Cl_2]ClO_4$ in Glycerol

622CM1.1 [TIC=5167360, 100%=2420841 FAB

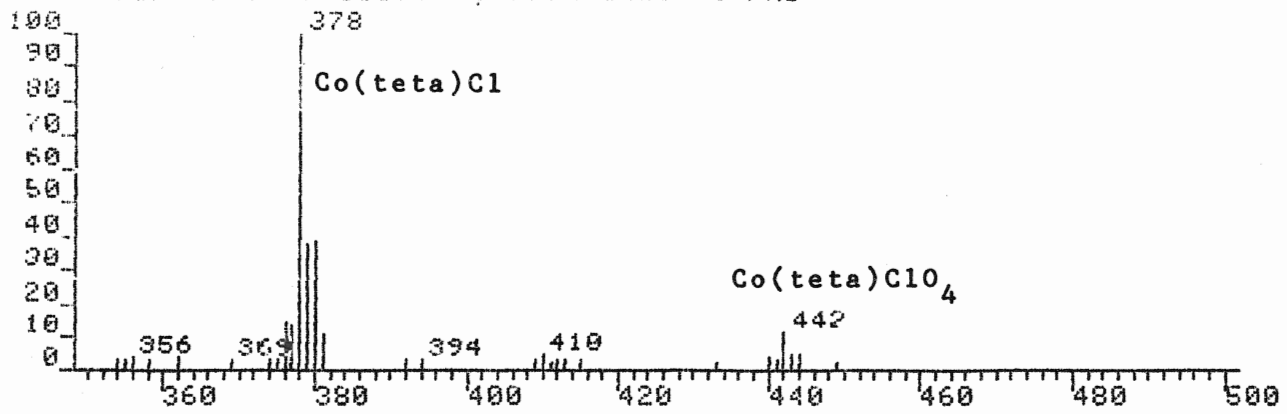

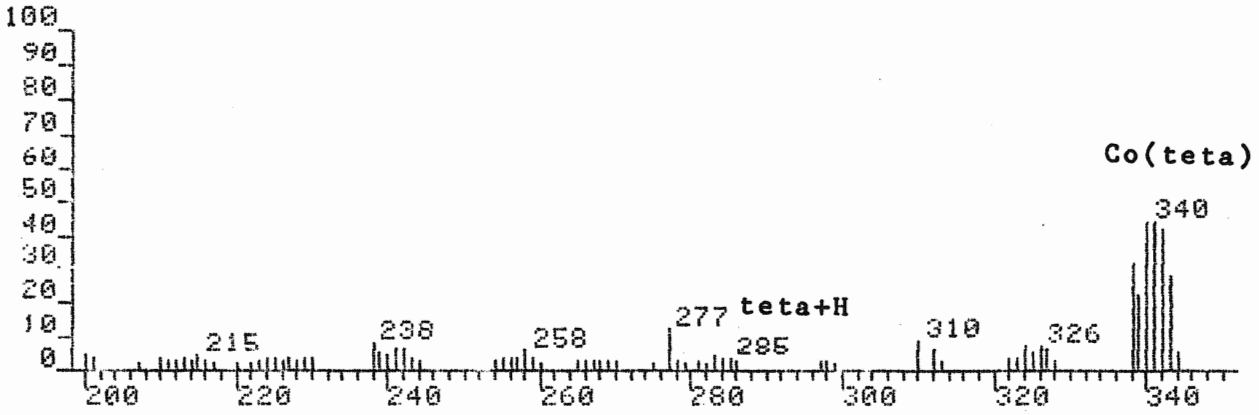

DP4:622CM1.MS
SCAN: 1, 6/22/84 12: 4

IONISATION: FAB
NO. PEAKS: 205
BASE/NREF INT: 869024./ 869024.
TIC: 5167360.
MASS RANGE: 53 - 449

PEAK NO.	MEASURED MASS	NO. POINTS	ABSOLUTE INTENSITY	% INT. BASE	% INT. NREF	% TOT. ION
2	444	51	11392.	1.3	1.3	0.2*
3	443	51	11655.	1.3	1.3	0.2
4	442	59	27993.	3.2	3.2	0.5
12	410	51	11091.	1.3	1.3	0.2
16	381	59	27389.	3.2	3.2	0.5
17	380	87	93768.	10.8	10.8	1.8*
18	379	87	91700.	10.6	10.6	1.8*
19	378	103	242084.	27.9	27.9	4.7*
20	377	71	33577.	3.9	3.9	0.6*
21	376	71	35786.	4.1	4.1	0.7*
30	344	59	13296.	1.5	1.5	0.3
31	343	71	67704.	7.8	7.8	1.3
32	342	103	101872.	11.7	11.7	2.0*
33	341	103	107848.	12.4	12.4	2.1*
34	340	175	108004.	12.4	12.4	2.1*
35	339	143	53437.	6.1	6.1	1.0*
36	338	287	78632.	9.0	9.0	1.5*
38	327	59	16662.	1.9	1.9	0.3
39	326	59	18686.	2.2	2.2	0.4
40	325	59	13460.	1.5	1.5	0.3
41	324	71	17827.	2.1	2.1	0.3
42	323	87	9159.	1.1	1.1	0.2
43	322	71	9293.	1.1	1.1	0.2
45	312	59	16901.	1.9	1.9	0.3
46	310	239	22695.	2.6	2.6	0.4
51	285	71	10353.	1.2	1.2	0.2
53	283	71	11408.	1.3	1.3	0.2
58	277	59	29163.	3.4	3.4	0.6
68	258	59	13913.	1.6	1.6	0.3

PEAK NO.	MEASURED MASS	NO. POINTS	ABSOLUTE INTENSITY	% INT. BASE	% INT. NREF	% TOT. ION
69	257	51	9702.	1.1	1.1	0.2
70	256	71	9838.	1.1	1.1	0.2
71	255	59	8782.	1.0	1.0	0.2
74	243	59	9712.	1.1	1.1	0.2
75	242	71	16290.	1.9	1.9	0.3
76	241	59	15814.	1.8	1.8	0.3
77	240	59	11180.	1.3	1.3	0.2
78	239	59	13263.	1.5	1.5	0.3
79	238	59	21295.	2.5	2.5	0.4
81	229	51	9208.	1.1	1.1	0.2
83	227	51	9074.	1.0	1.0	0.2
85	225	71	9506.	1.1	1.1	0.2
86	224	59	8917.	1.0	1.0	0.2
92	215	51	11389.	1.3	1.3	0.2
99	201	51	9362.	1.1	1.1	0.2
100	200	59	11358.	1.3	1.3	0.2

FAB of $[Co(teta)Cl_2]Cl$ in Thioglycerol

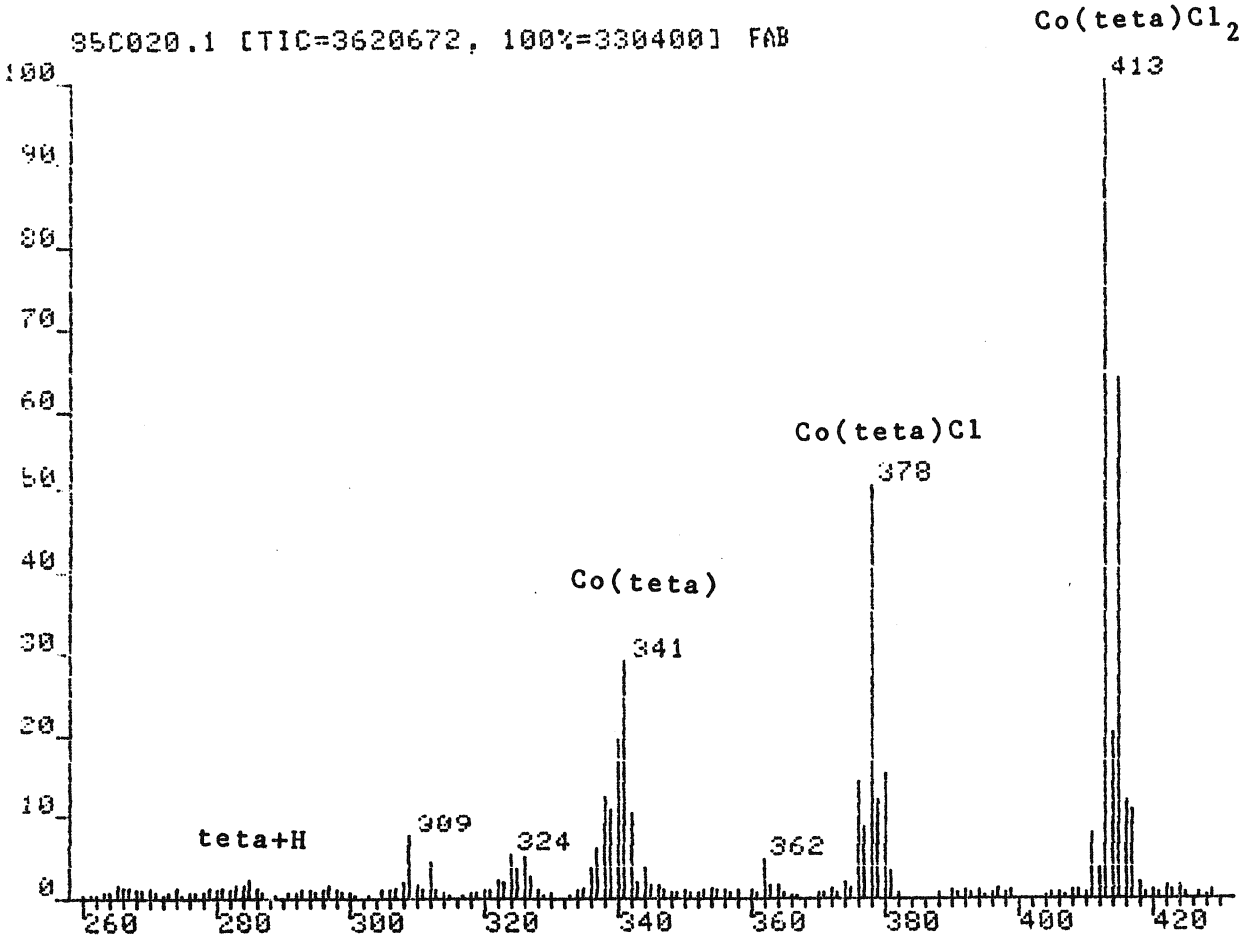

DP4:85C020.MS
SCAN: 1. 6/25/85 14:49

IONISATION: FAB
NO. PEAKS: 362
BASE/NREF INT: 330400./ 330400.
TIC: 3620672.
MASS RANGE: 69 - 867

PEAK NO.	MEASURED MASS	NO. POINTS	ABSOLUTE INTENSITY	% INT. BASE	% INT. NREF	% TOT. ION
32	424	35	5141.	1.6	1.6	0.1
34	422	29	5124.	1.6	1.6	0.1
38	418	35	6790.	2.1	2.1	0.2
39	417	51	35600.	10.8	10.8	1.0
40	416	59	40141.	12.1	12.1	1.1%
41	415	71	209924.	63.5	63.5	5.8%
42	414	59	66788.	20.2	20.2	1.8%
43	413	103	330400.	100.0	100.0	9.1%
44	412	51	11999.	3.6	3.6	0.3%
45	411	51	26009.	7.9	7.9	0.7%
55	397	35	4329.	1.3	1.3	0.1
65	381	43	9979.	3.0	3.0	0.3
66	380	51	51238.	15.5	15.5	1.4%
67	379	51	39806.	12.0	12.0	1.1%
68	378	71	166824.	50.5	50.5	4.6%
69	377	71	28340.	8.6	8.6	0.8%
70	376	59	47082.	14.2	14.2	1.3
71	375	35	4108.	1.2	1.2	0.1
72	374	43	6357.	1.9	1.9	0.2%
74	372	35	3863.	1.2	1.2	0.1
80	364	35	5198.	1.6	1.6	0.1
81	363	35	4441.	1.3	1.3	0.1
82	362	43	15021.	4.5	4.5	0.4
85	358	35	3383.	1.0	1.0	0.1%
89	354	35	3927.	1.2	1.2	0.1
97	346	71	5089.	1.5	1.5	0.1%
98	345	71	4875.	1.5	1.5	0.1%
99	344	87	12030.	3.6	3.6	0.3%
100	343	59	6595.	2.0	2.0	0.2%
101	342	71	34236.	10.4	10.4	0.9%
102	341	71	96196.	29.1	29.1	2.7%
103	340	71	64169.	19.4	19.4	1.8%
104	339	71	35551.	10.8	10.8	1.0%
105	338	87	40555.	12.3	12.3	1.1%
106	337	87	19738.	6.0	6.0	0.5%
107	336	71	11684.	3.5	3.5	0.3%
108	335	59	4190.	1.3	1.3	0.1%
114	327	43	8360.	2.5	2.5	0.2
115	326	43	15903.	4.8	4.8	0.4
116	325	51	11978.	3.6	3.6	0.3%
117	324	51	16980.	5.1	5.1	0.5%
118	323	51	6872.	2.1	2.1	0.2%
119	322	51	7555.	2.3	2.3	0.2%
127	313	29	3411.	1.0	1.0	0.1
128	312	43	13903.	4.2	4.2	0.4
130	310	51	4607.	1.4	1.4	0.1%
131	309	175	24616.	7.5	7.5	0.7%
132	308	71	6029.	1.8	1.8	0.2%
133	307	51	3556.	1.1	1.1	0.1%
141	297	43	5166.	1.6	1.6	0.1
150	286	43	4192.	1.3	1.3	0.1
151	285	51	7250.	2.2	2.2	0.2
152	284	35	4654.	1.4	1.4	0.1
153	283	43	5869.	1.8	1.8	0.2
155	281	35	3463.	1.0	1.0	0.1%
157	279	35	3666.	1.1	1.1	0.1
162	274	43	4123.	1.2	1.2	0.1
166	270	35	4394.	1.3	1.3	0.1
169	267	35	3611.	1.1	1.1	0.1
170	266	35	3492.	1.1	1.1	0.1
171	265	35	5444.	1.6	1.6	0.2

FAB of $[Co(teta)Cl_2]Cl$ in Glycerol

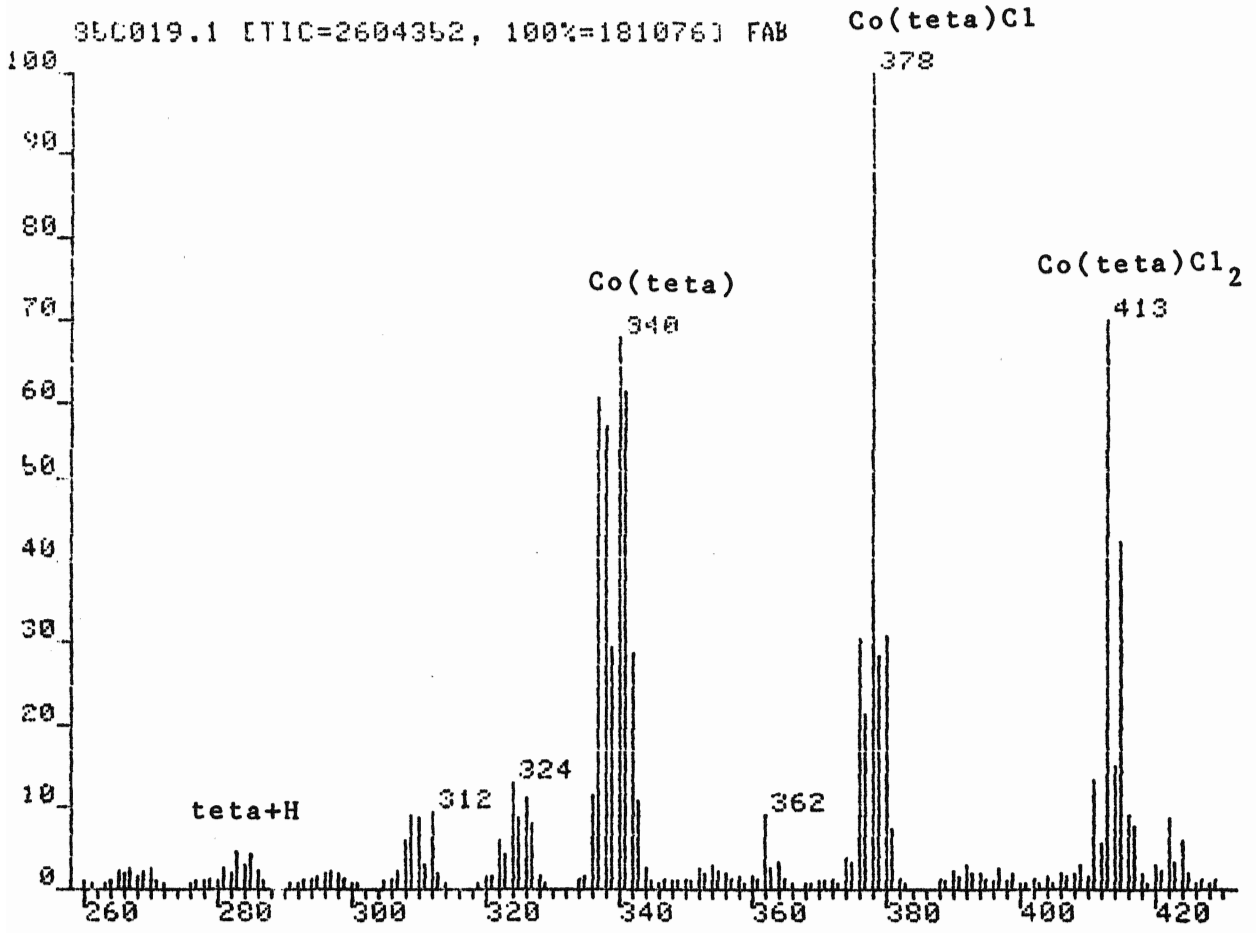

DP4:85C019.MS
SCAN: 1. 6/25/85 14:23

IONISATION: FAB
NO. PEAKS: 339
BASE/NREF INT: 181076./ 181076.
TIC: 2604352.
MASS RANGE: 68 - 865

PEAK NO.	MEASURED MASS	NO. POINTS	ABSOLUTE INTENSITY	% INT. BASE	% INT. NREF	% TOT. ION
44	424	43	10823.	6.0	6.0	0.4
45	423	35	5698.	3.1	3.1	0.2
46	422	43	15076.	8.3	8.3	0.6
47	421	35	3936.	2.2	2.2	0.2
48	420	35	5241.	2.9	2.9	0.2
51	417	43	13257.	7.3	7.3	0.5
52	416	43	16232.	9.0	9.0	0.6%
53	415	59	76412.	42.2	42.2	2.9
54	414	51	27318.	15.1	15.1	1.0%
55	413	71	126756.	70.0	70.0	4.9%
56	412	43	10218.	5.6	5.6	0.4%
57	411	43	24201.	13.4	13.4	0.9%
59	409	35	5263.	2.9	2.9	0.2
60	408	35	3730.	2.1	2.1	0.1
71	397	35	4775.	2.6	2.6	0.2
74	394	35	3718.	2.1	2.1	0.1
76	392	35	4913.	2.7	2.7	0.2
78	390	35	3896.	2.2	2.2	0.1
83	381	43	12869.	7.1	7.1	0.5%
84	380	51	55726.	30.8	30.8	2.1%
85	379	71	51701.	28.6	28.6	2.0%
86	378	87	181076.	100.0	100.0	7.0%
87	377	71	38702.	21.4	21.4	1.5%
88	376	59	55321.	30.6	30.6	2.1%
89	375	43	5900.	3.3	3.3	0.2%
90	374	43	7288.	4.0	4.0	0.3%
99	364	35	5929.	3.3	3.3	0.2
100	363	35	4546.	2.5	2.5	0.2
101	362	43	16321.	9.0	9.0	0.6
107	356	35	3751.	2.1	2.1	0.1
108	355	35	4005.	2.2	2.2	0.2%
109	354	43	4899.	2.7	2.7	0.2%
111	352	43	4367.	2.4	2.4	0.2
119	344	51	4382.	2.4	2.4	0.2%
120	343	51	19360.	10.7	10.7	0.7%
121	342	87	52523.	29.0	29.0	2.0%
122	341	103	110512.	61.0	61.0	4.2%
123	340	119	122400.	67.6	67.6	4.7%
124	339	103	53312.	29.4	29.4	2.0%
125	338	239	103148.	57.0	57.0	4.0%
126	337	351	109344.	60.4	60.4	4.2%
127	336	143	20293.	11.2	11.2	0.8%
132	327	43	14140.	7.8	7.8	0.5
133	326	51	19739.	10.9	10.9	0.8%
134	325	51	15253.	8.4	8.4	0.6%
135	324	71	23531.	13.0	13.0	0.9%
136	323	59	7506.	4.1	4.1	0.3%
137	322	71	10788.	6.0	6.0	0.4%
142	313	35	3729.	2.1	2.1	0.1
143	312	43	17158.	9.5	9.5	0.7
144	311	59	5358.	3.0	3.0	0.2%
145	310	143	15397.	8.5	8.5	0.6%
146	309	143	15598.	8.6	8.6	0.6%
147	308	103	10481.	5.8	5.8	0.4%
148	307	71	4325.	2.4	2.4	0.2%
155	297	43	4200.	2.3	2.3	0.2
156	296	35	3771.	2.1	2.1	0.1
163	286	43	4080.	2.3	2.3	0.2
164	285	51	7853.	4.3	4.3	0.3%
165	284	43	5095.	2.8	2.8	0.2
166	283	51	7969.	4.4	4.4	0.3
167	282	35	3625.	2.0	2.0	0.1
168	281	43	4520.	2.5	2.5	0.2%
176	270	35	4591.	2.5	2.5	0.2
177	269	43	4279.	2.4	2.4	0.2
179	267	43	4363.	2.4	2.4	0.2
181	265	43	4292.	2.4	2.4	0.2

FAB of Co(teta)($CoCl_4$) in Thioglycerol

:5C013.1 [TIC-2795840, 100%=432032] FAB

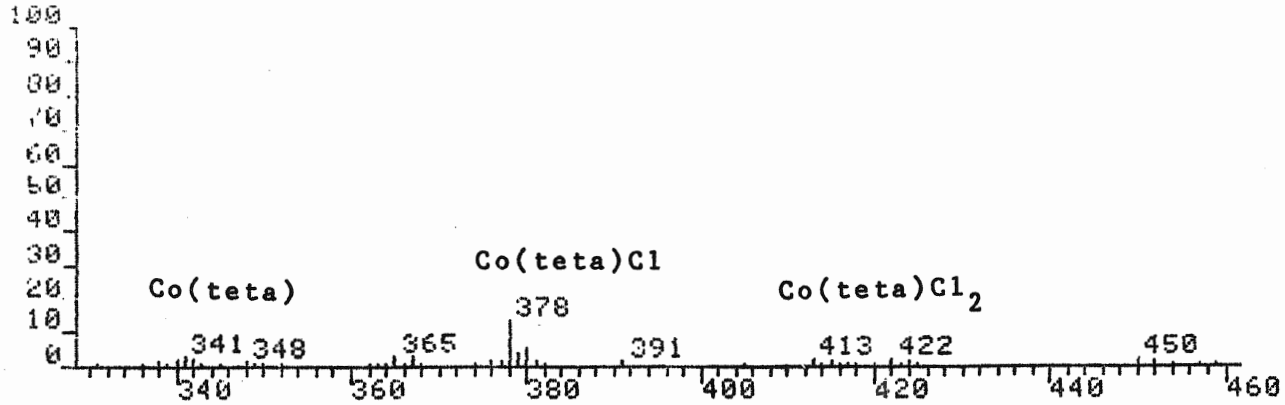

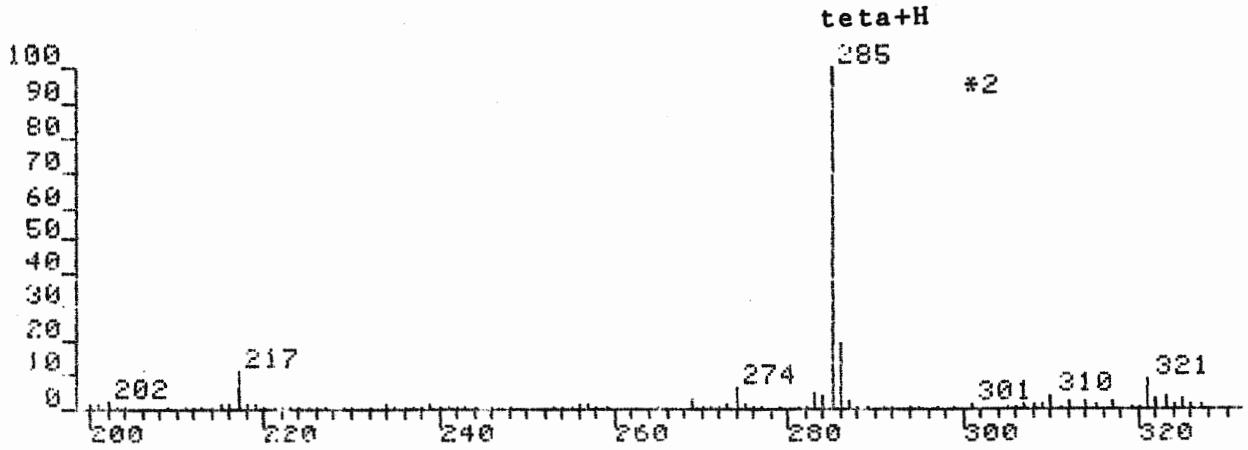

DP4:85C013.MS
SCAN: 1. 3/20/85 14: 9

IONISATION: FAB
NO. PEAKS: 328
BASE/NREF INT: 432032./ 432032.
TIC: 2795840.
MASS RANGE: 32 - 704

PEAK NO.	MEASURED MASS	NO. POINTS	ABSOLUTE INTENSITY	% INT. BASE	% INT. NREF	% TOT. ION
27	452	29	3457.	0.8	0.8	0.1
28	450	35	4234.	1.0	1.0	0.2
30	424	35	3505.	0.8	0.8	0.1
32	422	35	4431.	1.0	1.0	0.2
37	415	35	3362.	0.8	0.8	0.1
39	413	35	4803.	1.1	1.1	0.2
42	391	35	3420.	0.8	0.8	0.1
44	381	43	4101.	0.9	0.9	0.1
45	380	51	11603.	2.7	2.7	0.4
46	379	43	8660.	2.0	2.0	0.3
47	378	43	29041.	6.7	6.7	1.0
48	377	35	3682.	0.9	0.9	0.1
49	376	35	3319.	0.8	0.8	0.1
52	367	43	6329.	1.5	1.5	0.2
54	365	51	6879.	1.6	1.6	0.2
64	342	35	4506.	1.0	1.0	0.2
65	341	35	7035.	1.6	1.6	0.3
66	340	43	4813.	1.1	1.1	0.2
71	327	43	3047.	0.7	0.7	0.1
73	325	51	5541.	1.3	1.3	0.2
74	324	51	3627.	0.8	0.8	0.1
75	323	51	8489.	2.0	2.0	0.3
76	322	51	5639.	1.3	1.3	0.2
77	321	43	18133.	4.2	4.2	0.6
80	317	35	3813.	0.9	0.9	0.1
82	314	43	4073.	0.9	0.9	0.1
83	312	59	4820.	1.1	1.1	0.2
85	310	59	8138.	1.9	1.9	0.3
88	307	59	3500.	0.8	0.8	0.1
91	301	43	3325.	0.8	0.8	0.1
92	299	35	3210.	0.7	0.7	0.1
102	287	51	10446.	2.4	2.4	0.4
103	286	59	83560.	19.3	19.3	3.0*
104	285	87	432032.	100.0	100.0	15.5*
105	284	71	13849.	3.2	3.2	0.5*
106	283	51	21275.	4.9	4.9	0.8*
112	276	35	3759.	0.9	0.9	0.1
113	275	43	4441.	1.0	1.0	0.2
114	274	59	24823.	5.7	5.7	0.9
115	273	43	6126.	1.4	1.4	0.2
117	271	51	3244.	0.8	0.8	0.1
118	270	43	3207.	0.7	0.7	0.1
119	269	43	11093.	2.6	2.6	0.4
124	258	51	4348.	1.0	1.0	0.2
125	257	51	5604.	1.3	1.3	0.2
126	256	59	4439.	1.0	1.0	0.2
127	255	59	3148.	0.7	0.7	0.1*
134	242	59	3067.	0.7	0.7	0.1
135	241	59	3154.	0.7	0.7	0.1
137	239	59	4406.	1.0	1.0	0.2
142	234	35	5173.	1.2	1.2	0.2
145	229	59	3243.	0.8	0.8	0.1*
154	219	43	6906.	1.6	1.6	0.2
155	218	43	6804.	1.6	1.6	0.2
156	217	51	47123.	10.9	10.9	1.7
157	216	43	5069.	1.2	1.2	0.2
158	215	43	6141.	1.4	1.4	0.2
159	214	43	4093.	0.9	0.9	0.1
166	204	51	4309.	1.0	1.0	0.2
168	202	51	8553.	2.0	2.0	0.3
169	201	51	6981.	1.6	1.6	0.2*
170	200	71	5360.	1.2	1.2	0.2*

FAB of $[Co(teta)(SCN)_2]SCN$ in Thioglycerol

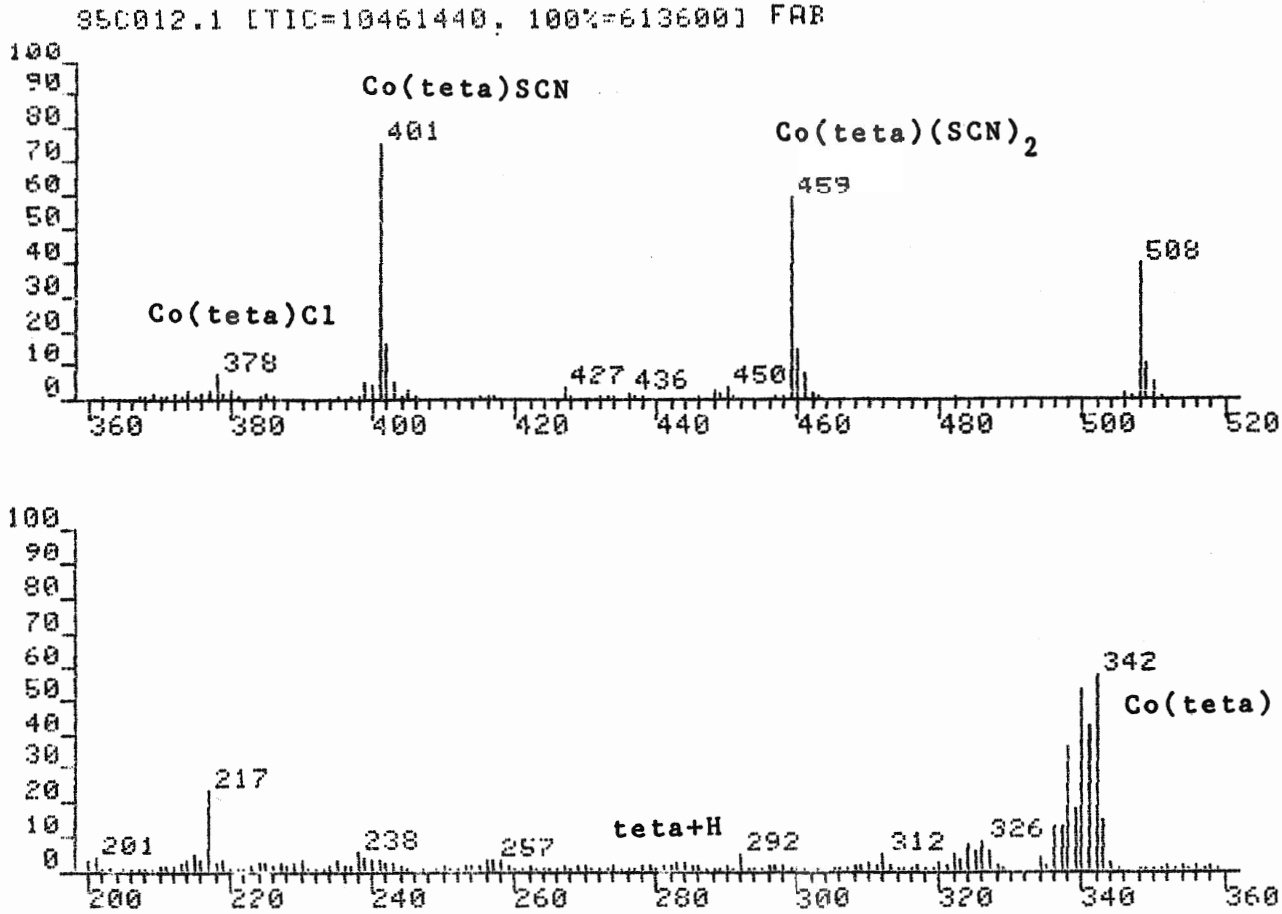

DP4:85C012.MS
SCAN: 1. 3/20/85 13:59

IONISATION: FAB
NO. PEAKS: 417
BASE/NREF INT: 613600./ 613600.
TIC: 10461440.
MASS RANGE: 32 - 565

PEAK NO.	MEASURED MASS	NO. POINTS	ABSOLUTE INTENSITY	% INT. BASE	% INT. NREF	% TOT. ION
9	510	43	29461.	4.8	4.8	0.3
10	509	43	62103.	10.1	10.1	0.6*
11	508	71	241664.	39.4	39.4	2.3*
22	461	43	41831.	6.8	6.8	0.4
23	460	59	85300.	13.9	13.9	0.8*
24	459	87	359664.	58.6	58.6	3.4*
29	450	43	17421.	2.8	2.8	0.2
31	448	35	13780.	2.2	2.2	0.1
50	427	35	16929.	2.8	2.8	0.2
59	405	35	13608.	2.2	2.2	0.1
61	403	43	31059.	5.1	5.1	0.3
62	402	59	100168.	16.3	16.3	1.0*
63	401	103	463520.	75.5	75.5	4.4*
64	400	51	24167.	3.9	3.9	0.2*
65	399	51	28957.	4.7	4.7	0.3*
80	380	43	14423.	2.4	2.4	0.1
82	378	43	43428.	7.1	7.1	0.4
83	377	35	13121.	2.1	2.1	0.1
86	374	43	14866.	2.4	2.4	0.1
114	343	51	89692.	14.6	14.6	0.9*
115	342	103	352624.	57.5	57.5	3.4*
116	341	103	259948.	42.4	42.4	2.5*
117	340	119	326992.	53.3	53.3	3.1*
118	339	87	112656.	18.4	18.4	1.1*
119	338	207	223652.	36.4	36.4	2.1*
120	337	87	80780.	13.2	13.2	0.8*
121	336	143	79124.	12.9	12.9	0.8*
123	334	87	20870.	3.4	3.4	0.2*
126	327	51	30714.	5.0	5.0	0.3
127	326	51	53259.	8.7	8.7	0.5
128	325	59	33909.	5.5	5.5	0.3
129	324	71	48018.	7.8	7.8	0.5*
130	323	71	17532.	2.9	2.9	0.2*
131	322	87	26565.	4.3	4.3	0.3*
141	312	51	28433.	4.6	4.6	0.3
143	310	59	14703.	2.4	2.4	0.1*
160	292	239	30325.	4.9	4.9	0.3*
169	283	59	14357.	2.3	2.3	0.1*
194	258	51	16175.	2.6	2.6	0.2*
195	257	51	17396.	2.8	2.8	0.2
196	256	59	15997.	2.6	2.6	0.2
209	242	51	13561.	2.2	2.2	0.1
210	241	51	19514.	3.2	3.2	0.2
211	240	51	16153.	2.6	2.6	0.2
212	239	59	22388.	3.6	3.6	0.2*
213	238	51	31654.	5.2	5.2	0.3
216	235	43	16659.	2.7	2.7	0.2
221	230	43	15547.	2.5	2.5	0.1
222	229	51	12653.	2.1	2.1	0.1
224	227	51	13596.	2.2	2.2	0.1
226	225	51	12834.	2.1	2.1	0.1
227	224	43	12710.	2.1	2.1	0.1
232	219	43	15939.	2.6	2.6	0.2
233	218	51	14831.	2.4	2.4	0.1
234	217	51	142900.	23.3	23.3	1.4
235	216	59	15703.	2.6	2.6	0.2
236	215	51	26994.	4.4	4.4	0.3
237	214	51	16283.	2.7	2.7	0.2
250	201	51	22157.	3.6	3.6	0.2
251	200	51	18590.	3.0	3.0	0.2

FAB of [Co(teta)(SCN)$_2$]SCN in Glycerol

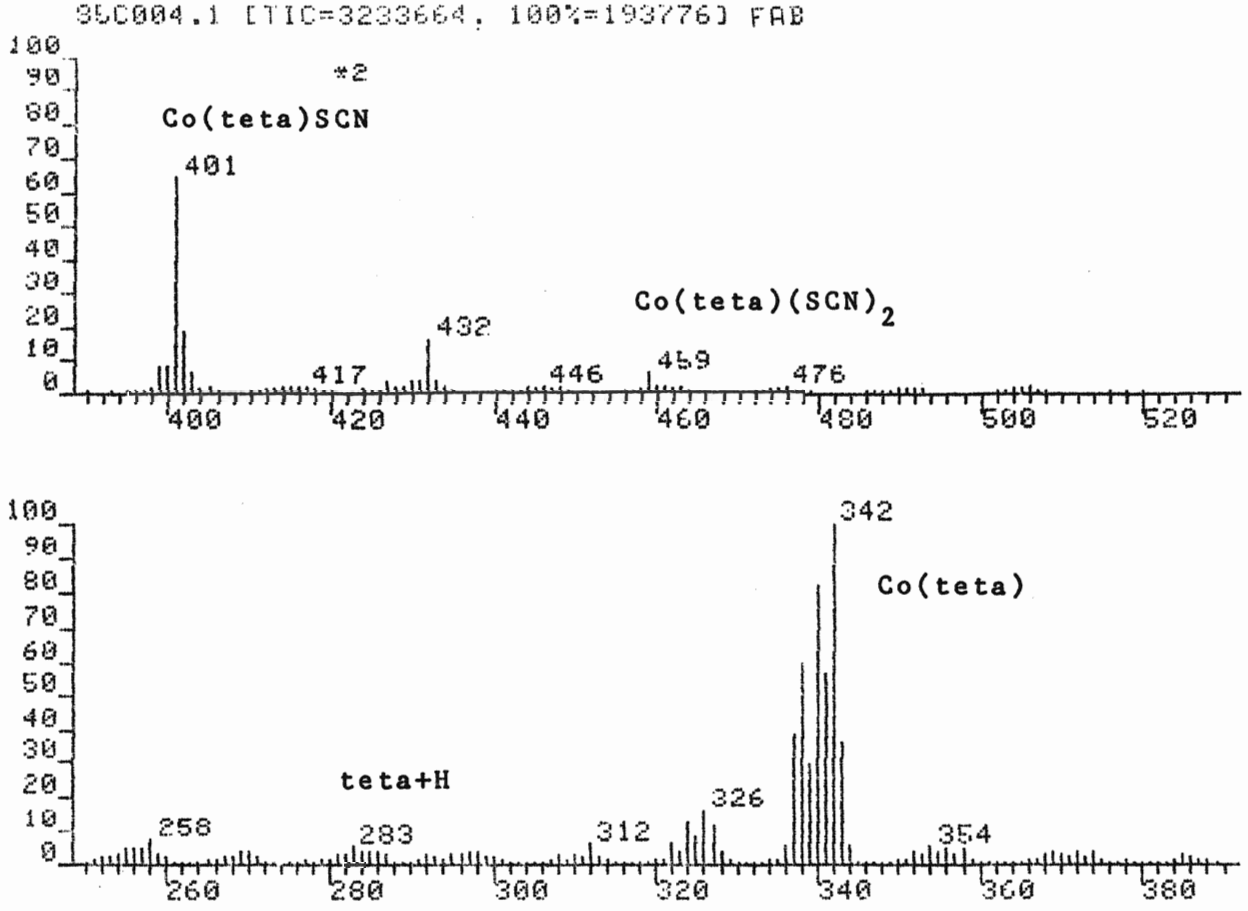

DP4:85C004.MS
SCAN: 1. 3/ 5/85 15:12

IONISATION: FAB
NO. PEAKS: 397
BASE/NREF INT: 193776./ 193776.
TIC: 3233664.
MASS RANGE: 68 - 840

PEAK NO.	MEASURED MASS	NO. POINTS	ABSOLUTE INTENSITY	% INT. BASE	% INT. NREF	% TOT. ION
35	459	35	6418.	3.3	3.3	0.2
52	432	43	16189.	8.4	8.4	0.5
64	417	35	4981.	2.6	2.6	0.2
65	416	35	4944.	2.6	2.6	0.2
75	403	43	11499.	5.9	5.9	0.4
76	402	43	37367.	19.3	19.3	1.2
77	401	59	124660.	64.3	64.3	3.9*
78	400	43	16076.	8.7	8.7	0.5*
79	399	43	14954.	7.7	7.7	0.5
92	385	43	5827.	3.0	3.0	0.2
103	374	35	6678.	3.4	3.4	0.2
105	372	43	7751.	4.0	4.0	0.2
107	370	43	5997.	3.1	3.1	0.2
108	369	35	6600.	3.4	3.4	0.2
109	368	43	5141.	2.7	2.7	0.2
119	358	43	9199.	4.7	4.7	0.3
120	357	35	4903.	2.5	2.5	0.2
121	356	43	9324.	4.8	4.8	0.3
122	355	35	6675.	3.4	3.4	0.2
123	354	43	9736.	5.0	5.0	0.3
124	353	35	5255.	2.7	2.7	0.2*
125	352	35	6592.	3.4	3.4	0.2
133	344	43	10597.	5.5	5.5	0.3
134	343	51	69288.	35.8	35.8	2.1
135	342	87	193776.	100.0	100.0	6.0*
136	341	87	109924.	56.7	56.7	3.4*
137	340	119	159048.	82.1	82.1	4.9*
138	339	103	56989.	29.4	29.4	1.8*
139	338	287	114952.	59.3	59.3	3.6*
140	337	175	75272.	38.8	38.8	2.3*
141	336	59	10002.	5.2	5.2	0.3
149	328	35	6267.	3.2	3.2	0.2
150	327	43	22807.	11.8	11.8	0.7*
151	326	43	31094.	16.0	16.0	1.0
152	325	43	15992.	8.3	8.3	0.5*
153	324	51	26351.	13.6	13.6	0.8*
154	323	51	7583.	3.9	3.9	0.2*
155	322	51	11269.	5.8	5.8	0.3*
165	312	43	11315.	5.8	5.8	0.3
167	310	43	6093.	3.1	3.1	0.2
169	308	43	5142.	2.7	2.7	0.2
179	298	43	6697.	3.5	3.5	0.2
180	297	43	6809.	3.5	3.5	0.2
181	296	43	5013.	2.6	2.6	0.2*
182	295	51	5282.	2.7	2.7	0.2
185	292	87	5911.	3.1	3.1	0.2*
190	287	43	5199.	2.7	2.7	0.2
191	286	43	7581.	3.9	3.9	0.2
192	285	51	7140.	3.7	3.7	0.2*
193	284	43	7931.	4.1	4.1	0.2
194	283	51	9761.	5.0	5.0	0.3
195	282	43	5003.	2.6	2.6	0.2
196	281	51	5690.	2.9	2.9	0.2
206	270	43	6743.	3.5	3.5	0.2
207	269	43	6284.	3.2	3.2	0.2
217	259	43	5028.	2.6	2.6	0.2
218	258	43	14547.	7.5	7.5	0.4
219	257	43	9339.	4.8	4.8	0.3
220	256	51	9444.	4.9	4.9	0.3
221	255	43	8656.	4.5	4.5	0.3
222	254	51	5260.	2.7	2.7	0.2

FAB of $[Co(teta)(CN)_2]ClO_4$ in Thioglycerol

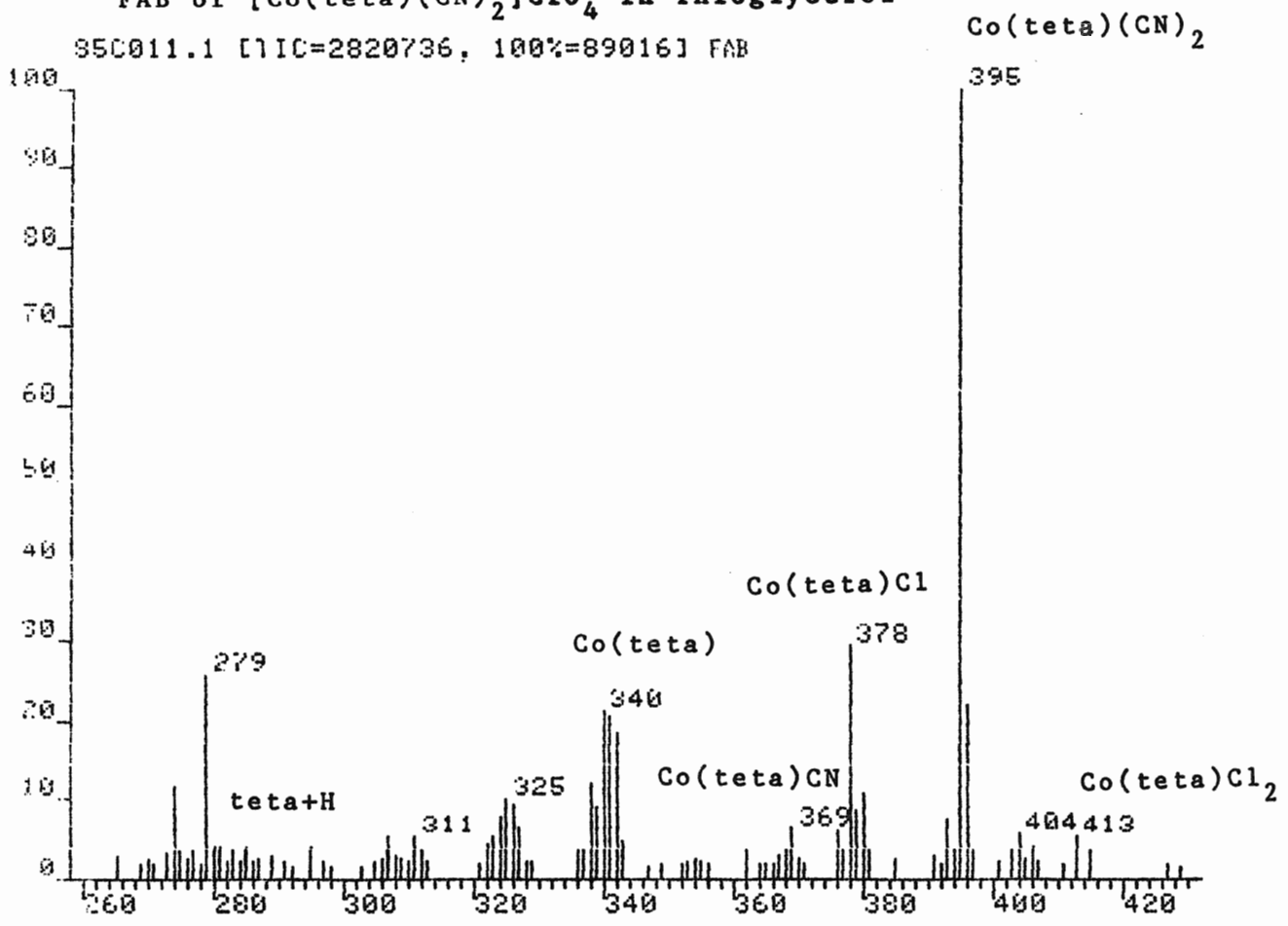

DP4:85C011.MS
SCAN: 1. 3/20/85 12:39

IONISATION: FAB
NO. PEAKS: 287
BASE/NREF INT: 280384./ 280384.
TIC: 2820736.
MASS RANGE: 31 - 455

PEAK NO.	MEASURED MASS	NO. POINTS	ABSOLUTE INTENSITY	% INT. BASE	% INT. NREF	% TOT. ION
5	415	35	3257.	1.2	1.2	0.1
6	413	35	4498.	1.6	1.6	0.2
9	406	35	3398.	1.2	1.2	0.1
11	404	35	4822.	1.7	1.7	0.2
12	403	43	3143.	1.1	1.1	0.1
14	397	35	2999.	1.1	1.1	0.1
15	396	43	19454.	6.9	6.9	0.7
16	395	43	89016.	31.7	31.7	3.2
17	394	35	3066.	1.1	1.1	0.1
18	393	35	6585.	2.3	2.3	0.2
22	381	35	3013.	1.1	1.1	0.1
23	380	35	9545.	3.4	3.4	0.3
24	379	35	7554.	2.7	2.7	0.3
25	378	43	26201.	9.3	9.3	0.9
26	377	35	2974.	1.1	1.1	0.1
27	376	35	5207.	1.9	1.9	0.2
30	369	35	5422.	1.9	1.9	0.2
31	368	29	3208.	1.1	1.1	0.1
36	362	35	3231.	1.2	1.2	0.1
44	343	43	4097.	1.5	1.5	0.1
45	342	43	16356.	5.8	5.8	0.6
46	341	43	18461.	6.6	6.6	0.7
47	340	51	19038.	6.8	6.8	0.7
48	339	59	8103.	2.9	2.9	0.3
49	338	59	10683.	3.8	3.8	0.4
50	337	35	3142.	1.1	1.1	0.1
51	336	43	3084.	1.1	1.1	0.1
54	327	43	5395.	1.9	1.9	0.2
55	326	43	8431.	3.0	3.0	0.3

PEAK NO.	MEASURED MASS	NO. POINTS	ABSOLUTE INTENSITY	% INT. BASE	% INT. NREF	% TOT. ION
56	325	43	9086.	3.2	3.2	0.3
57	324	43	6989.	2.5	2.5	0.2
58	323	43	4553.	1.6	1.6	0.2
59	322	35	3658.	1.3	1.3	0.1
62	312	35	3104.	1.1	1.1	0.1
63	311	43	4632.	1.7	1.7	0.2
67	307	35	4511.	1.6	1.6	0.2
73	295	35	3365.	1.2	1.2	0.1
79	285	43	3497.	1.2	1.2	0.1
81	283	51	3318.	1.2	1.2	0.1
83	281	35	3509.	1.3	1.3	0.1
84	280	35	3481.	1.2	1.2	0.1
85	279	43	23070.	8.2	8.2	0.8
87	277	35	3007.	1.1	1.1	0.1
89	275	35	3332.	1.2	1.2	0.1
90	274	43	10423.	3.7	3.7	0.4

FAB of $[Co(teta)(CN)_2]ClO_4$ in Glycerol

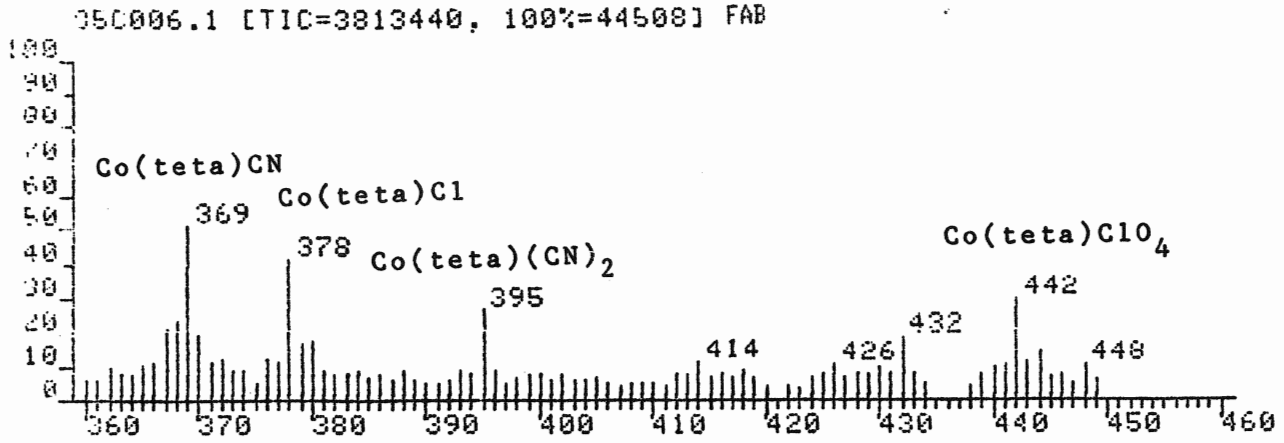

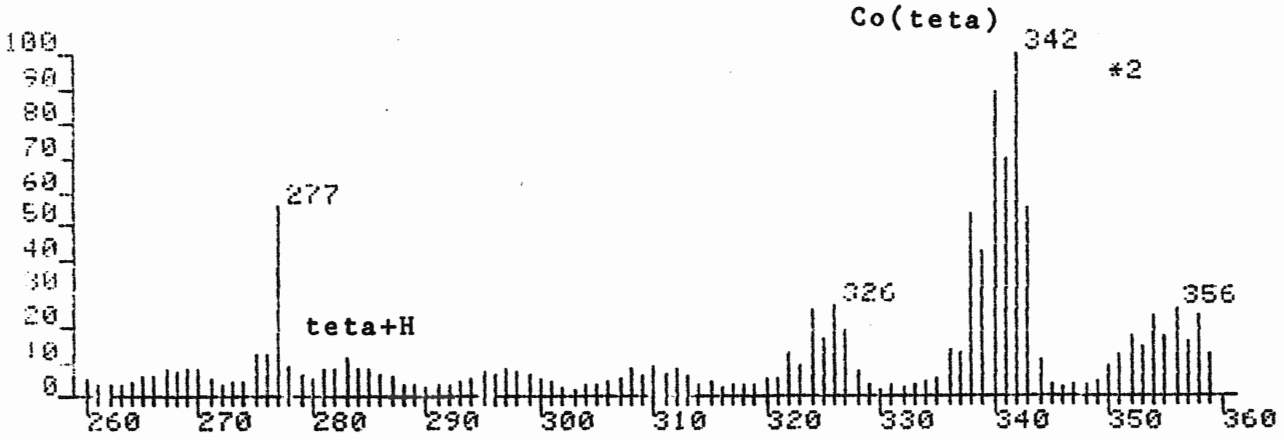

DP4:85C006.MS
SCAN: 1, 3/20/85 11:14

IONISATION: FAB
NO. PEAKS: 437
BASE/NREF INT: 511456./ 511456.
TIC: 3813440.
MASS RANGE: 31 - 553

PEAK NO.	MEASURED MASS	NO. POINTS	ABSOLUTE INTENSITY	% INT. BASE	% INT. NREF	% TOT. ION
33	444	35	3381.	0.7	0.7	0.1
34	443	35	2631.	0.5	0.5	0.1
35	442	35	6638.	1.3	1.3	0.2
42	432	35	4223.	0.8	0.8	0.1
59	414	35	2628.	0.5	0.5	0.1
78	395	35	5853.	1.1	1.1	0.2
93	380	35	3976.	0.8	0.8	0.1
94	379	35	3879.	0.8	0.8	0.1
95	378	43	9224.	1.8	1.8	0.2
96	377	35	2681.	0.5	0.5	0.1*
97	376	35	2777.	0.5	0.5	0.1
101	372	35	2733.	0.5	0.5	0.1
102	371	35	2597.	0.5	0.5	0.1
103	370	35	4383.	0.9	0.9	0.1
104	369	43	11314.	2.2	2.2	0.3
105	368	35	5262.	1.0	1.0	0.1
106	367	35	4640.	0.9	0.9	0.1
107	366	35	2624.	0.5	0.5	0.1
114	359	35	2682.	0.5	0.5	0.1
115	358	43	5221.	1.0	1.0	0.1
116	357	35	3574.	0.7	0.7	0.1
117	356	43	5778.	1.1	1.1	0.2
118	355	43	4062.	0.8	0.8	0.1
119	354	43	5262.	1.0	1.0	0.1
120	353	35	3223.	0.6	0.6	0.1
121	352	43	3877.	0.8	0.8	0.1
122	351	35	2692.	0.5	0.5	0.1
129	344	43	4780.	0.9	0.9	0.1
130	343	51	24301.	4.8	4.8	0.6*
131	342	51	44508.	8.7	8.7	1.2
132	341	51	31046.	6.1	6.1	0.8
133	340	87	39684.	7.8	7.8	1.0*
134	339	103	18828.	3.7	3.7	0.5*
135	338	103	23712.	4.6	4.6	0.6*
136	337	51	5933.	1.2	1.2	0.2*
137	336	51	6135.	1.2	1.2	0.2*
145	328	35	3224.	0.6	0.6	0.1
146	327	43	8569.	1.7	1.7	0.2*
147	326	43	11727.	2.3	2.3	0.3
148	325	43	7455.	1.5	1.5	0.2
149	324	43	10963.	2.1	2.1	0.3*
150	323	43	4128.	0.8	0.8	0.1*
151	322	43	5852.	1.1	1.1	0.2*
160	313	35	2704.	0.5	0.5	0.1
161	312	43	3949.	0.8	0.8	0.1*
162	311	43	3185.	0.6	0.6	0.1*
163	310	43	4005.	0.8	0.8	0.1
164	309	35	2697.	0.5	0.5	0.1
165	308	43	3623.	0.7	0.7	0.1*
174	299	35	3019.	0.6	0.6	0.1
175	298	43	3512.	0.7	0.7	0.1
176	297	43	3693.	0.7	0.7	0.1*
177	296	35	2988.	0.6	0.6	0.1*
178	295	51	3239.	0.6	0.6	0.1*
186	287	35	2587.	0.5	0.5	0.1
187	286	43	3106.	0.6	0.6	0.1*
188	285	43	3620.	0.7	0.7	0.1*
189	284	43	3930.	0.8	0.8	0.1*
190	283	51	5075.	1.0	1.0	0.1*
191	282	43	3663.	0.7	0.7	0.1
192	281	51	3537.	0.7	0.7	0.1
194	279	43	2930.	0.6	0.6	0.1
195	278	43	4180.	0.8	0.8	0.1
196	277	43	24775.	4.8	4.8	0.6
197	276	35	5482.	1.1	1.1	0.1
198	275	43	5673.	1.1	1.1	0.1
203	270	51	3707.	0.7	0.7	0.1*
204	269	43	3603.	0.7	0.7	0.1
205	268	43	3341.	0.7	0.7	0.1
206	267	51	3531.	0.7	0.7	0.1
207	266	43	2574.	0.5	0.5	0.1*
208	265	43	2657.	0.5	0.5	0.1

FAB of $[Co(teta)ClN_3]ClO_4$ in Thioglycerol

85C023.1 [TIC=4929792, 100%=291520] FAB

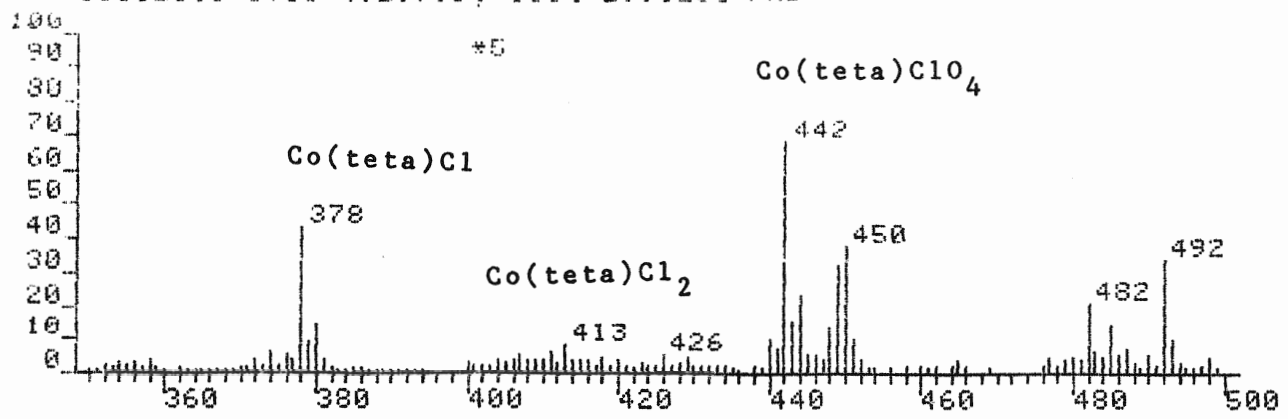

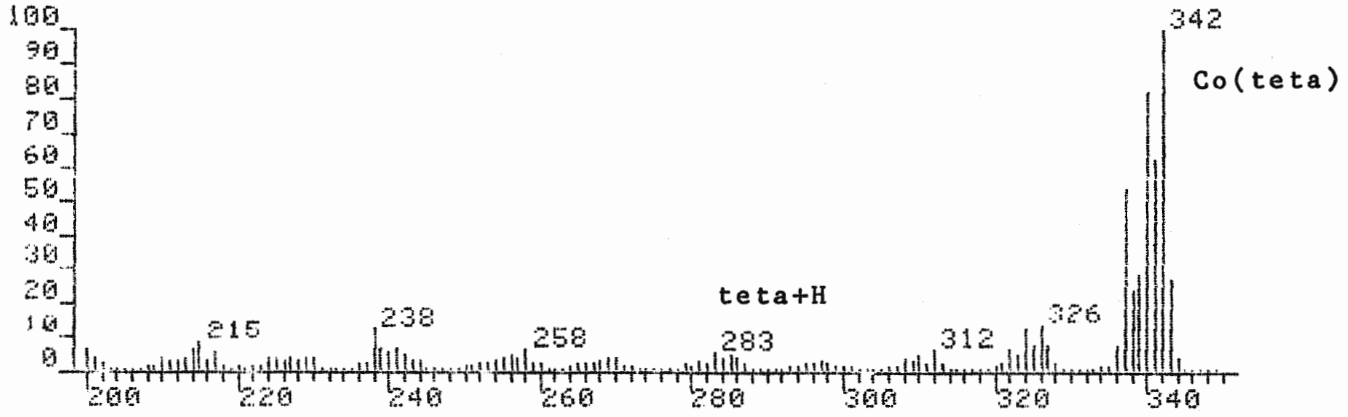

DP4:85C023.MS
SCAN: 1. 6/25/85 15:48

IONISATION: FAB
NO. PEAKS: 438
BASE/NREF INT: 291520./ 291520.
TIC: 4929792.
MASS RANGE: 69 - 819

PEAK NO.	MEASURED MASS	NO. POINTS	ABSOLUTE INTENSITY	% INT. BASE	% INT. NREF	% TOT. ION
29	492	43	19862.	6.8	6.8	0.4
39	482	35	12203.	4.2	4.2	0.2
59	450	43	21940.	7.5	7.5	0.4
60	449	43	18695.	6.4	6.4	0.4
65	444	43	13851.	4.8	4.8	0.3
66	443	43	9203.	3.2	3.2	0.2
67	442	51	39949.	13.7	13.7	0.8
126	381	43	9965.	3.4	3.4	0.2
127	380	51	42487.	14.6	14.6	0.9
128	379	51	27971.	9.6	9.6	0.6*
129	378	71	125320.	43.0	43.0	2.5*
130	377	51	12000.	4.1	4.1	0.2*
131	376	43	15677.	5.4	5.4	0.3*
133	374	43	19291.	6.6	6.6	0.4*
135	372	43	10987.	3.8	3.8	0.2
149	358	43	11253.	3.9	3.9	0.2
151	356	43	9591.	3.3	3.3	0.2
153	354	43	9291.	3.2	3.2	0.2
163	344	43	11020.	3.8	3.8	0.2*
164	343	71	79824.	27.4	27.4	1.6*
165	342	119	291520.	100.0	100.0	5.9*
166	341	103	181032.	62.1	62.1	3.7*
167	340	119	239004.	82.0	82.0	4.8*
168	339	103	84480.	29.0	29.0	1.7*
169	338	103	70776.	24.3	24.3	1.4*
170	337	287	157264.	53.9	53.9	3.2*
171	336	103	22194.	7.6	7.6	0.5*
180	327	51	21737.	7.5	7.5	0.4
181	326	71	40619.	13.9	13.9	0.8*
182	325	59	22930.	7.9	7.9	0.5*
183	324	71	36771.	12.6	12.6	0.7*
184	323	71	13358.	4.6	4.6	0.3*
185	322	87	18151.	6.2	6.2	0.4*
195	312	51	18297.	6.3	6.3	0.4*
197	310	87	12886.	4.4	4.4	0.3*
199	308	71	9788.	3.4	3.4	0.2*
221	286	51	9307.	3.2	3.2	0.2
222	285	59	14255.	4.9	4.9	0.3*
223	284	51	9792.	3.4	3.4	0.2
224	283	59	15494.	5.3	5.3	0.3
237	270	51	9460.	3.2	3.2	0.2*
238	269	51	10277.	3.5	3.5	0.2
249	258	59	18530.	6.4	6.4	0.4*
250	257	59	11582.	4.0	4.0	0.2*
251	256	71	14410.	4.9	4.9	0.3*
252	255	51	9666.	3.3	3.3	0.2*
264	243	51	9023.	3.1	3.1	0.2*
265	242	59	14413.	4.9	4.9	0.3
266	241	59	20075.	6.9	6.9	0.4*
267	240	59	16441.	5.6	5.6	0.3*
268	239	59	19020.	6.5	6.5	0.4*
269	238	59	35105.	12.0	12.0	0.7*
277	230	51	12227.	4.2	4.2	0.2
278	229	51	10864.	3.7	3.7	0.2
280	227	51	11937.	4.1	4.1	0.2
282	225	59	12215.	4.2	4.2	0.2*
283	224	59	11847.	4.1	4.1	0.2*
290	217	51	16059.	5.5	5.5	0.3
291	216	43	9109.	3.1	3.1	0.2
292	215	51	24405.	8.4	8.4	0.5
293	214	59	18177.	6.2	6.2	0.4
294	213	51	9989.	3.4	3.4	0.2*
295	212	59	9252.	3.2	3.2	0.2*
296	211	51	9270.	3.2	3.2	0.2*
297	210	59	10459.	3.6	3.6	0.2
306	201	51	12397.	4.3	4.3	0.3
307	200	59	17418.	6.0	6.0	0.4*

FAB of $[Co(teta)ClN_3]ClO_4$ in Glycerol

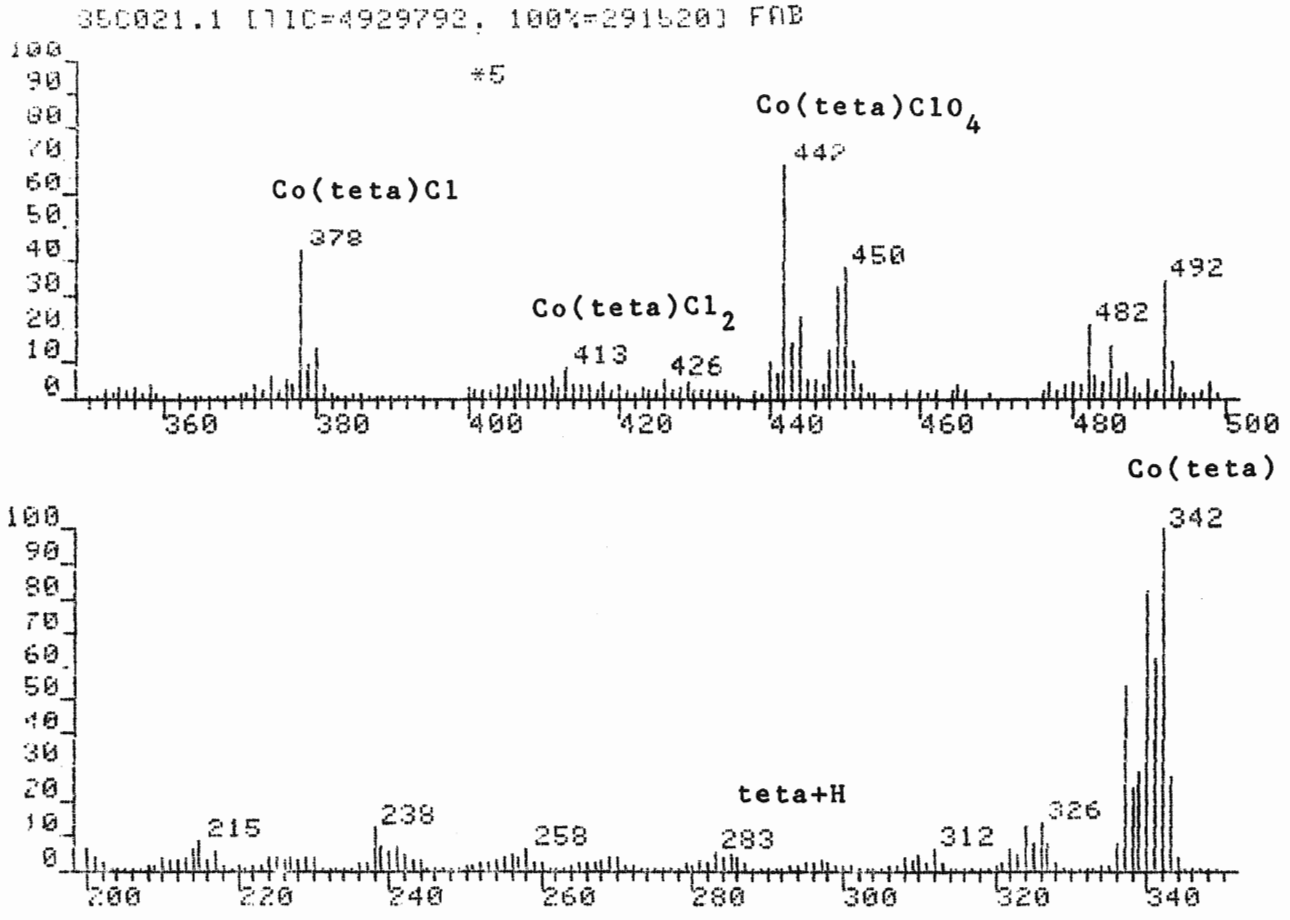

DP4:85C021.MS
SCAN: 1, 6/25/85 15:41

IONISATION: FAB
NO. PEAKS: 438
BASE/NREF INT: 291520./ 291520.
TIC: 4929792.
MASS RANGE: 69 - 819

PEAK NO.	MEASURED MASS	NO. POINTS	ABSOLUTE INTENSITY	% INT. BASE	% INT. NREF	% TOT. ION
29	492	43	19862.	6.8	6.8	0.4
39	482	35	12203.	4.2	4.2	0.2
59	450	43	21940.	7.5	7.5	0.4
60	449	43	18695.	6.4	6.4	0.4
65	444	43	13851.	4.8	4.8	0.3
66	443	43	9203.	3.2	3.2	0.2
67	442	51	39949.	13.7	13.7	0.8
126	381	43	9965.	3.4	3.4	0.2
127	380	51	42487.	14.6	14.6	0.9
128	379	51	27971.	9.6	9.6	0.6%
129	378	71	125320.	43.0	43.0	2.5%
130	377	51	12000.	4.1	4.1	0.2%
131	376	43	15677.	5.4	5.4	0.3%
133	374	43	19291.	6.6	6.6	0.4%
135	372	43	10987.	3.8	3.8	0.2
149	358	43	11253.	3.9	3.9	0.2
151	356	43	9591.	3.3	3.3	0.2
153	354	43	9291.	3.2	3.2	0.2
163	344	43	11020.	3.8	3.8	0.2%
164	343	71	79824.	27.4	27.4	1.6%
165	342	119	291520.	100.0	100.0	5.9%
166	341	103	181032.	62.1	62.1	3.7%
167	340	119	239004.	82.0	82.0	4.8%
168	339	103	84480.	29.0	29.0	1.7%
169	338	103	70776.	24.3	24.3	1.4%
170	337	287	157264.	53.9	53.9	3.2%
171	336	103	22194.	7.6	7.6	0.5%
180	327	51	21737.	7.5	7.5	0.4
181	326	71	40619.	13.9	13.9	0.8%
182	325	59	22930.	7.9	7.9	0.5%
183	324	71	36771.	12.6	12.6	0.7%
184	323	71	13358.	4.6	4.6	0.3%
185	322	87	18151.	6.2	6.2	0.4%
195	312	51	18297.	6.3	6.3	0.4%
197	310	87	12886.	4.4	4.4	0.3%
199	308	71	9788.	3.4	3.4	0.2%
221	286	51	9307.	3.2	3.2	0.2
222	285	59	14255.	4.9	4.9	0.3%
223	284	51	9792.	3.4	3.4	0.2
224	283	59	15494.	5.3	5.3	0.3
237	270	51	9460.	3.2	3.2	0.2%
238	269	51	10277.	3.5	3.5	0.2
249	258	59	18530.	6.4	6.4	0.4%
250	257	59	11582.	4.0	4.0	0.2%
251	256	71	14410.	4.9	4.9	0.3%
252	255	51	9666.	3.3	3.3	0.2%
264	243	51	9023.	3.1	3.1	0.2%
265	242	59	14413.	4.9	4.9	0.3
266	241	59	20075.	6.9	6.9	0.4%
267	240	59	16441.	5.6	5.6	0.3%
268	239	59	19020.	6.5	6.5	0.4%
269	238	59	35105.	12.0	12.0	0.7%
277	230	51	12227.	4.2	4.2	0.2
278	229	51	10864.	3.7	3.7	0.2
280	227	51	11937.	4.1	4.1	0.2
282	225	59	12215.	4.2	4.2	0.2%
283	224	59	11847.	4.1	4.1	0.2%
290	217	51	16059.	5.5	5.5	0.3
291	216	43	9109.	3.1	3.1	0.2
292	215	51	24405.	8.4	8.4	0.5
293	214	59	18177.	6.2	6.2	0.4
294	213	51	9989.	3.4	3.4	0.2%
295	212	59	9252.	3.2	3.2	0.2%
296	211	51	9270.	3.2	3.2	0.2%
297	210	59	10459.	3.6	3.6	0.2
306	201	51	12397.	4.3	4.3	0.3
307	200	59	17418.	6.0	6.0	0.4%

FAB of $[Co(teta)(NO_2)_2]ClO_4$ in Thioglycerol

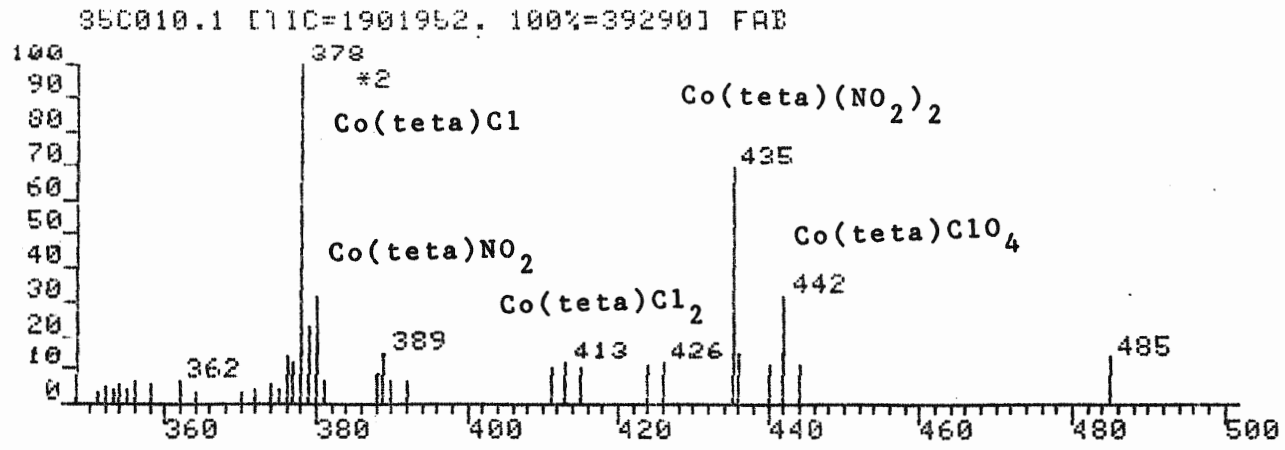

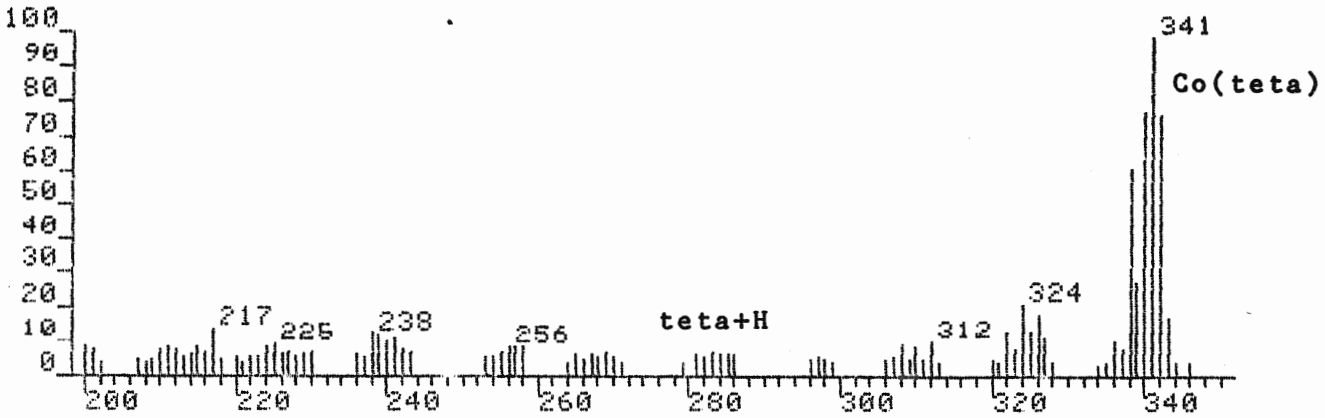

DP4:85C010.MS
SCAN: 1, 3/20/85 11:44

IONISATION: FAB
NO. PEAKS: 276
BASE/NREF INT: 68428./ 68428.
TIC: 1901952.
MASS RANGE: 31 - 485

PEAK NO.	MEASURED MASS	NO. POINTS	ABSOLUTE INTENSITY	% INT. BASE	% INT. NREF	% TOT. ION
1	485	35	2664.	3.9	3.9	0.1
3	442	35	6247.	9.1	9.1	0.3
5	436	35	2901.	4.2	4.2	0.2
6	435	35	13540.	19.8	19.8	0.7
14	389	35	2916.	4.3	4.3	0.2
17	380	43	12172.	17.8	17.8	0.6
18	379	35	8934.	13.1	13.1	0.5
19	378	43	39290.	57.4	57.4	2.1
20	377	35	4702.	6.9	6.9	0.2
21	376	35	5177.	7.6	7.6	0.3
27	362	35	2440.	3.6	3.6	0.1
37	343	43	6553.	9.6	9.6	0.3
38	342	51	29773.	43.5	43.5	1.6*
39	341	51	38784.	56.7	56.7	2.0
40	340	87	30002.	43.8	43.8	1.6*
41	339	59	10839.	15.8	15.8	0.6*
42	338	103	23701.	34.6	34.6	1.2
43	337	43	2887.	4.2	4.2	0.2
44	336	43	3886.	5.7	5.7	0.2
48	327	35	4335.	6.3	6.3	0.2
49	326	35	7089.	10.4	10.4	0.4
50	325	35	4957.	7.2	7.2	0.3
51	324	43	8184.	12.0	12.0	0.4
52	323	35	3033.	4.4	4.4	0.2
53	322	43	4968.	7.3	7.3	0.3
57	312	35	4029.	5.9	5.9	0.2
59	310	35	3125.	4.6	4.6	0.2
61	308	43	3657.	5.3	5.3	0.2
68	286	35	2439.	3.6	3.6	0.1
69	285	35	2397.	3.5	3.5	0.1
70	284	43	2441.	3.6	3.6	0.1
71	283	51	2738.	4.0	4.0	0.1
77	269	43	2639.	3.9	3.9	0.1
79	267	35	2512.	3.7	3.7	0.1
81	265	35	2404.	3.5	3.5	0.1
83	258	35	3135.	4.6	4.6	0.2
84	257	43	3210.	4.7	4.7	0.2
85	256	35	3366.	4.9	4.9	0.2
86	255	43	2650.	3.9	3.9	0.1
89	243	43	2646.	3.9	3.9	0.1
90	242	43	2934.	4.3	4.3	0.2
91	241	43	4206.	6.1	6.1	0.3*
92	240	43	3901.	5.7	5.7	0.2
93	239	35	4466.	6.5	6.5	0.2
94	238	43	4899.	7.2	7.2	0.3
97	230	43	2628.	3.8	3.8	0.1
100	227	35	2723.	4.0	4.0	0.1
101	226	43	2453.	3.6	3.6	0.1*
102	225	43	3590.	5.2	5.2	0.2
103	224	35	3148.	4.6	4.6	0.2
109	217	43	5436.	7.9	7.9	0.3
110	216	43	2575.	3.8	3.8	0.1
111	215	43	3155.	4.6	4.6	0.2
112	214	35	2507.	3.7	3.7	0.1
114	212	43	3087.	4.5	4.5	0.2
115	211	43	3114.	4.6	4.6	0.2
116	210	43	3038.	4.4	4.4	0.2
121	201	35	3010.	4.4	4.4	0.2
122	200	43	3441.	5.0	5.0	0.2

FAB of $[Co(teta)(NO_2)_2]ClO_4$ in Glycerol

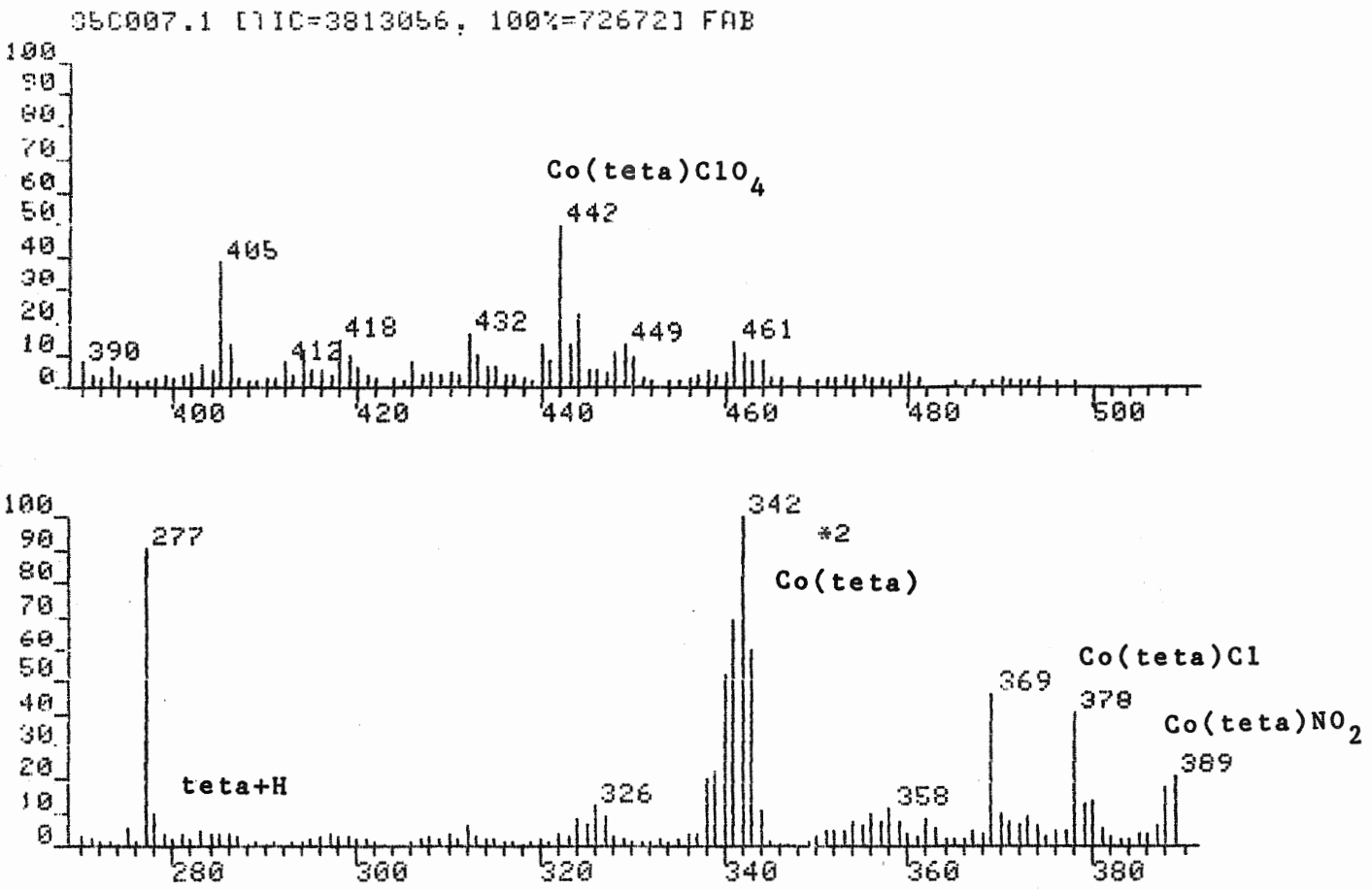

DP4:85C007.MS
SCAN: 1, 3/19/85 15:46

IONISATION: FAB
NO. PEAKS: 431
BASE/NREF INT: 1090624./ 1090624.
TIC: 3813056.
MASS RANGE: 68 - 884
RETN TIME/MISC: 0: 0/ 0/ 0/ 0

PEAK NO.	MEASURED MASS	NO. POINTS	ABSOLUTE INTENSITY	% INT. BASE	% INT. NREF	% TOT. ION
68	450	35	3444.	0.3	0.3	0.1*
69	449	43	4917.	0.5	0.5	0.1*
70	448	43	4045.	0.4	0.4	0.1*
74	444	43	7984.	0.7	0.7	0.2*
75	443	35	4991.	0.5	0.5	0.1
76	442	43	17826.	1.6	1.6	0.5
77	441	35	2972.	0.3	0.3	0.1
78	440	35	4662.	0.4	0.4	0.1
83	435	35	2355.	0.2	0.2	0.1*
84	434	35	2324.	0.2	0.2	0.1*
85	433	35	3605.	0.3	0.3	0.1
86	432	43	5886.	0.5	0.5	0.2*
92	426	35	2904.	0.3	0.3	0.1
97	420	35	2338.	0.2	0.2	0.1*
98	419	35	3654.	0.3	0.3	0.1
99	418	43	5418.	0.5	0.5	0.1*
103	414	35	4305.	0.4	0.4	0.1
105	412	35	2778.	0.3	0.3	0.1
111	406	35	4734.	0.4	0.4	0.1
112	405	43	13938.	1.3	1.3	0.4
114	403	35	2488.	0.2	0.2	0.1
124	393	35	2265.	0.2	0.2	0.1*
127	390	35	2849.	0.3	0.3	0.1
128	389	43	7481.	0.7	0.7	0.2
129	388	35	6345.	0.6	0.6	0.2
130	387	35	2248.	0.2	0.2	0.1
137	380	35	5071.	0.5	0.5	0.1
138	379	35	4844.	0.4	0.4	0.1
139	378	43	14633.	1.3	1.3	0.4
143	374	35	2226.	0.2	0.2	0.1
144	373	35	3337.	0.3	0.3	0.1
145	372	35	2383.	0.2	0.2	0.1
146	371	35	2864.	0.3	0.3	0.1
147	370	35	3592.	0.3	0.3	0.1
148	369	43	16759.	1.5	1.5	0.4
155	362	35	3139.	0.3	0.3	0.1
158	359	35	2655.	0.2	0.2	0.1
159	358	35	4221.	0.4	0.4	0.1
160	357	35	2823.	0.3	0.3	0.1
161	356	35	3766.	0.3	0.3	0.1
162	355	35	2248.	0.2	0.2	0.1
163	354	35	2706.	0.2	0.2	0.1
172	344	43	8058.	0.7	0.7	0.2
173	343	51	43596.	4.0	4.0	1.1
174	342	59	72672.	6.7	6.7	1.9*
175	341	59	49782.	4.6	4.6	1.3*
176	340	71	37782.	3.5	3.5	1.0*
177	339	103	16727.	1.5	1.5	0.4*
178	338	71	14876.	1.4	1.4	0.4*
179	337	43	2696.	0.2	0.2	0.1*
180	336	35	2788.	0.3	0.3	0.1*
189	327	43	6874.	0.6	0.6	0.2
190	326	43	8806.	0.8	0.8	0.2
191	325	35	4723.	0.4	0.4	0.1
192	324	43	6111.	0.6	0.6	0.2
194	322	35	2677.	0.2	0.2	0.1
203	313	35	2228.	0.2	0.2	0.1
204	312	35	4506.	0.4	0.4	0.1
206	310	35	2368.	0.2	0.2	0.1
216	298	35	2209.	0.2	0.2	0.1
217	297	35	2362.	0.2	0.2	0.1
226	287	35	2290.	0.2	0.2	0.1
227	286	35	2389.	0.2	0.2	0.1
228	285	35	2366.	0.2	0.2	0.1
229	284	35	2430.	0.2	0.2	0.1
230	283	43	3521.	0.3	0.3	0.1
232	281	35	2337.	0.2	0.2	0.1

FAB of $[Co(teta)NO_2OH]ClO_4$ in Thioglycerol

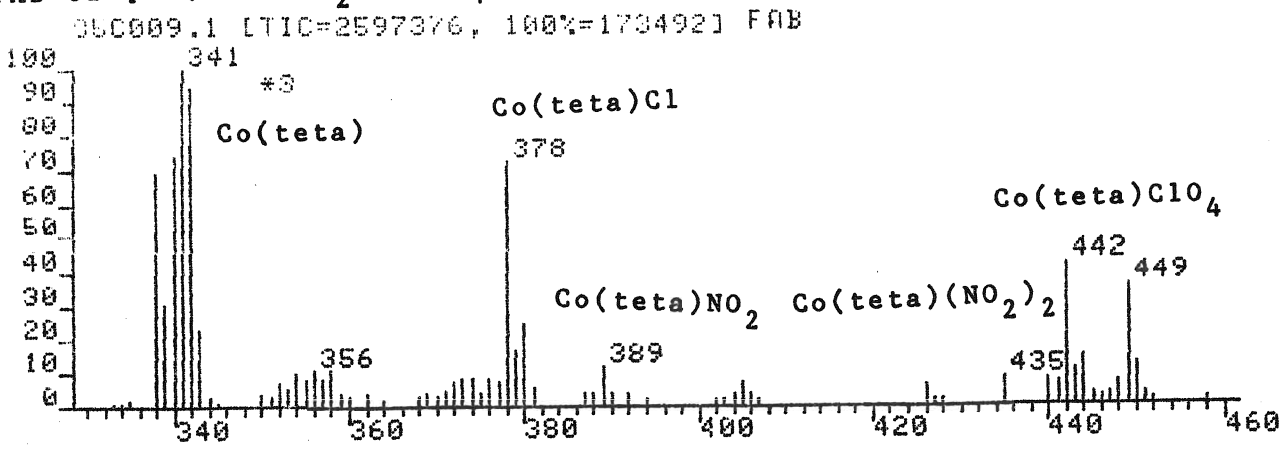

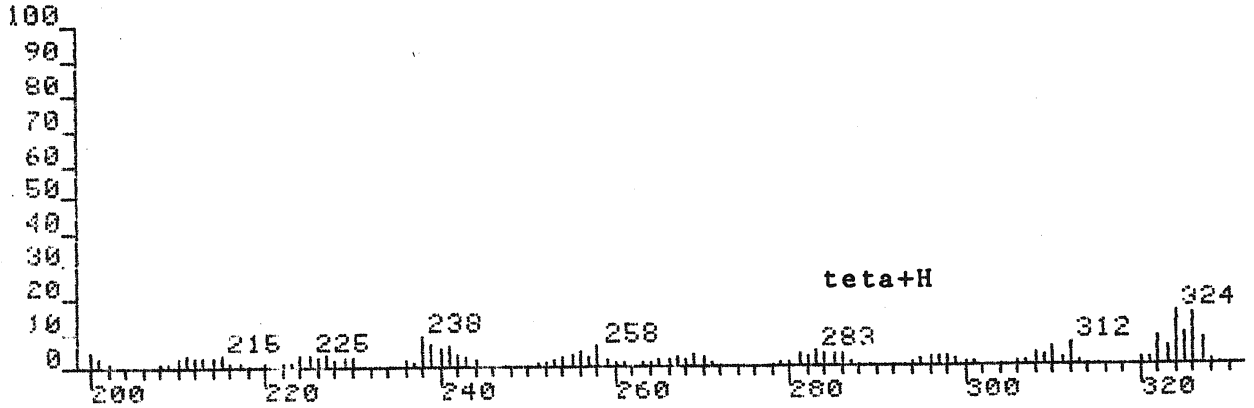

DR4:85C009.MS
SCAN: 1. 3/20/85 10:54

IONISATION: FAB
NO. PEAKS: 309
BASE/NREF INT: 173492./ 173492.
TIC: 2597376.
MASS RANGE: 31 - 497
RETN TIME/MISC: 0: 0/ 0/ 0/ 0

PEAK NO.	MEASURED MASS	NO. POINTS	ABSOLUTE INTENSITY	% INT. BASE	% INT. NREF	% TOT. ION
10	450	35	7309.	4.2	4.2	0.3
11	449	43	20700.	11.9	11.9	0.8
12	448	35	3936.	2.3	2.3	0.2
16	444	35	8456.	4.9	4.9	0.3
17	443	35	6367.	3.7	3.7	0.2
18	442	43	24700.	14.2	14.2	1.0
19	441	35	3953.	2.3	2.3	0.2
20	440	35	4382.	2.5	2.5	0.2
21	435	35	4869.	2.8	2.8	0.2
24	426	35	3564.	2.1	2.1	0.1
27	405	35	4241.	2.4	2.4	0.2
34	389	35	6876.	4.0	4.0	0.3
37	381	35	3260.	1.9	1.9	0.1
38	380	35	14157.	8.2	8.2	0.5
39	379	35	9339.	5.4	5.4	0.4
40	378	51	41939.	24.2	24.2	1.6
41	377	35	3964.	2.3	2.3	0.2
42	376	35	4540.	2.6	2.6	0.2
44	374	35	5084.	2.9	2.9	0.2
45	373	35	4334.	2.5	2.5	0.2
46	372	35	3915.	2.3	2.3	0.2
47	371	43	2959.	1.7	1.7	0.1
55	358	35	6206.	3.6	3.6	0.2
56	357	43	4424.	2.5	2.5	0.2
57	356	43	6527.	3.8	3.8	0.3*
58	355	35	4672.	2.7	2.7	0.2
59	354	43	6035.	3.5	3.5	0.2
60	353	35	3343.	1.9	1.9	0.1
61	352	43	4088.	2.4	2.4	0.2
65	344	43	4963.	2.9	2.9	0.2
66	343	51	38830.	22.4	22.4	1.5
67	342	71	163516.	94.2	94.2	6.3*
68	341	119	173492.	100.0	100.0	6.7*
69	340	119	128308.	74.0	74.0	4.9*
70	339	87	53552.	30.9	30.9	2.1*
71	338	351	119368.	68.8	68.8	4.6*
76	328	35	2851.	1.6	1.6	0.1
77	327	43	13134.	7.6	7.6	0.5
78	326	51	26149.	15.1	15.1	1.0
79	325	59	15717.	9.1	9.1	0.6
80	324	71	27341.	15.8	15.8	1.1*
81	323	87	9174.	5.3	5.3	0.4*
82	322	71	14240.	8.2	8.2	0.5*
83	321	59	3052.	1.8	1.8	0.1*
84	320	51	3436.	2.0	2.0	0.1
87	313	35	2952.	1.7	1.7	0.1
88	312	43	11304.	6.5	6.5	0.4
89	311	43	4021.	2.3	2.3	0.2*
90	310	71	8910.	5.1	5.1	0.3*
91	309	71	4716.	2.7	2.7	0.2*
92	308	51	6265.	3.6	3.6	0.2
98	299	43	3864.	2.2	2.2	0.1
99	298	43	5036.	2.9	2.9	0.2
100	297	43	5462.	3.1	3.1	0.2
101	296	43	4331.	2.5	2.5	0.2*
102	295	43	3401.	2.0	2.0	0.1
103	294	35	2716.	1.6	1.6	0.1
108	287	35	2822.	1.6	1.6	0.1
109	286	43	6172.	3.6	3.6	0.2
110	285	59	6415.	3.7	3.7	0.2
111	284	43	6429.	3.7	3.7	0.2
112	283	59	8206.	4.7	4.7	0.3
113	282	51	4550.	2.6	2.6	0.2
114	281	43	5667.	3.3	3.3	0.2

FAB of $[Co(teta)NO_2OH]ClO_4$ in Glycerol

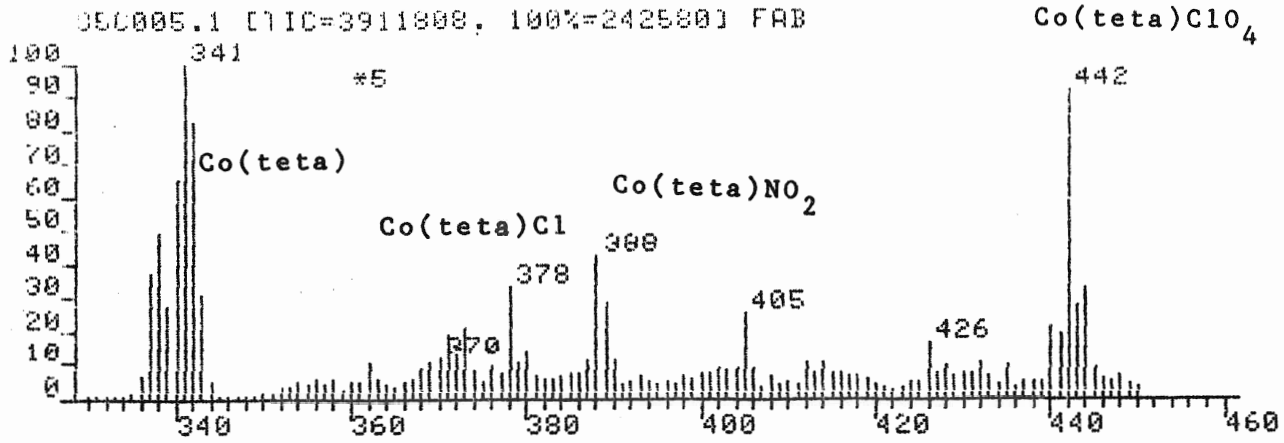

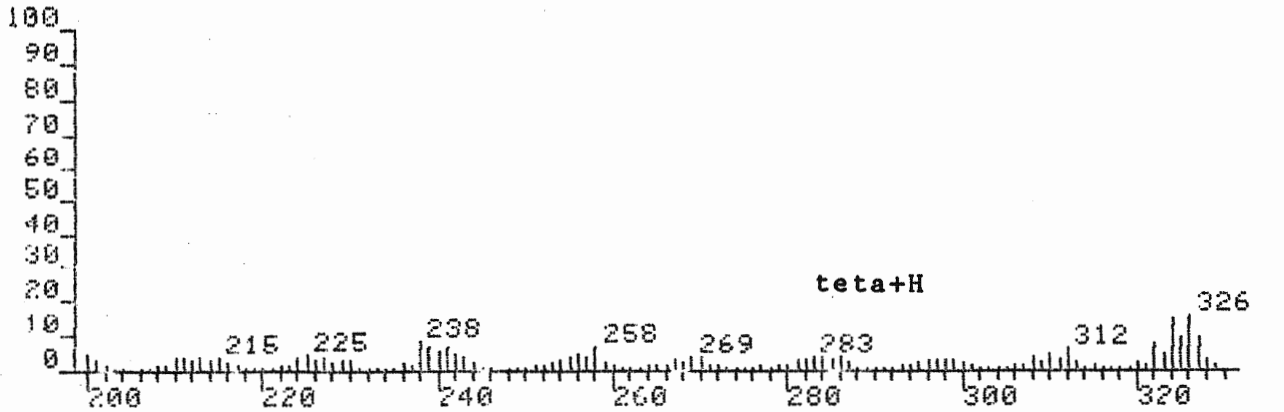

DP4:85C005.MS
SCAN: 1. 3/20/85 9:56

IONISATION: FAB
NO. PEAKS: 448
BASE/NREF INT: 242580./ 242580.
TIC: 3911808.
MASS RANGE: 30 - 532

PEAK NO.	MEASURED MASS	NO. POINTS	ABSOLUTE INTENSITY	% INT. BASE	% INT. NREF	% TOT. ION
50	444	43	15577.	6.4	6.4	0.4
51	443	43	13067.	5.4	5.4	0.3
52	442	51	44231.	18.2	18.2	1.1
53	441	43	9233.	3.8	3.8	0.2
54	440	43	10300.	4.2	4.2	0.3
68	426	43	7985.	3.3	3.3	0.2
89	405	43	12046.	5.0	5.0	0.3
105	389	43	13795.	5.7	5.7	0.4
106	388	43	20668.	8.5	8.5	0.5
116	378	43	15877.	6.5	6.5	0.4
121	373	43	10173.	4.2	4.2	0.3
123	371	43	9039.	3.7	3.7	0.2
136	358	43	13668.	5.6	5.6	0.3
137	357	43	10168.	4.2	4.2	0.3
138	356	43	13442.	5.5	5.5	0.3
139	355	43	9747.	4.0	4.0	0.2
140	354	51	11045.	4.6	4.6	0.3
150	344	43	11585.	4.8	4.8	0.3
151	343	59	73816.	30.4	30.4	1.9%
152	342	87	199712.	82.3	82.3	5.1%
153	341	103	242580.	100.0	100.0	6.2%
154	340	103	157652.	65.0	65.0	4.0%
155	339	87	67156.	27.7	27.7	1.7%
156	338	287	118940.	49.0	49.0	3.0%
157	337	239	89812.	37.0	37.0	2.3%
158	336	87	14513.	6.0	6.0	0.4
167	327	51	22960.	9.5	9.5	0.6
168	326	51	37418.	15.4	15.4	1.0
169	325	51	23531.	9.7	9.7	0.6%
170	324	71	35689.	14.7	14.7	0.9%
171	323	71	11352.	4.7	4.7	0.3%
172	322	71	18386.	7.6	7.6	0.5%
182	312	51	14385.	5.9	5.9	0.4
184	310	51	10604.	4.4	4.4	0.3
186	308	43	8155.	3.4	3.4	0.2
196	298	43	7692.	3.2	3.2	0.2
208	286	43	8672.	3.6	3.6	0.2
209	285	51	7682.	3.2	3.2	0.2
210	284	51	9813.	4.0	4.0	0.3
211	283	51	10068.	4.2	4.2	0.3
213	281	51	7288.	3.0	3.0	0.2
224	270	51	7900.	3.3	3.3	0.2
225	269	51	8803.	3.6	3.6	0.2
236	258	51	15864.	6.5	6.5	0.4
237	257	51	9053.	3.7	3.7	0.2
238	256	51	11500.	4.7	4.7	0.3
239	255	43	8908.	3.7	3.7	0.2
250	243	43	7860.	3.2	3.2	0.2
251	242	51	11780.	4.9	4.9	0.3
252	241	51	15654.	6.5	6.5	0.4
253	240	51	12923.	5.3	5.3	0.3
254	239	51	15927.	6.6	6.6	0.4
255	238	51	20860.	8.6	8.6	0.5
263	230	43	7441.	3.1	3.1	0.2
264	229	43	7649.	3.2	3.2	0.2
266	227	51	9887.	4.1	4.1	0.3
268	225	51	10439.	4.3	4.3	0.3
269	224	51	8811.	3.6	3.6	0.2
270	215	43	9585.	4.0	4.0	0.2
280	213	43	8029.	3.3	3.3	0.2
282	211	43	7785.	3.2	3.2	0.2
283	210	51	8155.	3.4	3.4	0.2
291	201	51	7734.	3.2	3.2	0.2
292	200	51	10872.	4.5	4.5	0.3

APPENDIX II

The Positive Ion FAB Mass Spectra of the Teta Metal Containing Complexes other than Cobalt

FAB Mass Spectrum of $(HgCl_2)_2(tetb)$

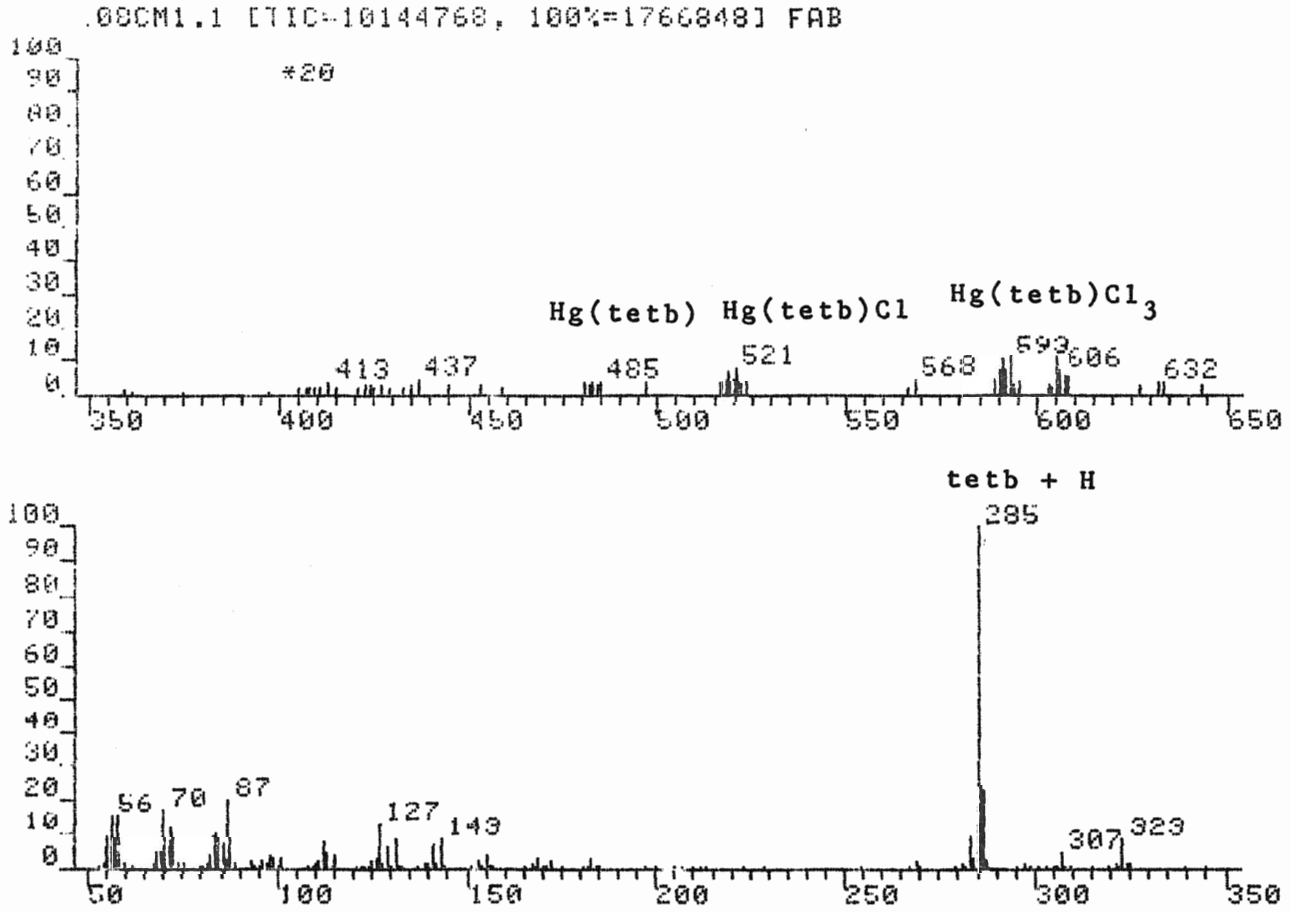

Quantitative Report for the Complex $(HgCl_2)_2(tetb)$

DP4:108CM1.MS
SCAN: 1. 1/ 8/85 11:40

IONISATION: FAB
NO. PEAKS: 327
BASE/NREF INT: 1766848./ 1766848.
TIC: 10144768.
MASS RANGE: 14 - 643

PEAK NO.	MEASURED MASS	NO. POINTS	ABSOLUTE INTENSITY	% INT. BASE	% INT. NREF	% TOT. ION
1	643	29	2544.	0.1	0.1	0.0
2	633	51	3574.	0.2	0.2	0.0*
3	632	35	3602.	0.2	0.2	0.0
4	627	35	2970.	0.2	0.2	0.0
5	608	51	4813.	0.3	0.3	0.0*
6	607	43	5077.	0.3	0.3	0.1*
7	606	43	5957.	0.3	0.3	0.1*
8	605	43	9811.	0.6	0.6	0.1
9	604	35	2084.	0.1	0.1	0.0
10	603	35	2473.	0.1	0.1	0.0
11	595	35	3105.	0.2	0.2	0.0
12	594	35	2847.	0.2	0.2	0.0
13	593	35	9886.	0.6	0.6	0.1
14	592	35	6090.	0.3	0.3	0.1
15	591	43	9055.	0.5	0.5	0.1
16	590	35	5885.	0.3	0.3	0.1
17	589	43	4551.	0.3	0.3	0.0
18	568	35	4246.	0.2	0.2	0.0
19	566	29	2300.	0.1	0.1	0.0
20	523	35	3528.	0.2	0.2	0.0
21	522	35	2818.	0.2	0.2	0.0
22	521	35	7129.	0.4	0.4	0.1
23	520	35	3941.	0.2	0.2	0.0
24	519	35	6314.	0.4	0.4	0.1
25	518	35	3985.	0.2	0.2	0.0
26	517	35	3270.	0.2	0.2	0.0
27	497	35	3115.	0.2	0.2	0.0
28	485	35	3664.	0.2	0.2	0.0
29	484	35	2690.	0.2	0.2	0.0
30	483	35	3529.	0.2	0.2	0.0
31	482	35	2554.	0.1	0.1	0.0
32	481	35	3111.	0.2	0.2	0.0
33	459	35	2328.	0.1	0.1	0.0
34	453	35	2789.	0.2	0.2	0.0
75	359	51	24778.	1.4	1.4	0.2
94	325	43	21651.	1.2	1.2	0.2
95	324	51	29689.	1.7	1.7	0.3
96	323	51	149760.	8.5	8.5	1.5
98	321	51	26029.	1.5	1.5	0.3
109	307	59	77920.	4.4	4.4	0.8
119	297	51	18509.	1.0	1.0	0.2
126	287	51	37683.	2.1	2.1	0.4
127	286	87	397824.	22.5	22.5	3.9*
128	285	175	1766848.	100.0	100.0	17.4*^
129	284	87	47005.	2.7	2.7	0.5*
130	283	103	165612.	9.4	9.4	1.6
132	281	71	24920.	1.4	1.4	0.2
139	269	51	39724.	2.2	2.2	0.4
193	184	59	17832.	1.0	1.0	0.2
194	183	71	47143.	2.7	2.7	0.5
202	172	51	37569.	2.1	2.1	0.4
205	169	87	44891.	2.5	2.5	0.4
207	167	71	19905.	1.1	1.1	0.2
218	155	71	67872.	3.8	3.8	0.7
220	153	87	41387.	2.3	2.3	0.4
227	143	71	150368.	8.5	8.5	1.5
228	142	51	22683.	1.3	1.3	0.2
229	141	71	115348.	6.5	6.5	1.1*
230	140	87	19042.	1.1	1.1	0.2*
231	139	87	24359.	1.4	1.4	0.2*
239	131	87	141012.	8.0	8.0	1.4
241	129	87	105224.	6.0	6.0	1.0*
242	128	51	22605.	1.3	1.3	0.2
243	127	71	237128.	13.4	13.4	2.3
244	126	59	50876.	2.9	2.9	0.5
245	125	51	31737.	1.8	1.8	0.3
253	115	103	64255.	3.6	3.6	0.6*
255	113	119	77464.	4.4	4.4	0.8*
256	112	71	132968.	7.5	7.5	1.3
257	111	51	31831.	1.8	1.8	0.3
258	110	51	28410.	1.6	1.6	0.3
265	101	51	44145.	2.5	2.5	0.4
267	99	71	44937.	2.5	2.5	0.4*
268	98	59	58736.	3.3	3.3	0.6
269	97	103	27759.	1.6	1.6	0.3*
270	96	59	34508.	2.0	2.0	0.3
273	93	51	43450.	2.5	2.5	0.4
275	88	59	21440.	1.2	1.2	0.2
276	87	71	356944.	20.2	20.2	3.5
277	86	71	36382.	2.1	2.1	0.4
278	85	71	117892.	6.7	6.7	1.2
279	84	71	182248.	10.3	10.3	1.8
280	83	71	164612.	9.3	9.3	1.6
281	82	59	74328.	4.2	4.2	0.7
282	81	59	24173.	1.4	1.4	0.2
286	75	51	23901.	1.4	1.4	0.2
288	73	71	23636.	1.3	1.3	0.2
289	72	71	205572.	11.6	11.6	2.0
290	71	71	129800.	7.3	7.3	1.3
291	70	71	302496.	17.1	17.1	3.0
292	69	87	84292.	4.8	4.8	0.8*
293	68	71	82476.	4.7	4.7	0.8
294	67	51	23054.	1.3	1.3	0.2
299	59	51	24789.	1.4	1.4	0.2
300	58	71	271200.	15.3	15.3	2.7
301	57	87	143372.	8.1	8.1	1.4
302	56	71	275488.	15.6	15.6	2.7
303	55	71	166888.	9.4	9.4	1.6
304	54	51	20991.	1.2	1.2	0.2

FAB of $Cd(teta)Cl_2$ in Thioglycerol

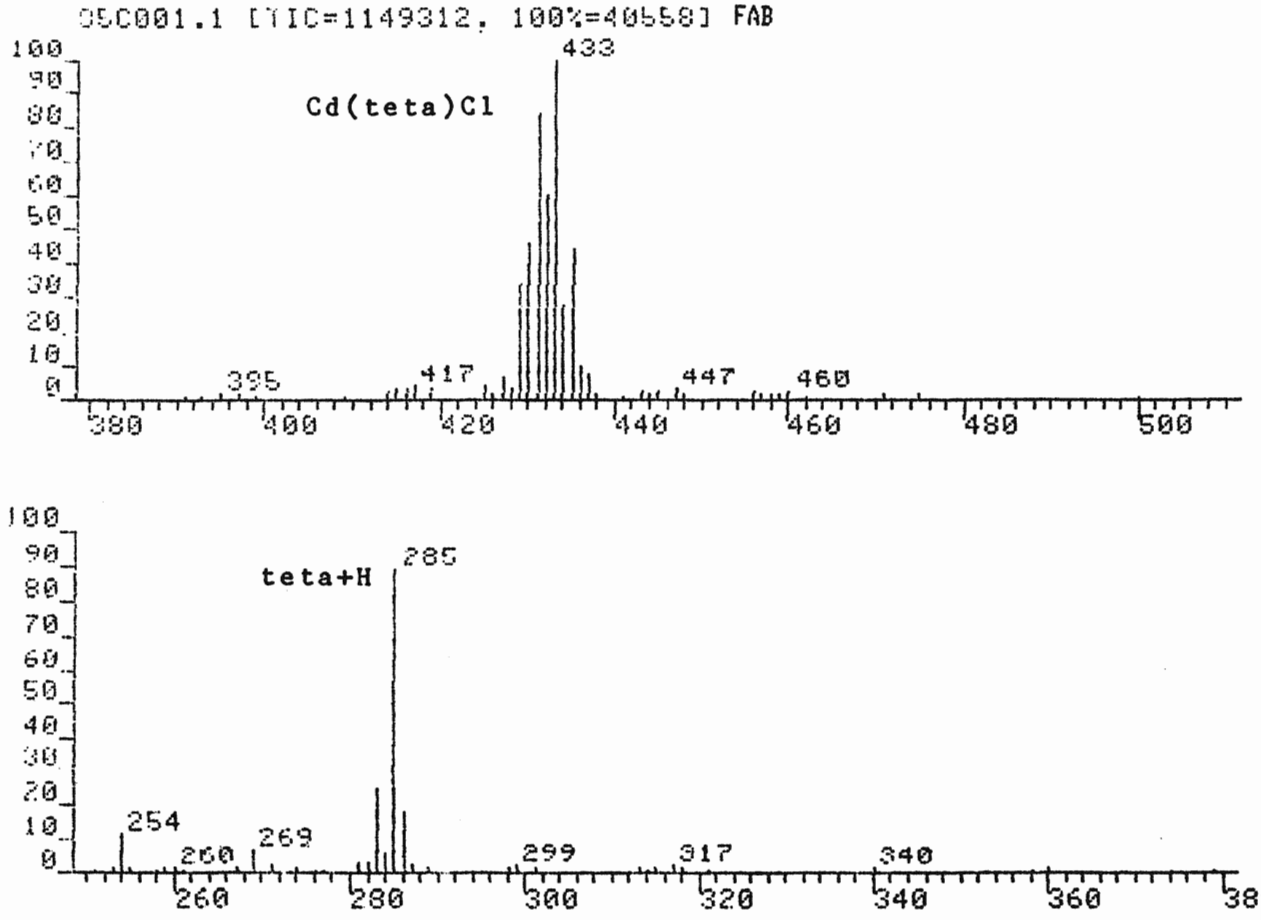

DPA:85C001.MS
SCAN: 1, 2/20/85 11: 1

IONISATION: FAB
NO. PEAKS: 272
BASE/NREF INT: 49348./ 49348.
TIC: 1149312.
MASS RANGE: 18 - 903
RETN TIME/MISC: 0: 0/ 0/ 0/ 0

PEAK NO.	MEASURED MASS	NO. POINTS	ABSOLUTE INTENSITY	% INT. BASE	% INT. NREF	% TOT. ION	PEAK NO.	MEASURED MASS	NO. POINTS	ABSOLUTE INTENSITY	% INT. BASE	% INT. NREF	% TOT. ION
22	437	35	2805.	5.7	5.7	0.2	171	119	87	5568.	11.3	11.3	0.5*
23	436	43	4034.	8.2	8.2	0.4*	177	113	103	6098.	12.4	12.4	0.5*
24	435	43	17771.	36.0	36.0	1.5	178	112	119	8224.	16.7	16.7	0.7*
25	434	43	11094.	22.5	22.5	1.0	179	111	59	3838.	7.8	7.8	0.3
26	433	51	40558.	82.2	82.2	3.5	180	110	103	3436.	7.0	7.0	0.3*
27	432	51	24003.	48.6	48.6	2.1	182	108	87	3189.	6.5	6.5	0.3*
28	431	59	34155.	69.2	69.2	3.0*	189	101	87	5262.	10.7	10.7	0.5*
29	430	43	18396.	37.3	37.3	1.6	190	100	87	6404.	13.0	13.0	0.6*
30	429	43	13834.	28.0	28.0	1.2							
32	427	35	2621.	5.3	5.3	0.2							
62	286	43	7233.	14.7	14.7	0.6							
63	285	59	36355.	73.7	73.7	3.2							
65	283	43	10214.	20.7	20.7	0.9							
72	269	35	2843.	5.8	5.8	0.2							
79	254	35	4634.	9.4	9.4	0.4							
123	183	43	4133.	8.4	8.4	0.4							
125	181	71	5253.	10.6	10.6	0.5							
131	169	71	3416.	6.9	6.9	0.3*							
133	167	71	2915.	5.9	5.9	0.3*							
138	155	87	5835.	11.8	11.8	0.5*							
147	143	87	5881.	11.9	11.9	0.5							
149	141	59	9915.	20.1	20.1	0.9							
159	131	87	11359.	23.0	23.0	1.0*							
161	129	71	3132.	6.3	6.3	0.3*							
162	128	43	2887.	5.9	5.9	0.3							
163	127	51	22706.	46.0	46.0	2.0							
164	126	51	4819.	9.8	9.8	0.4							
165	125	35	4156.	8.4	8.4	0.4							
166	124	103	4237.	8.6	8.6	0.4*							

FAB of $Cd(teta)Cl_2$ in Glycerol

[13CM2.1 [TIC=1725184, 100%=154252] FAB

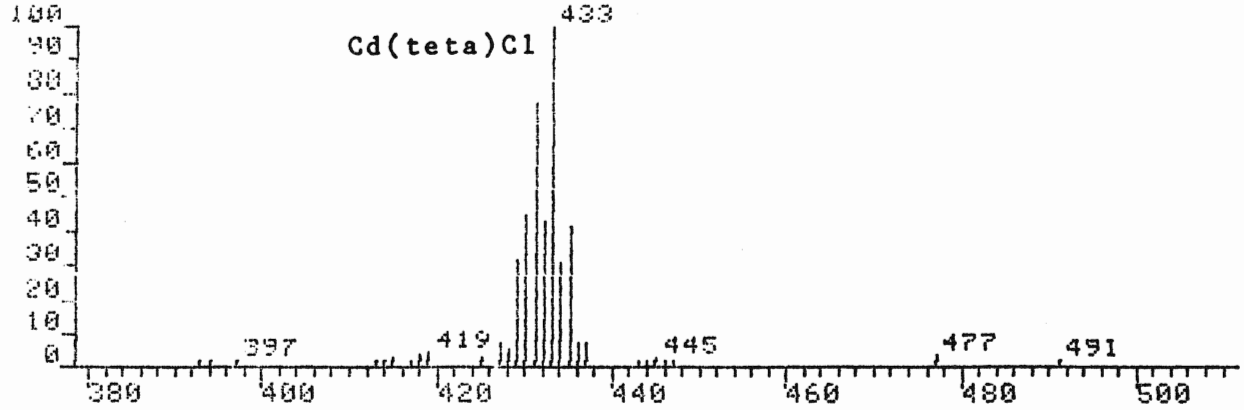

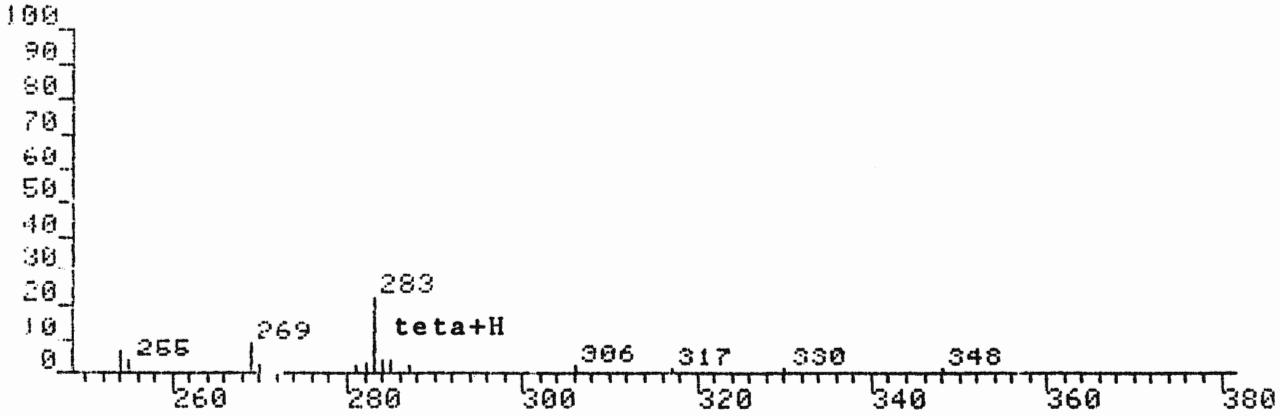

DP1:113CM2.MS
SCAN: 1. 1/13/84 9:36

IONISATION: FAB
NO. PEAKS: 112
BASE/NREF INT: 154252./ 154252.
TIC: 1725184.
MASS RANGE: 60 - 539
RETN TIME/MISC: 0: 0/ 0/ 0/ 0

PEAK NO.	MEASURED MASS	NO. POINTS	ABSOLUTE INTENSITY	% INT. BASE	% INT. NREF	% TOT. ION	PEAK NO.	MEASURED MASS	NO. POINTS	ABSOLUTE INTENSITY	% INT. BASE	% INT. NREF	% TOT. ION
3	491	21	2994.	1.9	1.9	0.2	32	330	25	2224.	1.4	1.4	0.1
4	477	35	5304.	3.4	3.4	0.3	33	317	21	2599.	1.7	1.7	0.2
5	447	29	2640.	1.7	1.7	0.2	34	306	21	3196.	2.1	2.1	0.2
6	446	21	2553.	1.7	1.7	0.1	35	287	25	3007.	1.9	1.9	0.2
7	445	21	5142.	3.3	3.3	0.3	36	285	35	4923.	3.2	3.2	0.3
8	444	25	2223.	1.4	1.4	0.1	37	284	35	4928.	3.2	3.2	0.3
9	443	25	2541.	1.6	1.6	0.1	38	283	87	34786.	22.6	22.6	2.0
10	437	59	10836.	7.0	7.0	0.6%	39	282	25	4355.	2.8	2.8	0.3
11	436	71	11252.	7.3	7.3	0.7%	40	281	25	3587.	2.3	2.3	0.2
12	435	119	64269.	41.7	41.7	3.7							
13	434	103	47384.	30.7	30.7	2.7							
14	433	119	154252.	100.0	100.0	8.9							
15	432	119	66872.	43.4	43.4	3.9%							
16	431	143	119208.	77.3	77.3	6.9							
17	430	103	68760.	44.6	44.6	4.0							
18	429	119	48171.	31.2	31.2	2.8							
19	428	59	8897.	5.8	5.8	0.5%							
20	427	51	10714.	6.9	6.9	0.6%							
21	425	51	4564.	3.0	3.0	0.3							
22	419	59	7429.	4.8	4.8	0.4%							
23	418	25	6595.	4.3	4.3	0.4							
24	417	25	2529.	1.6	1.6	0.1							
25	415	35	4162.	2.7	2.7	0.2							
26	414	21	3428.	2.2	2.2	0.2							
27	413	21	3101.	2.0	2.0	0.2							
28	397	29	3592.	2.3	2.3	0.2							
29	394	25	3169.	2.1	2.1	0.2							
30	393	29	3473.	2.3	2.3	0.2							
31	348	29	2252.	1.5	1.5	0.1							

FAB of $[Mn(teta)Cl_2]Cl$ in Thioglycerol

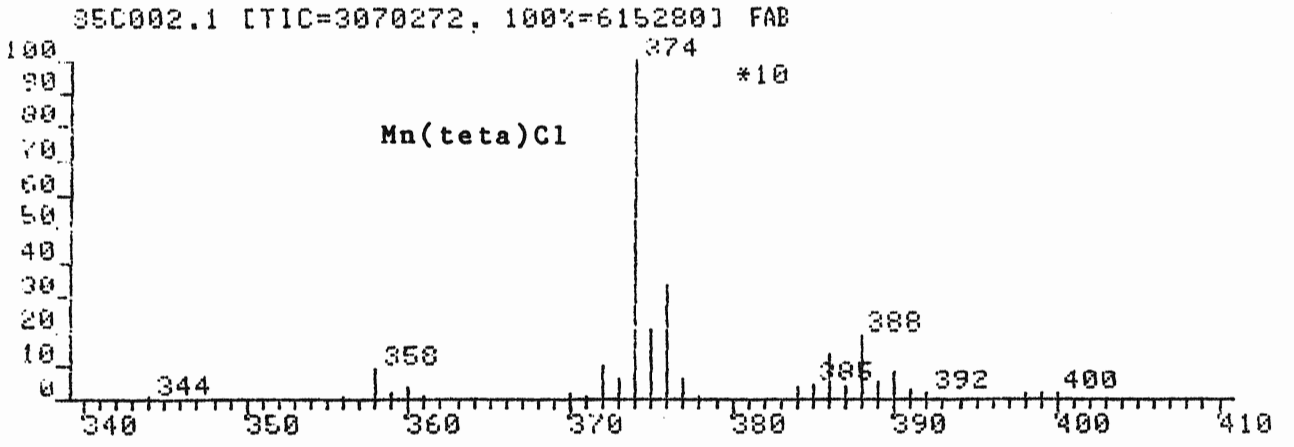

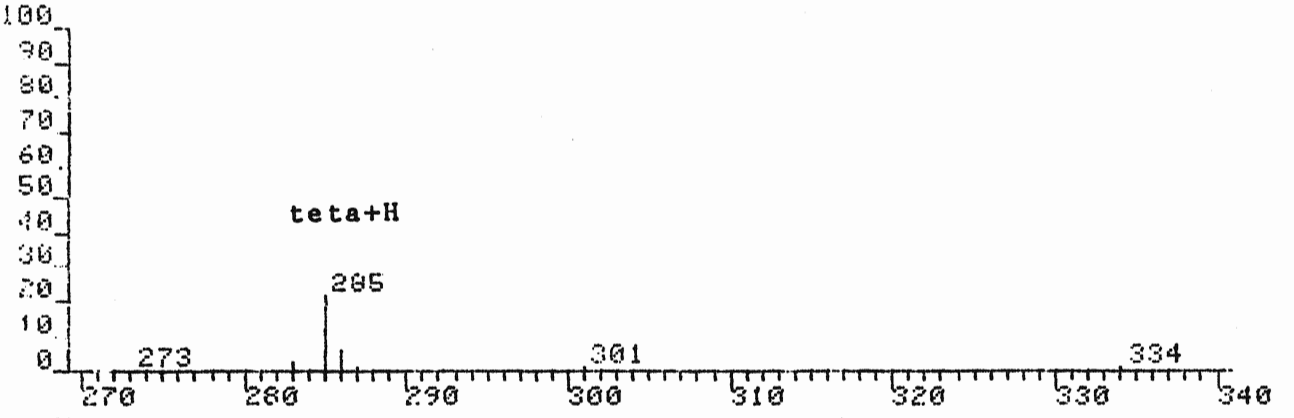

DRA:85C002.MS
SCAN: 1. 2/20/85 14:20

IONISATION: FAB
NO. PEAKS: 352
BASE/NREF INT: 615280./ 615280.
TIC: 3070272.
MASS RANGE: 18 - 911
RETN TIME/MISC: 0: 0/ 0/ 0/ 0

PEAK NO.	MEASURED MASS	NO. POINTS	ABSOLUTE INTENSITY	% INT. BASE	% INT. NREF	% TOT. ION
15	420	35	4206.	0.7	0.7	0.1
17	418	35	4630.	0.8	0.8	0.2
25	408	29	2032.	0.3	0.3	0.1
26	406	35	2003.	0.3	0.3	0.1
28	404	29	1874.	0.3	0.3	0.1
30	402	35	3536.	0.6	0.6	0.1
31	401	35	10062.	1.6	1.6	0.3
37	390	35	5269.	0.9	0.9	0.2
38	389	29	3375.	0.5	0.5	0.1
39	388	35	11627.	1.9	1.9	0.4
40	387	29	2432.	0.4	0.4	0.1
41	386	35	8146.	1.3	1.3	0.3
42	385	35	3026.	0.5	0.5	0.1
43	384	35	2351.	0.4	0.4	0.1
44	378	35	3585.	0.6	0.6	0.1
45	377	43	37104.	6.0	6.0	1.2*
46	376	71	202380.	32.9	32.9	6.6*
47	375	71	125200.	20.3	20.3	4.1*
48	374	103	615280.	100.0	100.0	20.0*
49	373	51	37657.	6.1	6.1	1.2*
50	372	51	65154.	10.6	10.6	2.1
51	371	35	3222.	0.5	0.5	0.1*
52	370	35	8305.	1.3	1.3	0.3
57	361	35	4287.	0.7	0.7	0.1
58	360	43	22088.	3.6	3.6	0.7
59	359	43	12525.	2.0	2.0	0.4
60	358	51	58782.	9.6	9.6	1.9
61	357	35	2301.	0.4	0.4	0.1
62	356	35	5575.	0.9	0.9	0.2
64	354	35	1980.	0.3	0.3	0.1
69	346	35	2660.	0.4	0.4	0.1
70	345	29	1849.	0.3	0.3	0.1
71	344	35	6644.	1.1	1.1	0.2
73	342	35	2025.	0.3	0.3	0.1
76	337	35	3213.	0.5	0.5	0.1
77	336	35	3254.	0.5	0.5	0.1
78	335	35	2967.	0.5	0.5	0.1
79	334	43	8363.	1.4	1.4	0.3
81	332	35	4410.	0.7	0.7	0.1
84	329	29	2152.	0.3	0.3	0.1
89	320	35	6076.	1.0	1.0	0.2
91	318	43	5617.	0.9	0.9	0.2
92	317	43	2998.	0.5	0.5	0.1
93	316	35	3701.	0.6	0.6	0.1
94	315	43	4291.	0.7	0.7	0.1
101	304	35	2264.	0.4	0.4	0.1
102	303	35	3297.	0.5	0.5	0.1*
103	302	43	4065.	0.7	0.7	0.1*
104	301	51	8624.	1.4	1.4	0.3*
105	300	43	2618.	0.4	0.4	0.1
106	299	59	3787.	0.6	0.6	0.1*
108	297	35	2368.	0.4	0.4	0.1
115	289	35	3440.	0.6	0.6	0.1
116	288	35	3803.	0.6	0.6	0.1
117	287	71	9162.	1.5	1.5	0.3*
118	286	51	37139.	6.0	6.0	1.2
119	285	59	133356.	21.7	21.7	4.3
120	284	43	3272.	0.5	0.5	0.1*
121	283	43	15789.	2.6	2.6	0.5*
123	281	35	2697.	0.4	0.4	0.1
124	280	35	2760.	0.4	0.4	0.1
126	278	35	3067.	0.5	0.5	0.1
128	276	35	2268.	0.4	0.4	0.1
129	275	35	3695.	0.6	0.6	0.1

FAB of [Mn(teta)Cl$_2$]Cl in Glycerol

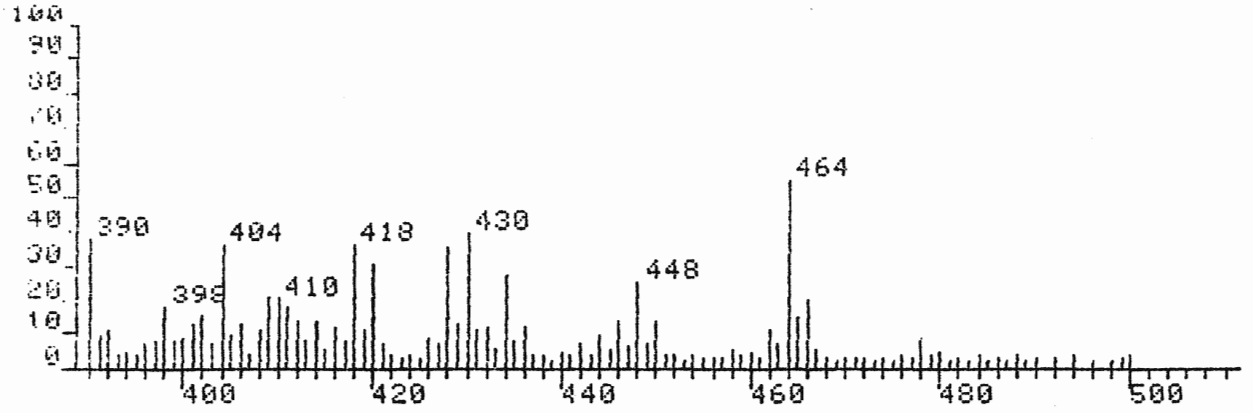

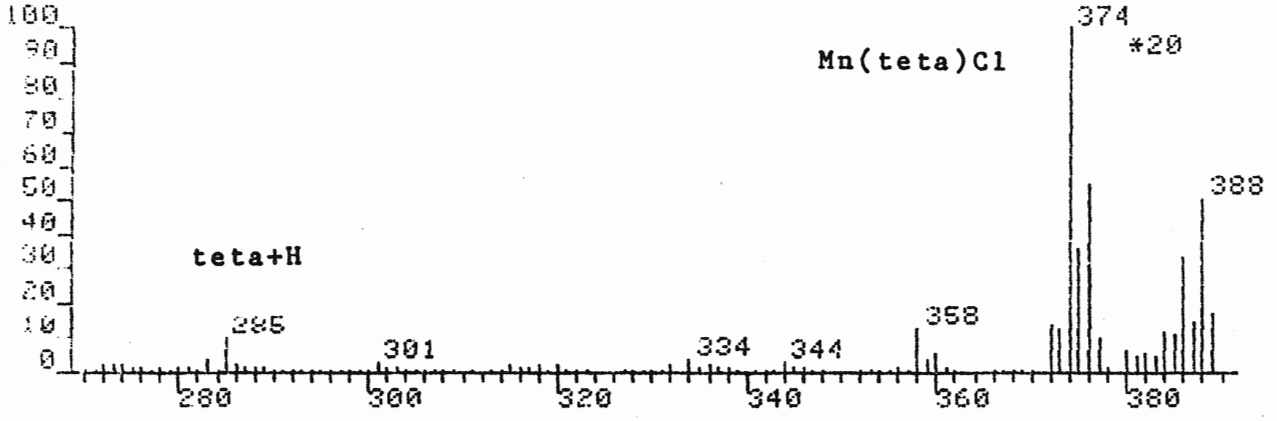

DB:111CM1.MS
SCAN: 1, 10/11/84 13:41

IONISATION: FAB
NO. PEAKS: 435
BASE/NREF INT: 2247808./ 2247808.
TIC: 15707136.
MASS RANGE: 53 - 500
RETN TIME/MISC: 0: 0/ 0/ 0/ 0

PEAK NO.	MEASURED MASS	NO. POINTS	ABSOLUTE INTENSITY	% INT. BASE	% INT. NREF	% TOT. ION
31	466	51	22307.	1.0	1.0	0.1
33	464	51	62208.	2.8	2.8	0.4
49	448	51	28104.	1.3	1.3	0.2
63	434	51	30840.	1.4	1.4	0.2
67	430	51	43730.	1.9	1.9	0.3
69	428	51	39573.	1.8	1.8	0.3
77	420	51	34409.	1.5	1.5	0.2
79	418	51	40098.	1.8	1.8	0.3
86	411	51	20508.	0.9	0.9	0.1
87	410	59	22958.	1.0	1.0	0.1
88	409	51	24102.	1.1	1.1	0.2
93	404	51	40126.	1.8	1.8	0.3
99	398	51	20328.	0.9	0.9	0.1
107	390	51	42334.	1.9	1.9	0.3
108	389	51	19227.	0.9	0.9	0.1
109	388	59	57670.	2.6	2.6	0.4
111	386	59	38160.	1.7	1.7	0.2
119	378	71	26536.	1.2	1.2	0.2*
120	377	103	233928.	10.4	10.4	1.5*
121	376	103	1231872.	54.8	54.8	7.8*
122	375	87	797936.	35.5	35.5	5.1*
123	374	119	2247808.	100.0	100.0	14.3*^
124	373	87	275440.	12.3	12.3	1.8*
125	372	175	323952.	14.4	14.4	2.1*
126	370	71	20722.	0.9	0.9	0.1
135	361	59	26721.	1.2	1.2	0.2
136	360	71	112504.	5.0	5.0	0.7
137	359	87	76548.	3.4	3.4	0.5*
138	358	103	293072.	13.0	13.0	1.9*
139	357	71	19750.	0.9	0.9	0.1
140	356	71	28265.	1.3	1.3	0.2
142	354	51	18303.	0.8	0.8	0.1
150	346	71	29861.	1.3	1.3	0.2
151	345	87	26491.	1.2	1.2	0.2
152	344	87	66696.	3.0	3.0	0.4
153	343	71	18168.	0.8	0.8	0.1
158	338	59	38165.	1.7	1.7	0.2
159	337	59	36865.	1.6	1.6	0.2
160	336	103	50849.	2.3	2.3	0.3*
161	335	103	30788.	1.4	1.4	0.2*
162	334	175	83912.	3.7	3.7	0.5*
163	332	143	45743.	2.0	2.0	0.3*
165	330	71	20397.	0.9	0.9	0.1
166	329	71	18529.	0.8	0.8	0.1
174	321	71	18154.	0.8	0.8	0.1
175	320	71	46280.	2.1	2.1	0.3
177	318	87	48956.	2.2	2.2	0.3
178	317	71	23905.	1.1	1.1	0.2
179	316	71	35606.	1.6	1.6	0.2
180	315	71	41309.	1.8	1.8	0.3
192	303	71	24447.	1.1	1.1	0.2
193	302	87	29406.	1.3	1.3	0.2
194	301	119	59902.	2.7	2.7	0.4
196	299	87	19380.	0.9	0.9	0.1
198	297	71	19518.	0.9	0.9	0.1
201	294	59	18036.	0.8	0.8	0.1
206	289	71	27757.	1.2	1.2	0.2
207	288	71	24937.	1.1	1.1	0.2
208	287	71	33564.	1.5	1.5	0.2
209	286	71	47021.	2.1	2.1	0.3
210	285	87	220524.	9.8	9.8	1.4
211	284	71	22062.	1.0	1.0	0.1
212	283	71	77236.	3.4	3.4	0.5
213	282	71	18077.	0.8	0.8	0.1
214	281	71	36073.	1.6	1.6	0.2
215	280	71	29952.	1.3	1.3	0.2
216	279	71	19635.	0.9	0.9	0.1
217	278	71	27015.	1.2	1.2	0.2
219	276	71	27215.	1.2	1.2	0.2
220	275	71	32765.	1.5	1.5	0.2

FAB of $Zn(teta)Cl_2$ in Thioglycerol

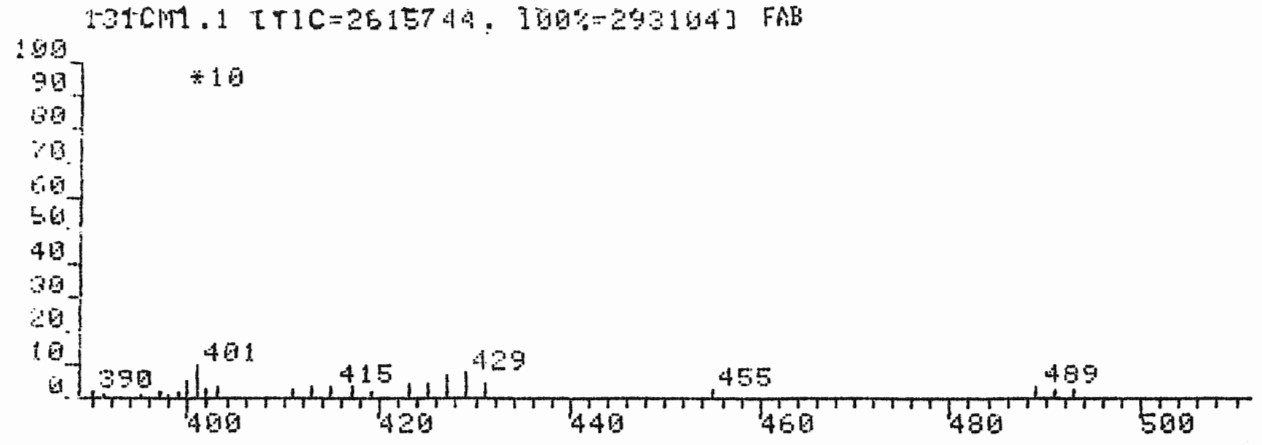

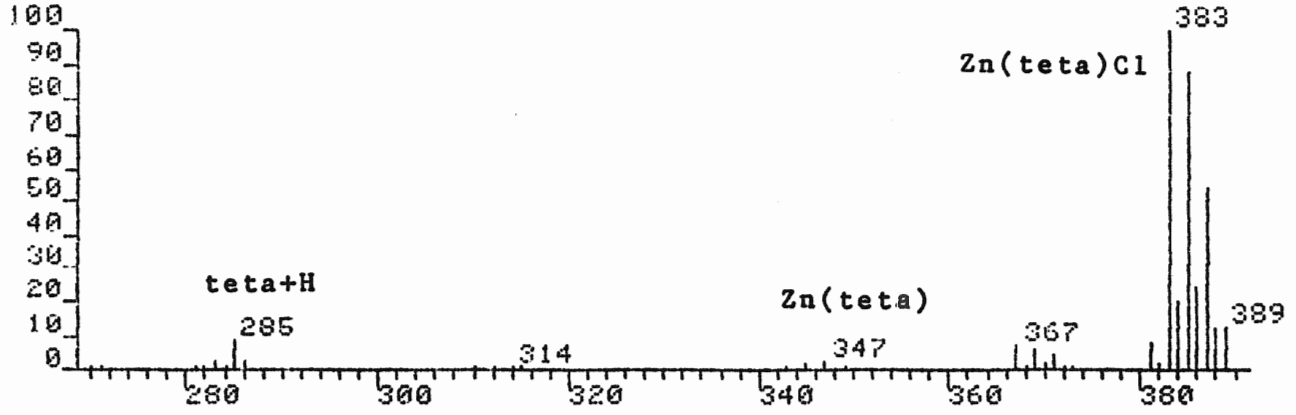

DB4:131CM1.MS
SCAN: 1. 1/31/85 13:18

IONISATION: FAB
NO. PEAKS: 330
BASE/NREF INT: 293104./ 293104.
TIC: 2615744.
MASS RANGE: 18 - 493
RETN TIME/MISC: 0: 0/ 0/ 0/ 0

PEAK NO.	MEASURED MASS	NO. POINTS	ABSOLUTE INTENSITY	% INT. BASE	% INT. NREF	% TOT. ION	PEAK NO.	MEASURED MASS	NO. POINTS	ABSOLUTE INTENSITY	% INT. BASE	% INT. NREF	% TOT. ION
17	401	29	2971.	1.0	1.0	0.1	85	315	71	3646.	1.2	1.2	0.1*
19	399	29	4941.	1.7	1.7	0.2	86	314	59	3980.	1.4	1.4	0.2*
21	397	35	5936.	2.0	2.0	0.2	88	312	35	3593.	1.2	1.2	0.1
23	395	29	2659.	0.9	0.9	0.1	90	310	29	3713.	1.3	1.3	0.1
26	390	35	6928.	2.4	2.4	0.3	100	298	35	2501.	0.9	0.9	0.1
27	389	35	39164.	13.4	13.4	1.5	108	289	35	2970.	1.0	1.0	0.1
28	388	35	36826.	12.6	12.6	1.4	111	286	59	7416.	2.5	2.5	0.3*
29	387	59	158536.	54.1	54.1	6.1*	112	285	59	27255.	9.3	9.3	1.0
30	386	43	71924.	24.5	24.5	2.7*	113	284	51	4701.	1.6	1.6	0.2*
31	385	71	259140.	88.4	88.4	9.9	114	283	59	8948.	3.1	3.1	0.3
32	384	59	59628.	20.3	20.3	2.3*	115	282	35	3528.	1.2	1.2	0.1
33	383	71	293104.	100.0	100.0	11.2*	116	281	43	4153.	1.4	1.4	0.2*
34	382	35	6410.	2.2	2.2	0.2							
35	381	35	24004.	8.2	8.2	0.9							
37	379	29	2874.	1.0	1.0	0.1							
40	373	35	3583.	1.2	1.2	0.1							
41	372	29	3002.	1.0	1.0	0.1							
42	371	35	13041.	4.4	4.4	0.5							
43	370	35	5218.	1.8	1.8	0.2							
44	369	35	18899.	6.4	6.4	0.7							
45	368	35	4628.	1.6	1.6	0.2							
46	367	35	21076.	7.2	7.2	0.8							
56	351	29	2590.	0.9	0.9	0.1							
58	349	35	5088.	1.7	1.7	0.2							
60	347	43	8392.	2.9	2.9	0.3							
62	345	43	5927.	2.0	2.0	0.2*							
64	343	51	3123.	1.1	1.1	0.1*							
73	331	35	2656.	0.9	0.9	0.1							
78	326	29	2579.	0.9	0.9	0.1							

FAB of $Zn(teta)Cl_2$ in Glycerol

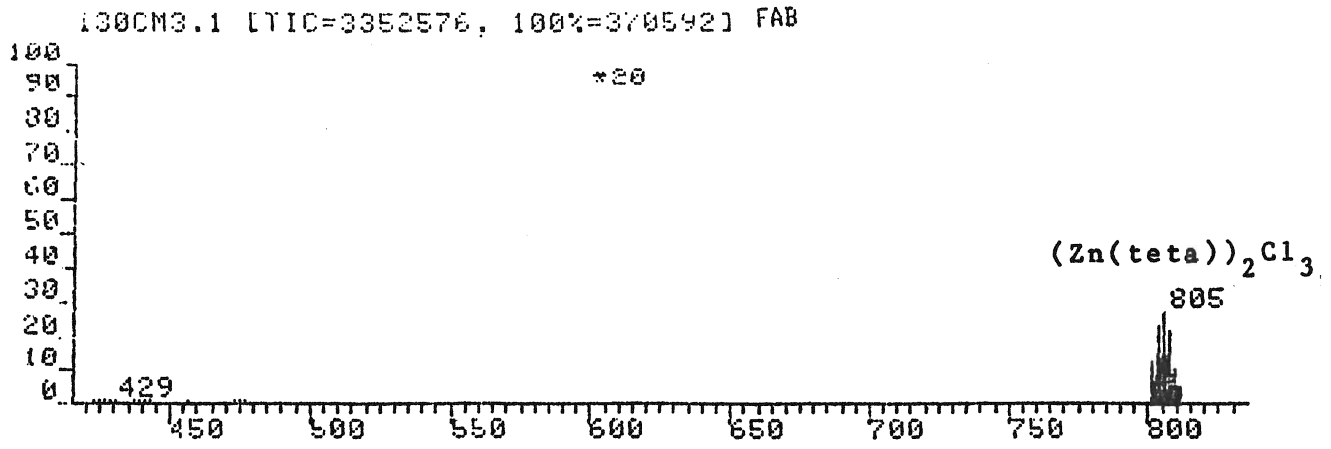

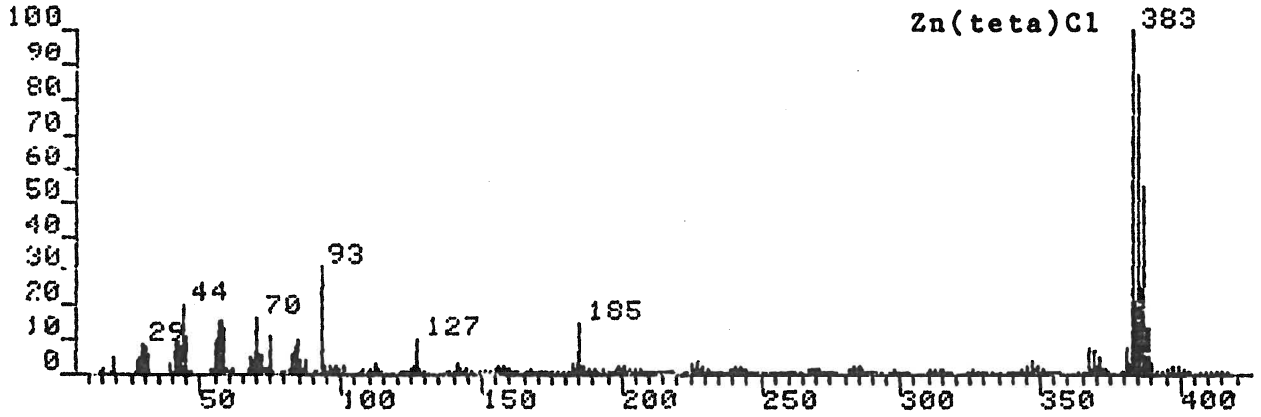

DP4:130CM3.MS
SCAN: 1. 1/30/85 16: 8

IONISATION: FAB
NO. PEAKS: 397
BASE/NREF INT: 370592./ 370592.
TIC: 3352576.
MASS RANGE: 14 - 811
RETN TIME/MISC: 0: 0/ 0/ 0/ 0

PEAK NO.	MEASURED MASS	NO. POINTS	ABSOLUTE INTENSITY	% INT. BASE	% INT. NREF	% TOT. ION	PEAK NO.	MEASURED MASS	NO. POINTS	ABSOLUTE INTENSITY	% INT. BASE	% INT. NREF	% TOT. ION
5	807	29	4061.	1.1	1.1	0.1	111	345	59	7341.	2.0	2.0	0.2%
7	805	29	5080.	1.4	1.4	0.2	113	343	59	4240.	1.1	1.1	0.1%
9	803	29	4423.	1.2	1.2	0.1	129	326	35	4249.	1.1	1.1	0.1
40	429	35	3960.	1.1	1.1	0.1	138	315	71	3974.	1.1	1.1	0.1%
60	401	35	4507.	1.2	1.2	0.1	139	314	71	5181.	1.4	1.4	0.2%
62	399	35	7549.	2.0	2.0	0.2	141	312	43	5139.	1.4	1.4	0.2%
64	397	35	7509.	2.0	2.0	0.2	143	310	35	4912.	1.3	1.3	0.1
66	395	35	4197.	1.1	1.1	0.1	154	298	35	3776.	1.0	1.0	0.1
70	390	35	9196.	2.5	2.5	0.3	166	286	43	4396.	1.2	1.2	0.1
71	389	43	50498.	13.6	13.6	1.5	167	285	71	7046.	1.9	1.9	0.2%
72	388	43	46965.	12.7	12.7	1.4	168	284	43	6246.	1.7	1.7	0.2%
73	387	59	201524.	54.4	54.4	6.0	169	283	59	8400.	2.3	2.3	0.3
74	386	59	92504.	25.0	25.0	2.8	170	282	51	5477.	1.5	1.5	0.2%
75	385	71	323216.	87.2	87.2	9.6%	171	281	43	5469.	1.5	1.5	0.2%
76	384	71	76276.	20.6	20.6	2.3%							
77	383	87	370592.	100.0	100.0	11.1							
78	382	51	9854.	2.7	2.7	0.3%							
79	381	43	27748.	7.5	7.5	0.8							
85	373	35	5136.	1.4	1.4	0.2							
86	372	35	4255.	1.1	1.1	0.1							
87	371	43	16566.	4.5	4.5	0.5							
88	370	43	7499.	2.0	2.0	0.2							
89	369	43	26337.	7.1	7.1	0.8							
90	368	35	6157.	1.7	1.7	0.2							
91	367	43	28032.	7.6	7.6	0.8							
105	351	35	4319.	1.2	1.2	0.1							
107	349	43	7734.	2.1	2.1	0.2%							
108	348	35	3966.	1.1	1.1	0.1							
109	347	51	12194.	3.3	3.3	0.4%							

FAB of [Cu(teta)]$(ClO_4)_2$ in Thioglycerol

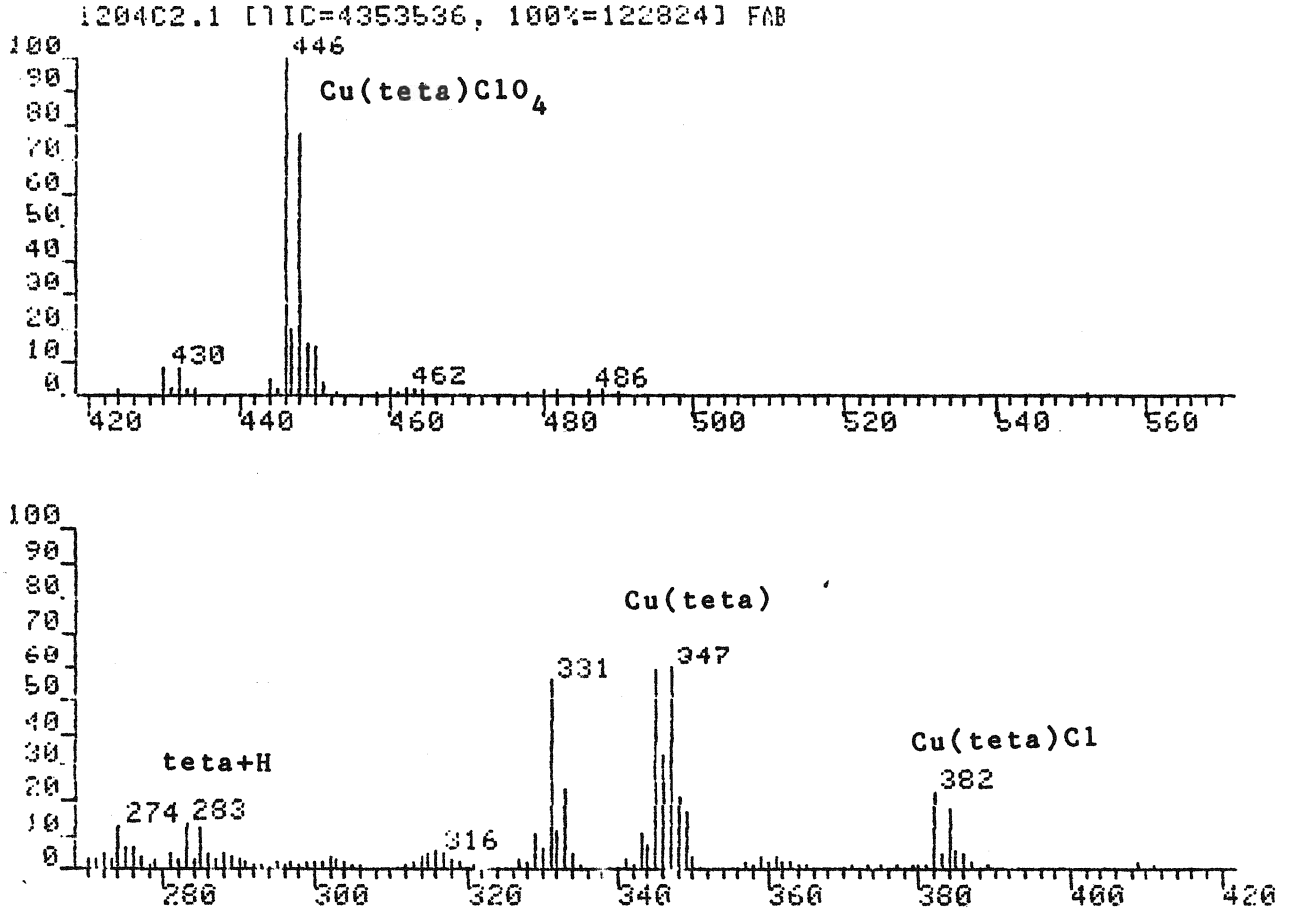

Quantitative Report for $[Cu(teta)](ClO_4)_2$ in Thioglycerol

DP4:1204C2.MS
SCAN: 1, 12/ 4/85 11:48

IONISATION: FAB
NO. PEAKS: 375
BASE/NREF INT: 168632./ 168632.
TIC: 4353536.
MASS RANGE: 14 - 552
RETN TIME/MISC: 0: 0/ 0/ 0/ 0

PEAK NO.	MEASURED MASS	NO. POINTS	ABSOLUTE INTENSITY	% INT. BASE	% INT. NREF	% TOT. ION
3	488	29	2059.	1.2	1.2	0.0
4	486	25	2107.	1.2	1.2	0.0
10	462	29	3110.	1.8	1.8	0.1
12	460	29	3052.	1.8	1.8	0.1
15	451	35	4587.	2.7	2.7	0.1
16	450	35	18586.	11.0	11.0	0.4
17	449	35	19120.	11.3	11.3	0.4*
18	448	51	95224.	56.5	56.5	2.2
19	447	43	24189.	14.3	14.3	0.6*
20	446	59	122824.	72.8	72.8	2.8*
21	445	29	2069.	1.2	1.2	0.0
22	444	35	6192.	3.7	3.7	0.1
23	434	29	2687.	1.6	1.6	0.1
24	433	29	2311.	1.4	1.4	0.1
25	432	35	9190.	5.4	5.4	0.2
26	431	35	3166.	1.9	1.9	0.1
27	430	35	10368.	6.1	6.1	0.2
31	409	35	2972.	1.8	1.8	0.1
34	387	29	2873.	1.7	1.7	0.1
35	386	29	5564.	3.3	3.3	0.1
36	385	35	6877.	4.1	4.1	0.2
37	384	35	21608.	12.8	12.8	0.5
38	383	29	6032.	3.6	3.6	0.1
39	382	35	28036.	16.6	16.6	0.6
44	377	35	2036.	1.2	1.2	0.0
51	363	35	2406.	1.4	1.4	0.1
52	362	25	2286.	1.4	1.4	0.1
53	361	35	4124.	2.4	2.4	0.1
54	360	35	2807.	1.7	1.7	0.1
55	359	35	4303.	2.6	2.6	0.1
56	358	25	1774.	1.1	1.1	0.0
57	357	29	2212.	1.3	1.3	0.1
61	350	35	4325.	2.6	2.6	0.1
62	349	35	20417.	12.1	12.1	0.5
63	348	43	25595.	15.2	15.2	0.6
64	347	51	73596.	43.6	43.6	1.7
65	346	51	41370.	24.5	24.5	1.0*
66	345	59	72216.	42.8	42.8	1.7*
67	344	35	9469.	5.6	5.6	0.2
68	343	71	13033.	7.7	7.7	0.3*
69	342	35	2014.	1.2	1.2	0.0
70	341	43	3602.	2.1	2.1	0.1*
74	334	35	5680.	3.4	3.4	0.1
75	333	43	28562.	16.9	16.9	0.7
76	332	35	13877.	8.2	8.2	0.3
77	331	59	68832.	40.8	40.8	1.6*
78	330	43	7309.	4.3	4.3	0.2*
79	329	43	13519.	8.0	8.0	0.3
80	328	29	2286.	1.4	1.4	0.1
81	327	35	3477.	2.1	2.1	0.1
84	321	35	2043.	1.2	1.2	0.0*
86	319	43	2853.	1.7	1.7	0.1*
87	318	35	3515.	2.1	2.1	0.1
88	317	43	5737.	3.4	3.4	0.1*
89	316	43	6728.	4.0	4.0	0.2*
90	315	35	5625.	3.3	3.3	0.1
91	314	43	4303.	2.6	2.6	0.1*
92	313	43	2879.	1.7	1.7	0.1
93	312	25	1861.	1.1	1.1	0.0
95	306	25	1763.	1.0	1.0	0.0
96	305	35	2048.	1.2	1.2	0.0
97	304	25	2685.	1.6	1.6	0.1
98	303	35	3251.	1.9	1.9	0.1
99	302	35	4168.	2.5	2.5	0.1
100	301	35	2887.	1.7	1.7	0.1
101	300	29	2619.	1.6	1.6	0.1
102	299	35	2222.	1.3	1.3	0.1
103	298	35	1849.	1.1	1.1	0.0
104	297	35	2709.	1.6	1.6	0.1
105	296	35	1921.	1.1	1.1	0.0
106	295	25	2192.	1.3	1.3	0.1
108	293	29	1782.	1.1	1.1	0.0
110	291	29	2269.	1.3	1.3	0.1
111	290	35	3795.	2.3	2.3	0.1
112	289	35	4056.	2.4	2.4	0.1
113	288	35	5715.	3.4	3.4	0.1
114	287	43	3512.	2.1	2.1	0.1
115	286	43	5369.	3.2	3.2	0.1
116	285	51	15282.	9.1	9.1	0.4
117	284	35	3912.	2.3	2.3	0.1
118	283	43	17601.	10.4	10.4	0.4*
119	282	35	3496.	2.1	2.1	0.1
120	281	43	6016.	3.6	3.6	0.1*
121	279	43	3347.	2.0	2.0	0.1
122	278	35	1998.	1.2	1.2	0.0
123	277	43	4185.	2.5	2.5	0.1
124	276	35	8284.	4.9	4.9	0.2
125	275	43	7899.	4.7	4.7	0.2

FAB of $[Cu(teta)](ClO_4)_2$ in Glycerol

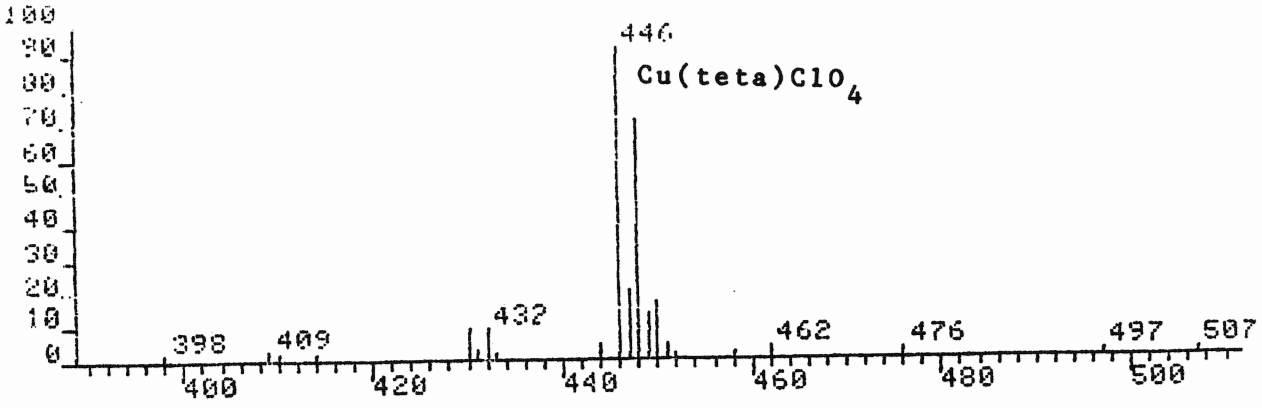

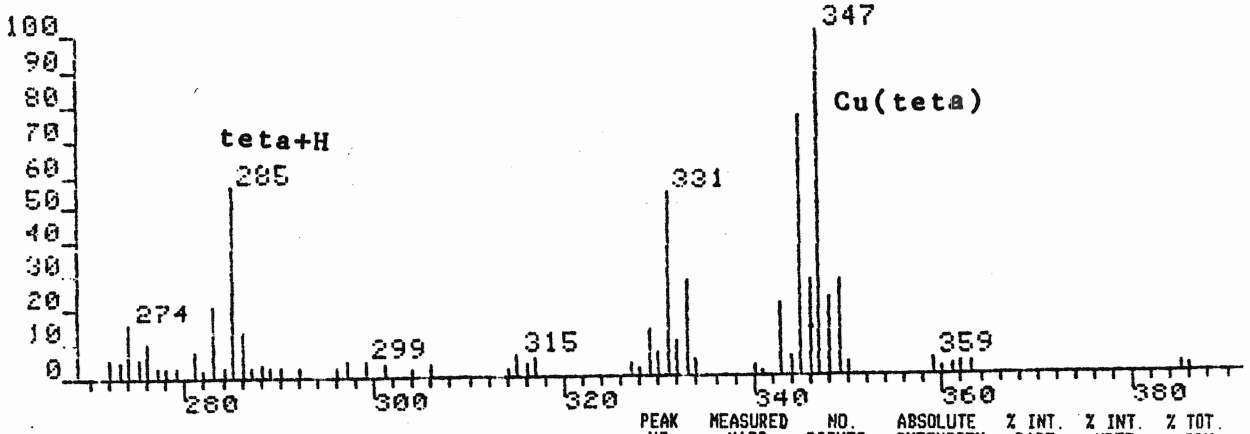

DP4:113CM1.MS
SCAN: 1. 1/13/84 9:13

IONISATION: FAB
NO. PEAKS: 247
BASE/NREF INT: 235728./ 235728.
TIC: 4206080.
MASS RANGE: 68 - 507
RETN TIME/MISC: 0: 0/ 0/ 0/ 0

PEAK NO.	MEASURED MASS	NO. POINTS	ABSOLUTE INTENSITY	% INT. BASE	% INT. NREF	% TOT. ION
1	507	21	2447.	1.0	1.0	0.1
2	497	21	3241.	1.4	1.4	0.1
3	476	35	4001.	1.7	1.7	0.1
4	462	43	4966.	2.1	2.1	0.1
5	458	35	2568.	1.1	1.1	0.1
7	451	43	6548.	2.8	2.8	0.2
8	450	71	20517.	8.7	8.7	0.5
9	449	71	16693.	7.1	7.1	0.4
10	448	103	89656.	38.0	38.0	2.1
11	447	87	25315.	10.7	10.7	0.6
12	446	143	117024.	49.6	49.6	2.8
13	444	43	6282.	2.7	2.7	0.1*
14	433	29	2888.	1.2	1.2	0.1
15	432	71	12142.	5.2	5.2	0.3
16	431	35	3367.	1.4	1.4	0.1
17	430	71	11753.	5.0	5.0	0.3
18	414	21	2683.	1.1	1.1	0.1
19	410	25	2909.	1.2	1.2	0.1
20	409	21	3868.	1.6	1.6	0.1
21	398	21	2677.	1.1	1.1	0.1
22	386	29	2843.	1.2	1.2	0.1
23	385	29	4017.	1.7	1.7	0.1
24	363	29	4251.	1.8	1.8	0.1
25	362	25	4621.	2.0	2.0	0.1
26	361	25	3997.	1.7	1.7	0.1
27	360	35	2883.	1.2	1.2	0.1
28	359	35	5920.	2.5	2.5	0.1
29	350	43	5078.	2.2	2.2	0.1
30	349	103	36013.	15.3	15.3	0.9
31	348	103	28452.	12.1	12.1	0.7*
32	347	119	127052.	53.9	53.9	3.0*
33	346	103	35964.	15.3	15.3	0.9*
34	345	143	96516.	40.9	40.9	2.3*
35	344	59	7183.	3.0	3.0	0.2*
36	343	103	26836.	11.4	11.4	0.6*
38	340	35	3617.	1.5	1.5	0.1
39	334	35	6264.	2.7	2.7	0.1*
40	333	103	35576.	15.1	15.1	0.8*
41	332	59	12902.	5.5	5.5	0.3*
42	331	103	68228.	28.9	28.9	1.6
43	330	51	9065.	3.8	3.8	0.2
44	329	71	16278.	6.9	6.9	0.4
45	328	21	3042.	1.3	1.3	0.1
46	327	35	4762.	2.0	2.0	0.1
47	317	59	6973.	3.0	3.0	0.2
48	316	43	4576.	1.9	1.9	0.1
49	315	71	7455.	3.2	3.2	0.2*
51	306	35	4971.	2.1	2.1	0.1
52	304	29	3077.	1.3	1.3	0.1
53	301	35	4224.	1.8	1.8	0.1*
54	299	43	6090.	2.6	2.6	0.1*
55	297	35	5622.	2.4	2.4	0.1
56	296	29	3565.	1.5	1.5	0.1
57	292	35	3894.	1.7	1.7	0.1
58	290	25	3955.	1.7	1.7	0.1
59	289	35	3565.	1.5	1.5	0.1
60	288	29	5170.	2.2	2.2	0.1
61	287	25	3581.	1.5	1.5	0.1
62	286	87	16892.	7.2	7.2	0.4*
63	285	103	71908.	30.5	30.5	1.7
64	284	29	3747.	1.6	1.6	0.1
65	283	87	26405.	11.2	11.2	0.6*
66	282	25	2786.	1.2	1.2	0.1
67	281	71	9435.	4.0	4.0	0.2*
68	279	35	4025.	1.7	1.7	0.1
69	278	21	3233.	1.4	1.4	0.1
70	277	29	3981.	1.7	1.7	0.1
71	276	59	12720.	5.4	5.4	0.3
72	275	35	6394.	2.7	2.7	0.2

FAB of $[Cu(teta)]Cl_2$ in Thioglycerol

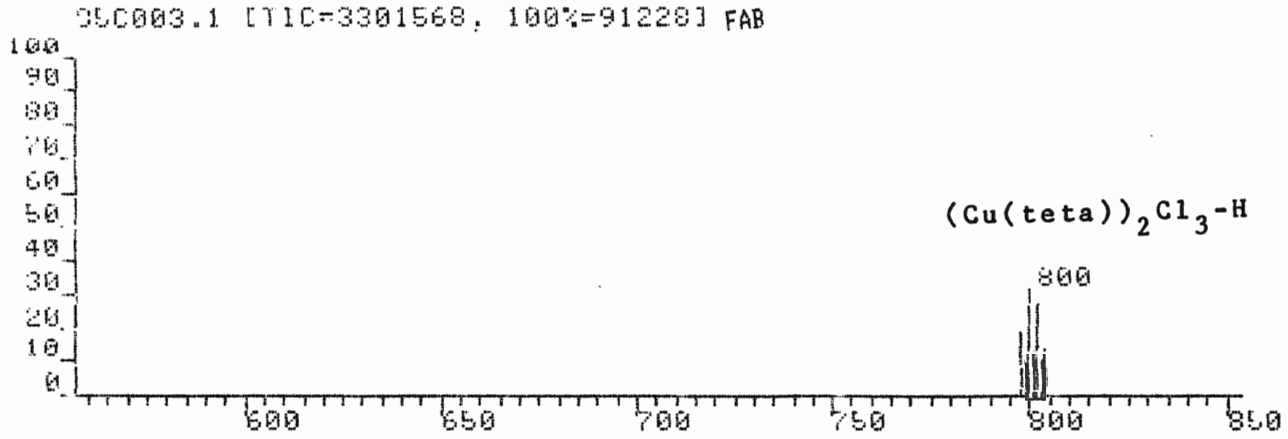

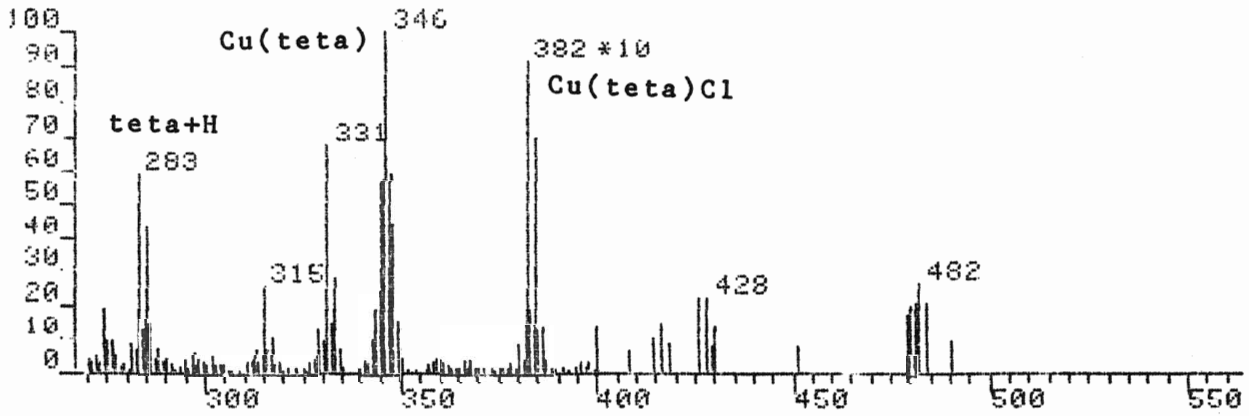

DP4:85C003.MS
SCAN: 1. 2/20/85 14:46

IONISATION: FAB
NO. PEAKS: 380
BASE/NREF INT: 136500./ 136500.
TIC: 3301568.
MASS RANGE: 18 - 804
RETN TIME/MISC: 0: 0/ 0/ 0/ 0

PEAK NO.	MEASURED MASS	NO. POINTS	ABSOLUTE INTENSITY	% INT. BASE	% INT. NREF	% TOT. ION
3	802	29	2481.	1.8	1.8	0.1
5	800	35	2826.	2.1	2.1	0.1
10	482	29	2393.	1.8	1.8	0.1
17	428	29	2063.	1.5	1.5	0.1
25	398	29	2262.	1.7	1.7	0.1
27	396	35	2388.	1.7	1.7	0.1
33	387	35	3845.	2.8	2.8	0.1
34	386	35	13152.	9.6	9.6	0.4
35	385	35	12999.	9.5	9.5	0.4
36	384	51	63959.	46.9	46.9	1.9
37	383	43	17383.	12.7	12.7	0.5
38	382	59	83716.	61.3	61.3	2.5*
39	381	35	3157.	2.3	2.3	0.1
40	380	35	7615.	5.6	5.6	0.2
42	378	29	2313.	1.7	1.7	0.1
51	368	35	3314.	2.4	2.4	0.1
53	366	35	3535.	2.6	2.6	0.1
57	362	29	2208.	1.6	1.6	0.1
58	361	35	2664.	2.0	2.0	0.1
59	360	29	3042.	2.2	2.2	0.1
60	359	35	3574.	2.6	2.6	0.1
61	358	35	2569.	1.9	1.9	0.1
66	350	35	3271.	2.4	2.4	0.1
67	349	43	14132.	10.4	10.4	0.4
68	348	51	40846.	29.9	29.9	1.2
69	347	59	53475.	39.2	39.2	1.6*
70	346	71	91228.	66.8	66.8	2.8*
71	345	59	52301.	38.3	38.3	1.6*
72	344	59	17504.	12.8	12.8	0.5*
73	343	51	9231.	6.8	6.8	0.3*
74	342	43	2851.	2.1	2.1	0.1*
75	341	71	3651.	2.7	2.7	0.1*
79	334	35	6123.	4.5	4.5	0.2
80	333	43	25496.	18.7	18.7	0.8
81	332	43	13229.	9.7	9.7	0.4
82	331	59	61624.	45.1	45.1	1.9
83	330	43	8712.	6.4	6.4	0.3*
84	329	43	10851.	7.9	7.9	0.3
85	328	43	2983.	2.2	2.2	0.1
86	327	43	2840.	2.1	2.1	0.1
92	319	43	2715.	2.0	2.0	0.1*
94	317	87	9457.	6.9	6.9	0.3*
95	316	51	5775.	4.2	4.2	0.2
96	315	175	23478.	17.2	17.2	0.7
97	314	51	2789.	2.0	2.0	0.1
98	313	71	5415.	4.0	4.0	0.2*
99	312	71	3170.	2.3	2.3	0.1*
100	311	59	2530.	1.9	1.9	0.1*
105	304	29	2201.	1.6	1.6	0.1
106	303	29	2090.	1.5	1.5	0.1
107	302	35	4099.	3.0	3.0	0.1
108	301	35	2112.	1.5	1.5	0.1
109	300	43	2672.	2.0	2.0	0.1*
110	299	35	3196.	2.3	2.3	0.1
112	297	35	4802.	3.5	3.5	0.1
114	295	29	2916.	2.1	2.1	0.1
118	290	35	3447.	2.5	2.5	0.1
119	289	35	2849.	2.1	2.1	0.1
120	288	35	6300.	4.6	4.6	0.2
121	287	51	3429.	2.5	2.5	0.1
122	286	59	13688.	10.0	10.0	0.4
123	285	51	39231.	28.7	28.7	1.2
124	284	35	11637.	8.5	8.5	0.4
125	283	51	53392.	39.1	39.1	1.6
126	282	43	6012.	4.4	4.4	0.2
127	281	35	7792.	5.7	5.7	0.2

FAB of $[Cu(teta)]Cl_2$ in Glycerol

122CM1.1 [1]C=3283072, 100%=1990281 FAB

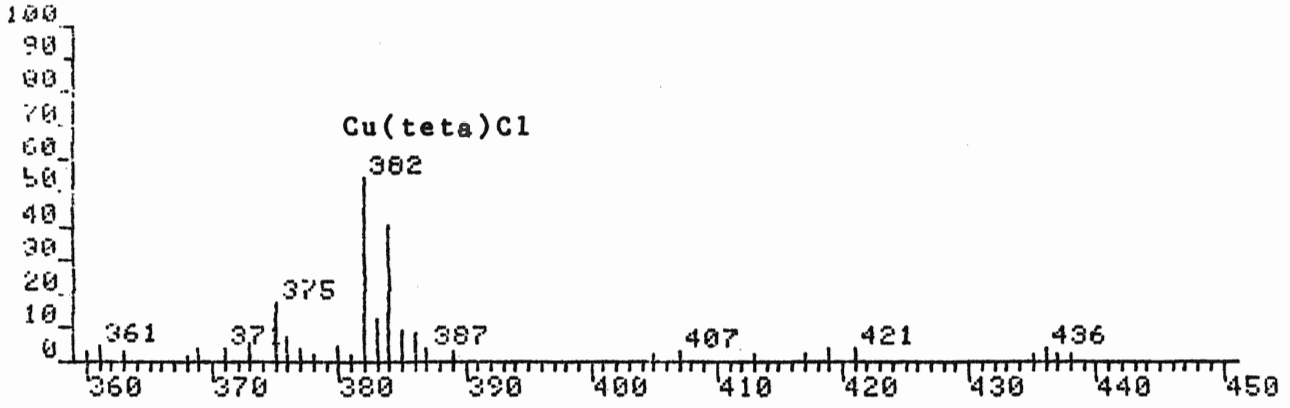

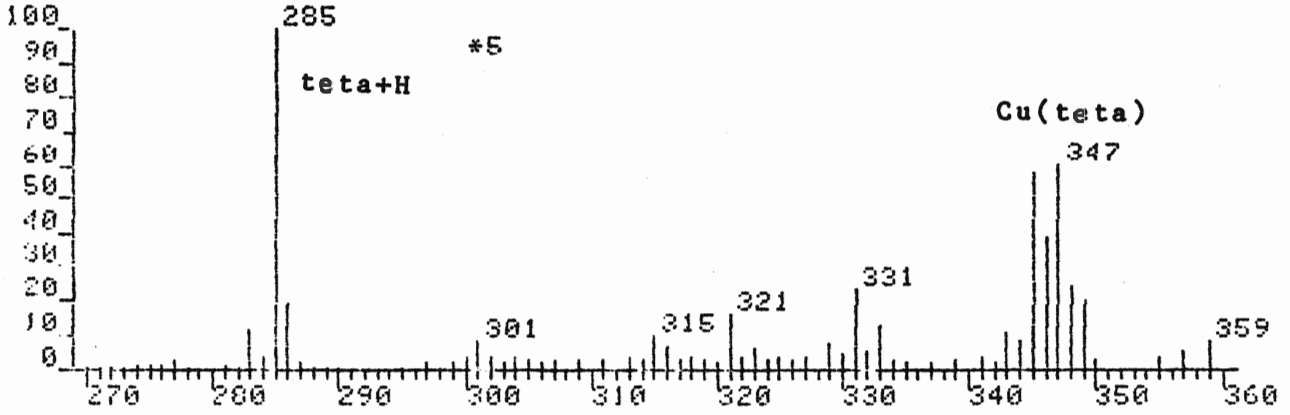

DB4:122CM1.MS
SCAN: 1. 1/22/85 15:32

IONISATION: FAB
NO. PEAKS: 315
BASE/NREF INT: 363376./ 363376.
TIC: 3283072.
MASS RANGE: 30 - 608
RETN TIME/MISC: 0: 0/ 0/ 0/ 0

PEAK NO.	MEASURED MASS	NO. POINTS	ABSOLUTE INTENSITY	% INT. BASE	% INT. NREF	% TOT. ION
15	386	59	3429.	0.9	0.9	0.1
16	385	59	3826.	1.1	1.1	0.1
17	384	71	16148.	4.4	4.4	0.5
18	383	71	4985.	1.4	1.4	0.2
19	382	71	21534.	5.9	5.9	0.7
21	380	51	1880.	0.5	0.5	0.1
24	376	59	2917.	0.8	0.8	0.1*
25	375	71	6817.	1.9	1.9	0.2
26	373	51	2139.	0.6	0.6	0.1
31	361	51	1927.	0.5	0.5	0.1
33	359	71	3373.	0.9	0.9	0.1
34	357	59	2013.	0.6	0.6	0.1
37	349	71	8035.	2.2	2.2	0.2
38	348	71	9750.	2.7	2.7	0.3
39	347	87	24103.	6.6	6.6	0.7
40	346	71	15527.	4.3	4.3	0.5
41	345	87	23108.	6.4	6.4	0.7
42	344	71	3281.	0.9	0.9	0.1
43	343	71	4398.	1.2	1.2	0.1
50	333	71	5166.	1.4	1.4	0.2
51	332	59	2247.	0.6	0.6	0.1
52	331	71	9372.	2.6	2.6	0.3
53	330	51	1947.	0.5	0.5	0.1*
54	329	59	2926.	0.8	0.8	0.1
59	323	51	2329.	0.6	0.6	0.1
61	321	71	6332.	1.7	1.7	0.2
66	316	59	2715.	0.7	0.7	0.1
67	315	87	4023.	1.1	1.1	0.1
78	301	71	3360.	0.9	0.9	0.1

PEAK NO.	MEASURED MASS	NO. POINTS	ABSOLUTE INTENSITY	% INT. BASE	% INT. NREF	% TOT. ION
80	299	71	4398.	1.2	1.2	0.1
82	297	71	4580.	1.3	1.3	0.1
88	287	87	4668.	1.3	1.3	0.1*
89	286	87	39223.	10.8	10.8	1.2
90	285	119	199028.	54.8	54.8	6.1
91	284	71	7775.	2.1	2.1	0.2
92	283	71	22332.	6.1	6.1	0.7
94	281	51	2577.	0.7	0.7	0.1
96	277	59	5548.	1.5	1.5	0.2
97	276	59	2273.	0.6	0.6	0.1
98	275	59	2533.	0.7	0.7	0.1

FAB of [Ni(teta)]Cl_2 in Thioglycerol

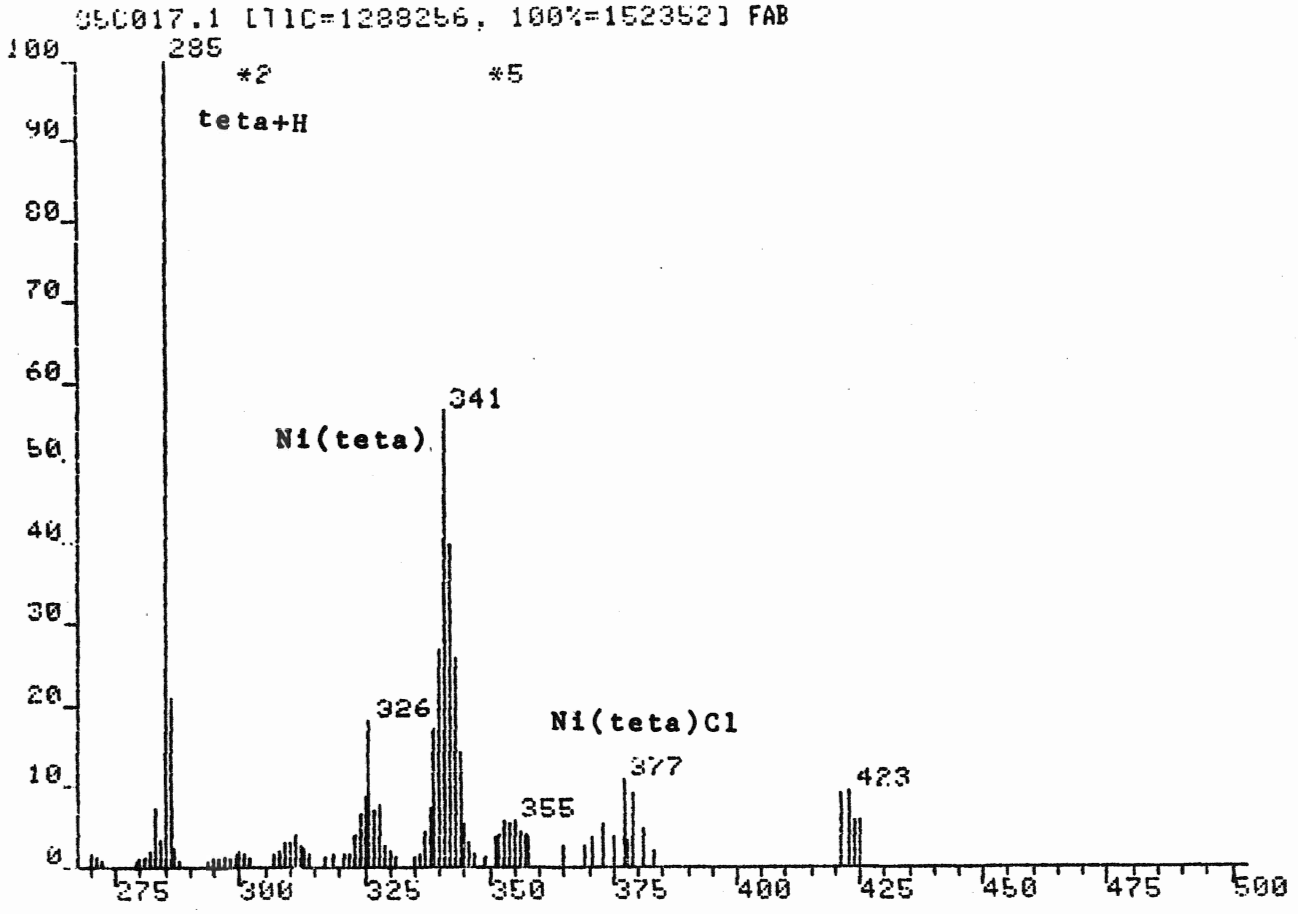

BR4 050017.MS 6/25/85 13:53
SCAN 1:

IONISATION: FAB
NO. PEAKS: 249
BASE/NREF INT: 152352./ 152352.
TIC: 1288256.
MASS RANGE: 68 - 651
RETN TIME/MISC: 0: 0/ 0/ 0/ 0

PEAK NO.	MEASURED MASS	NO. POINTS	ABSOLUTE INTENSITY	% INT. BASE	% INT. NREF	% TOT. ION
1	651	21	1608.	1.1	1.1	0.1
2	649	29	2131.	1.4	1.4	0.2
4	425	29	1729.	1.1	1.1	0.1
5	424	25	1615.	1.1	1.1	0.1
6	423	29	2850.	1.9	1.9	0.2
7	421	29	2637.	1.7	1.7	0.2
10	379	29	2797.	1.8	1.8	0.2
12	377	35	3284.	2.2	2.2	0.3
21	355	29	1736.	1.1	1.1	0.1
23	353	25	1633.	1.1	1.1	0.1
28	346	29	2091.	1.4	1.4	0.2
29	345	29	3966.	2.6	2.6	0.3
30	344	35	10604.	7.0	7.0	0.8
31	343	43	19716.	12.9	12.9	1.5%
32	342	43	30225.	19.8	19.8	2.3
33	341	51	42731.	28.0	28.0	3.3%
34	340	59	20555.	13.5	13.5	1.6%
35	339	51	12899.	8.5	8.5	1.0%
36	338	59	5326.	3.5	3.5	0.4%
37	337	35	3210.	2.1	2.1	0.2%
42	329	29	1854.	1.2	1.2	0.1
43	328	35	5689.	3.7	3.7	0.4
44	327	35	5275.	3.5	3.5	0.4
45	326	43	13615.	8.9	8.9	1.1
46	325	35	6402.	4.2	4.2	0.5
47	324	35	5036.	3.3	3.3	0.4
48	323	35	3012.	2.0	2.0	0.2
54	313	25	1610.	1.1	1.1	0.1
55	312	29	1959.	1.3	1.3	0.2

PEAK NO.	MEASURED MASS	NO. POINTS	ABSOLUTE INTENSITY	% INT. BASE	% INT. NREF	% TOT. ION
56	311	35	3009.	2.0	2.0	0.2
57	310	29	2246.	1.5	1.5	0.2
58	309	29	2282.	1.5	1.5	0.2
59	308	35	1555.	1.0	1.0	0.1
63	300	29	1535.	1.0	1.0	0.1
64	299	35	2227.	1.5	1.5	0.2%
66	297	35	2002.	1.3	1.3	0.2
71	287	35	3355.	2.2	2.2	0.3
72	286	59	31653.	20.8	20.8	2.5
73	285	71	152352.	100.0	100.0	11.8%
74	284	51	4923.	3.2	3.2	0.4
75	283	51	10680.	7.0	7.0	0.8
76	282	35	3166.	2.1	2.1	0.2
77	281	35	1863.	1.2	1.2	0.1%

FAB of [Ni(teta)]Cl_2 in Glycerol

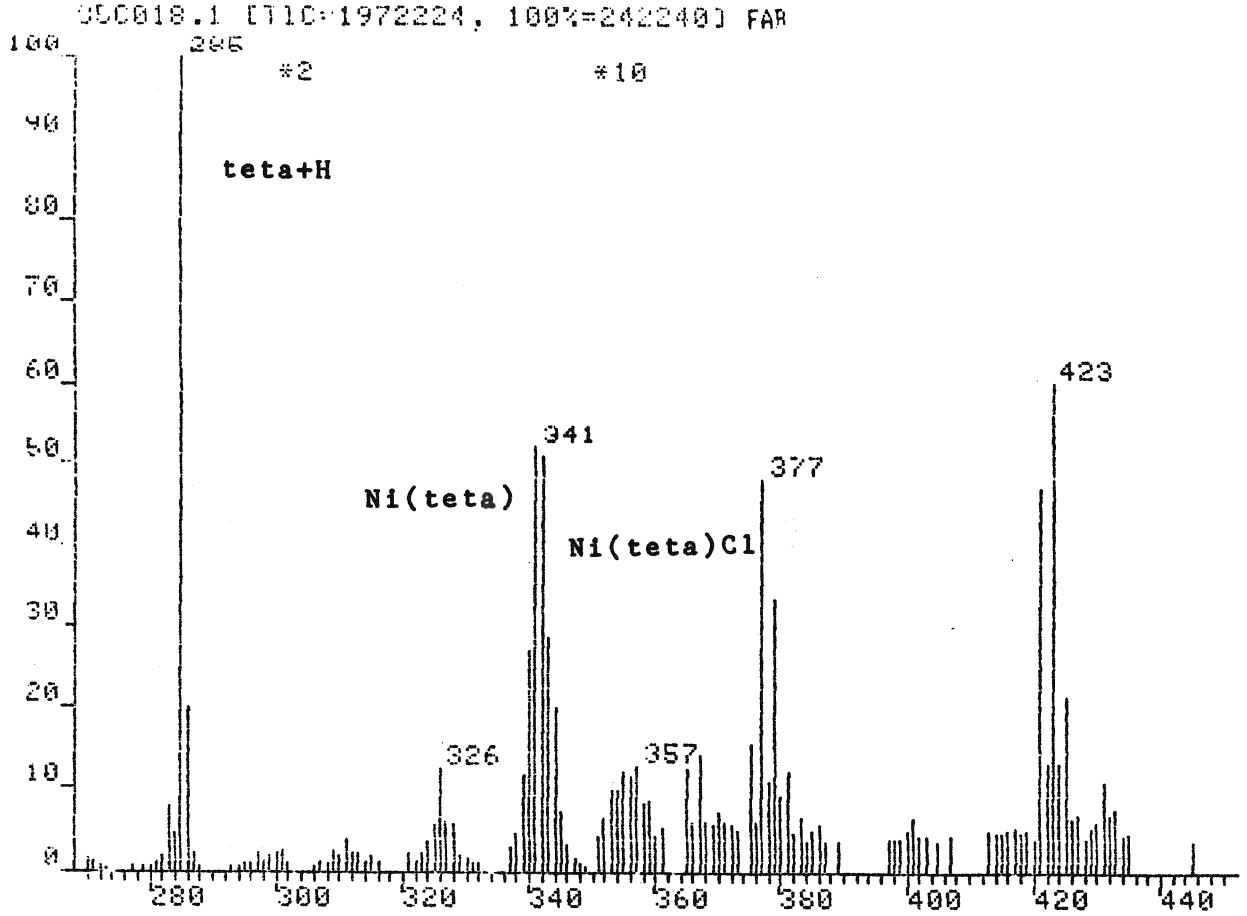

...050018.MS
SCAN: 1. 6/25/85 14: 8

IONISATION: FAB
NO. PEAKS: 301
BASE/NREF INT: 242240./ 242240.
TIC: 1972224.
MASS RANGE: 68 - 651
RETN TIME/MISC: 0: 0/ 0/ 0/ 0

PEAK NO.	MEASURED MASS	NO. POINTS	ABSOLUTE INTENSITY	% INT. BASE	% INT. NREF	% TOT. ION	PEAK NO.	MEASURED MASS	NO. POINTS	ABSOLUTE INTENSITY	% INT. BASE	% INT. NREF	% TOT. ION
10	431	35	2611.	1.1	1.1	0.1	83	338	43	5442.	2.2	2.2	0.3*
16	425	35	5144.	2.1	2.1	0.3	84	337	43	3324.	1.4	1.4	0.2*
17	424	35	3127.	1.3	1.3	0.2	88	329	29	2459.	1.0	1.0	0.1
18	423	43	14601.	6.0	6.0	0.7	89	328	35	6670.	2.8	2.8	0.3
19	422	35	3221.	1.3	1.3	0.2	90	327	43	7227.	3.0	3.0	0.4
20	421	43	11468.	4.7	4.7	0.6	91	326	43	15172.	6.3	6.3	0.8
45	381	35	2905.	1.2	1.2	0.1	92	325	43	6893.	2.8	2.8	0.3
46	380	25	2172.	0.9	0.9	0.1	93	324	35	4321.	1.8	1.8	0.2
47	379	35	8122.	3.4	3.4	0.4	94	323	35	2573.	1.1	1.1	0.1
48	378	29	2626.	1.1	1.1	0.1	96	321	35	2622.	1.1	1.1	0.1
49	377	43	11669.	4.8	4.8	0.6	98	315	35	2462.	1.0	1.0	0.1
51	375	35	3705.	1.5	1.5	0.2	100	313	35	2618.	1.1	1.1	0.1
58	367	35	3408.	1.4	1.4	0.2	101	312	35	2662.	1.1	1.1	0.1
60	365	35	2992.	1.2	1.2	0.2	102	311	43	4760.	2.0	2.0	0.2
63	359	29	2073.	0.9	0.9	0.1*	103	310	35	2498.	1.0	1.0	0.1
64	358	25	1987.	0.8	0.8	0.1	104	309	43	2926.	1.2	1.2	0.1*
65	357	35	3104.	1.3	1.3	0.2	109	301	35	3073.	1.3	1.3	0.2*
66	356	35	2804.	1.2	1.2	0.1	110	300	35	2842.	1.2	1.2	0.1
67	355	29	2953.	1.2	1.2	0.1	111	299	43	4876.	2.0	2.0	0.2
68	354	29	2410.	1.0	1.0	0.1	112	298	35	2855.	1.2	1.2	0.1*
69	353	29	2350.	1.0	1.0	0.1	113	297	43	5564.	2.3	2.3	0.3
75	346	35	3935.	1.6	1.6	0.2	115	295	35	2343.	1.0	1.0	0.1*
76	345	43	8696.	3.6	3.6	0.4	119	287	43	5699.	2.4	2.4	0.3*
77	344	43	24150.	10.0	10.0	1.2	120	286	59	48659.	20.1	20.1	2.5
78	343	51	34561.	14.3	14.3	1.8	121	285	103	242240.	100.0	100.0	12.3*
79	342	51	61559.	25.4	25.4	3.1	122	284	59	10746.	4.4	4.4	0.5
80	341	71	63309.	26.1	26.1	3.2*	123	283	51	19112.	7.9	7.9	1.0
81	340	59	32594.	13.5	13.5	1.7*	124	282	43	5008.	2.1	2.1	0.3
82	339	59	14419.	6.0	6.0	0.7*	125	281	43	2900.	1.2	1.2	0.1*

FAB of $Zn(teta)ClNO_2$ in Thioglycerol

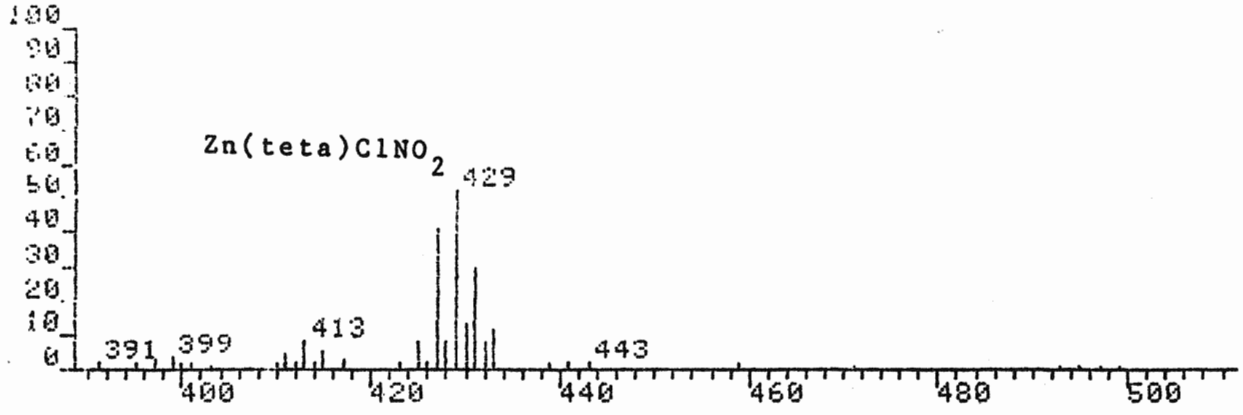

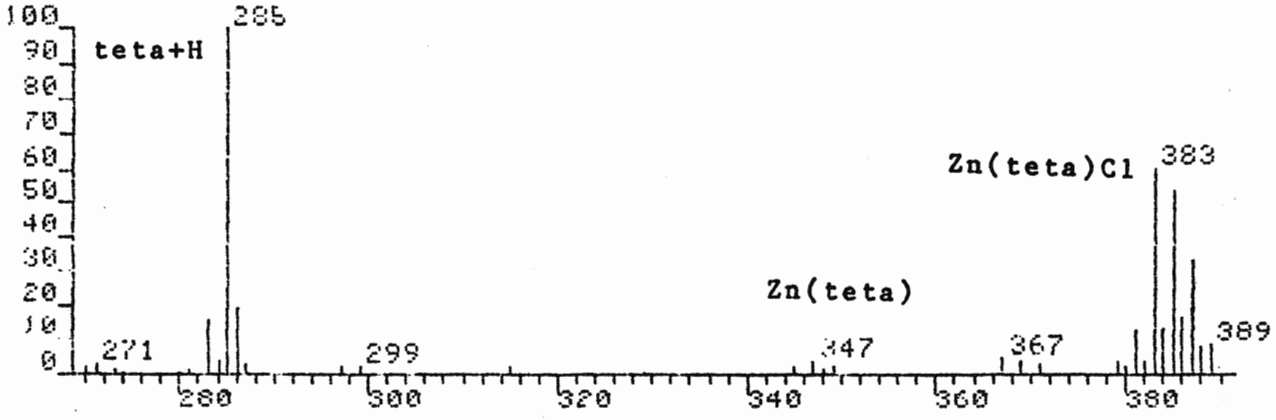

DE:4.1107C1.MS
SCAN: 1. 11/ 7/84 11: 4

IONISATION: FAB
NO. PEAKS: 206
BASE/NREF INT: 155076./ 155076.
TIC: 2049728.
MASS RANGE: 53 - 600
RETN TIME/MISC: 0: 0/ 0/ 0/ 0

PEAK NO.	MEASURED MASS	NO. POINTS	ABSOLUTE INTENSITY	% INT. BASE	% INT. NREF	% TOT. ION	PEAK NO.	MEASURED MASS	NO. POINTS	ABSOLUTE INTENSITY	% INT. BASE	% INT. NREF	% TOT. ION
29	495	43	1544.	1.0	1.0	0.1	59	391	51	3594.	2.3	2.3	0.2
31	471	29	1627.	1.0	1.0	0.1	60	389	43	13872.	8.9	8.9	0.7
32	459	29	1870.	1.2	1.2	0.1	61	388	35	11393.	7.3	7.3	0.6
33	443	25	3982.	2.6	2.6	0.2	62	387	71	52669.	34.0	34.0	2.6
34	441	29	3547.	2.3	2.3	0.2	63	386	43	24825.	16.0	16.0	1.2
35	439	29	2293.	1.5	1.5	0.1	64	385	87	83180.	53.6	53.6	4.1
36	433	43	18556.	12.0	12.0	0.9	65	384	43	20781.	13.4	13.4	1.0
37	432	43	12376.	8.0	8.0	0.6	66	383	87	93396.	60.2	60.2	4.6
38	431	43	46653.	30.1	30.1	2.3	67	382	43	5314.	3.4	3.4	0.3
39	430	43	19989.	12.9	12.9	1.0	68	381	35	19114.	12.3	12.3	0.9
40	429	71	81124.	52.3	52.3	4.0	69	380	35	2763.	1.8	1.8	0.1
41	428	43	13770.	8.9	8.9	0.7	70	379	43	6163.	4.0	4.0	0.3
42	427	51	62567.	40.3	40.3	3.1	71	371	35	3888.	2.5	2.5	0.2
43	426	35	3097.	2.0	2.0	0.2	72	369	29	5888.	3.8	3.8	0.3
44	425	43	12846.	8.3	8.3	0.6	73	367	29	7534.	4.9	4.9	0.4
45	423	43	3462.	2.2	2.2	0.2	74	349	35	3586.	2.3	2.3	0.2
46	417	43	4619.	3.0	3.0	0.2	75	348	25	1652.	1.1	1.1	0.1
47	415	35	8204.	5.3	5.3	0.4	76	347	35	6235.	4.0	4.0	0.3
48	414	43	3470.	2.2	2.2	0.2	77	345	35	3747.	2.4	2.4	0.2
49	413	51	12690.	8.2	8.2	0.6	78	329	29	1496.	1.0	1.0	0.1
50	412	35	3955.	2.6	2.6	0.2	79	315	43	2902.	1.9	1.9	0.1
51	411	35	7945.	5.1	5.1	0.4	80	299	29	3208.	2.1	2.1	0.2
52	410	43	2845.	1.8	1.8	0.1	81	297	35	3149.	2.0	2.0	0.2
53	403	29	1828.	1.2	1.2	0.1	82	287	71	4626.	3.0	3.0	0.2
54	401	35	2903.	1.9	1.9	0.1	83	286	71	29746.	19.2	19.2	1.5
55	400	35	2527.	1.6	1.6	0.1	84	285	103	155076.	100.0	100.0	7.6
56	399	51	5471.	3.5	3.5	0.3	85	284	51	6155.	4.0	4.0	0.3
57	397	35	4893.	3.2	3.2	0.2	86	283	51	23646.	15.2	15.2	1.2
58	395	29	3111.	2.0	2.0	0.2	87	281	25	2625.	1.7	1.7	0.1

FAB of $Zn(teta)ClNO_2$ in Glycerol

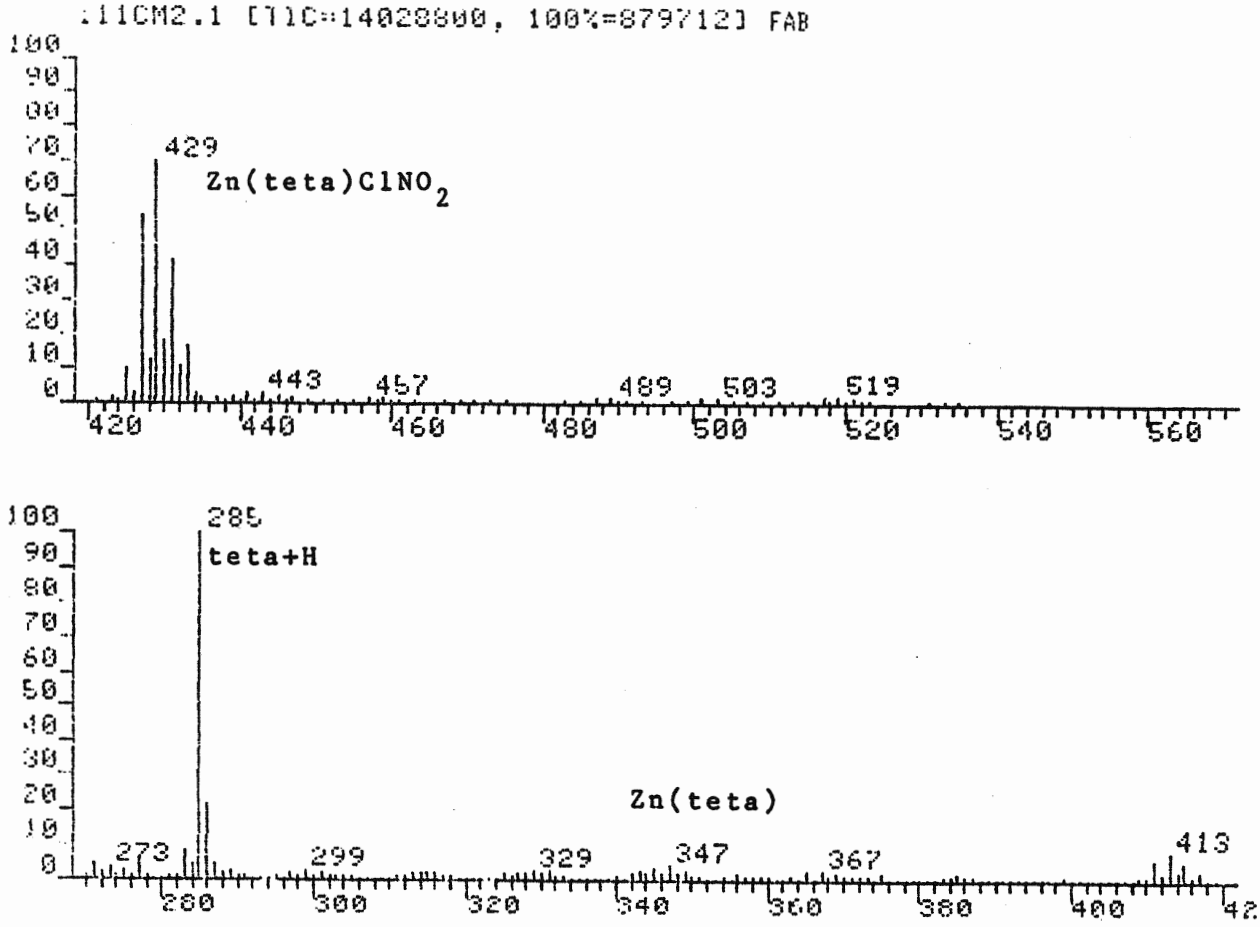

DP4:111CM2.MS
SCAN: 1, 10/11/84 15: 8

IONISATION: FAB
NO. PEAKS: 482
BASE/NREF INT: 1405248./ 1405248.
TIC: 14028800.
MASS RANGE: 53 - 549
RETN TIME/MISC: 0: 0/ 0/ 0/ 0

PEAK NO.	MEASURED MASS	NO. POINTS	ABSOLUTE INTENSITY	% INT. BASE	% INT. NREF	% TOT. ION
22	521	43	15102.	1.1	1.1	0.1
24	519	43	23028.	1.6	1.6	0.2
26	517	43	18817.	1.3	1.3	0.1
81	459	43	14427.	1.0	1.0	0.1
83	457	51	15339.	1.1	1.1	0.1
95	445	51	22047.	1.6	1.6	0.2
97	443	51	28161.	2.0	2.0	0.2
99	441	51	27073.	1.9	1.9	0.2
101	439	51	19491.	1.4	1.4	0.1
103	437	51	15067.	1.1	1.1	0.1
106	434	51	28116.	2.0	2.0	0.2
107	433	71	142224.	10.1	10.1	1.0
108	432	71	97612.	6.9	6.9	0.7*
109	431	87	365024.	26.0	26.0	2.6*
110	430	87	162640.	11.6	11.6	1.2*
111	429	103	613984.	43.7	43.7	4.4*
112	428	71	106476.	7.6	7.6	0.8*
113	427	103	478400.	34.0	34.0	3.4*
114	426	71	28680.	2.0	2.0	0.2*
115	425	71	87232.	6.2	6.2	0.6*
117	423	51	15667.	1.1	1.1	0.1
123	417	51	23051.	1.6	1.6	0.2
124	416	51	14255.	1.0	1.0	0.1
125	415	59	48203.	3.4	3.4	0.3
126	414	51	22237.	1.6	1.6	0.2
127	413	71	71768.	5.1	5.1	0.5
128	412	51	18002.	1.3	1.3	0.1
129	411	59	51641.	3.7	3.7	0.4
153	387	51	14156.	1.0	1.0	0.1
155	385	51	16067.	1.1	1.1	0.1
157	383	59	14429.	1.0	1.0	0.1
165	375	71	15911.	1.1	1.1	0.1
171	369	59	16456.	1.2	1.2	0.1
173	367	59	27587.	2.0	2.0	0.2
175	365	51	27233.	1.9	1.9	0.2
184	356	59	19341.	1.4	1.4	0.1
189	351	59	14381.	1.0	1.0	0.1
191	349	71	27549.	2.0	2.0	0.2
192	348	71	21612.	1.5	1.5	0.2
193	347	71	43164.	3.1	3.1	0.3
194	346	87	19140.	1.4	1.4	0.1
195	345	87	36063.	2.6	2.6	0.3
196	344	71	21381.	1.5	1.5	0.2*
197	343	87	21808.	1.6	1.6	0.2*
198	342	59	16378.	1.2	1.2	0.1
209	331	71	22953.	1.6	1.6	0.2
210	330	71	17818.	1.3	1.3	0.1
211	329	71	23837.	1.7	1.7	0.2
212	328	71	19372.	1.4	1.4	0.1
213	327	71	21323.	1.5	1.5	0.2
214	326	71	14332.	1.0	1.0	0.1
215	325	71	21008.	1.5	1.5	0.1
224	316	71	17983.	1.3	1.3	0.1
225	315	71	20758.	1.5	1.5	0.1
226	314	71	18618.	1.3	1.3	0.1
227	313	71	18031.	1.3	1.3	0.1
239	301	71	20336.	1.4	1.4	0.1
241	299	87	21809.	1.6	1.6	0.2
243	297	87	20672.	1.5	1.5	0.1
251	289	71	21929.	1.6	1.6	0.2
252	288	71	18526.	1.3	1.3	0.1
253	287	87	42559.	3.0	3.0	0.3*
254	286	119	188200.	13.4	13.4	1.3*
255	285	143	879712.	62.6	62.6	6.3*
256	284	103	39326.	2.8	2.8	0.3*
257	283	103	78480.	5.6	5.6	0.6
259	281	71	15306.	1.1	1.1	0.1
263	277	71	49471.	3.5	3.5	0.4

APPENDIX III

The BMASABD and Bayesian Results for the Metal Complexes of Teta

The BMASABD data for $[Co(teta)(CN)_2]ClO_4$

(a) The % Composition of the Dehydrogenated Fragments

Fragment	% Composition
Co(teta)	9.75333
Co(teta)-H	23.61660
Co(teta)-2H	14.18570
Co(teta)-3H	22.00590
Co(teta)-4H	8.59596
Co(teta)-5H	13.68690
Co(teta)-6H	2.89647
Co(teta)-7H	3.32421
Co(teta)-8H	1.93941

(b) Observed and Calculated Averaged Intensities

m/z	Observed	Calculated	Difference
347	0.00000	0.00002	-0.00002
346	0.00000	0.00053	-0.00053
345	0.00000	0.00920	-0.00920
344	0.12500	0.10474	0.02026
343	0.63700	0.64087	-0.00387
342	1.16700	1.16660	0.00040
341	0.81400	0.81403	-0.00003
340	1.04100	1.04100	0.00000
339	0.49400	0.49400	0.00000
338	0.62200	0.62200	0.00000
337	0.15600	0.15600	0.00000
336	0.16100	0.16100	0.00000
335	0.08400	0.08400	0.00000

Average Deviation = 0.003

The BMASABD Data for $[Co(teta)Cl_2]ClO_4$ Spectrum 622CM1

(a) The % Composition of the Dehydrogenated Fragments

Fragment	% Composition
Co(teta)	11.44300
Co(teta)-H	18.96260
Co(teta)-2H	20.07160
Co(teta)-3H	22.75850
Co(teta)-4H	8.68362
Co(teta)-5H	18.08070

(b) Observed and Calculated Averaged Intensities

m/z	Observed	Calculated	Difference
347	0.00000	0.00005	-0.00005
346	0.00000	0.00117	-0.00117
345	0.00000	0.02012	-0.02012
344	0.25700	0.22468	0.03232
343	1.31000	1.31608	-0.00608
342	1.97100	1.97037	0.00063
341	2.08700	2.08704	-0.00004
340	2.09000	2.09000	0.00000
339	1.03400	1.03400	0.00000
338	2.52200	2.52200	0.00000

Average Deviation = 0.006

The BMASABD Data for $[Co(teta)Cl_2]ClO_4$ Spectrum 85RP1

(a) The % Composition of the Dehydrogenated Fragments

Fragment	% Composition
Co(teta)	8.49768
Co(teta)-H	14.94480
Co(teta)-2H	23.40100
Co(teta)-3H	23.58770
Co(teta)-4H	6.76771
Co(teta)-5H	18.02470
Co(teta)-6H	2.69371
Co(teta)-7H	1.33924
Co(teta)-8H	0.74346

(b) Observed and Calculated Averaged Intensities

m/z	Observed	Calculated	Difference
347	0.10000	0.00006	0.09994
346	0.00000	0.00139	-0.00139
345	0.10000	0.02407	0.07593
344	0.30000	0.27013	0.02987
343	1.60000	1.60741	-0.00741
342	2.70000	2.69917	0.00083
341	3.80000	3.80006	-0.00006
340	3.40000	3.40000	0.00000
339	1.40000	1.40000	0.00000
338	2.50000	2.50000	0.00000
337	0.40000	0.40000	0.00000
336	0.20000	0.20000	0.00000
335	0.10000	0.10000	0.00000

Average Deviation = 0.017

The BMASABD Data for $[Co(teta)Cl_2]ClO_4$ Spectrum 85RP2

(a) The % Composition of the Dehydrogenated Fragments

Fragment	% Composition
Co(teta)	8.09828
Co(teta)-H	13.89950
Co(teta)-2H	24.49290
Co(teta)-3H	25.52100
Co(teta)-4H	7.09154
Co(teta)-5H	20.89670

(b) Observed and Calculated Averaged Intensities

m/z	Observed	Calculated	Difference
347	0.10000	0.00005	0.09995
346	0.10000	0.00123	0.09877
345	0.10000	0.02118	0.07882
344	0.30000	0.23766	0.06234
343	1.40000	1.41407	-0.01407
342	2.40000	2.39846	0.00154
341	3.70000	3.70011	-0.00011
340	3.40000	3.39999	0.00001
339	1.40000	1.40000	0.00000
338	2.60000	2.60000	0.00000

Average Deviation = 0.036

The BMASABD data for $[Co(teta)Cl_2]Cl$

(a) The % Composition of the Dehydrogenated Fragments

Fragment	% Composition
Co(teta)	2.30138
Co(teta)-H	6.72428
Co(teta)-2H	17.77230
Co(teta)-3H	23.22440
Co(teta)-4H	7.14924
Co(teta)-5H	16.70200
Co(teta)-6H	21.51210
Co(teta)-7H	4.02417
Co(teta)-8H	0.59011

(b) Observed and Calculated Averaged Intensities

m/z	Observed	Calculated	Difference
347	0.00000	0.00002	-0.00002
346	0.00000	0.00055	-0.00055
345	0.00000	0.00979	-0.00979
344	0.16800	0.11441	0.05359
343	0.74300	0.75352	-0.01052
342	2.01700	2.01590	0.00110
341	4.24300	4.24308	-0.00008
340	4.70000	4.70000	0.00000
339	2.04700	2.04700	0.00000
338	3.96100	3.96100	0.00000
337	4.19900	4.19900	0.00000
336	0.77900	0.77900	0.00000
335	0.11100	0.11100	0.00000

Average Deviation = 0.006

The BMASABD data for $[Co(teta)(SCN)_2]SCN$ in Thioglycerol

(a) The % Composition of the Dehydrogenated Fragments

Fragment	% Composition
Co(teta)	1.91758
Co(teta)-H	24.39170
Co(teta)-2H	15.61000
Co(teta)-3H	24.52270
Co(teta)-4H	5.53024
Co(teta)-5H	16.59440
Co(teta)-6H	5.15946
Co(teta)-7H	6.27394

(b) Observed and Calculated Averaged Intensities

m/z	Observed	Calculated	Difference
347	0.00000	0.00001	-0.00001
346	0.00000	0.00041	-0.00041
345	0.00000	0.00779	-0.00779
344	0.10400	0.10400	0.00000
343	0.85700	0.85685	0.00015
342	3.37100	3.37102	-0.00002
341	2.48500	2.48500	0.00000
340	3.12600	3.12600	0.00000
339	1.07700	1.07700	0.00000
338	2.13800	2.13800	0.00000
337	0.77200	0.77200	0.00000
336	0.75600	0.75600	0.00000

Average Deviation = 0.001

The BMASABD data for $[Cu(teta)](ClO_4)_2$

(a) The % Composition of the Dehydrogenated Fragments

Fragment	% Composition
Cu(teta)	38.88720
Cu(teta)-H	7.07896
Cu(teta)-2H	40.34430
Cu(teta)-3H	1.10324
Cu(teta)-4H	12.58620

(b) Observed and Calculated Averaged Intensities

m/z	Observed	Calculated	Difference
350	0.12000	0.17969	-0.05969
349	0.86000	0.95391	-0.09391
348	0.68000	0.73524	-0.05524
347	3.02000	2.95977	0.06023
346	0.86000	0.83727	0.02273
345	2.29000	2.31680	-0.02680
344	0.17000	0.18018	-0.01018
343	0.64000	0.62801	0.01199

Average Deviation = 0.043

The BMASABD data for $[Cu(teta)]Cl_2$

(a) The % Composition of the Dehydrogenated Fragments

Fragment	% Composition
Cu(teta)	25.19750
Cu(teta)-H	18.97250
Cu(teta)-2H	22.57460
Cu(teta)-3H	-1.54535
Cu(teta)-4H	34.80070

(b) Observed and Calculated Averaged Intensities

m/z	Observed	Calculated	Difference
350	0.00000	0.04505	-0.04505
349	0.24500	0.25073	-0.00573
348	0.29700	0.29238	0.00462
347	0.73400	0.72817	0.00583
346	0.47300	0.47541	-0.00241
345	0.70400	0.70658	-0.00258
344	0.10000	0.09892	0.00108
343	0.64000	0.63885	0.00115

Average Deviation = 0.009

The BMASABD data for $[Ni(teta)]Cl_2$

(a) The % Composition of the Dehydrogenated Fragments

Fragment	% Composition
Ni(teta)	18.04170
Ni(teta)-H	41.52240
Ni(teta)-2H	19.72100
Ni(teta)-3H	14.43990
Ni(teta)-4H	6.27507

(b) Observed and Calculated Averaged Intensities

m/z	Observed	Calculated	Difference
346	0.20000	0.12932	0.07068
345	0.30000	0.31268	-0.01268
344	0.80000	0.81750	-0.01750
343	1.50000	1.48521	0.01479
342	2.30000	2.29923	0.00077
341	3.30000	3.30447	-0.00447
340	1.60000	1.60076	-0.00076
339	1.00000	0.99888	0.00112
338	0.40000	0.39939	0.00061

Average Deviation = 0.014

The Results from the Single Precision Bayesian Analysis using Twenty Scans

Compostion (%)

	least squares	Bayes
Co(teta)	8.91	8.38
Co(teta)-H	15.10	16.30
Co(teta)-2H	25.07	24.65
Co(teta)-3H	27.68	25.02
Co(teta)-4H	0.00	0.00
Co(teta)-5H	23.26	25.66

(b) Observed and Calculated Averaged Intensities

m/z	Obsd (%)	Calcd (%) least squares	Calcd (%) Bayes
347	0.4661	0.0003	0.0003
346	0.3056	0.0089	0.0084
345	0.5297	0.1532	0.1460
344	1.6782	1.7177	1.6487
343	8.9381	10.1888	9.9406
342	15.9052	16.9065	17.7856
341	24.0697	25.0977	24.3232
340	22.0227	23.0493	20.9110
339	9.3387	3.7985	4.1902
338	16.7457	19.0789	21.0460

sum of squares, least squares = 41.26

sum of squares, Bayes = 51.29

The Results from the Double Precision Bayesian Analysis using Fifteen Scans

Compostion (%)

	least squares	Bayes
Co(teta)	9.03	7.13
Co(teta)-H	15.09	15.93
Co(teta)-2H	25.06	25.36
Co(teta)-3H	27.13	29.46
Co(teta)-4H	0.00	0.00
Co(teta)-5H	23.69	22.12

(b) Observed and Calculated Averaged Intensities

m/z	Obsd (%)	Calcd (%) least squares	Calcd (%) Bayes
347	0.4597	0.0004	0.0003
346	0.2810	0.0090	0.0073
345	0.5593	0.1550	0.1263
344	1.6934	1.7370	1.4391
343	9.0622	10.2844	8.8710
342	15.9140	16.8925	17.6675
341	24.0018	25.0063	25.6350
340	21.6088	22.6116	24.4974
339	9.2609	3.8693	3.6123
338	17.1588	19.4344	18.1438

sum of squares, least squares = 39.16

sum of squares, Bayes = 47.54

APPENDIX IV

The $Zn(NO_3)_2.6H_2O$ was reported to have less than 0.005% chloride. The zinc nitrate complex was tested with $AgNO_3$ solution and gave a negative indication for chloride. The zinc teta complex was tested with $AgNO_3$ and a positive result was obtained. The preliminary results indicated chloride contamination of the teta ligand.

A sodium fusion on the teta Strem lot# 158k was done. The test confirmed the presence of chloride. A melting point of the ligand clearly indicated the compound to be impure. The Strem Chemical Co. was informed of the impurity. After a number of denials and some checking by the company the faulty chemical was replaced. A check on the melting point of the new batch showed the chemical to be pure.

The impurity of the ligand was a concern as a number of the cobalt complexes not containing chloride as a ligand, had peaks due to chloride. A number of theses complexes were resynthesized and their FAB spectra repeated. The complexes for which resynthesis was deemed necessary included all the cobalt complexes with the exception of the dichloro and azide complexes, as these already contained chloride as a ligand.

APPENDIX V

The oxidative dehydrogenation reaction was proposed as an explanation for the hydrogen loss observed in the teta complexes. The reaction was believed to proceed through oxidation of the +I species to a +II species (ie Co(I)(teta)--->Co(II)(teta)) followed by hydrogen loss, and reduction of the complex to the +I species. Therefore, the use of an oxidizing matrix should increase the intensity of the species obtained due to loss of hydrogens if this reaction is occurring.

The positive FAB mass spectra of $[Co(teta)(CN)_2]ClO_4$ and $[Cu(teta)](ClO_4)_2$ were obtained using nitrobenzyl alcohol as the matrix. The spectra of these complexes in nitrobenzyl alcohol are given on pages A49 and A50 respectively. The spectrum of the $[Cu(teta)](ClO_4)_2$ complex was similar to the spectrum obtained in glycerol (page A28), with the exception that the peak at m/z 345 was equivalent in intensity to the peak at m/z 347. The peak at m/z 345 has been identified as loss of two hydrogens from the $[Cu(teta)]^+$ species. The nitrobenzyl alcohol matrix has enhanced hydrogen loss in the copper complex.

The $[Co(teta)(CN)_2]ClO_4$ complex also produced a similar spectrum in nitrobenzyl alcohol to the one obtained in glycerol (page A10). The peaks due to hydrogen loss, however were altered to a great extent in the oxidizing matrix. The peak due to the $[Co(teta)]^+$ at m/z 343 was much greater in intensity in the glycerol matrix than in the nitrobenzyl alcohol matrix. The

FAB of $[Co(teta)(CN)_2]ClO_4$ in Nitrobenzyl alcohol

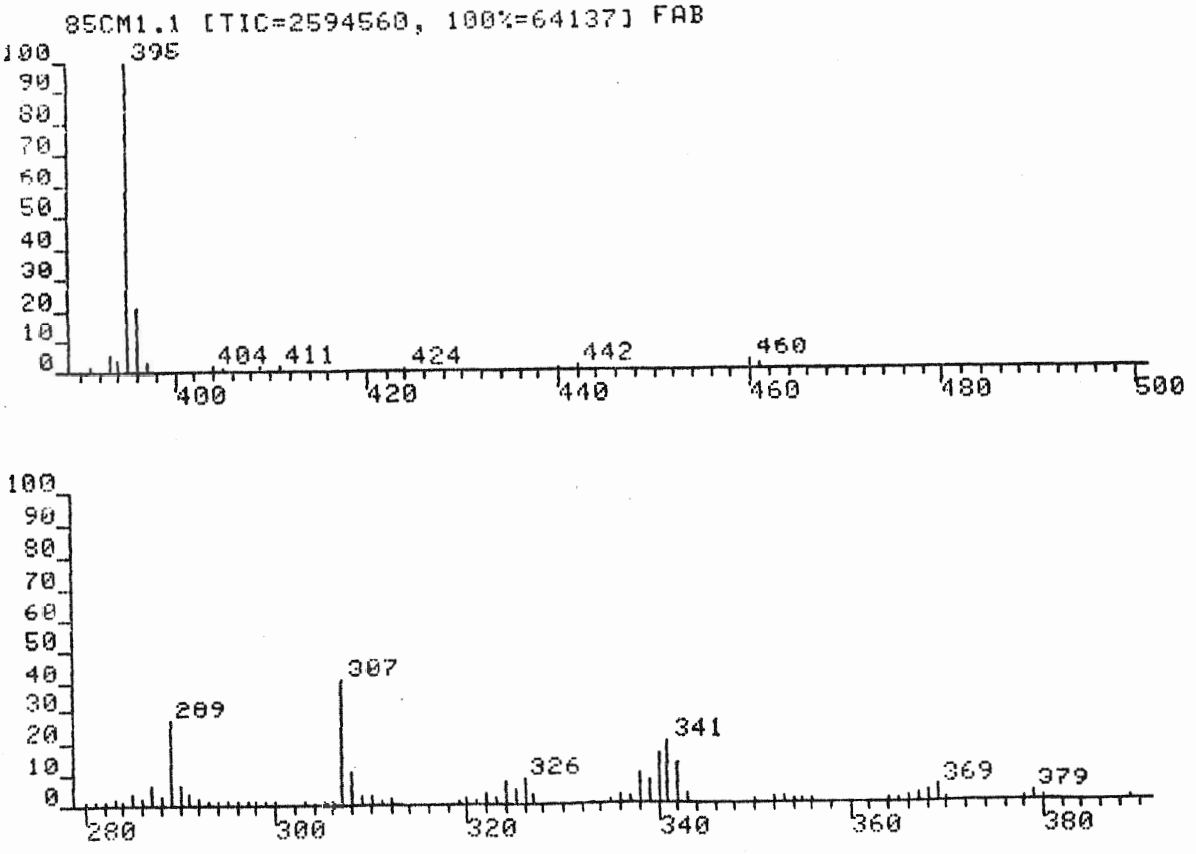

DATA:85CM1 MS
SCAN: 1: 10/25/85 12:36
IONISATION: FAB
NO. PEAKS: 317
BASE/NREF INT: 192044./ 192044.
TIC: 2594560.
MASS RANGE: 30 - 509
RETN TIME/MISC: 0: 0/ 0/ 0/ 0

PEAK NO.	MEASURED MASS	NO. POINTS	ABSOLUTE INTENSITY	% INT. BASE	% INT. NREF	% TOT. ION
3	460	25	1809.	0.9	0.9	0.1
7	411	25	1132.	0.6	0.6	0.0
10	404	17	1032.	0.5	0.5	0.0
11	397	25	1837.	1.0	1.0	0.1
12	396	35	13612.	7.1	7.1	0.5
13	395	43	64137.	33.4	33.4	2.5*
14	394	25	2318.	1.2	1.2	0.1
15	393	29	3751.	2.0	2.0	0.1
16	391	21	969.	0.5	0.5	0.0
19	379	25	1794.	0.9	0.9	0.1*
21	370	21	1031.	0.5	0.5	0.0
22	369	29	3548.	1.8	1.8	0.1
23	368	29	2327.	1.2	1.2	0.1
24	367	25	2006.	1.0	1.0	0.1
25	366	25	1202.	0.6	0.6	0.0*
28	356	25	1113.	0.6	0.6	0.0
30	354	21	1094.	0.6	0.6	0.0
31	353	21	1215.	0.6	0.6	0.0
32	352	21	1133.	0.6	0.6	0.0
34	343	29	1992.	1.0	1.0	0.1
35	342	35	8684.	4.5	4.5	0.3
36	341	35	13005.	6.8	6.8	0.5
37	340	35	10221.	5.3	5.3	0.4*
38	339	35	4872.	2.5	2.5	0.2*
39	338	35	6484.	3.4	3.4	0.2*
40	337	25	1457.	0.8	0.8	0.1*
41	336	25	1818.	0.9	0.9	0.1
44	327	25	1804.	0.9	0.9	0.1
45	326	35	5648.	2.9	2.9	0.2
46	325	29	2881.	1.5	1.5	0.1
47	324	35	4847.	2.5	2.5	0.2
48	323	25	1551.	0.8	0.8	0.1
49	322	29	2519.	1.3	1.3	0.1
51	320	25	1150.	0.6	0.6	0.0
52	319	25	984.	0.5	0.5	0.0*
53	312	25	1344.	0.7	0.7	0.1
54	311	25	1094.	0.6	0.6	0.0
55	310	25	1763.	0.9	0.9	0.1
56	309	25	1846.	1.0	1.0	0.1
57	308	35	6710.	3.5	3.5	0.3
58	307	35	26114.	13.6	13.6	1.0
59	306	21	1029.	0.5	0.5	0.0
60	305	21	1021.	0.5	0.5	0.0
62	303	21	1048.	0.5	0.5	0.0
64	299	21	1019.	0.5	0.5	0.0
65	298	21	1038.	0.5	0.5	0.0
67	296	21	1019.	0.5	0.5	0.0
69	294	25	1057.	0.6	0.6	0.0
71	292	21	1341.	0.7	0.7	0.1
72	291	25	2120.	1.1	1.1	0.1
73	290	29	3953.	2.1	2.1	0.2
74	289	35	17710.	9.2	9.2	0.7
75	288	25	1655.	0.9	0.9	0.1
76	287	29	4051.	2.1	2.1	0.2
77	286	21	1201.	0.6	0.6	0.0
78	285	29	2076.	1.1	1.1	0.1
79	284	25	1114.	0.6	0.6	0.0
80	283	29	1318.	0.7	0.7	0.1
81	282	21	1021.	0.5	0.5	0.0
82	281	25	1035.	0.5	0.5	0.0
83	280	21	974.	0.5	0.5	0.0

FAB of $[Cu(teta)](ClO_4)_2$ in Nitrobenzyl alcohol

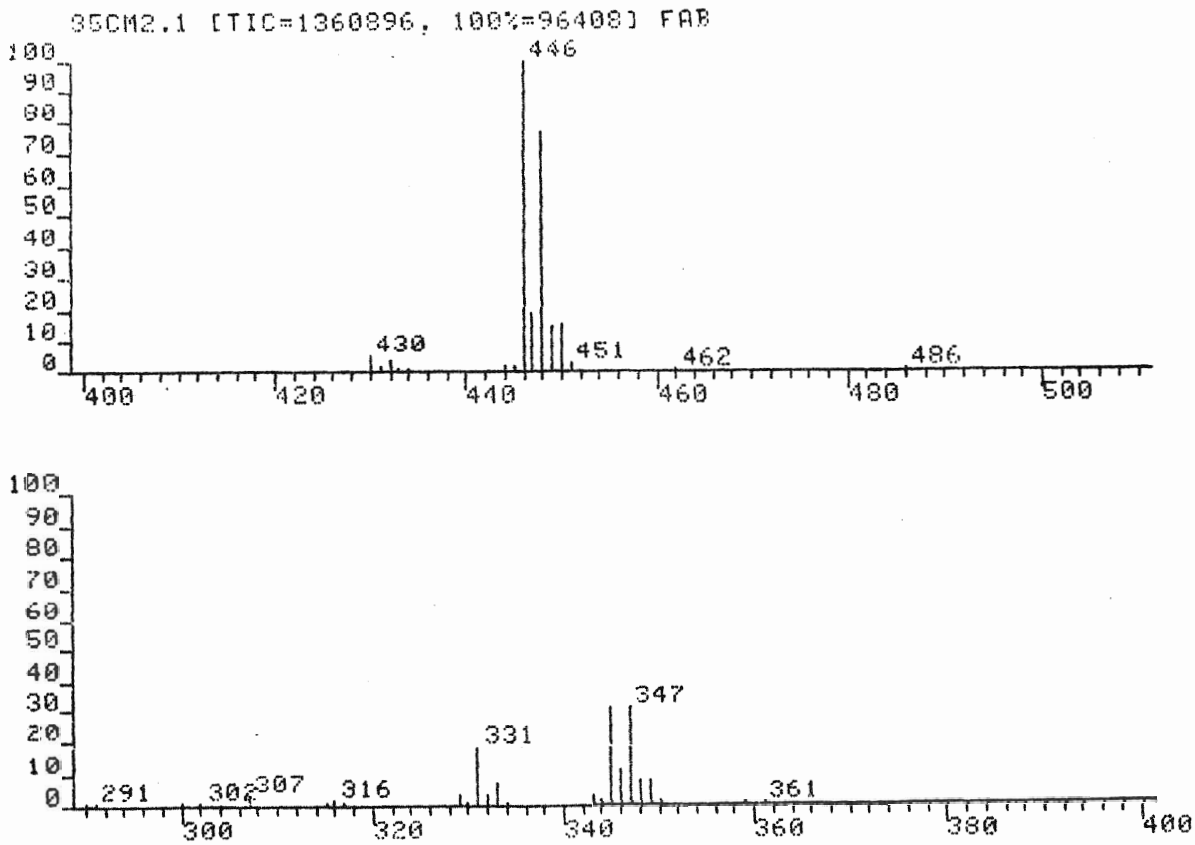

DP0.85CM2.MS
SCAN: 1, 10/28/85 13:25
IONISATION: FAB
NO. PEAKS: 230
BASE/NREF INT: 96408./ 96408.
TIC: 1360896.
MASS RANGE: 30 - 486
RETN TIME/MISC: 0: 0/ 0/ 0/ 0

PEAK NO.	MEASURED MASS	NO. POINTS	ABSOLUTE INTENSITY	% INT. BASE	% INT. NREF	% TOT. ION
1	486	17	1024.	1.1	1.1	0.1
2	462	21	1140.	1.2	1.2	0.1
3	451	25	2796.	2.9	2.9	0.2
4	450	35	15197.	15.8	15.8	1.1
5	449	35	14407.	14.9	14.9	1.1
6	448	43	74288.	77.1	77.1	5.5
7	447	35	18482.	19.2	19.2	1.4
8	446	43	96408.	100.0	100.0	7.1
9	445	29	1401.	1.5	1.5	0.1
10	444	21	1929.	2.0	2.0	0.1
11	434	21	1013.	1.1	1.1	0.1
12	433	21	860.	0.9	0.9	0.1
13	432	29	4131.	4.3	4.3	0.3
14	431	21	1297.	1.3	1.3	0.1
15	430	29	5576.	5.8	5.8	0.4
16	363	21	931.	1.0	1.0	0.1
17	361	21	1135.	1.2	1.2	0.1
18	354	21	1028.	1.1	1.1	0.1
19	350	25	1680.	1.7	1.7	0.1
20	349	35	7946.	8.2	8.2	0.6
21	348	35	7819.	8.1	8.1	0.6
22	347	35	30903.	32.1	32.1	2.3
23	346	35	10913.	11.3	11.3	0.8
24	345	43	30590.	31.7	31.7	2.2
25	344	25	1746.	1.8	1.8	0.1
26	343	29	3366.	3.5	3.5	0.2
27	334	21	1432.	1.5	1.5	0.1
28	333	35	7591.	7.9	7.9	0.6
29	332	29	3704.	3.8	3.8	0.3

PEAK NO.	MEASURED MASS	NO. POINTS	ABSOLUTE INTENSITY	% INT. BASE	% INT. NREF	% TOT. ION
30	331	35	18102.	18.8	18.8	1.3
31	330	25	1465.	1.5	1.5	0.1
32	329	35	3974.	4.1	4.1	0.3
33	318	21	938.	1.0	1.0	0.1
34	317	21	1134.	1.2	1.2	0.1
35	316	25	1685.	1.7	1.7	0.1
36	315	25	1455.	1.5	1.5	0.1
37	314	21	907.	0.9	0.9	0.1
38	308	17	909.	0.9	0.9	0.1
39	307	29	3451.	3.6	3.6	0.3
40	304	21	859.	0.9	0.9	0.1
41	303	21	868.	0.9	0.9	0.1
42	302	21	1041.	1.1	1.1	0.1
43	300	21	1006.	1.0	1.0	0.1
44	291	21	1108.	1.1	1.1	0.1
45	290	25	1313.	1.4	1.4	0.1

peaks at m/z 341, 340, 339, and 338, which were due to loss of hydrogens from the species at m/z 343 are increased in intensity with respect to the peak at m/z 342. In the spectrum of the cobalt compound, using glycerol the peak at m/z 342 was the largest peak and all the others were of lower intensity. Again hydrogen loss was elevated by the use of the more oxidizing matrix nitrobenzyl alcohol. This increase in hydrogen loss supports the theory that an oxidative dehydrogenation mechanism is occurring.